THE
LONDON, EDINBURGH, AND DUBLIN
PHILOSOPHICAL MAGAZINE
AND
JOURNAL OF SCIENCE.

[SEVENTH SERIES.]

FEBRUARY 1927.

XXIX. *Measurements of the Velocity of Sound in Steam, Nitrous Oxide, and Carbon Dioxide, with special reference to the Temperature Coefficient of the Molecular Heats.* *By* W. G. SHILLING, *M.C., M.Sc.**

Introduction.

IN the experiments to be described the molecular heats of nitrous oxide and carbon dioxide have been investigated from room temperature upwards, whilst that of steam has been determined from 100° C. up to 1000° C.

Preliminary experiments at room temperature † had led to the detection and elimination of small inherent errors in the method devised by Kundt for the measurement of the velocity of sound in a gas. For the higher temperature measurements the velocity of sound method seems to contain the least number of immanent errors. Hence it was employed in this work. The method which employs a constant flow calorimeter seems always to yield results slightly greater than those obtained by any other method. The "explosion" method is full of uncertainties. The modern form of the adiabatic method ‡ of Desormes and Clement yields accurate values, but its application to high temperatures would be a matter of considerable experimental

* Communicated by the Author.

† Phil. Mag. xlv. p. 416 (1923).

‡ Partington, Proc. Roy. Soc. A, c. p. 27 (1921). Partington and Howe, Proc. Roy. Soc. A, cv. p. 225 (1924). Brinkworth, Proc. Roy. Soc. A, cvii. p. 510 (1925); cxi. p. 124 (1926).

difficulty. There are many difficulties in the determination of the true velocity of sound in a gas at high temperatures, but none of them have been insurmountable.

Principle of the Method of Experiment.

Sound waves of known frequency are set up in a long tube maintained at the desired temperature and filled with the required gas, and their length accurately measured. Fig. 1 is a diagrammatic sketch of the apparatus.

The tube could be maintained at any temperature from that of the room to an upper limit of about 1100° C. The stationary, reflected wave motion is set up by a telephone, T, the diaphragm, D, of which is placed perpendicular to the axis of the tube, thus forming one of the reflecting surfaces.

Fig. 1.

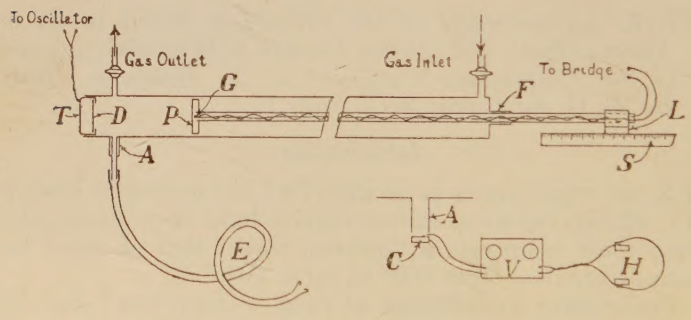

The other reflecting surface is the flat face of a piston, P, which is capable of movement throughout the whole length of the tube. Alternate increase and decrease in the intensity of the sound takes place as the piston is moved along the heated tube, the exact points of the maximum and minimum sound intensity being quite distinct. Between any two maxima or minima the piston has travelled a distance equal to one half wave-length of the sound in the gas. The side tube, A, placed near the telephone diaphragm, is used to detect maximum intensity by methods which will be described later. The mean value of the half wave-length of the sound in the tube is deduced from a series of readings along it. Since the frequency of the oscillation is accurately known, the apparent velocity of the sound in the tube can be deduced. The temperature of the heated tube is determined by measuring the e.m.f. of a thermocouple, the hot junction, C, of which moves along the tube with the piston.

Description of the Apparatus.

The central part of the apparatus is the long silica tube forming a narrow electric furnace. The physical properties of silica limit its use to temperatures not exceeding 1150° C. for any prolonged period. It becomes devitrified and very brittle above 1200° C.* The outer layer of the piston rod used in these experiments became devitrified after long exposure to temperatures which never exceeded 1150° C. The resistivity of silica to chemical action is, however, a great asset.

The first experiments were carried out in a tube of one metre length and 4 cm. bore. But, at temperatures of 700° C. and over, the uniformly heated portion of this tube was only long enough to allow the measurement of three or four half wave-lengths. Disturbances due to the movement of the piston were also rather marked at the higher temperatures. It was therefore decided to employ a much longer tube.

The new silica tube had also a bore of 4 cm. but a total length of 210 cm., the portion actually heated being 180 cm. long. The remaining 30 cm. projected from the furnace for 15 cm. at each end. The tube was wound with 17 S.W.G. nichrome wire, the turns being spaced at 1 cm. apart. The subsidiary heating coils were formed of 14 turns of the same wire, the turns varying from 7 mm. to 2 cm. apart towards the centre. Between the supplementary and the main coils there were four or five layers of asbestos paper of 1 mm. thickness. Normally the short coils were connected in series with the main windings, but provision was made for a separate circuit if necessary. The Uralite case had a cross-section of 30 cm. and was filled with slag wool. The external adjusting resistances were made by covering a sheet iron former with asbestos paper and winding with nichrome wire of various gauges (Nos. 17, 23, 26, and 30 S.W.G.). The total resistance of about 700 ohms was contained on two formers each measuring $7 \times 4 \times 50$ cm.

To one of the projecting ends of the furnace the telephone fitting was attached. A direct attachment of the telephone to the end of the tube was found to be useless. The telephone must be adjustable in respect of the distance of the diaphragm from the side tube, A (fig. 1), since this distance must always be the same proportion of the wave-length being measured. The end-piece finally designed and used

* Information obtained from the Thermal Syndicate Ltd., and confirmed by my experiments.

with complete success is shown in section in fig. 2. The telephone, T, provided with a metal cap in place of the usual vulcanite one, is attached to a rod, R, half of which is threaded. The other half passes through a packing gland of the usual pattern, in which a "hat" washer is used as the packing material. The cover-plate, L, is removable for inspection of the telephone or furnace interior. Insulated telephone terminals are shown at t_1 and t_2. The tubes M, for the microphone, and H, for the gas outlet, go through the water-jacket to the inside tubes. Water is circulated in the jacket by means of the tubes w_1 and w_2. For the experiments on steam the water-jacket was not fitted. The telephone is an easy fit in its cylinder, the packing-gland being sufficient to ensure a gas-tight fitment which is cemented to the furnace tube by a cement of dry litharge and glycerine.

For inert gases the escape of gas through the ear-tube was not objectionable. The gas, cooled by the time it reached the ear, caused no inconvenience to the operator. No further device was necessary since the maxima could be easily and distinctly heard. The case of steam was different, as would also be the case of a poisonous gas. A diaphragm, however thin, could not be inserted between the apparatus and the ear since the energy of the sound waves was extremely small. The Rayleigh disk method * was tried, using a quartz-fibre suspension with a small aluminium disk at its lower end. The available energy was insufficient to cause any marked deflexion of a spot of light reflected from a very light galvanometer mirror attached to the fibre. An application of the microphonic flame method †, which depends on the difference in conductivity produced in a flame containing ions of some salt when any disturbance takes place across its path, is impossible in this case. The difficulty lies in the impracticability of enclosing the flame. Methods of measuring air-pressure changes ‡ are only applicable to comparatively large changes. The most promising type of apparatus seemed to be that using either

*Rayleigh, Phil. Mag. xiv. p. 186 (1882). Grünsehl, *Ann. Phys.* xxxiv. p. 1028 (1888). Zernov, *Ann. Phys.* xxi. p. 131 (1906); xxvi. p. 79 (1908).

† Lee de Forest, 'Nature,' p. 739 (1923).

‡ Raps, *Ann. Phys.* xxxvi. p. 273 (1889). Dvorak, *Ann. Phys.* xxii. p. 606 (1907). Wien, *Ann. Phys.* xxxvi. p. 834 (1889). Altberg, *Ann. Phys.* xi. p. 405 (1903). Wood, Phys. Rev. xx. p. 113 (1905); *Phys. Zeit.* vi. p. 22 (1905).

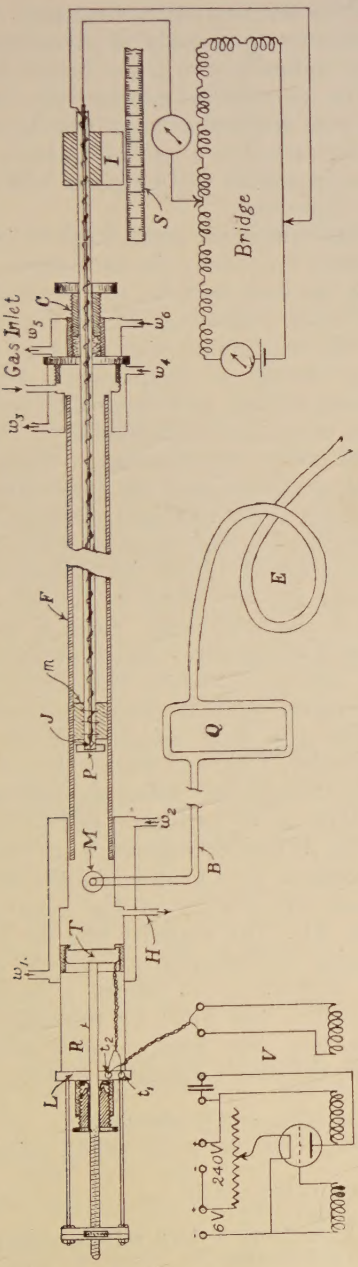
Bridge
S
I
C
Gas Inlet
ω_3
ω_6
ω_4
ω_5
F
m
J
P
M
ω_2
B
E
Q
T
H
ω_1
R_1
t_2
t_1
L
V
240V
6V

Fig. 2.

a telephonic * or microphonic † method. A general survey of the instruments applicable is given by Webster ‡, and many further references will be found in Winkelmann §. In the device eventually adopted the sound waves were received by a microphone, magnified by a two-stage valve amplifier and received in a pair of ordinary head telephones. Details of the apparatus will be given when the experiments on steam are described.

To excite the telephone, some form of interrupter giving a very constant frequency is necessary. The wire interrupter, which has been used for this type of work ‖, has two serious drawbacks. Heating effects are caused in the thin steel wire with consequent expansion of the latter and a corresponding change of frequency. Duplication of the apparatus, using one set as a check on the frequency, seems to be the only solution of this difficulty. This would render the apparatus very cumbersome. Secondly, it is not practicable to construct such an interrupter having a frequency much over 1000 vibrations per second. The resulting half wave-length of sound in most gases is much too long (*e. g.* in air it is about 17 cm.) to be convenient. It would be necessary to use the third or fourth overtone of the fundamental of the telephone. Such a note, forming only about 5 per cent. of the total sound intensity, would be very weak indeed, and it would be difficult to damp down the strong fundamental without destroying entirely the weaker overtones. For the final solution of the problem of a suitable interrupter, I have to thank Prof. J. T. MacGregor-Morris of this College, for whose suggestion of the use of a thermionic valve as an oscillator and valuable advice as to the construction of the instrument, I am indebted.

It is not proposed here to describe the oscillator in detail. The connexions are shown in the general figure of the apparatus (fig. 2). The capacity and the inductance of the circuit determine the frequency. Special precautions were taken in our instrument to secure a constant inductance, whilst the capacity was fixed by preliminary trials with a variable condenser. The final capacity selected, 0·01 mfd., using 240 v. as the anode potential and an anode current of

* Schaefer, *Ann. Phys.* lvii. p. 786 (1896).

† Oberbeck, *Ann. Phys.* xiii. p. 222 (1881). Stern, *Ann. Phys.* xlii. p. 622 (1891).

‡ Phys. Rev. xvi. p. 248 (1903).

§ "Akustik," p. 245 (1909).

‖ Pupin, Sill. Amer. Journ. series 3, vol. xlv. p. 325 (1893). Furstenau, *Ann. Phys.* xxvii. p. 735 (1908).

3·5 milliamperes, gave a frequency of 2992·8 vibrations per second. The instrument was first calibrated by comparison with a standard wave-meter, and afterwards sent to the National Physical Laboratory to be tested. The following table gives the results of the calibrations at the latter institution.

TABLE I.

Frequency of the Oscillator. Anode voltage of 240 v.

Anode Current milliamps.	Frequency.	Anode Current milliamps.	Frequency.
2·8	3007·3	3·2	3000·9
2·9	3005·3	3·3	2998·6
3·0	3003·2	3·4	2995·2
3·1	3002·2	3·5	2992·8

A change of frequency of only 0·06 per cent. was produced by an increase, from 240 v., of 3 per cent. in the anode voltage, the anode current being kept constant at 3·0 milliamperes. The temperature coefficient of the oscillator may be neglected for normal changes in room temperature. The inductance was specially wound to obviate, as far as possible, changes with temperature and the condenser was constructed for this work by the Dubilier Condenser Co., Ltd.

The silica piston was constructed by The Thermal Syndicate, Ltd. A flat disk of silica forms the piston head, which is 4 mm. thick and 4 mm. less in diameter than the bore of the furnace-tube. The piston "rod," a tube of 2 metres length and 1 cm. external diameter, is joined by fusion to the disk the face of which is perpendicular to the axis of the tube. The rod is recessed into the disk so that the covering at the centre of the latter is only very thin, although the face of the disk is perfectly flat. The hot junction of the thermocouple, situate immediately behind this thin covering, is thus quickly affected by any changes in the temperature.

For brevity, the end of the furnace from which the piston projects will be called the "piston end" and the opposite end the "telephone end." The piston rod slides through a packing gland cemented to the piston end of the furnace. The gland is of the usual type having asbestos fibre as the packing material. The latter can be tightened onto the piston rod by means of a large milled thumb-screw. This form of gland is quite suitable since there is always a

slight excess pressure inside the furnace and any diffusion which does take place is outwards from, and not into, the furnace. Fig. 2 shows the general lay-out of the apparatus.

If the piston head touched the furnace-tube as it moved along it, the noise produced rendered measurements much more difficult. For this reason, and also to allow free circulation of the gas, the disk was made 4 mm. less in diameter than the bore of the furnace-tube in which it was held centrally by plates of mica, *m* (fig. 2), strapped to it immediately behind the piston head. Stout platinum wire was used to strap these plates which were about 8 cm. long. Movement of the piston then generated no extraneous noise since mica is relatively soft.

A steadying guide, which also served as a reading index, completed the fittings attached to the piston. At a distance of about 5 cm. vertically below the piston rod, placed parallel with the axis of the latter, was arranged a silvered steel scale of 150 cm. in length. The scale was made for this work by Messrs. Chesterman and Co., Ltd., of Sheffield, and has a guaranteed accuracy of one part in ten thousand. It is divided for the whole of its length into millimetres. The reading index of the apparatus is at the zero of the scale when the piston is at a distance of about 50 cm. from the telephone diaphragm.

A square prism of cork, of the same cross-section as the width of the scale, and 5 cm. long, was bored to fit tightly on the end of the piston rod. Two glass plates were then cut and glued to two sides of the cork prism. When fixed in position on the piston rod, the index formed a saddle, the glass plates sliding on the wood support of the scale and touching both sides of the latter. One edge of the front plate is used as the reading index.

To measure the temperature of the furnace-tube a thermocouple of *pure platinum*/90 *per cent. platinum* + 10 *per cent. rhodium* is used. It runs throughout the whole length of the piston rod with the hot junction situated immediately behind the face of the piston. The cold junctions, which are outside the piston rod, are brought under the reading index and fixed to the top of the cork prism by means of drawing pins. The e.m.f. of the thermocouple was measured directly in microvolts on a bridge, using a mirror galvanometer as a null instrument. The bridge consisted of ten coils of 0·1 ohm resistance in series with a bridge wire of 0·1 ohm resistance. The latter was divided into 1000 parts. With a current of 10 milliamperes flowing in the circuit, the fall of potential down each coil or down the whole of

the bridge wire, was thus one millivolt. The whole of the apparatus was made in the Department. Every care was taken to ensure relative accuracy of the divisions and the thermocouple was calibrated with the bridge as it is normally used. The *absolute* values of the potential differences are obviously immaterial under these conditions. In the measurements described, the absolute values were probably accurate to ± 2 per cent. The galvanometer (Gambrell Bros. Ltd., Southfields) had the following constants:— Resistance 160 ohms, sensibility 320 mm. per microampere, period 8 seconds. The corresponding deflexion for a potential difference of 10 microvolts is 20 mm. on a scale placed one metre from the mirror. This deflexion corresponds roughly to 1° C. for the thermocouple used. The required accuracy of 1° C. can therefore easily be obtained. The total error involved in the contacts and in manipulation is of the order 0°·1 C. Thus the probable error in reading the temperature is considerably less than 1° C. at all the temperatures used. The fixed points used to calibrate the thermocouple and the corresponding readings in millivolts are given below.

TABLE II.

Temp. ° C.	Fixed Point.	Millivolts.
100·0	B.P. of water at 760 mm.	0·612
217·9	,, naphthalene at 760 mm.	1·675
357·3	,, mercury at 760 mm.	3·051
444·5	,, sulphur at 760 mm.	3·498
630·0	M.P. of antimony.	5·830
801·0	,, sodium chloride.	7·868
960·0	,, silver.	9·676

In all these calibrations the cold junctions were maintained at room temperature which was carefully noted during the experiment. To reduce the readings to a cold junction temperature of 0° C. the cold junctions were immersed in ice-water at 0° C., and readings taken with the hot junction at temperatures of 5°, 10°, etc., up to 50° C. All subsequent temperature readings can then be reduced to a cold junction temperature of 0° C. from the carefully noted room temperature at the time of the experiment. This method of procedure was necessary since it would be very inconvenient always to maintain the cold junctions at 0° C. under experimental conditions. The resulting curve for the e.m.f. plotted against temperature runs practically parallel to the typical curve for such a thermocouple as given by Henning *. A

* 'Temperaturmessung,' p. 122 (1915).

large scale graph was used to deduce the centigrade temperatures from the experimental readings in microvolts.

The gas generating and purifying apparatus will be described separately for each gas. One other part of the general apparatus remains to be described in detail. This is the ear-tube through which the sound is conveyed to the ear of the observer. It is joined to the glass tube, B (fig. 2), and is of hard, black, thick-walled rubber tubing. Other kinds of rubber tubing tried transmitted a large part of the sound through the walls of the tubing and the note of the telephone could be heard continuously In this case the maxima were much less distinct. Between the glass tube and the ear-tube, a Quincke interference tube, Q (fig. 2) is inserted to reduce the intensity of undesirable harmonics.

Method of Experiment.

The gas used as a standard of comparison throughout the experiments was dry air from which carbon dioxide had been removed. Air thus treated will be called "pure air" in all subsequent references. To standardize the apparatus, the velocity of sound in pure air at 0° C. and 760 mm. pressure was taken to be 331·4 m./sec.* This figure is the basis of all the calculations.

To dry the tube, air was passed through the furnace which had been heated to about 900° C., until no moisture was observed in the exit tube for several hours. The air from a blower was first passed through a sulphuric acid wash-bottle to observe the rate of flow and also partially dry the gas. It was then passed through a long tower packed with broken stick sodium hydroxide, to remove any carbon dioxide, and then through long drying tubes containing calcium chloride and phosphorus pentoxide. The process of drying the tube occupied three days. The air was kept circulating until the furnace had again attained room temperature, when the supply was cut down until it was just sufficient to ensure that there could be no diffusion of the outside atmosphere into the dry furnace. The telephone was then set vibrating and the piston moved along the furnace with the ear-tube held to the ear. Adjustment of the telephone was then made by a method of oscillations until the best maxima were heard. It is impossible to describe the adjustment since the sound which is most suitable for measurement of accurate maxima is a matter of experience. The best adjustment gives quite weak, but very distinct, maxima. The louder sounds, which

* See 'Specific Heats of Gases,' Partington & Shilling, p. 77 (1924),

at first appeared to be easier to measure, were really less accurately measured. At room temperature the maxima could easily be fixed to $\pm 0{\cdot}5$ mm. Series of 25 to 30 half wave-lengths have been obtained in which the maximum deviation from the mean did not exceed $\pm 0{\cdot}004$ cm. on a half wave-length of about 6 cm. A probable error in the velocity of sound of one part in 11,000 was obtained from a series of 93 experiments. At higher temperatures the measurements are much more difficult and the error is increased to something of the order one part in 800 in the region of 1000° C. The corresponding probable errors in the values of C_v are 0·05 per cent. and 1 per cent. respectively. At room temperature a maximum as near the zero end of the scale as possible is chosen as the zero, or starting point. The maximum next measured would be, say, the tenth from this point, the intervening maxima being merely counted as they are passed. Readings are then taken at each successive maximum as far as the apparatus will allow. With air 25 maxima can be measured, whilst for carbon dioxide 30 are obtainable. The temperature of the experiment is taken from the readings of calibrated thermometers at each end of the furnace.

When satisfactory measurements at room temperature have been completed, the furnace is heated to the vicinity of 100° C. When the desired temperature has been reached and no deviation greater than that corresponding to 1° or 2° C. has been observed for half an hour, the temperature is taken as constant for the purpose of the experiment. A series of measurements can usually be completed in less than this time. With the furnace at any temperature above that of the room, there is a temperature gradient from the cooled ends to the heated portion. Measurements are never taken in this portion of the furnace, since the magnitude of the correction necessary would be very uncertain. The particular maximum which is chosen as the zero for any series of measurements is always well within the uniformly heated portion of the furnace. The exact temperature gradient is then immaterial provided it is never disturbed by any violent movement of the piston, which exerts a pumping action when rapidly moved. Gentle movement of the piston and a pause between each two movements of one half wave-length obviates any disturbance of the temperature gradient. The zero must be farther within the tube the higher the temperature of the latter, a distance of about 30 cm. being necessary in the region of 1000° C. The pause between each two successive measurements is also necessary to ensure that the

thermocouple has attained the temperature of the surrounding gas. When the temperature of the central part of the furnace was steady near 100° C., the temperatures at the ends were adjusted, if necessary, by regulating the current through the supplementary heating coils. The piston was then pushed into the furnace until the end of the uniformly heated portion was reached. The first point of maximum sound inside this limit was then chosen as the zero for the series of measurements. The position of the telephone diaphragm relative to the side tube was then adjusted before finally fixing this point. The Quincke interference tube was removed, the ear-tube placed to the ear, and the piston placed at what was judged to be the position of maximum sound.

The telephone was then moved until the maximum was loudest, and the piston again moved to the best position for maximum sound. Alternate movements of the telephone and the piston were then made until the best position of the former was determined. The Quincke tube was then replaced and adjusted to damp down the undesirable overtones. The incidental damping of the fundamental had the effect of rendering the maxima more distinct. Later, when using the microphone and valve amplifier to receive the sounds, the adjustment of the telephone was similar. When a short, loud maximum had been obtained, the filament current of the amplifier was so adjusted that the maximum was only just audible. The fine control thus obtained of the intensity of the note received by the telephones rendered it possible just to eliminate all sound except in the immediate neighbourhood of the maximum. But there was always audible a faint reproduction of the note emitted by the telephone. This was due, partly to the mutual action of the oscillator circuit and the amplifier and partly to direct action of the telephone on the microphone.

With the telephone adjusted, the point of maximum sound was accurately determined and the corresponding thermocouple e.m.f. read. The temperature of the cold junctions was read from a calibrated mercury thermometer placed near them. The series of maxima was then read along the furnace until the temperature began to fall at the end of the uniformly heated portion. Tables III. to VI. show the type of result obtained. The piston was pushed back into the furnace and the zero checked after each series. The reading must agree to $\pm 0{\cdot}5$ mm. with the first one. The anode current of the oscillator valve was also checked several times during each series of readings.

When several concordant sets of readings had been obtained near 100° C., the process was repeated at intervals of about 100° C. up to 1000° C. Measurements were made as high as 1050° C. in order to fix accurately the position of the velocity curve at 1000° C. The apparatus described above was used in the experiments on carbon dioxide. The work on nitrous oxide and steam will be described a little more in detail, since the former is decomposed by heat and the latter required modifications of the apparatus.

Preparation of the Gases.

Air.—The purification of the air used to standardize the apparatus has already been described.

Carbon dioxide.—The commercial gas was used as obtained from cylinders. After blowing off the first portions of the gas, the remainder contained a very uniform amount of 0·5 per cent. of air (by volume). Analyses were made during each day's run. Since the velocities of sound in air had already been accurately investigated, a correction for the amount of air present could easily be made at each temperature.

Nitrous oxide.—This gas was prepared by the interaction of a solution of pure hydroxylamine hydrochloride dissolved in air-free water and an air-free solution of pure recrystallized sodium nitrite. The central portions of gas from a cylinder of nitrous oxide were also used. No difference could be detected in the velocity of sound in the gases from the two different sources. A very small percentage of nitrogen, the only impurity not easily removed from the cylinder gas, would certainly be detected by the method of experiment used. Hence, although the first and last portions of the gas from a cylinder were found to contain 1 per cent. and 4 per cent. of nitrogen respectively, the central portions were quite pure. Nitrous oxide begins to decompose into oxygen and nitrogen just above 500° C. Hence the velocity of sound in nitrous oxide is abnormal above this temperature and the apparent molecular heat begins to decrease instead of increase with rising temperature. The break in the velocity of sound curve was not abrupt, so that the exact point at which decomposition began could not be determined. The change first became noticeable at 530° C. Some decomposition would probably have taken place just before this temperature. Berthelot * estimated 520° C. as the temperature of initiation of decomposition. At 600° C. the results show that an appreciable

* 'Sur la Force des Matières Explosives,' vol. i. p. 290 (1883).

amount of nitrogen and oxygen must be present. The data obtained have been tabulated in two ways for 600° C. The first, *a*, Table XII., gives the figures actually obtained, and the second, *b*, Table XII., the figures obtained by extrapolating the velocity curves to follow a normal course through 600° C.

Steam.—Several important modifications of the apparatus were found necessary for the determination of the velocity of sound in steam. The two important alterations were: (*a*) the introduction of a separator and superheater to obtain a steady flow of dry steam into the furnace: (*b*) a modification of the method of reception of the sound intensity.

The method of introducing dry steam into the furnace will be described first. For the superheater, the original short furnace was adapted. It was placed with its axis at right angles to that of the main furnace and sloping downwards from the latter at an angle of about 15 degrees. To each end of the superheater was cemented a gauze separator.

Fig. 3.

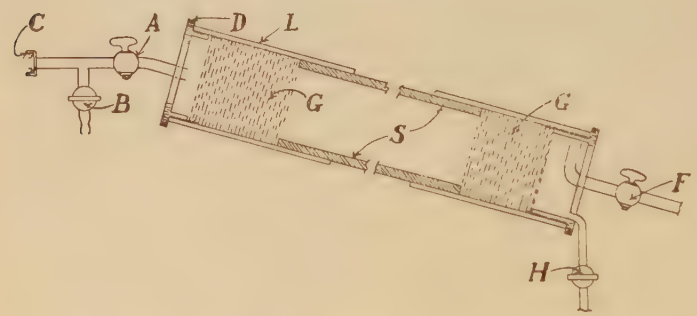

The two end-pieces are shown in fig. 3. Preliminary experiments before a separator was employed clearly showed the necessity for such a device. Without its use, the moisture carried over by the steam rendered it impossible to attain any uniformity of temperature in the main furnace. The temperature near the end at which the steam was admitted remained 150° to 200° C. below that near the exit end when the temperature of the latter was raised to 800° C. A few disks of copper gauze placed in the end of the superheater reduced this discrepancy to about 50° C. Although it is not possible to attain temperatures quite so uniform as when an easily controlled gas is being used, the end-pieces shown in fig. 3 have proved very satisfactory,

The upper end-piece, left of fig. 3, is connected directly to the gas inlet of the main furnace by means of the union

joint, C. The outer tube, L, was cemented to the silica tube of the superheater. The space of about 5 cm. between the end of the tube, S, and the cap, D, was filled with disks of fine copper gauze, the number of the latter being so arranged that, on screwing up the cap tightly, the disks were well pressed together. The connecting tube carried the brass tap, A, which controlled the flow of steam into the furnace, and also the tap, B. The latter was provided to admit the ready replacement of steam by air for the purpose of checking the frequency without disturbing any other parts of the apparatus.

The lower end-piece contained a similar gauze separator. Steam was admitted at F, the end of which was bent inside the brass cap so that it almost touched the side of the latter. Most of the surplus water was drained from the drain-cock, H, which also served to regulate the steam supply to the furnace, as will be described later.

To generate the steam, a large can was fitted with a delivery tube and safety tube as in the ordinary laboratory method of steam distillation. A can holding four to five litres was found to be sufficient to do a day's run without refilling. Some difficulty was experienced in obtaining a slow, steady current of dry steam. It was finally accomplished as follows. The whole of the projecting pieces of the furnace and superheater tubes was covered with a layer of asbestos cement of about 8 mm. thickness. Over this cement was wound a coil of 23 S.W.G. nichrome wire. The coils were spaced 2 cm. apart, since it was only necessary to maintain the external parts at a temperature just above the condensation point of water. The superheater was also wound with the same gauge wire so that the whole of the coils were placed in series in the same circuit. Thus the superheater, the right-angled connexion between this and the main furnace, and the projecting end of the latter near the telephone were all maintained at approximately the same temperature. When properly working, no condensed water could ever be drawn from the tap, B. The lower, projecting end of the superheater was also lagged with the same cement, but it was found unnecessary to lag the steam lead from the boiler. The latter was placed on the floor directly under the lower end of the superheater, thus needing only a very short length of vertical tubing to the tap, F. Any moisture condensing in this tube would then either fall back into the boiler or be drained off from the tap, H.

The most important factor in obtaining a steady flow of steam seemed to be the heating of the boiler. A shielded four-tube Bunsen burner was employed. When properly

shielded from draughts, this arrangement was quite satisfactory although electrical heating might have been better. The flame was adjusted until the steam was generated at a slightly greater rate than actually required. The tap, A, was then shut down until the requisite amount of steam was passing to the furnace. The amount of steam required was somewhat greater than needed for the permanent gases, since a slow flow caused the temperature gradient from the end of the furnace to the telephone to be easily disturbed. With the tap, A, adjusted, the tap, H, was so arranged that the head of water in the safety tube was about 5 cm. The definite pressure set up in the superheater could then be measured by means of the safety tube. If any but very small pressures were used, the noise of the steam as it was forced through the tap, A, considerably added to the difficulty of measuring the points of maximum resonance, since any sound at the tap, A, was transmitted to the headphones. The steam left the furnace at a point just in front of the telephone diaphragm (see H, fig. 2).

A summary of the methods available for the modification of the method of receiving the sounds has already been given. The arrangement actually adopted will therefore be described now.

The side tube, M, fig. 2, had been made 2·5 cm. in diameter to enable a microphone button to be placed in it. Attempts were first made to measure directly the changes in current flowing through a microphone placed in this side tube by connecting it in series with a delicate milliammeter and an accumulator cell. Although the maxima could be detected, the method was not sufficiently sensitive to enable measurements to be made. But by first magnifying these current changes by a three-electrode valve a great improvement was effected. The sounds, however, were still rather weak. The addition of a second stage of amplification has, however, given results which are even better than those obtained for other gases by the use of the ear-tube. The valve panel scarcely needs description. It is sufficient to say that the current from a microphone, in series with a 2 v. accumulator, is passed to the primary of a simple step-up transformer, the secondary of which is connected to the grid of the first valve. The amplified current is then passed to the second valve, by means of the intervalve transformer. From the second valve it is taken to the headphones.

Several types of microphone were tried. The best results were obtained by using an ordinary Weston Electric solid-back transmitter. The usual mouthpiece was replaced by a

short piece of brass tubing of 2·5 cm. diameter, screwed into the microphone by means of the thread which had previously held the mouthpiece. This transmitter had several advantages. The microphone was mounted on a large steel disk bedded on a rubber washer, thus forming a gas-tight joint. Thus the furnace gas did not come into contact with the microphone button. An adjustable damper-spring at the back of the large steel disk afforded a method of modifying the natural vibration frequency of the latter. Since a note of constant frequency, but of small amplitude, was to be received, the adjustment of this damper-spring afforded an excellent method of rendering the receiver more sensitive. A metal to metal connexion of the microphone to the side tube was not permissible since direct transmission of the sound took place along the metal. A rubber connexion minimized this trouble. One piece of tube was fitted to the microphone and a slightly larger piece to the side tube on the furnace. A telescopic arrangement was thus made so that the distance of the microphone button from the centre of the furnace tube could be varied. This adjustment was by no means so essential as the corresponding movement of the main telephone, but it was found to be a distinct advantage in the production of good maxima.

Experiments were carried out with varying speeds of the current of steam through the apparatus. With a very slow current equilibrium in the temperature gradient at the telephone end of the furnace was too easily disturbed. A series of measurements with a very slow current had to be carried out with such slow movements of the piston, or such long pauses after each movement, that it became difficult to maintain other conditions unchanged throughout the series. In addition, the measurement of one series was very laborious and personal fatigue reduced the accuracy of the measurements. With faster currents of steam this drawback disappeared but the uniformity of temperature suffered. A compromise was eventually adopted by adjusting the current of steam so that very little temperature lowering took place, but the measurements were somewhat more protracted than in the case of other gases. The effect on the temperature was merely a gradual lowering towards the end of the furnace at which the steam entered. Since the drop was quite small, the mean temperature with the corresponding mean half wave-length were taken as the result of the series of measurements. Many series of measurements were, however, discarded because the zero was found to have changed when the piston was moved back to its original position after

a series of readings had been taken. Owing to the greatly increased difficulties in the case of steam, the experimental errors are slightly greater than in the case of the other gases, but it is believed that the results obtained represent a considerable advance on our previous knowledge of the molecular heat of steam at one atmosphere pressure, especially in the temperature region 200° to 1000° C.

Reduction of the Results.

From the experimental measurements of the half wave-length of sound in the gases at the respective temperatures, the true velocity of sound in the gas must first be determined. Tables III. to VI. show the type of measurement actually

TABLE III.

Air at room temperature. 2/3/23.

Temperature..... 15°·5 C.
15°·7 C.

Mean temp. ..... 15°·6 C.

No. of wave-lengths.	Scale reading.	Difference.	λ/2 cm.
0	4·75	—	—
6	38·80	34·05	5·675
7	44·40	39·65	5·664
8	50·15	45·40	5·675
9	55·75	51·00	5·666
10	61·35	56·60	5·660
11	67·00	62·25	5·659
12	72·80	68·05	5·663
13	78·40	73·65	5·665
14	84·15	79·40	5·671
15	89·85	85·10	5·673
16	95·50	90·75	5·672
17	101·20	96·45	5·673
18	106·85	102·10	5·672
19	112·55	107·80	5·673
20	118·20	113·45	5·672
21	123·90	119·15	5·673
22	129·60	124·85	5·675
23	135·40	130·65	5·680
24	141·00	136·25	5·677
25	146·60	141·85	5·674
	Mean half wave-length		5·671

obtained. The date and the mean cold junction temperature are given at the top of the table. The three columns for each gas contain the number of half wave-lengths, the corresponding mean half wave-length and the temperature in millivolts respectively. At the foot of each table is added the cold junction correction and the equivalent temperature in degrees centigrade is also given.

TABLE IV.

Carbon dioxide.			Steam.		Nitrous oxide.	
13/12/23.		16°·3 C.	12/6/24.	20° C.	8/2/24.	14°·9 C.
No.	λ/2.	M.V.	λ/2.	M.V.	λ/2.	M.V.
0		1·142		1·400		1·140
6			8·32	1·400		
7			8·40	1·355		
8			8·42	1·340		
9	5·400	1·210	8·43	1·315		
10	5·395	1·215	8·44	1·305	5·420	1·155
11	5·272	1·225	8·39	1·305	5·409	1·155
12	5·400	1·228	8·42	1·275	5·409	1·155
13	5·400	1·238	8·44	1·275	5·392	1·155
14	5·393	1·238	8·41	1·260	5·400	1·158
15	5·400	1·230	8·40	1·280	5·407	1·160
16	5·375	1·230	8·44	1·000	5·394	1·160
17	5·400	1·215			5·397	1·155
18	5·395	1·215			5·400	1·140
19	5·400	1·190			5·415	1·140
20	5·400	1·112			5·405	1·172
Means	5·394	1·207	8·41	1·293	5·405	1·154
C. J.		0·073		0·090		0·067
Temp.		1·280		1·383		1·221
or,		174° C.		185° C.		167° C.

When sets of measurements had been taken over the whole temperature range, the mean half wave-length of each set was squared and plotted against the temperature on a large scale graph. The resulting smoothed line was only slightly curved. From this curve the exact square of the half wave-length was read off at each hundred degrees centigrade. The square root of this figure multiplied by twice the frequency employed gives the apparent velocity of sound in the gas.

Table V.

Carbon dioxide.			Steam.		Nitrous oxide.	
21/1/24. 15°·1 C.			26/5/24. 18°·9 C.		30/10/22. 14°·8 C.	
No.	λ/2.	M.V.	λ/2.	M.V.	λ/2.	M.V.
0		6·481		7·090		6·203
4			12·27	7·090		
5			12·07	7·050		
6	7·777	6·330	12·18	7·050		
7	7·700	6·310	12·23	6·860		
8	7·712	6·455	12·16	6·730	7·930	6·210
9	7·722	6·400	12·21	6·650	7·926	6·225
10	7·725	6·400	12·07	6·500	7·932	6·278
11	7·755	6·420	12·14	6·350	7·936	6·308
12	7·742	6·470	12·20	6·100	7·925	6·325
13	7·777	6·600			7·928	6·265
14	7·793	6·880			7·927	6·260
15					7·929	6 223
Means	7·738	6 474	12·17	6·747	7·929	6·255
C. J.		0·068		0·085		0·066
Temp.		6·542		6·832		6·321
or,		693° C.		719° C.		678° C.

Table VI.

	Carbon dioxide.		Steam.	
	23/1/24. 15°·9 C.		12/8/24. 24°·0 C.	
No.	λ/2.	M.V.	λ/2.	M.V.
0		10·10.)		10·640
3			13·30	10·780
4	8·900	10·380	13·30	10 780
5	8·900	10·570	13·30	10·520
6	8·867	10·680	13·40	10·520
7	8·886	10·700	13·30	10·480
8	8·900	10·640	13·30	10·420
9	8·911	10·550	13·30	10·320
10	8·910	10·460	13·30	10·275
11	8·909	10·400		
12	8·958	10·565		
Means	8·905	10·585	13·31	10·526
C. J.		0·071		0·108
Temp.		10·666		10·634
or,		1034° C.		1032° C.

The true velocity of sound in the free gas must then be calculated. This has been done by the method fully described elsewhere ‡. Equations (81) and (83) (*loc. cit.*) were employed for the calculations.

The true velocity, V, of sound in the gases, calculated from the apparent velocity, V′, in the tube, is given in Table VII. In Table VIII. the values of the velocity of sound in carbon dioxide obtained by the author are compared with those obtained by Professor H. B. Dixon and his co-workers.

TABLE VII.

Sound Velocities in metres per second.

Temp. ° C.	Carbon dioxide.		Steam.		Nitrous oxide.	
	V′.	V †.	V′.	V.	V′.	V.
Room*	263·2	264·7	—	—	—	264·6
100 ...	297·7	299·9	467·3	471·5	296·6	299·0
200 ...	332·6	335·8	530·6	536·7	330·9	334·3
300 ...	363·2	367·5	585·0	593·2	361·0	365·4
400 ...	391·7	397·1	632·8	643·2	388·4	393·9
500 ...	417·4	424·0	675·4	688·2	413·6	420·3
600 ...	441·4	449·2	712·6	727·8	439·1	446·9
700 ...	462·9	472·0	744·9	762·5	—	—
800 ...	484·1	494·5	775·0	795·3	—	—
900 ...	504·0	515·8	802·3	825·0	—	—
1000 ...	523·4	536·5	828·7	853·9	—	—

* 15° C. for CO_2; 14·5° C. for N_2O.
† Corrected also for the 0·5 per cent. of air present.

TABLE VIII.

Comparison of the Velocities of Sound in Carbon Dioxide.
(Velocities in metres per second.)

Temp. ° C.	Dixon.	Author *.
100.....	300·4	299·9
200.....	336·9	335·8
300.....	369·3	367·5
400.....	398·6	397·1
500	425·7	424·0
600.....	450·9	449·2

* The author's figures for carbon dioxide, uncorrected for the 0·5 per cent. of air present, are much nearer to those of Dixon than are those tabulated above.

‡ See 'The Specific Heats of Gases,' § 20 and § 21, pp. 51–54.

The calculation of the ratio of the specific heats of the various gases from the velocity of sound in them is carried out by means of the equation

$$\gamma = V^2 M\phi/RT, \quad . \quad . \quad . \quad . \quad . \quad . \quad (1)$$

where

$\gamma = C_p/C_v$ = the ratio of the specific heats,

M = the molecular weight of the gas,

R = the Gas Constant ($8{\cdot}3156 \times 10^7$ ergs/° C.; V in m./sec.),

T = the absolute temperature,

ϕ = a correction term for the deviation from the ideal gas laws.

The factor ϕ may be deduced when a suitable equation of state for the gas is available. For carbon dioxide and nitrous oxide, Berthelot's equation of state may be used. In this case,

$$\phi = 1 - \frac{9}{64}\pi\tau(1 - 6\tau^2) \quad . \quad . \quad . \quad . \quad (2)$$

and

$$C_p - C_v = R\left(1 + \frac{27}{16}\pi\tau^3\right), \quad . \quad . \quad . \quad . \quad . \quad (3)$$

in which

$\pi = p/p_c$ = actual/critical pressure,

$\tau = T_c/T$ = critical/actual temperature (abs.).

R, the Gas Constant, in equation 3 is expressed in calories (15° C.) per gram-molecule of the gas. (1·9875 cals.)

For steam, Callendar's equation of state has been used. The corresponding correction factors then become

$$\phi = (1 + pc/RT)^2, \quad . \quad . \quad . \quad . \quad . \quad (4)$$

$$C_p - C_v = R(1 + ncp/RT)^2, \quad . \quad . \quad . \quad . \quad (5)$$

where

p is the pressure in atmospheres,

$c = c'(373/T)^n$, in which n for steam is taken as 10/3. The constant c' has a value 0·47367 litres/gm. molecule in the case of steam. In equation (4), the Gas Constant must be expressed in litre atm.; in equation (5), in gm. cals. The

values of ϕ and $C_p - C_v$ were also calculated for steam by using Berthelot's equation of state. As might be expected, the discrepancies between the two sets of results are greatest below the critical temperature for steam and practically negligible above 600° C., at which temperature steam is fast conforming to the ideal gas laws. In Table IX. are given the physical constants used in the calculation of the

TABLE IX.

Constant.	Gas.		
	Carbon dioxide.	Nitrous oxide.	Steam.
Molecular Weight, M	44·0	44·02	18·01
Critical Temp., T_c	304·4	308·5	638
Critical pressure, p_c	72·9	75	204
Viscosity at 0° C., η_0	$0{\cdot}0_3 1366$	$0{\cdot}0_3 1366$	$0{\cdot}0_4 900$ *
Density at 0° C., ρ_0	0·001963	0·00197	0·0008039†
$\epsilon = K/C_v$	1·540	1·673	1·150
Ratio $C_p/C_v = \gamma$	1·302	1·30	1·33
Sutherland Constant, S ..	239·7	286	548
Thermal Conductivity, K	$0{\cdot}0_4 332$	$0{\cdot}0_4 351$	$0{\cdot}0_4 380$
Specific Heat, c_v (approx.)	0·1531	0·1536	0·367
The Gas Constant, R	$8{\cdot}3157 \times 10^7$ ergs/° C. or 1·9875 cals./gm. mole.		

* Extrapolated from measurements at higher temperatures.

† Ideal; the experimental value, extrapolated from measurements at 110° C., is 0·000788.

various factors which were employed to reduce the experimental results. In all cases they have been selected from the literature after a careful search and are believed to be as accurate as available experimental data will allow.

If the constants in the above table are employed, the values contained in Tables X. and XI. are obtained.

From equation (1) the values of γ can be calculated from the experimental value of V, the true velocity of sound in the free gas. Then, with γ and $C_p - C_v$ known, the quantities can be separately evaluated. The following Tables give these values.

Table X.

Constants for Carbon dioxide and Nitrous oxide.

Temp. ° C.	Carbon dioxide.			Nitrous oxide.		
	φ by (2).	$C_p - C_v$ by (3).	Eqn. 81. See p. 293.	ϕ by (2).	$C_p - C_v$ by (3).	Eqn. 81. See p. 293.
0 ..	1·0138	2·051	—	1·0141	2·052	—
Room *.	1·0110	2·041	0·368	1·0119	2·042	0·371
100 ...	1·0047	2·012	0·473	1·0048	2·013	0·479
200 ..	1·0018	2·000	0·591	1·0019	2·000	0·601
300 ..	1·0007	1·994	0·703	1·0007	1·994	0·718
400 ...	1·0002	1·992	0·811	1·0002	1·992	0·831
500 ...	1·0000	1·990	0·916	1·0000	1·990	0·940
600 ...	0·9998	1·989	1·017	0·9998	1·989	1·047
700 ...	0·9998	1·989	1·116	—	—	—
800 ...	0·9997	1·988	1·212	—	—	—
900 ...	0·9997	1·988	1·306	—	—	—
1000 ...	0·9997	1·988	1·398	—	—	—

* 15° C. for CO_2; 14·5° C. for N_2O.

Table XI.

Constants for Steam.

Temp. ° C.	Eqn. 81. See p. 293.	$c = c'\left[\frac{373}{T}\right]^n$.	Callendar's equation.		Berthelot's equation.	
			ϕ by (4).	$C_p - C_v$ by (5).	ϕ by (2).	$C_p - C_v$ by (3).
100 ...	0·498	0·47367	1·0362	2·198	1·0195	2·070
200 ...	0·637	0·21461	1·0111	2·061	1·0092	2·028
300 ...	0·772	0·11324	1·0048	2·021	1·0049	2·010
400 ...	0·905	0·06624	1·0024	2·003	1·0029	2·002
500 ...	1·035	0·04507	1·0014	1·997	1·0018	1·997
600 ...	1·161	0·02783	1·0008	1·993	1·0011	1·994
700 ...	1·285	0·01939	1·0005	1·991	1·0007	1·992
800 ...	1·407	0·01399	1·0003	1·990	1·0005	1·991
900 ...	1·527	0·01040	1·0002	1·989	1·0003	1·990
1000 ...	1·643	0·00791	1·0002	1·988	1·0002	1·990

Table XII.

C_v, C_p, and C_p/C_v for Carbon dioxide and Nitrous oxide.

Temp. ° C.	Carbon dioxide.			Nitrous oxide.		
	C_v.	C_p.	C_p/C_v.	C_v.	C_p.	Cp/C_v.
Room *	6·760	8·801	1·3020	6·704	8·746	1·3046
100 ...	7·135	9·147	1·2820	7·312	9·325	1·2753
200 ...	7·573	9·573	1·2641	7·908	9·908	1·2529
300 ...	8·037	10·031	1·2481	8·496	10·490	1·2347
400 ...	8·297	10·289	1·2401	9·018	11·010	1·2209
500 ...	8·637	10·627	1·2304	9·499	11·489	1·2095
600 ...	8·927	10·916	1·2228	(*a*) 9·422	11·411	1·2111
				(*b*) 9 910	11·899	1·2007
700 ...	9·418	11·407	1·2112	—	—	—
800 ...	9·679	11·667	1·2054	—	—	—
900 ...	9·960	11·948	1·1996	—	—	—
1000 ...	10·143	12·131	1·1960	—	—	—

(*a*) Experimental results showing the effect of decomposition.

(*b*) Velocity curves extrapolated from 500° C. to follow the normal course.

* 15° C. for CO_2; 14·5° C. for N_2O.

Table XIII.

C_v, C_p, and C_p/C_v for Steam.

Temp. ° C.	Callendar's equation.			Berthelot's equation.		
	C_v.	C_p.	C_p/C_v.	C_v	C_p.	C_p/C_v.
100 ...	6·63	8·82	1·332	6·54	8·61	1·317
200 ...	6·17	8·23	1·334	6·11	8·14	1·332
300 ...	5·99	8·01	1·337	5·96	7·97	1·337
400 ...	5·98	7·98	1·335	5·96	7·96	1·336
500 ...	6·06	8·06	1·329	6·06	8·05	1·330
600 ...	6·31	8·30	1·316	6·31	8·30	1·316
700 ...	6·74	8·73	1·295	6·74	8·73	1·296
800 ...	7 18	9·17	1·277	7·18	9·17	1·277
900 ...	7 73	9·72	1·257	7·73	9·72	1·257
1000 ...	8·24	10·23	1·241	8·25	10·24	1·241

Fig. 4.

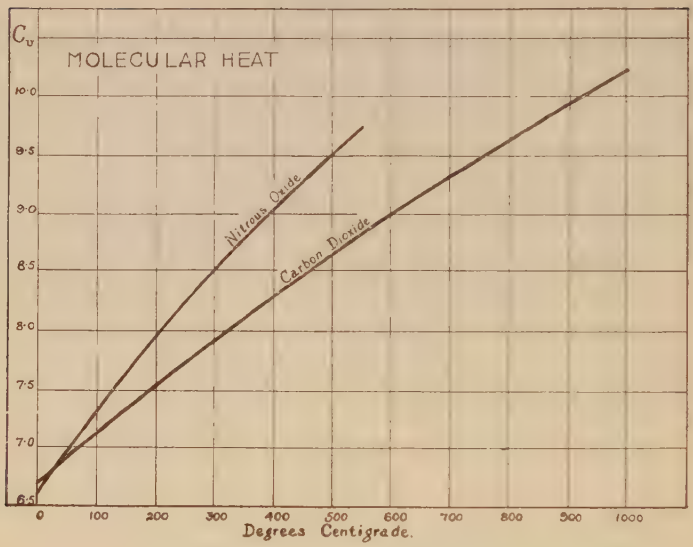

Fig. 5.

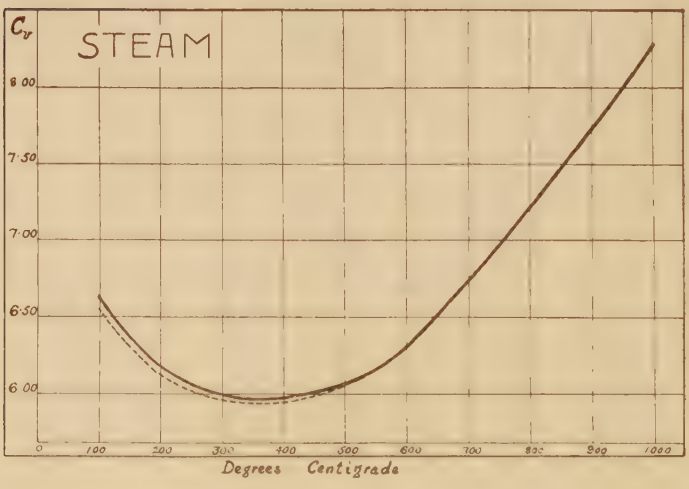

The results for the molecular heats are plotted graphically in figs. 4 and 5. In fig. 4 the results for carbon dioxide and nitrous oxide are plotted on the same scale. It will be seen

that the molecular heats of the two are equal only at room temperature. The temperature coefficient of the molecular heat of nitrous oxide is much greater than that of carbon dioxide. The peculiar results for steam, fig. 5, show a minimum at 365° C. and then increase normally from about 500° C. The minimum value occurs near the critical temperature for steam. The solid line of fig. 5 represents the values calculated by the use of Callendar's equation of state, whilst the broken line shows the results obtained when Berthelot's equation is employed. Above 500° C. the two equations yield almost the same results, the differences being confined to the temperature region in which steam by no means behaves as an ideal gas.

From the smoothed curves of figs. 4 and 5, the values of C_v and C_p given in Tables XIV. and XV. have been deduced.

TABLE XIV.

Molecular Heats at Constant Volume.

Temp. ° C.	Carbon dioxide.	Nitrous oxide	Steam †.
0	6·69	—	—
Room* ...	6·76	6·70	—
100	7·10	7·30	6·63
200	7·51	7·92	6·17
300	7·89	8·50	5·99
400	8·27	9·02	5·98
500	8·63	9·50	6·06
600	8·97	9·42	6·31
700	9·30	—	6·73
800	9·62	—	7·20
900	9·92	—	7·73
1000	10·21	—	8·24

* 15° C. for CO_2; 14·5° C. for N_2O.

† Using Callendar's equation of state.

They are tabulated only to two places of decimals although the actual results are probably correct to ± 3 in the third decimal place. Tables XVI. and XVII. give the empirical equations which reproduce the figures of Tables XIV. and XV.

Table XV.

Molecular Heats at Constant Pressure.

Temp. ° C.	Carbon dioxide.	Nitrous oxide.	Steam †.
0	8·74	—	—
Room * ...	8·80	8·75	—
100	9·12	9·31	8·82
200	9·51	9·92	8·23
300	9·89	10·49	8·01
400	10·26	11·01	7·98
500	10·62	11·49	8·06
600	10·96	11·41	8·30
700	11·29	—	8·72
800	11·61	—	9·19
900	11·91	—	9·72
1000	12·20	—	10·23

* 15° C. for CO_2; 14·5° C. for N_2O.
† Using Callendar's equation of state.

Table XVI.

Molecular Heats at Constant Volume.

Gas.	C_v in cals./gm. mole. at t° C.
Carbon dioxide...	$6{\cdot}688+0{\cdot}00423\,t-0{\cdot}0_6712\,t^2$
Nitrous oxide ...	$6{\cdot}629+0{\cdot}00694\,t-0{\cdot}0_5241\,t^2$
Steam.....	$7{\cdot}266-0{\cdot}00763\,t+0{\cdot}0_4{1261}\,t^2-0\,0_8401\,t^3$

Table XVII.

Molecular Heats at Constant Pressure.

Gas.	C_p in cals./gm. mole. at t° C.
Carbon dioxide...	$8{\cdot}708+0{\cdot}00415\,t-0{\cdot}0_6650\,t^2$
Nitrous oxide ...	$8{\cdot}659+0{\cdot}00677\,t-0{\cdot}0_5222\,t^2$
Steam	$9{\cdot}596-0{\cdot}00925\,t+0{\cdot}0_4148\,t^2-0{\cdot}0_6508\,t^3$

Note.—These equations should not be employed below 0° C. (or 100° C. in the case of steam) or above 1000° C.

Summary.

The molecular heats of carbon dioxide, nitrous oxide, and steam have been determined over a temperature range 0° to 1000° C. by a method depending on the measurement of the velocity of sound in the gases up to 1100° C. The dependence of the molecular heats on the temperature was found to be as represented by the equations given in Tables XVI. and XVII. Chemically pure gases only were employed.

In conclusion I wish to thank Professor J. R. Partington, M.B.E., D.Sc., for his supervision and suggestions throughout the course of the work. My thanks are due also to the Mines Research Board and the Department of Industrial and Scientific Research for maintenance grants and for funds with which most of the required apparatus was purchased.

This publication formed part of a Thesis approved for the Degree of Doctor of Science in the University of London.

Chemistry Department,
East London College,
University of London.

XXX. *A Note on the Connexion between Chemical Valency, Electron Grouping, and Crystal Structure.* *By* WILLIAM HUME-ROTHERY, *M.A., Ph.D.* *

IN a recent paper by Grimm and Sommerfeld † additional evidence is given in favour of the classification of electron sub-groups suggested by Stoner ‡ and Main Smith §. It is considered desirable to draw attention to certain points in connexion with the third section of this paper which deals with the crystal structure of elements and compounds. This is not done with any intention of criticising the Stoner-Main Smith classification, but rather to ensure that the latter shall be supported only by arguments which are entirely sound.

In the first place, the above authors point out that of the elements C, Si, Ge, Sn, and Pb which stand four places before an inert gas, all except Pb crystallize in the diamond type of lattice, in which each atom is surrounded tetrahedrally by four others. On the other hand, of the elements Ti, Zr, Ce, Hf, and Th occupying the other half of group IV, those hitherto examined all show the face-centred cubic

* Communicated by the Author.
† *Z. Physik*, xxxvi. pp. 36–59 (1926).
‡ Phil. Mag. xlviii. pp. 719–736 (1924).
§ Chem. and Industry, xlii. p. 1073 (1923).

structure. This is taken as confirming the Stoner classification, according to which all the elements C, Si, Ge, Sn, and Pb contain two complete sub-groups of two electrons each, and require an additional group of four electrons in order to reach the (2, 2, 4) grouping characteristic of the inert gases.

The facts of stereo-chemistry so clearly indicate the tetrahedral disposition of the four valencies of the carbon atom that, without making any assumptions as to the nature of the orbits of the shared electrons, it seems reasonable to suppose that the carbon atoms in the diamond lattice are joined together by forces closely resembling those which bind the atoms of a molecule together. This supposition is confirmed by the fact that the diamond is extremely hard, infusible below about 3000° C., and practically an absolute non-conductor of electricity *, this absence of conductivity being clearly due to the fact that the whole of the four valency electrons of each carbon atom are required to bind it to its four neighbours.

It may be noted that in the metallic form of carbon, graphite †, each carbon atom is joined similarly to three others only, forming a series of layers of hexagonal rings separated by a comparatively large distance. The fourth electron is thus left free to give the substance its metallic properties, and the binding of the different layers is presumably of a somewhat similar type to that found in metallic crystals and not yet understood.

Now, whilst it is true that the elements Si, Ge, and Sn all crystallize in the diamond type of lattice, their physical properties are entirely different. Apart from obvious differences in appearance and optical properties, they are fusible and are all conductors of electricity, the difference in this last property being of an absolutely different order of magnitude as compared with the diamond (diamond sp. resistance 10^{+14} ohms) ; silicon sp. resistance ca. 10^{-3} ohm). Without entering into any discussion of the part played by the electrons and atoms in the crystal lattices, it is clear that the electronic configuration in the diamond must be profoundly different from that in the metallic crystals of Si, Ge, and Sn, and that the mere similarity of the atomic lattices can not yet be regarded as indicating any particular electronic grouping. Whilst it may reasonably be hoped that our knowledge of atomic structure will eventually lead to an understanding of the way in which the elementary lattices

* Specific resistance ca. 10^{+14} ohms.

† Specific resistance $2{\cdot}9\times10^{-3}$ ohm.

are built up, the subject at present is full of apparent contradictions and anomalies. Thus the face-centred cubic lattice is formed by the elements copper, silver, and gold, in which the chemical, physical, and spectroscopic evidence all lead to the conclusion that the atoms are univalent and each give one free valency electron. The same type of lattice is, however, formed by the admittedly divalent calcium, and the non-valent argon. These and many similar examples all appear to indicate that the same *atomic* configuration can be produced by more than one method of binding together of the atoms, or by more than one electronic configuration, and for the present at any rate we cannot justifiably use the fact of similar space lattices being formed by different elements as indicating anything in the way of similar electronic structure.

The second point dealt with by the above authors is the formation of the diamond or wurtzite types of structure by the compounds CSi, BN, AlN, BeO, ZnO, ZnS, ZnSe, CdS, HgS, and the elements C and Si, whereas the simple halides of the alkali metals, and the oxides and sulphides of magnesium and the alkaline earth metals give the sodium-chloride or cæsium-chloride types of structure. In the case of the first two short periods, this is considered as indicating that all of the elements and compounds C, CSi, Si, BN, AlN, and BeO are non-polar compounds (or elements) in the solid state, and that the atoms are held together in the solid in the same way as the atoms of carbon in the diamond lattice. This is regarded as confirmed by X-ray evidence that the compounds are not ionized in the solid state. The compound AlN is then regarded as one in which the nitrogen atom has given one electron to the aluminium atom, thus giving four electrons to each atom and enabling the atoms to bind themselves together in the same way as the carbon atoms in the diamond. On the same grounds we must presumably look at the beryllium atom in BeO as having gained two electrons from the oxygen atom, thus again giving four electrons to each atom and so enabling the tetrahedral arrangement to be formed.

The evidence that the compounds BN, AlN, CSi and BeO, are non-polar in the solid state is based upon the intensities of the X-ray reflexions from the different crystal faces. The general principle is that the intensities of reflexion are proportional to the numbers of electrons associated with each atom, and that by measuring the relative intensities of

reflexions from planes containing both kinds of atoms, and from planes consisting alternately of one kind or the other, it is possible to estimate the number of electrons associated with each atom. The subject is, however, complex and the greatest care is necessary in the interpretation of the results*. While it is undoubtedly wrong to ignore the evidence, it is unwise to place too much reliance on evidence of this nature, especially where the crystal structure has been determined by the ordinary methods without the special precautions which are necessary if the relative intensities are to be interpreted accurately †. But if the matter is complex in the case of simple ionized compounds in which each electron can be regarded as belonging wholly to one particular atom, it is clearly even more complicated in the case of structures such as that of the diamond in which some electrons are associated with two atoms, and it is doubtful whether we can at present accept evidence of this sort as conclusive.

Even, however, if we assume that the intensities of reflexion do indicate neutral atoms in the crystals of AlN and BeO, it can be shown that the above authors' conclusions do not necessarily follow. In a simple polar compound such as NaCl, the atoms are almost certainly present as ions; each chlorine and sodium ion is surrounded by 18 and 10 electrons respectively and no electrons are held in common. In the case of the diamond the condition is different. Each neutral carbon atom has four valency electrons and is completing its octet by sharing with four others. It does not, however, thereby gain a negative charge, since for each share in the electron which a particular carbon atom gains from one of its neighbours, it loses a corresponding share in one of its own electrons. The atom as a whole remains neutral in agreement with X-ray evidence as far as the latter can be trusted.

This applies to the crystals of C and CSi ‡. It does not, however, apply to the crystals of AlN and BeO as formulated by the above authors. If we write the formula as $Al^{+}N^{-}$ and then imagine that sharing of electrons takes place as in

* See Darwin, Phil. Mag. May 1922.

† In this connexion the chapter on "Intensity of X-Ray Reflexion" in W. H. and W. L. Bragg's book on 'X-Rays and Crystal Structure' may be read with interest. The curves in fig. 76, p. 224, will show how very speculative is the extrapolation to the value $\theta = 0°$ corresponding to the number of electrons in the atom. The same chapter will show that the attempts to divide electrons into shells are even more speculative.

‡ The case of silicon is more complex on account of the electrical conductivity.

the diamond lattice, we shall have a negative Al^- ion and a positive N^+ ion, since it is assumed that in the sharing of electrons in the diamond lattice an individual atom gains just as much as it loses. Even if the difference in nuclear charges prevents a shared electron from being *equally* shared by the two atoms, the conclusion is inevitable that the aluminium atom must acquire some kind of negative charge, even if not that of a whole electron, in order that the compound AlN may resemble the diamond or carborundum CSi, in the solid state. If beryllium oxide is regarded as $Be^{--}O^{++}$, the same objection applies with even greater force. The above authors' suggestions are therefore definitely not in agreement with a structure of neutral atoms, but require negatively charged Be or Al atoms and positively charged N or O. Even, therefore, if we accept the X-ray evidence as indicating a structure of neutral atoms, it cannot be regarded as in agreement with the above authors' theory.

It is doubtful whether BeO is really to be regarded as so abnormal, since its heat of formation is of the same order of magnitude as that of barium oxide, which is a typical ionized oxide forming the NaCl type of lattice. The formation of the different types of lattices may be due to the fact that in MgO, SrO and BaO the constituent Mg^{++}, Sr^{++}, and Ba^{++} ions have an outer group of (2, 2, 4) electrons, whilst the Be^{++} ion would have a group of (2) only, as a result of which the symmetry of its field of force might well be different, and this together with the small size of the Be^{++} ion might account for the formation of different kinds of lattices. It is also possible that too much importance may be ascribed to the occurrence of tetrahedral arrangement in crystals, since the conditions of repetition through space so greatly restrict the possible numbers of atoms of one kind surrounding those of another, that in simple structures 4's, 6's, 8's and 12's are almost inevitable.

The author wishes to express his thanks to Dr. N. V. Sidgwick, F.R.S., for his kind interest in this note.

Magdalen College, Oxford.
June 1926.

XXXI. *The "Hetero-Normal" Current-density Effect.* By William Stephenson, *M.Sc., College Fellow, Armstrong College, Newcastle-on-Tyne* *.

Introduction.

PHENOMENAL deviations from the ordinary properties of the glow discharge in gases at pressures of the order 10 to 0·1 mm. Hg. have previously been noticed by many workers. Paschen [1] employed an exceptionally bright negative glow obtained inside a box-shaped cathode in early spectrographic work; Hermann Schuler [2] has recently described experiments in which it was shown that under suitable conditions glow discharges pass more readily to the inside of a hollow cylindrical cathode which has its ends closed, there being only a small hole (1 to 4 mm. diameter) drilled in one of these ends. In earlier work with hollow cylindrical cathodes, Schuler [3] found decreases in the "normal cathode fall of potential" of glow discharges to the inside of the cathodes, and Aston [4], in his paper on discharge between co-axial cylinders, noticed an unusual decrease in the cathode fall of potential of the glow discharge to a concave cathode surface. Recently, Hufford [5], in work on the discharge of electricity between parallel equipotential plates, reports several peculiarities in the voltage and current characteristics of the glow discharge. All these interesting deviations in cathode fall and current density can be ascribed to the "hetero-normal" effect, upon which I was led to work by experiments on the effect of the shape of the cathode on the glow discharge. The name "hetero-normal" was given to a current increasing and cathode fall of potential decreasing effect described in my recent paper [6] in the Philosophical Magazine, and a continuation of this work is the subject of the present paper.

The recent paper was of an introductory nature, and was concerned chiefly with experimental examples of current increases which were ascribed to the "hetero-normal" effect, rather than with an exposition of the "hetero-normal" effect in its simplest terms, for the simplest experimental conditions: the introductory paper, however, together with the present work, should make clear the following statement of the experimental facts:—

(1) "Overlapping" of the Crookes's Dark Spaces (C.D.S.) or negative glows of two opposing cathode surfaces results in current-density increases.

* Communicated by Prof. Geo. W. Todd, M.A., D.Sc.

(2) The increased current density passes at a cathode fall of potential at most equal to, and generally less than, the "ordinary" cathode fall of potential for the discharge free from "overlapping."

(3) If "overlapping" of strictly "normal current density" glows is effected, the current density increases are carried by a constant ordinary "normal cathode fall of potential," or by a cathode fall which is less than the ordinary "normal" one.

(4) In the first place, "hetero-normal" was the name given to the various "normal" current densities obtained at opposing cathode surfaces for various distances apart of the opposing cathode surfaces. The "hetero-normal" glows are "normal" in the sense that, for a particular distance apart of two opposing cathode surfaces, a minimum current density is carried at a constant minimum cathode fall of potential.

The Empirical Laws of the Glow Discharge.

It will be convenient, for future reference as well as for the present purpose, to state here what I imply by the "ordinary" properties of the glow-discharge phenomena at the cathode, in gases at pressures of the order 10 to 0·1 mm. Hg. The glow discharges here considered are self-maintained, steady, and have the negative glow, Crookes's dark space, and cathode-glow phenomena, but the anode and cathode are sufficiently near each other to avoid positive column glows. The voltage across the discharge-tube terminals never exceeds 600 or 700 volts. Under these experimental conditions the following empirical relations obtain for discharge (free from "wall" effects) between a plane anode and cathode.

I. When the full cathode area is not utilized in the discharge:

(*a*) The current density to the cathode surface remains at a constant value at a particular pressure, no matter what the total current through the discharge-tube, and the relation

$$i_n/p^2 = \mathrm{G} \quad . \quad . \quad . \quad . \quad . \quad . \quad . \quad (1)$$

connects the "normal current density" i_n, and the gas-pressure p, where G is a constant for a particular gas and electrode material.

(*b*) The potential difference between the cathode and a region near the boundary of the C.D.S. and the negative glow remains constant, at the "normal cathode fall of potential."

(*c*) The thickness of the C.D.S. remains constant at a particular pressure, for all current values, and the relation

$$p \,.\, d_n^2 \,. = \mathrm{F} \quad . \quad . \quad . \quad . \quad . \quad . \quad . \quad (2)$$

connects the "normal thickness of the C.D.S." d_n, and the gas-pressure, where F is a constant for a particular gas and electrode material.

II. When the full cathode area is utilized in discharge, the glow discharges are then "abnormal," and

(*d*) the equation

$$i_a = \frac{1}{k}(\mathrm{V} - \mathrm{V}_n) \quad . \quad . \quad . \quad . \quad . \quad . \quad . \quad (3)$$

gives, approximately, the relation between the "abnormal current density" i_a and the voltage V across the discharge-tube terminals, where $1/k$ is termed the "conductance" (constant for a particular gas and gas-pressure), and V_n is a constant voltage almost equal to the "normal cathode fall of potential" in the same discharge-tube. Over a wider range of current values, the equation given by Aston [7],

$$\mathrm{V} = \mathrm{E} + \frac{\mathrm{F}\sqrt{i_a}}{p}, \quad . \quad . \quad . \quad . \quad . \quad . \quad . \quad (4)$$

expresses the same experimental result, that any increase of current density above the "normal" value for the given pressure is accompanied by a corresponding increase in the cathode fall of potential.

(*e*) The relation between the "abnormal thickness of the C.D.S." d_a and the "abnormal current density" is given by Aston's equation [7],

$$d_a = \frac{\mathrm{A}}{p} + \frac{\mathrm{B}}{\sqrt{i_a}} \quad . \quad . \quad . \quad . \quad . \quad . \quad (5)$$

It will be seen, on referring to my first paper, that an examination of the hetero-glows was made there, in terms of the equations (1) to (5). It was shown that the hetero-glows do not follow equations (1), (2), and (4), but that for "hetero-normal" conditions equation (5) is obeyed, *i. e.* for a constant or nearly constant cathode fall of potential the relation between the hetero-normal C.D.S. thickness (d_h) and the hetero-normal current density (i_h) is

$$d_h = \mathrm{B}/\sqrt{i_h}. \quad . \quad . \quad . \quad . \quad . \quad . \quad (5a)$$

This process of examination of the hetero-glows in terms of the above equations is to be continued in the present paper, and, in particular, equation (3) is to receive consideration.

The Relation i_n/p^2.

A discharge-tube (K) was made according to the following specifications:—B and C are parallel opposing cathode surfaces, aluminium plates, each 6·5 cm. in diameter. C is fixed, but the height of B above C is adjusted by means of a glass tap and a suspension thread, as in fig. 4 in my first paper [6]. B and C are turned from the same sheet of aluminium, 2 mm. thick, and their backs are covered with mica plate so that discharge is confined to the two opposing cathode surfaces. A large aluminium wire spiral, 3-mm. diameter wire, 4 turns in the spiral, each 14 cm. diameter, is co-axial with B and C, and serves as the anode. Thus, except for the material of which the electrodes were made, their sizes, and the shape of the anode, the discharge-tube (K) is the same in form as that shown in fig. 4 in the earlier paper.

In the following experiment, discharge was passed in dry hydrogen and, for purposes of comparison, in dry air. "*Normal*" currents were taken over a wide range of pressures with the surfaces B and C at constant distances: 0·57, 0·78, 1·15, 1·4, and 1·8 cm. apart. "*Normal*" in this case, it will be remembered from the previous paper, has a rather special meaning, it being the value of the current through the discharge-tube when the available cathode surface is just completely utilized in the glow discharge, the currents so obtained then being always proportional to the "normal current density," since the same cathode area is utilized in every case.

Fig. 1 shows graphed results for one series of experiments. The "*normal*" current is plotted against the gas-pressure for the particular values of the distance (D) apart of the cathode surfaces B and C. For general purposes of comparison, two series of results are given in fig. 1: (*a*) for air, and (*b*) for a hydrogen-air mixture. Curve ABC, fig. 1, is theoretical, having the equation

$$i_n/p^2 = 0{\cdot}036, \quad . \quad . \quad . \quad . \quad . \quad (1\,a)$$

the current units being the arbitrary ones used for the experimental curves. It is seen that the relation (1) is obeyed for each value of D for all pressures greater than a definite minimum, and that for these values of D the part AB of the curve ABC is common to all (this result extends to higher pressures than those shown in fig. 1). Equation (1 *a*) is the experimental expression of the general equation (1). Curves deviating from ABC represent hetero-glows, *i.e.* "hetero-normal" currents at the particular pressures.

Table I. shows the maximum pressures at which the hetero-effect appears for the various values of D, as obtained from the results shown in fig. 1, assuming ABC to be the ordinary curve of "normal current density" values. The relation

Fig. 1.

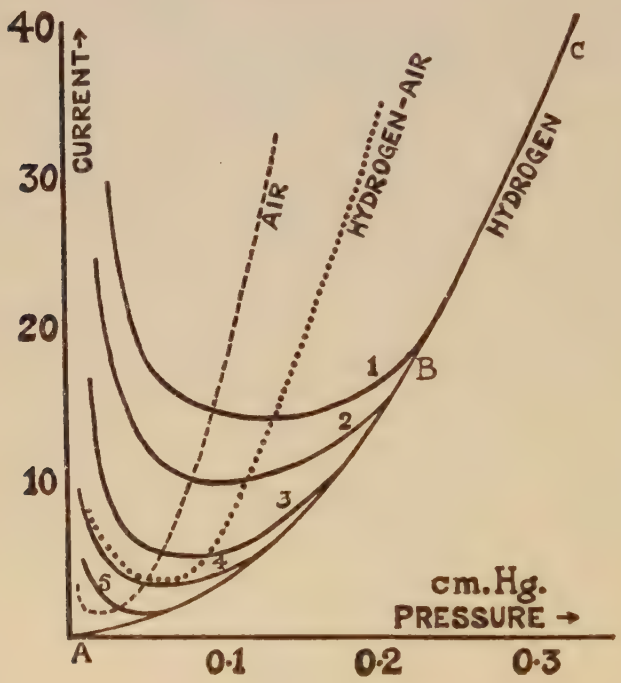

Table I.

D cm.	Pressure at which current increases begin.
1·8	$6{\cdot}5\times10^{-1}$ mm. Hg.
1·4	10
1·15	15·5
0·78	20
0·57	22

between D and these maximum pressures is nearly linear. Now, it was found in the case of discharge in air, with brass electrodes, that when $d_n = 0{\cdot}44$ D the hetero-normal effect was first observed, and if a similar simple relation between d_n and D is to obtain in the case of the results shown in Table I., it follows by substitution in this equation of the pressure relation (2) above that the results in Table I. should

conform to an equation of the type $D\sqrt{p} = \text{const.}$ Since in Table I. the relation between D and the maximum pressures is found to be linear, it follows that a relation of the type $d_n = k$. D is not to be obtained for the discharge in hydrogen. The results in Table I. suggest that the hetero-effect is obtained when the negative glows of two opposing cathode surfaces "overlap," and not necessarily only when the assumed "normal" values of the C.D.S. thicknesses "overlap."

In the early experiments with the small brass electrodes and the small "normal" currents, narrow negative glows were obtained in the case of discharge in air, and the "overlapping" of the negative glow did not appear to affect the current densities to any measurable extent. Under suitable conditions the length of the negative glow, at a particular pressure, is longer the greater the current density through the discharge-tube; and it follows that the hetero-effect should be obtained for "abnormal" currents when D is much greater than that demanded by the equation

$$d_n = 0{\cdot}5\ \text{D}, \quad . \quad . \quad . \quad . \quad . \quad . \quad (6)$$

which is a theoretical equation expressing the assumption that the current increases of the hetero-effect result when the thickness of the C.D.S. is equal to half the distance between the opposing cathode surfaces, *i. e.* that the current increases occur when "overlapping" of the C.D.Ss. is possible. Again, assuming that "overlapping" of opposing negative glows in discharge-tubes such as are used in these experiments results in current density increases, it is understood why the current increases obtained in the case of discharge in air occurred at the values of D given by $d_n = 0{\cdot}44$ D, instead of at values of D given by equation (6). The "overlapping" of negative glows as a factor contributing to the hetero-effect, and the dependence of the hetero-effect on the total current passing through the discharge-tube, are evinced in the following experiments.

The Hetero-effect for various Current Densities in the Discharge-tube.

A discharge-tube of the type shown in fig. 2 is best suited to the present experiments, partly because of the accentuation of the negative glows obtained in narrow vessels, and partly because I wish to refer, later, to work done by Hufford [5] on the discharge between equipotential plates in discharge-tubes having the electrodes bounded by the glass walls of the

containing vessel, as are B and C in fig. 2. The cathode surfaces B and C were 3·1 cm. in diameter, and were turned from the same plate of aluminium. The height of B above C could be varied between 0 to 12 cm., and discharge was confined to the two opposing surfaces B and C. In the following experiments discharge was passed in an argon-nitrogen mixture, got from a filament-damaged, gas-filled, electric lamp, so that the current range could be as large as possible with the batteries at my command, because of the low " normal cathode fall of potential " of this gas mixture.

Fig. 2.

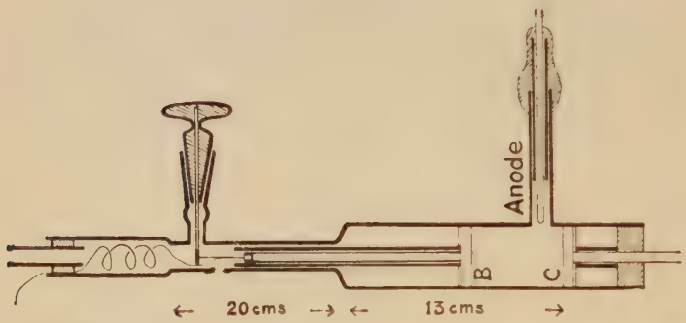

Fig. 3 shows a series of results taken in the following way. The pressure was constant (at 0·2 mm. Hg.), and the current through the discharge-tube was first adjusted so as to be nearly " *normal* " when both B and C were used together as the cathode, B being at the maximum distance, 12 cm. above C, and both B and C were utilized completely in the discharge. The circuit conditions were then left untouched throughout, whilst B was lowered and the current through the discharge-tube was read, together with the voltage across the terminals of the tube, for various values of the height of B above C (D cm.). Sufficient time was allowed between readings to avoid temporary pressure variations due to the movement of B. Curve (*a*), fig. 3, was obtained in this way. It is seen that the current through the tube is the same for all values of D greater than about 3·5 cm., and that at this value of D a current increase begins. At D = 1·5 cm. the cathode surfaces are just completely utilized in the discharge. At smaller values of D the total current through the tube remains the same, at 6 units, but the area of opposing cathodes used in the discharge becomes less and less with decrease in D, until finally a discharge ceases to pass between the surfaces B and C. The current density is thus rapidly increasing as D is made smaller and smaller. This process was repeated

for several initial "ordinary" values of the current at D = 12 cm., and typical results are shown in the curves (*b*) to (*e*) of fig. 3, the initial currents being 6·5, 13·5, 19, and 28 units respectively. In every case the voltage across the discharge-tube remained constant, or decreased with decrease in D, for the currents shown in the curves.

Fig. 3.—$p = 0{\cdot}2$ mm. Hg.

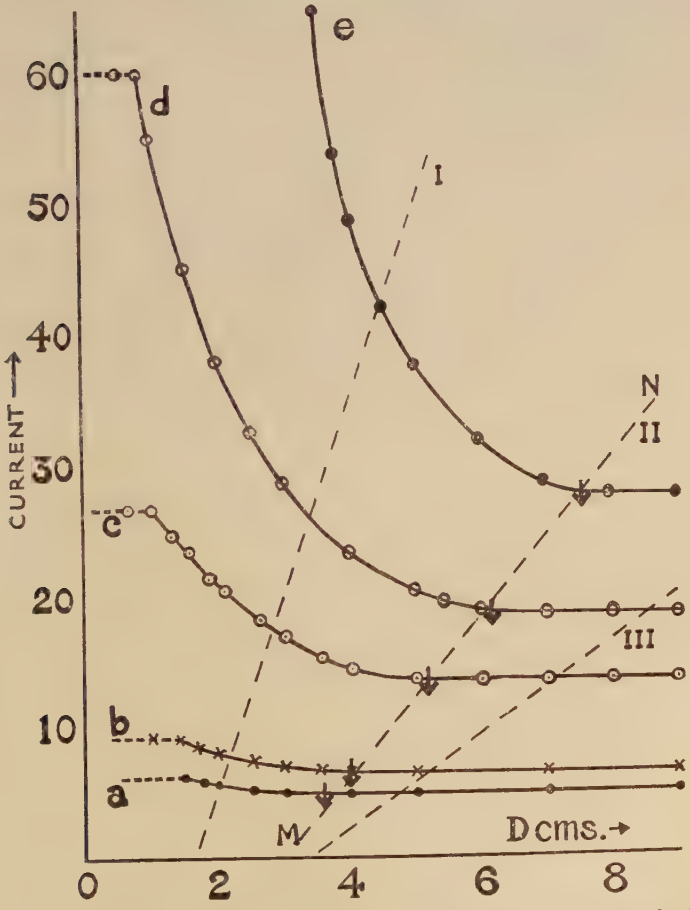

The current increases occur at the values of D marked with an inverted arrow in fig. 3. The relation between "ordinary" current and these arrowed D values is linear, and the increases in current begin at higher values of D the greater the value of the initial current, as is shown by the line MN in fig. 3.

Now, the thickness of the C.D.S. is greater the smaller the total current through the discharge-tube at a particular pressure : hence, were "overlapping" of the C.D.Ss. the only factor conditioning the current increases, these increases would be expected at greater values of D for the lower initial currents ; *i. e.*, in fig. 3 the arrows would occur at the maximum D for curve (*a*), and the minimum D for curve (*e*), and the line drawn like MN would slope in the opposite direction to MN of fig. 3. Further, lines drawn through the turning-points in the way MN is obtained slope increasingly towards the D-axis the smaller the gas-pressure is in the tube. This is indicated in fig. 3, where the lines I, II, and III are MN lines for the pressures 0·06, 0·02, and 0·01 cm. Hg. respectively. It is seen that the greater the pressure the more nearly the lines tend towards becoming what would be expected if "overlapping" of the C.D.Ss. alone determined the current increases. Since the negative glow is relatively narrower in such tubes the greater the gas-pressure (at 10 mm. Hg. the negative glow is merely a thin film of glow covering the cathode surfaces, whilst at 0·1 mm. Hg. the entire vessel is filled with negative glow), this effect is to be expected if "overlapping" of the negative glows leads to the current increases.

It is interesting to notice the following experimental facts :—

(i.) The current increases shown in fig. 3 are attended by a decrease in the voltage across the discharge-tube, below that for the initial condition when B was 12 cm. above C, except when the initial voltage was nearly "normal" (curve (*a*)), in which case the voltage remained constant for all values of D.

(ii.) When B alone was used as cathode, A being the anode as before, the current and voltage remain constant for all values of D, at a particular pressure, over the pressure range experimented upon.

(iii.) For the "ordinary" currents, represented by the horizontal parts of the curves (*a*) to (*e*) in fig. 3, the negative glows do not overlap. There is a dark space (ordinarily the Faraday space) dividing the two negative glows of the cathode surfaces B and C.

(iv.) When the current increases are obtained, the negative glows overlap, and there is a continuous band of negative glow between the boundaries of the C.D.Ss. and the glow nearest to B and C. For the larger D values this band of negative glow is brightest near the C.D.S. boundaries, but at the smaller values of D the band is of uniform brightness, so far as it is possible to see.

Variation of the "Normal" Current with change of D, *at Constant Pressure.*

It will be seen on referring to the early work with discharge in air, that the best illustration of the current increasing effect is shown when, at constant pressure, for various values of D, the "*normal*" current is measured (*i.e.*, the current through the discharge-tube when the available cathode surface is just completely utilized in the discharge). Using the discharge-tube (K) above, the same method was employed for discharge in hydrogen, nitrogen, and argon-nitrogen mixture, and in every case the same current-increasing effect was found. Thus, for the argon-nitrogen mixture, at $p = 0{\cdot}047$ cm. Hg., the results shown in Table II. were

TABLE II

D cm.	*i*n in arbitrary units.	V volts.
3	7·0	295
2	7·0	295
1·5	9·5	293
1·25	14	285
1	26·5	282
0·83	38	285
0·75	62	290
0·63	135	310
0·5	220	312
0·4	520	315
0·3	1400	325
0·2	off amm. scale.	335

obtained. The extremely large current density increases (a thousand times "normal" under suitable conditions, the restriction to these high densities in my experiments being merely lack of suitable batteries and heating effects) are obtained *without a corresponding rise in the cathode fall of potential.* The increase of 30–40 volts shown in Table II. between D = 3 cm. and D = 0·3 cm. is insignificant compared with the current increase from 7 to 1400 units over the same range: the "abnormal" cathode fall of potential for a current of 1400 under similar circumstances would be more than 1000 volts. The small increase of about 40 volts is most probably due to heating of the gas in the discharge-tube, because of the large current densities carried by the gas. This current-increasing phenomenon should have technical applications; for instance, the efficiency and usefulness of glow-discharge rectifying devices should be greatly

enhanced, as should be the well-known "Osglim" neon lamps.

In discharge in air[6] the hetero-glows were characterized by these large current density increases, and a decrease in the "normal cathode fall of potential" of about 20 volts, the "hetero-normal" cathode fall of potential being about 20 volts less than the "ordinary" "normal cathode fall of potential." It will be remembered that the decrease of 20 volts was observed over the whole range of pressures experimented upon. Experiments were made with the discharge-tube (K) used in the above experiments, series of "*normal*" currents being taken, as was done for Table II., in well-dried argon-nitrogen mixture, over the pressure range 0·3 to 0·03 cm. Hg. The "normal" voltage across the discharge-tube was constant over this range at 232 volts. *In no case was a decrease below this value obtained.* In all cases the minimum voltage across the discharge-tube terminals, when the discharge was strictly "hetero-normal," was the same as the "normal" value, 232 volts. This important result suggests that the current increases have their explanation, in this instance, in an increase in the "conductance" of the gas for a constant "normal cathode fall of potential." The decreases in the "normal cathode fall" were obtained for discharge in hydrogen. Thus it appears that the hetero-glows are not invariably attended by a decrease in the "normal cathode fall of potential," and that a fundamental change in the current mechanism results in the large current density increases, whilst any decrease in the "normal cathode fall," of course, enhances the current increases. This result is considered more fully in the experiments now to be described.

Volt-ampere Characteristics of the Hetero-glows.

A probe method of measurement of the "normal cathode fall of potential," whilst being the direct method, is attended by a difficulty that makes the method not easy to use in the case of the parallel cathode plates type of discharge-tube that is the subject of this research. Already the discharge-tube has to be made with means for varying the distance of one cathode surface from the other, and to construct a tube with the second adjustment device that the probe demands is no easy matter. Two indirect methods, however, can be used for determining the cathode falls and differences in cathode falls. The first was that used in the early work with air. It was assumed that the anode conditions remained constant

over the pressure range experimented upon, and the cathode fall of potential differences were given, under the particular comparable conditions, by the differences in the voltages across the discharge-tube under these conditions. The second method makes use of the empirical volt-ampere characteristics of the form given in equation (3) above. The current through the tube, and the voltage V across it, are measured for various "abnormal" values of the current, and from the graphed results, when the straight line connecting voltage and current is produced so as to meet the voltage axis, the intercept of voltage gives V_n (equation (3)), *i. e.* when $i_a = 0$, $V = V_n$. The intercept V_n is nearly equal to the "normal cathode fall of potential." Experiments showed that the decreases in cathode fall of potential obtained by the first method agreed excellently with those obtained from the volt-ampere characteristics, under the same experimental conditions. The volt-ampere characteristics were taken in the following experiments because, besides giving the required voltage decreases (if any were to be obtained), they also throw light on the current mechanism of the hetero-glows. Ryde, Taylor[8], and others have shown that equation (3) expresses the conditions in a low-tension discharge-tube with a fair degree of completeness, for currents not too strongly "abnormal," and for discharges that are free from positive column and anode complications. The discharges in the following experiments confirmed to that equation, and it is the purpose of the next experiments to show in what degree the current increases of the hetero-glows are due to the decrease in V_n, or due to a change in the "conductance," $1/k$, or due to a combination of the two effects.

Volt-ampere Characteristics in Hydrogen.

The discharge-tube with small brass electrodes * was used in these experiments. Discharge-tubes of the same design were made, of copper and aluminium, with large cathode plates, but limitations in the current supply restricted their use to a very small pressure range. With the small brass electrodes it was possible to take suitable volt-ampere characteristics over the pressures 0·3 to 0·03 cm. Hg. for discharge in hydrogen. The characteristics were taken in the following way. With a constant voltage supply, current through the discharge-tube was varied by means of non-inductive resistances placed in series with the discharge-tube and the

* See (6) p. 565.

batteries. A Kelvin multicellular electrostatic voltmeter was shunted across the terminals of the discharge-tube, and

Fig. 4.—$p = 2{\cdot}8$ mm. Hg.

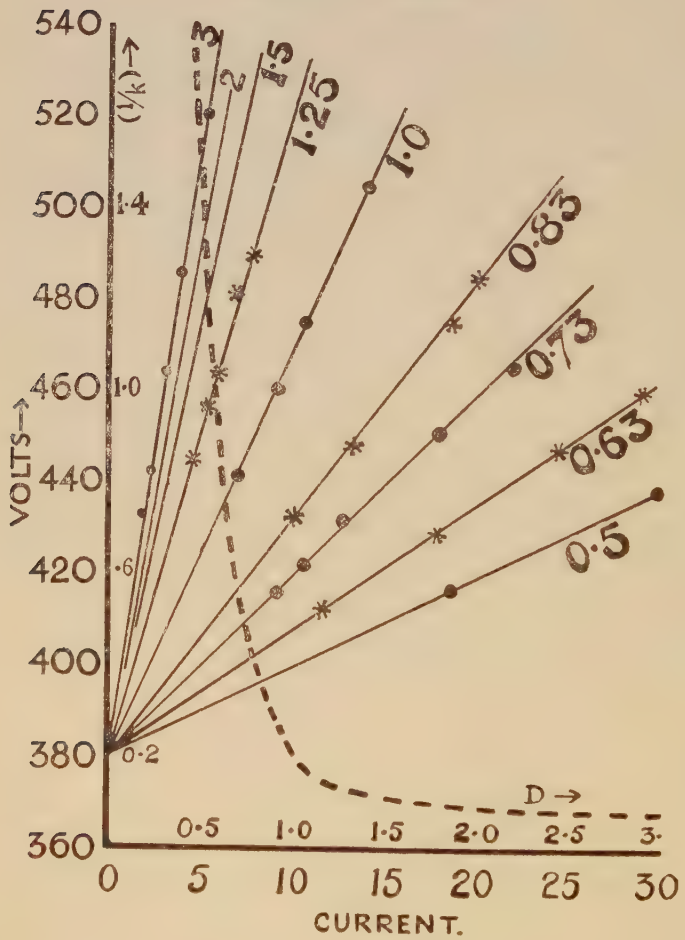

current was measured on a "Cambridge" uni-pivot galvanometer, provided with suitable shunts. In every case the "*normal*" discharge was first obtained, and the readings of current and voltage were taken for increasing values of the current through the discharge-tube. It is well known that

the characteristics obtained in this way differ slightly from those obtained for decreasing values of the current.

At a particular pressure, volt-ampere characteristics were taken in this way for various constant values of the distance D between the opposing cathode surfaces. Figs. 4 and 5

Fig. 5.—$p = 0{\cdot}4$ mm. Hg.

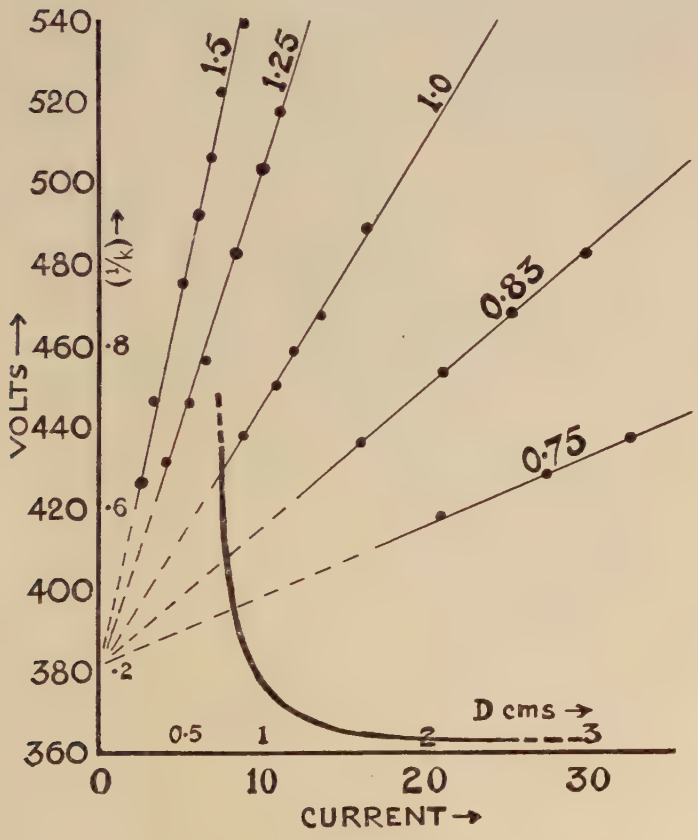

show representative results at pressures 0·28 and 0·04 cm. Hg. respectively. Similar results were obtained over the whole range of pressures and D values experimented upon. The curves show a complete change in "conductance," and the intercept V_n is constant.

A decrease in V_n may occur, however, along with a change

in the "conductance." Fig. 6 shows such experimental results. These changes in V_n at the lower D values occurred more readily when fresh supplies of gas were used, and for well-dried hydrogen and a thoroughly "run-in" tube a constant V_n was obtained, with all the current variations attributable to changes in the "conductance."

Fig. 6.—$p = 2{\cdot}12$ mm. Hg.

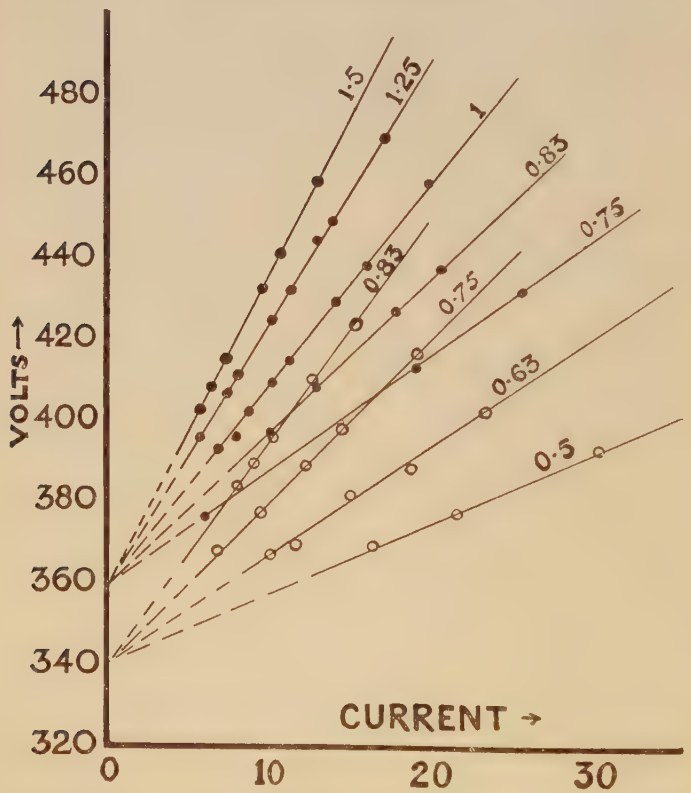

Using hollow cylindrical cathodes, obviously under conditions productive of hetero-glows, variations in the "normal cathode fall of potential" have been obtained by Schuler [3], who gives experiments in support of his theory that the "normal cathode fall" is a function of the ionization potential of the gas and the mean free path of the electron in the gas. I refrain from considering my experimental results for the potential differences until confirmatory evidence has been obtained by direct potential measurements.

Figs. 4 (*a*) and 5 (*a*) show the values of the "conductance" of the volt-ampere characteristics of figs. 4 and 5 respectively. As D is made small the "conductance" increases, at first slowly, and then extremely rapidly. From a large number of volt-ampere characteristics over wide D and pressure ranges, the result is confirmed that the current increases begin when the distance apart of the two opposing cathode surfaces is several times greater than the C.D.S. thicknesses obtaining under the given conditions.

The characteristics for one electrode (B) alone used in the discharge, the other (C) remaining insulated, are always the same, or of slightly smaller "conductance" for the smaller D values, for all distances of B above the insulated surface C, at a particular pressure.

Volt-ampere Characteristics for Discharge in Argon-nitrogen Mixture.

From a large number of characteristics, taken in the way described above for hydrogen, it was shown that, over the pressure range 5 to 0·1 mm. Hg. experimented upon :—

(*a*) The voltage V_n was constant at all pressures for all values of D. There appeared to be no decrease in the "normal cathode fall of potential."

(*b*) The hetero-glows were the result of a change in the "conductance" of the gas, of the same nature as that shown in figs. 5 (*a*) and 4 (*a*).

The Voltage Variations.

(i.) *For "Hetero-normal" Current Densities.*

Under the "normal" current density conditions of the hetero-glows the voltage across the discharge-tube terminals is nearly constant for all values of the distance D between the cathode surfaces, whilst the "normal" current density itself may be increased a few hundredfolds (see Table II.). This, I think, is a remarkable result, and it will be interesting to see how the various theories of the cathode fall of potential apply to the "hetero-normal" glows.

(ii.) *For "Abnormal" Hetero-glows.*

The volt-ampere characteristics above (figs. 4, 5, and 6) show the nature of the voltage variations for "abnormal" hetero-glows. For a particular current density the voltage rapidly diminishes as D is made smaller, the remaining variable being the C.D.S. thickness. Fig. 3 will afford a specific example.

Curves (*b*) to (*e*) of fig. 3 are for "abnormal" heteroglows over all parts of the curves except where the curves are horizontal. At the same time as the readings were made of current and D distances, readings were made of the voltage across the discharge-tube, and the thicknesses of the C.D.S. to each cathode surface (the values to each were always equal). Let us first consider the curve (*c*). Between D = 5 cm. and D = 8 cm. the voltage across the tube was constant at an "abnormal" value, 294 volts: the C.D.S. thickness and the current density were also constant. Over the range D = 5 to D = 1 cm. the current increases steadily from 13·5 to 27 units for decrease in D: at the same time the voltage steadily diminishes from 294 to 232 volts, while the C.D.S thickness also decreases. At D = 1 cm. the discharge is "hetero-normal," the voltage remains at 232 volts, and the current through the tube is such that the whole opposing cathode area is just completely utilized in the discharge. For smaller values of D the voltage remains at 232 and the total current at 27 units, but the area taken up by the discharge rapidly diminishes, and the current density correspondingly rapidly increases, as D is made smaller and smaller, the C.D.S. thickness meanwhile also decreasing. The same sequence of phenomena is observed for each curve of fig. 3: the voltage decreases from 330 to 232 in curve (*d*), and the current increases from 19 to 60 units; and decreased from 376 to 232 volts in curve (*e*) as the current increased from 28 to 250 of the same current units. In the latter case the C.D.S. decreased from 6 mm. to less than 3 mm. as the current increased from 28 to 250.

Aston's equation (4) above does not hold for the "hetero-abnormal" glows as obtained in the above experiment, and the generally-accepted law that current density increases are accompanied by increases in the cathode fall of potential is not true in the case of the above current density increases. Obviously, however, this result is not surprising, since for different distances D apart of the opposing cathode surfaces at which "overlapping" of the negative glow is effected the discharge-tube has different "conductances." This method of effecting changes in the "conductance" of a discharge-tube would seem to promise important results when applied to the experimental investigation of the various theories of the cathode fall of potential, and perhaps it will be instructive to consider the adaption of the "hetero-normal" measurements to the most important theories of the cathode fall of potential.

There are four glow-discharge variables—the current density, the cathode fall of potential, the C.D.S. thickness, and the gas-pressure, and two important theories have been given to connect these variables. Sir J. J. Thomson proposed that the product

$$\frac{i \cdot d^3 \cdot p \cdot}{V^2} = B, \quad . \quad . \quad . \quad . \quad . \quad . \quad (7)$$

where B is constant for any one gas, and this result was fairly well confirmed for large current densities by Aston [7]. Gunther-Schulze [9] and Ryde [10], however, have proposed that

$$\frac{i \cdot d^2}{V^{3/2}} = C, \quad . \quad . \quad . \quad . \quad . \quad (8)$$

this equation being the space-charge equation

$$\frac{i \cdot d^2}{V^{3/2}} = \frac{A}{9\pi} \cdot \sqrt{\frac{2e}{M}} \cdot \quad . \quad . \quad . \quad . \quad . \quad (9)$$

This latter theory is no doubt very extreme, and Aston [11] cannot admit that it gives even the semblance of an explanation of the conditions in the glow discharge at the cathode: and yet it leads to unexpectedly good agreement with experimental results.

Now, the "hetero-normal" current density, and the "hetero-normal" C.D.S. thickness, are very strictly in agreement with equation 5 (*a*) above. Thus the "*normal*" currents of the hetero-glows were obtained over the pressure range 1 to 0·1 mm. Hg., the corresponding values of the voltage across the tube and the C.D.S. thicknesses being read at the same time, for a wide range of D values. Fig. 7 shows typical results for discharge in air, the voltage across the terminals of the discharge-tube being constant at 330 volts. The figure shows I_h (arbitrary units of "hetero-normal" current) plotted against $1/d^2$. It is seen that equation 5 (*a*) expresses the results, and that the line passes through the origin. Further, the slope of the line in fig. 7 was found to be independent of pressure. Exactly similar results were obtained for air, nitrogen, argon-nitrogen mixture, and hydrogen, for electrodes of aluminium, copper, and brass. Thus equation (7) is certainly not true for the "hetero-normal" glows. The constant B in equation (7) involves only the mobility of the positive ions: it seems, therefore, that some fundamental simple change in the mobility of the positive ions must be postulated if Sir J. J. Thomson's theory of the cathode fall is to be applied to the hetero-glows.

At the first glance, however, the above experimental results are in complete agreement with equation (8). Equation (8) gives a remarkably accurate account of the hetero-glows. Further, whether merely fortuitous or not, the experimental results are in agreement with equation (9).

Fig. 7.—$p = 0{\cdot}43$ mm. Hg.

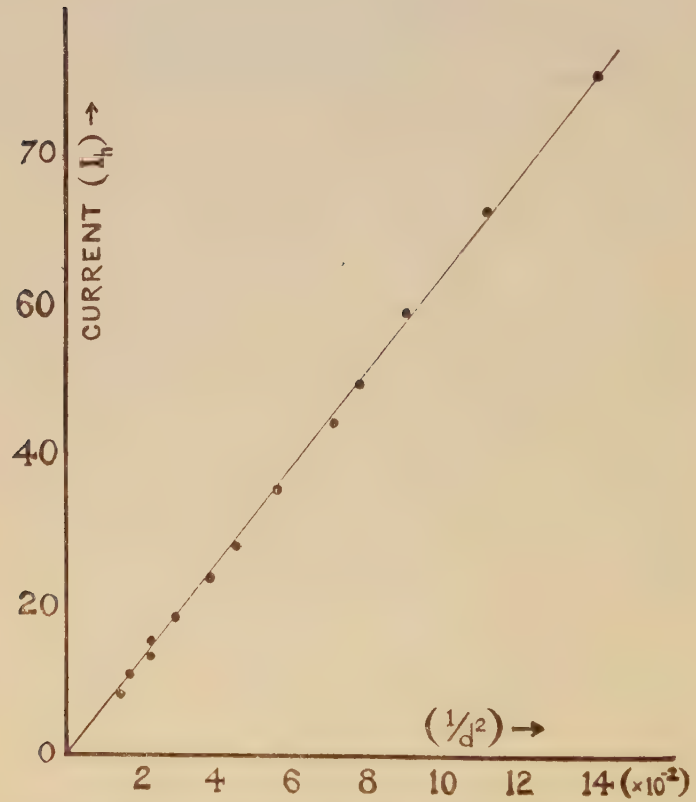

Let us take, for instance, readings of V, d, and i for various values of D at different pressures, the discharges being "hetero-normal," and the voltages therefore nearly constant. Fig. 7 shows such results. In this graph the ratio $i \cdot d^2/V^{3/2}$ is 104×10^{-5} in the arbitrary current units. In making this calculation the total voltage across the discharge-tube was read, less 25 volts to make some allowance for the anode fall of potential. In this way ratios $i \cdot d^2/V^{3/2}$ were taken from several graphs, and the results are shown in Table III.

TABLE III.

(1). Pressure mm. Hg.	(2). Range of D values.	(3). Ratio $i \cdot d^2 \cdot / V^{3/2} \times 10^{-5}$.
1·18	0·5 to 0·29	103
1·1	0·6 „ 0·28	87
0·82	1·2 „ 0·33	90
0·79	0·8 „ 0·4	114
0·75	0·7 „ 0·4	105
0·56	1·2 „ 0·3	93
0·42	2·2 „ 0·2	95
0·35	2·1 „ 0·3	109
0·3	1·4 „ 0·2	108
0·19	1·4 „ 0·3	124

The ratios in column 3 range from 85 to 124. Under the experimental conditions it is not unsound to say that these ratios are constant, because it is easy to account for the differences. The average of column 3 gives 103, whilst the average of all the separate results at the various pressures all grouped together gave 104. The average value of the ratios is therefore $0{\cdot}00103 \times 168 \times 3 \times 10^3 \times 300$ e.s.u., where the number 168 is the micro-ampere per scale-division factor of the current reading instrument used in the experiments, and the numbers 3×10^3 and 300 are those for conversion of the practical units of current and voltage to e.s.u. The ratio is thus 27×10^5 in e.s.u.

To apply the space-charge equation, we turn to equation (8), where A is the area of cathode surface utilized in the discharge in the above experiments, in this case twice the area of one of the brass disks of fig. 4 in the previous paper. A was $2\pi\left(\frac{3{\cdot}29}{2}\right)^2$ sq. cm. Let us assume that M for the combined oxygen and hydrogen molecules of air is $2 \times 14{\cdot}5 \times 1{\cdot}65 \times 10^{-24}$ gm., and taking e as $4{\cdot}77 \times 10^{-10}$ e.s.u., we have

$$\frac{A}{9\pi} \cdot \sqrt{\frac{2e}{M}} = \frac{2 \cdot \pi \cdot (3{\cdot}29/2)^2}{9\pi} \cdot \sqrt{\frac{4{\cdot}77 \times 10^{-10}}{14{\cdot}5 \times 1{\cdot}65 \times 10^{-24}}}$$

$$= 27 \times 10^5 \text{ expressed in e.s.u.}$$

This is precisely the average value obtained experimentally above. Apparently the general equation (8) is the experimental expression of the space-charge equation (9).

It would be interesting to proceed farther, to consider the above equations for the "hetero-abnormal" glows. Here, however, there is not sufficient difference between the two

equations (7) and (8) to definitely decide which agrees the better with experimental results. My experiments do not merit my going fully into the order of agreement with equations (7) and (8) of the measurements of V, d, i, and p for the "hetero-abnormal" glows of various gases and electrode materials, because of several disabilities, hitherto not specifically mentioned. Heating effects, electron emission; the faults of the apparatus, edge effects, and the smallness of the cathode area used in the discharge, and "wall" effects; the measurement of the total voltage across the discharge-tube instead of the actual cathode falls, and in particular the small C.D.S. thicknesses to be measured—these, and others, are some of the difficulties of the experimental work. The inaccuracy resulting from the above disabilities is sufficient to mask differences between the equations (7) and (8), especially over the limited pressures at which it was possible for me to work. However, the hetero-effect places at hand a new means for investigation of the relation between V, d, i, and p, and it is hoped that such an investigation will be made in the near future. Aston's work [4] on the glow discharge could very well be repeated, using, instead of concentric cylinders as anode and cathode, the hetero-effect between two opposing cathode surfaces as the means for altering the discharge conditions.

Consideration of Experiments described by Hufford.

It is now possible to consider the recent paper by M. E. Hufford on the discharge of electricity between equipotential plates (Phil. Mag. vol. l. No. 300, Dec. 1925, p. 1197), in the light of my experiments on the hetero-normal current density effect. Mention of Hufford's paper has been made already in my previous paper [6].

Strictly, Hufford's paper describes two independent effects: (i.) the discharge of electricity between equipotential plates, and (ii.) phenomena at a hole in a cathode. I proceed to examine the first of these two effects as described by Hufford.

First, several points require mention. The essential independence of the two effects above must be emphasized—the effect (ii.) merely acts as an obstruction to the full play of the effect (i.). The Hufford type * of discharge-tube, therefore, does not lend itself to observation of the discharge phenomena between equipotential plates under the simplest possible conditions. In Hufford's discharge-tube there is no

* See (5), p. 1197.

free access for the discharge between the inner glows (at the surfaces of P and P′, opposing each other) and the anode other than by way of the hole, and consequently discharge to the opposing cathode surfaces can be obtained only under very limited conditions, namely, generally only when a "bead" is present in the hole. Again, the current used by Hufford to give the "bead" effect and the glows within the space between P and P′ are all "abnormal."

Hufford found that the glow discharge within PP′ was at variance with the ordinary negative glow discharges. Two types of glow discharge are obtained within PP′. Fig. 8 (*a*)

Fig. 8.—Horizontal shading represents negative glow.

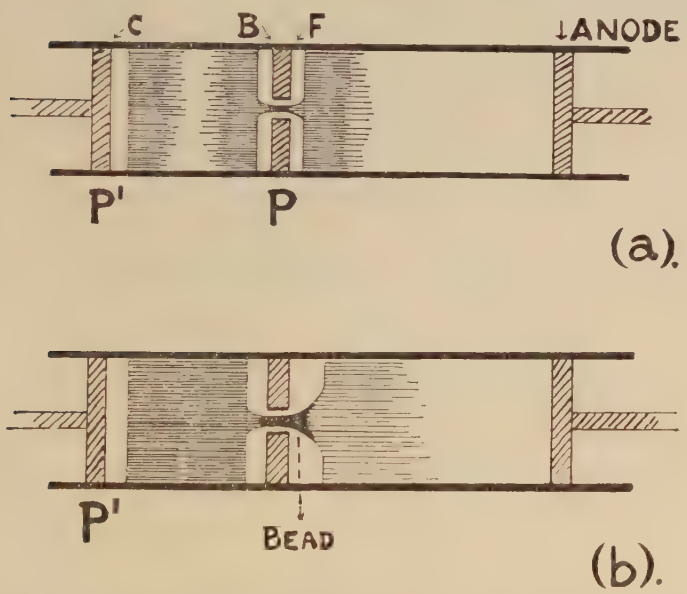

is a diagrammatical representation of the first type, the characterizing features of which are as follows :—The "conductance" to the front of P (at F) is slightly greater than, or generally equal to, that at the surfaces B and C. The negative glows of the surfaces B and C do not "overlap," and the cathode fall of potential is the same to each of the three surfaces B, C, and F. This type occurs at the higher pressures, when, for holes of the order 2 mm. diameter, there is nearly free access for the discharge between PP′ and the anode. Fig. 8 (*b*) shows the second type, which is the chief concern of Hufford. The glow to the surfaces B and C fills

the space between P and P′, except for the space taken up by the C.D.S. to the cathode surfaces B and C, *i.e.* the glows "overlap." The negative glow at F is fainter, has a higher potential, and a longer C.D.S. thickness, than the negative glows at B and C, which are obviously the same as those experimented upon in the present paper. Because of the phenomena at the hole in the cathode P, Hufford's paper resolves into the description of isolated "hetero-abnormal" glow-discharge effects between P and P′, for a "normal" discharge generally cannot be obtained within PP′, owing to the fact that large current densities are required before the bead effect is obtained at the hole in P, thus making possible the discharge within PP′. The potential measurements etc. given by Hufford confirm the chief characteristics of the hetero-glows as described in the above paragraphs and in my previous paper. Thus, because of the opposing cathode surfaces, it is not surprising that larger current densities are carried to the cathode surfaces B and C, for 200 volts or so less cathode fall of potential, than to the single surface F, as was obtained by Hufford for many different gases and electrode materials. Of the discharge obtained within PP′ Hufford says (p. 1201): "It was found that with each of the gases and gas mixtures, the dark space covering the metal surfaces between P and P′ increases in length as the pressure is diminished, until the pressure is reached at which the bead and glow disappear. The Crookes's dark space is usually slightly longer than the dark space which appears behind the cathode." The various deviations and peculiarities reported by Hufford are explained, for the most part, by the hetero-effect, and the restrictions put on the discharge between P and P′ by the hole in the surface P being the only means of access between PP′ and the anode. There is but little meaning in comparing (as Hufford compares) the potentials obtained under the circumstances of his work with the "normal cathode fall of potential" as given by Gunther-Schulze and others, because the currents employed by Hufford are nearly all "abnormal."

Conclusions.

1. It has been shown that large increases in current density (expressed as current density at the surface of the cathode, since in the above experiments only plane surfaces were used as cathodes) occur in discharge-tubes having "opposing" cathode surfaces, when a restriction of the volume of negative glow is effected through "overlapping" of the

opposing negative glows, or when the distance apart of the opposing surfaces is such that the "normal" C.D.Ss. would ordinarily "overlap."

The early experiments by Aston [4] on discharge to a concave cathode surface showed the same effect, but in a much smaller degree. It seems from the above work, however, that an explanation of the mechanism of the current increases and C.D.S. shrinkages is to be found, not at or very near the surface of the cathode (as Aston deduced from his experiments) so much as at the point of "overlapping" or contact of the opposing negative glows or C.D.Ss. (It will be remembered that if a piece of mica plate, or other obstruction, is placed in the negative glow region between the opposing cathode surfaces, the current-increasing effect cannot be obtained for parts of the cathode adjacent to the mica plate.)

2. On maintaining "normal glows, *i. e.* adjusting the current through the discharge-tube so that the cathode area is just completely utilized in the discharge, the increases in current density are greater the nearer together are the opposing cathode surfaces.

3. The generally-accepted law that current density increases are accompanied by increases in the cathode fall of potential is not true in the case of the above current density increases.

For the above "*normal*" glows, the cathode fall of potential remains at a constant value. This value is generally the ordinary "normal cathode fall of potential," but might be a voltage smaller than the ordinary "normal" one. (This reduction in the "normal cathode fall of potential," of the kind described by Schuler [3], requires substantiating by rigid experiment, however; and the observation is made with due regard to the need for better experimental methods, and thorough cleaning of the gases employed in the discharge, before the result can be accepted finally.)

4. The "hetero-normal" current densities, and the C.D.S. thicknesses in the above case (2), are connected by the equation

$$i \,.\, d^2 = \text{constant.}$$

The constant term is independent of pressure, but is different for different gases.

5. The seat of the mechanism giving the "hetero-normal" current densities appears to be at the points of "overlapping of opposing negative glows of Crookes's dark spaces.

6. The "conductance" of the discharge-tube is constant

for any particular distance apart of the opposing cathode surfaces, at any given pressure.

I wish to express my indebtedness to Prof. G. W. Todd, of Armstrong College, under whose supervision the experiments were carried out, and to the Department of Scientific and Industrial Research for the grant which enabled me to undertake the work.

List of References.

(1) Paschen, *Ann. d. Phys.* vol. l. p. 901 (1916).
(2) Hermann Schuler, *Zeits. f. Phys.* xxxv. p. 323 (1926).
(3) Hermann Schuler, *Phys. ZS.* xxii. p. 264 (1921).
(4) Aston, Proc. Roy. Soc. A, lxxxvii. p. 428 (1912).
(5) Hufford, Phil. Mag. vol. l. No. 300. p. 1197 (1925).
(6) Stephenson, Phil. Mag. vol. ii. p. 556 (1926).
(7) Aston, Proc. Roy. Soc. A, lxxix. p. 80 (1906).
(8) Taylor, Proc. Univ. Dur. Phil. Soc. vii. pt. 1, p. 14 (1923–24).
(9) Gunther-Schulze, *Zeits. f. Phys.* xx. pl. (1923).
(10) Ryde, Phil. Mag. xlv. p. 1149 (1923).
(11) Aston, Phil. Mag. xlvi. p. 211 (1923).

XXXII. *The Electric Moments of Disubstituted Benzene Derivatives.* *By* Robert N. Kerr, *B.Sc., Ph.D., Carnegie Research Scholar* *.

THE introduction of a substituent into the benzene ring is known to produce a molecule with a finite electric moment. No measurements, however, are yet available showing the effect on the moment of introducing a second substituent. Recently Sir J. J. Thomson † has made an interesting suggestion concerning the manner in which the moments of such disubstituted benzene compounds may vary with the three possible positions of the substituents relative to one another. He considers that the electrical effect of replacing an atom of hydrogen by another atom or radicle may be represented by the introduction of an electric doublet, the sign of which depends on the nature of the substituent. The latter may be one of two types according to the nature of its electron configuration. The first type consists of those radicles and atoms with a system which requires an electron to form a complete octet (halogens, OH, NH_2 CH_3), and the second those radicles in which there is one electron over after providing for complete octets (NO_2, COOH, CHO, CN). The positive end of the doublet will be toward the

* Communicated by Sir James Walker, F.R.S.
† Phil. Mag. xlvi. p. 497 (1923).

molecule with which the radicle is combined if the substituent be of the first type, but for the second group the direction is the opposite one. Accordingly the relative magnitudes of the moments of the three isomers depend on the nature of the substituents. If both are of the same kind then the moments will be in the order $o > m > p$, but if the substituents are of different types the effect of the two groups in the ortho position will be partially to neutralize one another, and the order of the moments will be $o < m < p$. These variations should have an effect on the dielectric action of the substances, and, accordingly, Thomson predicts that in certain cases the values of the dielectric constants for the three isomers should lie in one order and in other cases the reverse order. It was thought to be of interest therefore to determine the dielectric constants of a number of disubstituted benzene derivatives in the liquid state with the object of finding whether such differences existed, and, if so, whether they occurred in the cases predicted by Thomson.

Experimental.

The substances used were carefully purified, care being taken to obtain the isomers as free from one another as possible. The liquids were fractionally distilled until a fraction boiling constant over 0°·2 was obtained; the solids were crystallized from suitable solvents. The values of the melting-points and boiling-points were in good agreement with those quoted in the literature with the exception of *p*-nitrotoluene. The value found for the melting-point of this substance was 51°·5 ; the value generally quoted, 54°, appears to be erroneous, for Rintoul *, with carefully purified material, obtained a value of 51°·6–51°·9, and Holleman † found a value of 51°·4, with which values the figure quoted here is in good agreement. Before use the substances were all carefully dried, in the case of the more hygroscopic substances by distilling over P_2O_5 under reduced pressure.

The dielectric constants were determined by means of an apparatus described in a previous communication ‡. As several of the substances were solids with low melting-points the determinations were carried out at a temperature at which all were liquid (58°). The results obtained are given in the second column of Table I. ; each value was checked by the repetition (if necessary, more than once) of the

* Jour. Soc. Chem. Ind. xxxiv. p. 60 (1915).
† *Rec. Trav. Pays-Bas*, xxxiii. p. 5 (1914).
‡ Kerr, Jour. Chem. Soc. cxxix. p. 2797 (1926).

determination with a fresh quantity of substance. The values for the monosubstituted compounds have also been determined, and for comparison the results are given in the Table. The first column contains the results of density determinations carried out at 58° by means of a pyknometer. The values $\frac{k \times M}{d}$, the dielectric constant estimated for the same number of molecules *, and $\frac{k-1}{k+2} \cdot \frac{M}{d}$, the molecular polarization †, have been calculated and are given in the third and fourth columns respectively.

TABLE I.

Temp. = 58°. Wave-length = 95 metres.

	D_4^{58}.	Dielectric Constant (k).	$\frac{k \times M}{d}$.	$\frac{k-1}{k+2} \cdot \frac{M}{d}$.
Chlorobenzene	1·064	5·23	553	61·8
Dichlorobenzene $C_6H_4Cl_2$ { *o* ...	1·256	7·00	838	78·0
{ *m* ...	1·244	4·63	548	64·7
{ *p* ...	1·248	2·62	308	29·8
Aniline	·989	6·20	538	59·7
Toluidine $C_6H_4(NH_3)(CH_2)$ { *o* ..	·966	5·71	633	67·7
{ *m* ...	·959	5·45	609	66·7
{ *p* ...	·954	4·88	548	63·3
Nitrobenzene	1·165	28·00	2958	95·1
Nitrotoluene $C_6H_4(NO_2)(CH_3)$ { *o* ...	1·126	21·61	2631	106·3
{ *m* ...	1·121	21·86	2673	106·9
{ *p* ...	1·117	22·22	2728	107·5
Chlorobenzene	1·064	5·23	553	61·8
Chlorotoluene $C_6H_4Cl \cdot CH_3$ { *o* ...	1·044	4·16	504	62·1
{ *m* ...	1·035	5·04	616	70·1
{ *p* ...	1·031	5·55	681	73·9
Bromobenzene	1·444	4·92	535	61·2
Bromotoluene $C_6H_4Br \cdot CH_3$ { *o* ...	1·344	4·28	544	66·4
{ *m* ...	1·309	5·36	700	77·4
{ *p* ...	1·314	5·49	714	78·0
Phenol	1·075	9·90	836	65·1
Cresol $C_6H_4(OH)(CH_3)$ { *o* ...	1·012	6·02	643	66·9
{ *m* ...	1·013	9·68	1033	79·3
{ *p* ...	1·004	9·91	1064	80·5
Chlorophenol $C_6H_4Cl \cdot CH_3$ { *o* ...	1·218	5·41	571	62·5
{ *p* ...	1·247	9·46	975	76·0

* Thomson, *loc. cit.*

† Ebert, *Zeit. Phys. Chem.* cxiii. p. 1 (1924).

Discussion of Results.

The theoretical relationship between the electric moment and the dielectric constant is given by the equation of Gans *,

$$\frac{k-1}{k+2}\cdot\frac{1}{d}=C+\frac{A}{T}\phi\frac{(T\sqrt{1-\gamma d})}{B\sqrt{d}},$$

where C can be calculated from optical data. A, B, and γ are constants which depend on the electric moment and other molecular constants, and ϕ is a function introduced by Gans in his theory of paramagnetism. In the above equation it is not the dielectric constant itself which is taken to calculate the moment, but the function $\frac{k-1}{k+2}\cdot\frac{1}{d}$, and, accordingly, comparison of this expression multiplied by the molecular weight, *i. e.* the molecular polarization †, gives a truer comparison of the moments of two substances than is got by taking simply the dielectric constant. In using this quantity as a measure of the moments, however, no account is taken of the quantities entering into the remainder of Gans's equation which are a measure of the molecular fields exerted in the substances. Although there must be certain differences due to the varying electric moments of the isomers, it may be assumed that the molecular fields of the three disubstituted benzene isomers are of much the same nature, since the molecular volumes, and consequently the distances between the molecules therein, are nearly equal. Accordingly, the changes in molecular polarization for the three isomers may be taken as indicating actual changes in the value of the electric moment.

All the substituents in the above Table belong to the first group with the exception of NO_2, and therefore the moments of all the isomers, with the exception of the nitrotoluenes, should be in the order $o>m>p$. Examination of the above Table shows that this is not so, and the rules governing the variation of the moment cannot be so simple as those suggested by Thomson. The results obtained, however, show that there is either a regular increase or decrease of the moment in passing from ortho through meta to para.

The most striking agreement between the theory and the present results is got for the dichlorobenzenes. When both substituents are the same, Thomson shows ‡ that the meta

* *Ann. d. Phys.* lxiv. p. 481 (1921).
† Ebert, *loc. cit.*
‡ *Loc. cit.* p. 513.

and para compounds should have moments equal to those of the monosubstituted compound and benzene respectively. This is verified by the figures for the dichlorobenzenes; the value of the molecular polarization for the meta compound is nearly the same as that for chlorobenzene. The value of the molecular polarization for benzene at 60° is 27·0, which is quite of the same order as that for *p*-dichlorobenzene, the difference being easily accounted for by the additional electron polarization which must be present in the latter compound due to the two chlorine atoms. A similar gradation in the moments is exhibited by the xylenes, as shown in the following figures for the moment taken from Henri's 'Structure des Molecules'—xylenes *o* $\cdot 58 \times 10^{-18}$, *m* ·46, *p* ·23; toluene ·49; benzene ·2. Another example of a similar gradation is given by Höjendahl*. He has made a similar suggestion to Thomson's and has calculated the moments of several molecules as the vector sum of the moments of the polar groups in the molecule. He has tested his theory by determining the dipole moment for infinite dilution in benzene solution. The values obtained for the dinitrobenzenes (*o*, 5·95, *m*, 4·02, *p*, ·8; nitrobenzene, 3·75) are again in good accord with those required by this theory. It appears from these three examples that this is the general behaviour of disubstituted benzene derivatives when both substituents are the same, and it may be concluded therefore that this method of calculating the moment is applicable for such compounds.

The limitations of this method, however, are seen from examination of the derivatives of toluene. That compound itself has a small moment, and therefore the dipole moment associated with the CH_3 group must be small; accordingly, there should not be much difference between the moments of the three derivatives obtained by substitution of toluene. This is the case for the nitrotoluenes: the order of the moments for these isomers is $o < m < p$, and as the two substituents belong to different types, this is the order required by Thomson's theory. Likewise, the toluidines agree with this theory; the order in this case is $o > m > p$, as the two substituents are of the same type. With the other derivatives of toluene, however, the theory breaks down. The moments of the chlorotoluenes, bromotoluenes, and cresols are in the order $o < m < p$, which is the inverse to that required. Not only so, but the differences between the single isomers are much more marked than expected on this theory. That the deviation from the theory cannot be

* 'Nature,' cxvii. p. 892 (1926).

attributed to the wrong sign being given to the CH_3 group is shown from the values for the chlorophenols. From the similar behaviour of the chlorotoluenes and the cresols the doublets corresponding to the CH_3 and Cl groups must have the same sign, and therefore the moment of the ortho should be greater than that of the para compound, instead of smaller as found experimentally. These results therefore show that the simple rules suggested by Thomson are unable to account for the behaviour of disubstituted benzene derivatives when the two substituents are different.

The number of isomers examined and also the lack of experimental data of other kinds do not permit of any general conclusions being drawn as to what are the influences causing the ortho compound to have the greatest moment in some cases but the least in others. It appears to the author, however, that a possible explanation lies in consideration of the polarization of the molecule by the influence of the external field as distinct from the permanent dipole moment of the molecule. The polarization of the molecule consists of two parts*: (1) the "electron polarization" of the old theory of dielectrics; and (2) an atom polarization due to displacement of the atoms in the molecule. It appears possible that the variations from the theory for the chlorotoluenes, bromotoluenes, and cresols may be due to atom polarization taking place to a more marked extent in these compounds than in the toluidines and nitrotoluenes which obey the theory. The abnormally low value of the ortho compounds would be explained on this view as due to the near presence of the CH_3 group in the ortho position preventing atom polarization taking place to such an extent as happens when it is in the meta or para position. Such an explanation, however, in no way accounts for the behaviour of the chlorophenols. Thus there is no apparent reason why *p*-chlorophenol should have a moment quite comparable with each of the monosubstituted compounds, whereas *p*-dichlorobenzene has only a very small moment.

Summary.

The dielectric constants of a number of disubstituted benzene derivatives in the liquid state have been determined. The isomers in all cases show a gradation of this property from ortho through meta to para, but in some cases there is an increase and in others a decrease. A theory suggested by Sir J. J. Thomson regarding the method in which the

* Ebert, *loc. cit.*

electric moments of such isomers should vary has been tested ; it is found to hold when both substituents are the same, but when the latter are different the theory is found to fail for several cases.

The author wishes to express his thanks to Professor Sir James Walker, F.R.S., for his helpful advice throughout the investigation.

Chemistry Department,
Edinburgh University.

XXXIII. *Magnetism and Molecular Structure.* *By* EDMUND C. STONER, *Ph.D.* (*Cambridge*), *Lecturer in Physics at the University of Leeds* *.

Introduction.

RECENT work has shown that for many of the simpler molecules the multiplicity of the electronic levels in the band spectra schemes is of the same type as that in the line spectra schemes for atoms with the same number of valence electrons. In CN and BO, for example, there are 9 electrons in addition to two pairs of K electrons, and the electronic levels in the band spectra may be classified as S and doublet P levels just as can the atomic levels in Na with 9 electrons in addition to the single K pair. As is well known, the atomic (or ionic) spectral, chemical, and magnetic properties can be closely correlated. It is the main purpose of this paper to consider how far the correlation may be extended to the simpler molecules [1]. One of the questions which arises—as to whether molecules can be regarded as individual systems which, as wholes, assume quantum orientations in a magnetic field—has been brought prominently to the fore by Glaser's experiments. The numerical values of the molecular susceptibilities will be discussed, as serving as a test for the validity of present or future theories of molecular structure. Atomic and ionic magnetic properties will first be briefly considered in the light of the Heisenberg-Hund schemes, which have been so

* Communicated by the Author.

[1] A number of the questions treated in this paper are discussed in a preliminary manner in 'Magnetism and Atomic Structure' (Methuen, 1926) (see particularly Chaps. VI, VII, XII, XIV XV), where full references to earlier work are given.

extraordinarily fruitful in correlating the spectral properties with the electronic constitution of the atoms. It will be seen that there are still many unsolved problems in connexion with the magnetic properties. In spite of this, it would seem unwise to defer all discussion of molecules, for the main lines of attack are fairly clearly indicated, and any developments in atomic theory may be readily extended to molecular theory, while consideration of molecular properties may assist in the elucidation of the more fundamental atomic problems.

Mononuclear Systems.

Nomenclature and General Principles[2].—The spectroscopic state of an atom or ion may be conveniently represented by a symbol of the type ${}^{r}\mathrm{L}_{j}$ (e. g. ${}^{3}\mathrm{P}_{1}$), where r indicates the multiplicity, L the nature of the term (S, P, D, ...), and j is the "inner quantum number" associated with it. With L may be associated a quantum number l, which, following Heisenberg[3] and Hund[4], is usually taken as $\frac{1}{2}, \frac{3}{2}, \frac{5}{2}, \ldots$ for S, P, D, ... terms. Physically, but somewhat formally, l may be interpreted as the resultant angular momentum of the electrons in incompleted groups; for atoms or ions with a single series electron it is equal to k for this electron. (k is less by $\frac{1}{2}$ than the azimuthal quantum number k in the original Bohr theory. It is convenient to retain the Bohr k in referring to nk orbits.) The inner quantum number is connected with the angular momentum of the atom as a whole, and may be assigned the values 0 and $\frac{1}{2}$ for singlet and doublet S terms, values for other terms then following from the combination rule $\Delta j = \pm 1$ or 0. In a weak magnetic field each ${}^{r}\mathrm{L}_{j}$ level is revealed as a complex of levels, of magnetic energy $m_1 goh$, where g is the Landé splitting factor and o the Larmor precession frequency; m_1 has integral or half-integral values, differing by unity, symmetrical about zero, and ranging from $+j$ to $-j$. The number of magnetic terms associated with a given ${}^{r}\mathrm{L}_{j}$ level is thus $2j+1$. In a strong field the magnetic energy is given by $m_2 oh$. The spectroscopic properties of atoms

[2] For a summary of the Heisenberg-Hund scheme, see Fowler and Hartree, Proc. Roy. Soc. cxi. p. 83 (1926).

[3] Heisenberg, *Zeit. f. Phys.* xxxii. p. 841 (1925).

[4] Hund, *Zeit. f. Phys.* xxxiii. p. 345 (1925).

containing a number of electrons in incomplete groups may be interpreted as resulting from the properties of the individual electrons in these groups if to each of them are assigned four quantum numbers such as serve to specify the separate states of doublet atoms. (Pauli [5], Hund.)

The apparent necessity for the assignment of four quantum numbers to each individual electron, bound up with the "duplexity" in spectral terms of atoms with one valence electron, may be formally explained by the hypothesis of the spinning electron; but many difficulties are still encountered if any thorough-going physical interpretation is attempted on a classical quantum basis. For the present purpose, however, this question can be left on one side, and it is also unnecessary to enter into detail as to the theory of complex spectra.

An atom or ion will have zero moment and be diamagnetic if in an ${}^{r}\mathrm{L}_{j}$ state for which $j=0$. If j differs from zero, the atom can assume orientations in a magnetic field such that the resolved magnetic moment (as shown directly by the Gerlach and Stern experiments, and indirectly by the Zeeman effect) is equal to the possible values of mg. It is therefore possible to calculate the atomic or ionic susceptibility of mononuclear systems in a given ${}^{r}\mathrm{L}_{j}$ state. Ionic magnetic moments are conveniently specified by the Weiss magneton values (p) calculated in the usual way. By an extension of the Langevin treatment, taking into account quantum orientation, it may readily be shown [1] that

$$p=5\sqrt{3(mg)^2}=5g\sqrt{j(j+1)}. \quad . \quad . \quad . \quad . \quad (1)$$

Diamagnetic Configurations.—Systems with numbers of electrons capable of forming completed groups are, in general, diamagnetic [6]. This is illustrated by the zero moment of atoms of Sn (50), Pb (82), Zn (30), Cd (48) (Gerlach and Stern); by the diamagnetism of ions with 28, 46, 68, and 78 electrons (*e.g.* Zn^{++}, Hf^{++++}); and by the diamagnetism of inert gas configurations. It is these last which will be considered here.

The work of Wills and Hector [7] has shown that the inert gases have susceptibilities which are in close agreement with those predicted by Joos [8] by interpolation from the

[5] Pauli, *Zeit. f. Phys.* xxxi. p. 765 (1925).

[6] Grimm and Sommerfeld, *Zeit. f. Phys.* xxxvi. p. 36 (1926).

[7] Wills and Hector, Phys. Rev. xxiii. p. 209 (1924); Hector, Phys. Rev. xxiv. p. 418 (1924).

[8] Joos, *Zeit. f. Phys.* xix. p. 347 (1923); xxxii. p. 835 (1925).

susceptibilities of ions of neighbouring atoms (*e.g.* A from K^+ and Cl^-). The atomic susceptibilities, interpolated and observed, are shown in Table I.

TABLE I.

Gram-Atomic Susceptibilities of Inert Gases.

$-\chi_A \times 10^6$.

	Interpolated (Joos).	Observed (Hector and Willis).	Calculated from I.P.
He 2.....	(3·0)	1·7	·9
Ne 10.....	8·8	6·1	14·3
A 18.....	17·5	16·5	30·0

The "sizes" of ions which these values indicate have been shown by Joos to be in reasonable agreement with those deduced from crystal structure data.

A rough calculation of the value of the susceptibility to be expected from the ionizing potential of the atom may also readily be made.—From Langevin's theory, for the atomic susceptibility of an atom with N electronic orbits orientated at random,

$$\chi_{At} = -\frac{e^2}{6mc^2}\sum_N \overline{r^2}, \quad . \quad . \quad . \quad . \quad . \quad . \quad (2)$$

where $\overline{r^2}$ is the mean square radius of the orbit. This gives for the gram atomic susceptibility

$$\chi_A = -2{\cdot}85 \times 10^{10} \sum_N \overline{r^2}. \quad . \quad . \quad . \quad . \quad (2.1)$$

Let a_H be the radius of the normal (1, 1) hydrogen orbit ($\cdot 532 \times 10^{-8}$ cm.). For a hydrogen like n, k orbit about an effective nuclear charge Z,

$$\overline{r^2} = kn\left(\frac{n}{Z}\right)^2 a_H^2 = {\cdot}283 \times 10^{-16} kn\left(\frac{n}{Z}\right)^2. \quad . \quad . \quad (3)$$

Let I be the ionizing potential of an atom corresponding to removal of an n, k electron, I_H the ionizing potential of the hydrogen atom (13·5 volts),

$$I = \left(\frac{Z}{n}\right)^2 I_H = 13{\cdot}5\left(\frac{Z}{n}\right)^2. \quad . \quad . \quad . \quad (3.1)$$

Combining (3) and (3.1),

$$\overline{r^2} = kn\frac{3{\cdot}83}{I} \times 10^{-16}. \quad . \quad . \quad . \quad . \quad . \quad (4)$$

In Ne, the I.P. of 21·5 volts corresponds to removal of a (2, 2) electron; in A, 15·3 volts of a (3, 2) electron. The diamagnetism of neon and argon is mainly due to the eight least firmly bound electrons, and the effect of the contracted helium and neon-like cores is practically negligible. The susceptibility of neon—with 6(2, 2) and 2(2, 1) electrons, and of argon—with 6(3, 2) and 2(3, 1) electrons, can then be calculated from equations (2.1) and (4). The results are given in the last column of Table I. The values so calculated for Ne and A are much greater than those observed. The method, however, is crude, and the values must be taken as upper limits, for in equation (4) the "effective" n instead of the larger "rational" n should be used. Bearing this in mind, it seems that fairly close agreement would be obtained if more refined calculations could be made.

In considering the numerical values, the central question which arises is whether the observed values of the susceptibilities correspond to a random orientation of the atoms, or to a single definite orientation appropriate to systems in a $^1S_0$ state. It seems undoubted that paramagnetic systems do take up quantum orientations, as shown by the fact that the observed moments of ions, even in concentrated solutions, agree as to order of magnitude with those calculated on the orientation hypothesis; and that the molecular susceptibility of oxygen is definitely independent of the pressure (Glaser[9]). There is, however, so far, no evidence that the atomic susceptibility of the inert gases changes with pressure. Lehrer[10], in fact, has found no change for argon between 50 and 800 mm. Hg—but he also found no change for CO_2, while Glaser[11] found an increase by a factor of 3 at low pressures. The Glaser "anomaly" will be discussed more fully in connexion with molecular systems, but it may be stated here that it seems very unlikely that there is a change for atomic systems such as Glaser's work has been taken to indicate for diamagnetic molecular systems; but only experiment can decide definitely. If there is any change, it would be expected to occur at much higher pressures for the atomic systems; but it seems impossible to say quite definitely at present whether the values observed—both for the atoms and the diamagnetic ions—are for $^1S_0$ systems orientated

[9] Glaser, *Ann. der Phys.* lxxviii. p. 641 (1925).
[10] Lehrer, *Zeit. f. Phys.* xxxvii. p. 155 (1926).
[11] Glaser, *Ann. der Phys.* lxxv. p. 459 (1924).

discretely or at random, or whether there would actually be a difference in the two cases. Consideration of the discrepancy between the observed values and those calculated from the I.P.s must, therefore, await further evidence.

The case of helium is of particular interest. Assuming that there are two similar 1, 1 orbits, the I.P. of 24·5 volts leads to a value of $\sqrt{\overline{r^2}}$ of ·394 A.U. If the orbits (or the atoms) are orientated at random, this gives $\chi_A = -\cdot 90 \times 10^{-6}$; if both the orbits are at right angles to the field, $\chi_A = -1\cdot 35 \times 10^{-6}$. The higher value is still 20 per cent. less than that observed ($-1\cdot 7 \times 10^{-6}$). A number of lines of evidence now indicate that it is highly improbable that the helium atom has a magnetic moment which sets itself at right angles to the magnetic field; and it is reasonable to suppose that the two electron orbits in helium are arranged like the K pair generally, and like the two valence electron orbits in the alkaline earth atoms in the $^1S_0$ state. This led Sommerfeld [12] to suggest a provisional model in which the electrons move in opposite directions in coplanar elliptical orbits specified by a total quantum number 1 and an azimuthal quantum number $\frac{1}{2}$. For the major and minor axes, a and b, approximately $a = \frac{a_H}{2}$; $b = \frac{a_H}{4}$. From these dimensions the maximum susceptibility (assuming the orbits to set at right angles to the field) may be calculated, with the result $\chi_A = -\cdot 30 \times 10^{-6}$—a value about six times smaller than that observed. The experiments on helium are open to many sources of error, but, in so far as the results may be relied on, they rule out the Sommerfeld model, and suggest that the orbits approximate to the 1, 1 type. If the electrons move in opposite directions—as they must—they cannot move in the same plane as the nucleus. In spite of the instability which ordinary mechanical considerations would indicate, the model which gives a most satisfactory picture of the magnetic properties is one in which the electrons move in opposite directions in parallel orbits approximately circular. Other non-paramagnetic models of the helium atom could doubtless be devised with the spinning electron, but it is questionable whether these would possess any advantage from the point of view of simplicity or mechanical stability.

[12] Sommerfeld, 'Atombau und Spektrallinien' (4th ed., 1924) p. 197.

The diamagnetism of the inert gas configurations is, then, in agreement with general theory; and the order of magnitude of the susceptibilities accords fairly well with that anticipated from other evidence as to orbital dimensions. The significance of the discrepancies must remain doubtful until definite experimental evidence is available as to whether the susceptibilities observed correspond to the single orientation of a $^1S_0$ system, or to a random orientation. For helium, a model with two $(1, \frac{1}{2})$ orbits gives much too small a susceptibility; a model with two parallel (1, 1) orbits is suggested by the magnetic properties.

Paramagnetic configurations.—If the values of k for the individual electrons are known, it is possible, on the basis of the Heisenberg-Hund scheme (taking into account the Pauli restrictions), to deduce the $^{\prime}$L nature of the lower terms in the spectra of the configuration. Thus for a system with three $\frac{5}{2}$ electrons (in addition to a closed configuration) Hund gives the lower terms as ^2D, ^2P, ^2D, ^2F, ^2G, ^2H, ^4P, ^4F. It cannot be said *a priori* which of these is the lowest; but according to Hund's empirical rule, which seems to hold fairly generally, it may be taken as that among the terms of highest multiplicity for which the l value is greatest—in the example just given the ^4F term. The lowermost j component is still undetermined, for the term may be partially or wholly inverted. For the rare earth ions (54 to 68 electrons) with 0 to 14 uncompensated $\frac{1}{2}$ electrons, Hund [13] assumes that in those with 0 to 6 the component with the smallest j value is the lowest, and in those with 7 to 14 that with the largest. It is then possible to calculate the magneton values for the ions using equation (1), and, with one exception, the results are in fair agreement with experiment.

For the ions of the first transition series of elements, an analogous procedure is not successful. The ions concerned, with 18–28 electrons, contain in all probability 0–10 uncompensated $\frac{1}{2}$ electrons (3_3 electrons in the Bohr scheme). The problems which arise may be discussed with reference to Table II.

One of the difficulties in connexion with the magnetic properties is that while in some cases ionic moments deduced from measurements of the susceptibility of different salts (in solution or as solids) under different conditions are remarkably constant, in others there are considerable

[13] Hund, *Zeit. f. Phys.* xxxiii. p. 855 (1925).

Table II.

Magnetic Properties of Ions of the First Transition Series of Elements.

Total Number of Electrons	18	19	20	21	22	23	24	25	26	27	28
Number of $^5_2$ Electrons	0	1	2	3	4	5	6	7	8	9	10
Magneton Value p (Obs.)	0	8·5	—	19	24	29·5	26·0	24·5	16·0	9·5	0
Theoretical Ground Term ^rL	^1S	^2D	^3F	^4F	^5D	^6S	^5D	^4F	^3F	^2D	^1S
Empirical Ground Term ^rL	$^1S_0$	$^2S_{1/2}$		$^4S_{3/2}$	$^5S_2$	$^6S_{5/2}$	$^5D_3$	$^4F_{7/2}$	—	—	$^1S_0$
Magneton Value (Calc.).....	0	8·6	-	19·3	24·4	29·5	26·0	24·4	—	—	0

variations. The Weiss magneton values in the third row of the table are therefore only to be regarded as probable approximate values (to the nearest half integer) for ions with the number of electrons given in the first row. In the fourth row are given the ground terms for the ions anticipated from the Hund scheme, and in the next ${}^{r}L_j$ terms which would give rise to Weiss magneton values (row 6) approximating to those observed.

Among the eleven configurations considered, it is only for five—and two of these are of the closed diamagnetic type—that the Hund scheme predicts ground terms which can give rise approximately to the p values observed. For the remainder, none of the low-lying terms enumerated by Hund account for the observed p values. For the ions with less than 24 electrons, however, the moments are in close agreement with what would be expected if the ground terms were all S terms of systems of the appropriate multiplicity as originally suggested by Sommerfeld. Consider first an ion with 19 electrons such as Ti^{+++} (with $p \doteqdot 8{\cdot}6$). In K and Ca^{+} the 19th electron enters a 4_1 orbit (with $k=\frac{1}{2}$) which would give a ${}^{2}S$ term. The spectral term sequences indicate that the 19th electron in Sc^{++} would enter a 3_3 orbit, giving a ${}^{2}D$ term, and the same would be expected for Ti^{+++}. For neither of the ${}^{2}D$ components, however, do the p values—17·6 for ${}^{2}D_3$, 7·7 for ${}^{2}D_2$—agree with that observed. Too much reliance should perhaps not be placed on the experimental magneton value for Ti^{+++}; but for an ion with 27 electrons, where a ${}^{2}D$ ground term is expected, the observed values for Cu^{++} (ranging between 9 and 10) are again not in agreement. For ions with 21 and 22 electrons, ${}^{4}S$ and ${}^{5}S$ terms may occur owing to the interaction of the 3 and 4 electrons for which $k=\frac{5}{2}$—but not if these are all "equivalent." One at least must have a total quantum number greater than 3, so that ${}^{4}S$ and ${}^{5}S$ terms would not be expected for the ions in their most stable state; yet none of the components of the ${}^{4}F$ or ${}^{5}D$ terms give the magneton values observed. Among the right-hand half of this transition series of ions there is the difficulty with Cu^{++} (27) above mentioned; in addition, the magneton value for Ni^{++} (26) ($p=16{\cdot}0$—one of the most constant values, experimentally) does not seem to fit in with any of the possible ground terms. Tamm[14] has pointed out that ${}^{5}G_3$ gives $p=15{\cdot}9$,

[14] Tamm, *Zeit. f. Phys.* xxxii. p. 582 (1925).

but the Hund scheme suggests only multiplicities of 1 and 3 for systems with eight $\frac{5}{2}$ electrons.

The question of ionic moments, it will be seen, is full of difficulties which there has been a tendency to overlook. On the experimental side it seems desirable that investigations should be made as to whether the apparent moments depend on the strengths of the fields employed, for the splitting factor g is a function of the field. It seems highly improbable, however, with the fields used, that the appropriate g values will differ markedly from those for "weak fields"—and for S terms, in particular, there is no variation. Further, though the experimental magneton values do vary, they cluster round mean values sufficiently closely to show that they cannot be correlated completely with the possible spectroscopic ground terms suggested by the Hund scheme.

The spectra of titanium (22) and vanadium (23) show that the free atoms are normally in an F state. For ions in solids or solutions the conditions must be very different, for, from the magnetic characteristics, the ions with a smaller number of uncompensated electrons seem to exhibit a tendency to assume S states—that is, states in which the resultant electronic angular momentum is a minimum—even if this involves the movement of individual electrons in orbits of a total quantum number higher than the minimum possible; but in the conjugate systems (in which "empty spaces" take the place of electrons) there seems to be a tendency to assume states in which the l value is as large as possible. There is a slight analogy here with the fact that a 4_1 electron is at first (with lower resultant core charge) more firmly bound than a 3_3 electron; but the analogy is not far-reaching. The difficulties still remain of correlating the magnetic properties of the ions with their supposed electronic constitution and their predicted spectroscopic characteristics when in their normal state.

Binuclear Systems.

The great majority of gases whose susceptibilities have been measured are diamagnetic. With the striking exception of oxygen (with 16 electrons) those which are paramagnetic have "odd" molecules—NO (15), NO_2 (23), and ClO_2 (33). The simpler molecules H_2, N_2, NO, and O_2 will be mainly considered here, for a certain amount of information as to their structure may be derived from the band spectra associated with them as well as from their chemical properties.

The magneton value observed for O_2 (14·12) agrees closely with that calculated for a ^3S system, on the quantum orientation basis (14·1) ; that for NO (9·20) does not seem to agree closely with the value appropriate to any of the spectroscopic states, but the nearest value is that for a ^2S system (8·6) as was suggested by Pauli. N_2 is diamagnetic. As a preliminary statement, it may be said that the molecular systems N_2 (with 14 electrons), NO (15 and O_2 (16) have magnetic properties closely resembling those of atomic (or mononuclear) systems in ^1S, ^2S, and ^3S states.

In the interpretation of band spectra three types of transitions must be considered, involving changes in the electronic configuration of the molecule, and in the oscillational and rotational states. Considering the electronic levels in the simpler binuclear molecules, Birge[15] and Mulliken[16, 17] have shown that the energy levels associated with the valence electrons of molecules agree in all essential aspects with those associated with the valence electrons of atoms ; they may be specified as S, P, ... terms with the appropriate multiplicity, the separations frequently being of the same order as those for the "corresponding" atomic systems. The analogies found are far from complete, but the general outlook is of great value in considering magnetic properties.

As examples, the molecular systems CN, BO, and CO^+ may be mentioned. These have 13 electrons, of which 4 may be assumed to be K electrons, a pair moving in small orbits round each nucleus. There remain 9 electrons. The lowest electronic level in the band spectra is single (an S level), the next double (^2P), and the next single (S). Although the separation of the two P terms—126 for BO and CO^+, and 54 for CN—differs from that for the corresponding Na ^2P terms (17), the fact that the type of multiplicity is the same as that for mononuclear one-valence electron systems suggests that of the 9 outer electrons 8 form a closed configuration similar to that of the 8 L electrons in neon, and that the remaining electron may move in orbits similar to those of the valence electron in Na. A rough picture of molecules of this type may then be formed. Each nucleus has a pair of K electrons moving in small firmly bound orbits associated with it ; the binuclear system

[15] Birge, 'Nature,' cxvii p. 300 (1926).
[16] Mulliken, Phys. Rev. xxvi. p. 561 (1925).
[17] Mulliken, Proc. Nat. Acad. Sci. xii. p. 144 & p. 338 (1926).

rotates, and the nuclei oscillate along the line joining them; the whole of this system acts as a single nucleus for the outer electrons which distribute themselves among orbits in a similar way to electrons in atoms. In order that the molecular stability and symmetry may be maintained, it would seem that the orbital planes of the "outer" electrons must be orientated in some definite manner with respect to the plane of nuclear rotation.

Diamagnetic Configurations.—Free molecules will be diamagnetic if the electrons form closed configurations. (In this connexion it is interesting to note that pairs of atoms such as CC, BN, BeO, which contain the right number of electrons to produce a neon-like structure, do not unite into binuclear free molecular systems—they unite into crystalline assemblies usually of a tetrahedral type, as pointed out by Grimm and Sommerfeld [6].) Such molecules may be said to be in a ^1S state, and so, if completely quantized, will have a single orientation in an external magnetic field.

In investigating the variation in the susceptibility of a number of gases—H_2, N_2, CO_2—Glaser [11] found a surprising anomaly in that the volume susceptibility, below a certain critical pressure, did not decrease uniformly with the pressure; at low pressures the relation was again linear, but the slope of the curve was greater than that at high pressures, suggesting an apparent molecular susceptibility three times as great. As a rough empirical expression for the critical pressure, Glaser [9] gives the equation:

$$p_{\text{crit.}} = C\frac{Z\sqrt{H}}{\sqrt{\Theta}}, \quad \ldots\ldots\ldots \quad (5)$$

where C is a constant, H the magnetic field, Θ the moment of inertia of the molecule, and Z the number of electrons it contains. (As an example, for N_2, with $H = 5100$ gauss, $p_{\text{crit.}} = 415$ mm.) As already mentioned, Lehrer [10], using a different method, finds no anomaly with CO_2, and it seems possible that Glaser's observed anomaly is due to some secondary experimental factor inherent in his method. Consideration of the implications of the threefold increase, moreover, does not lend support to the reality of the phenomenon.—It has been supposed that the increase is due to the possibility of complete quantum orientation (as opposed to random orientation) occurring below the critical pressure. On the ordinary view this would account for an increase by a factor of $\frac{3}{2}$. If, however, it is assumed that

molecular precession can only occur about one axis—the axis of nuclear rotation—and that the molecule tends to set itself with this axis along the field, then the ratio of the observed susceptibility for the single setting to that for random orientation would be given by

$$H : H\overline{\cos\theta}\,.\,\overline{\cos\theta} = 3, \quad . \quad . \quad . \quad . \quad (6)$$

the bar indicating a spatial mean value.

If, then, Glaser's interpretation of his result—supplemented by some such assumption as that just considered—is correct, it is the low-pressure susceptibility value which is characteristic of the orientated molecules. Now for monatomic molecules such as those of the inert gases, the moment of inertia Θ is indefinitely small, and the critical pressure, according to Eq. (5), would be large, so that the ordinarily observed susceptibility would be that characterizing the fully orientated ^1S systems. Some numerical values may now be discussed in the light of this.

In the following table are given some gram-molecular susceptibilities derived from measurements of Soné[18], Wills and Hector[7], and Pascal.

TABLE III.—Gram-Molecular Susceptibilities.

$-\chi_M \times 10^6$.

(Soné.)	(Wills and Hector.)	(Pascal.)
(2) H_2..... 4·0	(2) He..... 1·7	(34) Cl_2 ..... 41·5
(14) N_2 ..... 7·4	(10) Ne..... 6·1	
(22) CO_2 ... 18·7	(18) A ..... 16·5	

The susceptibility of Cl_2 is a little more than twice that of A, and since the diamagnetism depends on the mean projected area of the electronic orbits (*cf.* Eq. 2) this at once suggests that Cl_2 has what may be called a double argon-like structure as suggested by chemical considerations. The two neon-like kernels do not act as a single positive nucleus for an outer electronic configuration of a mononuclear atomic type, but there are two atom-like configurations, some of the electronic orbits (probably two) being common to both. (In a similar way, the susceptibility of CO_2 suggests a triple neon-like structure.) In N_2, on the other hand, although there are more electrons than in Ne, the susceptibility is only slightly greater. This strongly

[18] Soné, Phil. Mag. xxxix. p. 305 (1920).

supports the view that in N_2 the two nuclei with four associated electrons constitute a central system about which the 10 outer electrons form an atom-like configuration similar to that of a closed ^1S system. If, however, the susceptibility of N_2 which is strictly comparable with that of Ne is a threefold enhanced value as suggested by the Glaser results, the coherence between the chemical, spectroscopic, and magnetic properties breaks down.

For H_2, Soné's value for the susceptibility (Table III.) is in good agreement with that of Wills and Hector ($-\chi_M \times 10^6 = 3{\cdot}7$). Taking Soné's value, and assuming that in H_2 there are two similar electronic orbits, using equation (2), the following results are obtained:

(*a*) Assuming "random" orientation of the orbits,

$$\overline{r^2} = {\cdot}7 \times 10^{-16}, \quad \sqrt{\overline{r^2}} = {\cdot}83 \text{ A.U.}$$

(*b*) Assuming both orbits are at right angles to the field,

$$\overline{r^2} = {\cdot}5 \times 10^{-16}, \quad \sqrt{\overline{r^2}} = {\cdot}67 \text{ A.U.}$$

(It may be noted that the distance between the atomic nuclei, from the band spectra, is of the order of ·5 A.U.)

According to Smyth, 16·4 volts corresponds to $H_2 \rightarrow H_2^+ +$ electron, and may be considered as the ionizing potential of the molecule. A rough calculation may then be made, using equations (3.1) and (4), treating one of the electrons as moving about a charge necessarily between 1 and 2, so that n cannot be greater than 2. Putting $Z=2$, $k=1$, $\overline{r^2} = {\cdot}42 \times 10^{-16}$. The observed susceptibility is thus greater than would be anticipated from other data. If at low pressures the molecular susceptibility is three times as great, the value would be quite incompatible with other evidence as to the molecular dimensions. It would indicate, on assumption (*a*) above, a mean square radius of $2{\cdot}1 \times 10^{-16}$ (giving $\sqrt{\overline{r^2}} = 1{\cdot}4$ A.U.) or, as a minimum, on the assumption (*b*), $1{\cdot}4 \times 10^{-16}$ ($\sqrt{\overline{r^2}} = 1{\cdot}2$ A.U.) This is of the same order as that deduced from kinetic theory data (1·36 A.U.—Jeans) and so is unquestionably too large, since the kinetic theory "radii" are generally much greater than those deduced from other evidence. (Thus for argon, the "radii" deduced from the susceptibility, ionizing potential, crystal data, and viscosity respectively, are approximately ·8, 1·2, 1·0, and 1·8 A.U.)

From another point of view the normal value of the susceptibility of H_2 is surprisingly high. The molecule, being diamagnetic, may be regarded as a ^1S system: and it would be expected that the orbits of the two electrons would be similar to those in the helium atom. The measured susceptibilities show that the projected area of the orbits in H_2 is two to three times as great as that in He. If the two H atoms are coupled together in such a way that the electrons move about the binuclear centre of charge two in orbits specified by quantum numbers the same as those for the orbits in He, the susceptibility would be of the same order of magnitude. This suggests that the total quantum number associated with each of the electronic orbits in the hydrogen molecule is greater than one. Even if the improbable assumption is made that the molecule consists of two very loosely coupled normal hydrogen atoms, the susceptibility would be less than that observed.—As may readily be shown, on the basis of the ordinary quantum theory of hydrogen-like nk orbits, making use of the numerical values in Eq. (2.1), the gram-atomic susceptibility associated with nk orbits (orientated at random) about an effective nuclear charge Z is given by

$$\chi_{(n,k)} = -\cdot 81 \times 10^{-6} \frac{kn^3}{Z^2}. \quad . \quad . \quad . \quad (7)$$

For two normal H atoms, this would give $-\chi_M \times 10^{-6} = 1\cdot 6$ —much smaller than the value observed.

If the magnetic measurements are even approximately accurate, the most probable conclusion to be drawn is that in the hydrogen molecule the two electronic orbits are parallel to each other, and also to the plane of nuclear rotation. The electrons move in opposite directions in quantum orbits for which the total quantum number is greater than one. The molecule as a whole behaves as a ^1S system, and when strongly quantized assumes a single definite orientation in a magnetic field. This view is in agreement with the spectroscopic evidence, as interpreted by Mulliken [17].

With regard to Glaser's experiments, the numerical data above considered render it probable that the observed anomaly is due not to an enhanced molecular susceptibility consequent on quantum orientation at low pressures, but to some secondary, as yet unrecognized, experimental factor inherent in Glaser's method. Generally, the consideration of numerical values of susceptibilities enables a number of

definite conclusions to be drawn as to molecular structure which are in good agreement with those based on spectroscopic and chemical properties.

Paramagnetic Configurations.—The paramagnetic molecules NO and O_2 may conveniently be considered as forming a sequence with the diamagnetic molecule N_2. The spectroscopic characteristics of a number of molecules of a similar type will first be summarized with reference to the following table.

TABLE IV.

Sequence of Binuclear Octet-Type Molecules.

Number of Outer Electrons	9	10	11	12
Examples	CN	N_2	NO	O_2
	BO	CO	O_2+	
	CO+			
	N_2+			

While the analysis of the band spectra associated with a number of these molecules is as yet very incomplete, from the results so far available, the electronic levels may be interpreted, according to Birge and Mulliken, as analogous to those of "corresponding" atoms. Of the outer electrons (those in addition to the two K pairs) eight are supposed to move in 2 quantum orbits, forming an L group. (The Bohr analogue of the Langmuir octet.) The remaining electrons will move in orbits giving rise to S, P, D, ... electronic levels in the band spectra. In the normal state of the molecule the electrons will move in 3 quantum orbits. These assumptions enable the main features—term type and multiplicity—of the electronic levels to be coherently interpreted. (Alternative explanations, however, are not excluded in some cases.) For the present purpose, it is the character of the ground level, corresponding to the normal state of the molecules N_2, NO, and O_2, which is of interest. The ground-term to be anticipated from the above scheme, making use of the Heisenberg-Hund principles, may readily be deduced. It is assumed that the 9th and 10th electron (see Table IV.) enter $k=\frac{1}{2}$ orbits, the 11th and 12th $k=\frac{3}{2}$ orbits. The possible ground terms, with the corresponding Weiss magneton number p, are then given in the following table.

TABLE V.

Magnetic and Spectroscopic Characteristics of N_2 NO, and O_2.

Molecule	N_2	NO		O_2				
p (Obs.)	0	9·20		14·12				
Theoretical Ground Term	^1S	^2P		^3P			(^1D)	(^1S)
	$^1S_0$	$^2P_1$	$^2P_2$	$^3P_0$	$^3P_1$	$^3P_2$	$^1D_2$	$^1S_0$
p (Calc.)	0	2·9	13·8	0	10·6	18·4	12·2	0
Empirical Ground Term	^1S	^2S		^3S				
p (Calc.)	0	8·6		14·1				

It will be seen at once that the magnetic properties of the molecules do not lend support to a distribution of electrons in them such as is suggested by the Birge-Mulliken interpretation of the band spectra data. Before discussing this further, however, a few chemical facts may be briefly recalled.

One of the most striking properties of molecular nitrogen is its chemical inertness. The molecule, in fact, possesses in a marked degree characteristics similar to those of the closed configuration of inert gas atoms. That two $k=\frac{1}{2}$ electrons outside a closed configuration can give rise to a further closed system has been emphasized by Sommerfeld [6]. But N_2 does not seem to possess combining properties in any way resembling those of a divalent closed system such as that of Mg.—Chemically, nitrogen behaves as though two of its outer electrons were internal (in 1 quantum orbits) to the L group of eight, and not external (in 3 quantum orbits) as usually supposed. Such a picture of the nitrogen molecule (again a Bohr analogue of the Langmuir model) raises many difficulties, but it may be noted that it is not formally debarred by the Pauli restriction rules, for the "molecular" 1-quantum electrons cannot be considered as equivalent to the "atomic" K electrons. The NO molecule would then

be supposed to have one additional electron moving in a 3-quantum orbit, giving rise to a ^2S molecular state, and to a "monovalent molecule". The monovalency is shown by the formation of compounds such as NO·Cl, NO·F, and NO·OH. Passing on to O_2, a "divalent molecule" would be expected. The existence of Bach's ozonic acid $O_2\begin{smallmatrix}\nearrow OH\\ \searrow OH\end{smallmatrix}$ lends support to this idea, and also, perhaps, ozone, which may be regarded as $O_2\rightarrow O$. If, however, oxygen has two $k=\frac{1}{2}$ electrons, and both of these move in 3 quantum orbits, the Pauli restriction rules would leave only the ^1S diamagnetic state possible. A ^3S state is possible if one of the electrons moves in a 4 quantum $k=\frac{1}{2}$ orbit. It is a ^3S state which the magnetic constants indicate. There is, moreover, perhaps some support for the view that one of the electrons is less firmly bound, in the formation of the compound ClO_2, which has always appeared anomalous on the ordinary views of valency. Even if this correlation of the chemical and magnetic properties of oxygen is correct, the problem is still unsolved as to why a ^1S state is not the normal one for the molecule. It will be noted that this picture of the oxygen molecule corresponds to a single Langmuir octet with two external electrons, and the difficulty of interpreting physically the sharing of four electrons, involved in the Langmuir double octet model, is avoided. Reverting to Table IV., it will be seen that the view here discussed—that it is molecules with 10 outer electrons, and not those with 8, which behave analogously to inert gas atoms—is again supported by the chemical properties of CN. The well-known halogen-like character of CN strongly suggests that it has one electron less than that required to form an inert gas configuration—that the 9 outer electrons move in orbits (about the binuclear centre) specified by quantum numbers the same as those for the electrons in the fluorine atom. Further, the non-formation of free molecules of the type CC, BN, as above mentioned, is readily intelligible if it is 10 and not 8 outer electrons which are required to form the closed neon-like structure.

The magnetic properties of the molecules N_2, NO, and O_2 (suggesting the "Empirical Ground Terms" of Table V.) can, then, be closely correlated with chemical properties, if it is assumed that binuclear molecules with 10 outer electrons (see Table IV.) have an inert gas atom-like structure. This view, however, disagrees with that of Mulliken, Birge and others, and it does not seem that

it can be brought into harmony with the band-spectra data as these are at present interpreted.

Both views lead to reasonable explanations of the types of multiplicity so far observed in the electronic levels of the band spectra schemes; but the ground levels to be anticipated are quite different. These are shown in the following table, which should be examined with reference to Table IV.

TABLE VI.—Anticipated Electronic Ground Levels for Molecular Systems.

Number of Outer Electrons		9	10	11	12
Ground level ...	Scheme I	^2S	^1S	^2P	$[^1S\ ^1D\ ^3P]$
	Scheme II ...	^2P	^1S	^2S	$[^3S]$

According to Scheme I (Mulliken-Birge) eight outer electrons form an inert gas-like configuration; according to Scheme II, ten. There seems to be general agreement that in the molecules with 9 outer electrons the ground level is single, as the first scheme suggests. (There is, however, a difficulty in that the lines in the spectra frequently have a fine doublet structure whose origin is still obscure.) For the 11-electron system there is disagreement, for while Mulliken[17] states that for NO it may be concluded (from Sponer's work) that the ground term is of the ^2P type, Mecke[19] gives the ground term as single.

Until the band spectra have been more fully analysed—until, in particular, the electronic level multiplicities have been unquestionably distinguished from rotational and other multiplicities, and the electronic level sequences are more extensive—it would be premature to attempt to draw definite conclusions. At present, however, the band spectra data do seem inconsistent in detail with the coherent chemical and magnetic data, but all point to the validity of the conception of atom-like molecular configurations. In this section, the magnetic properties of certain molecules have been set forth so as to exhibit their relation with the spectroscopic and chemical properties of a sequence of molecules of a particular type. It has been shown that the different modes of approach in many cases lead to similar conclusions as to molecular structure, but that there are inconsistencies indicating that it is only the initial stages in the solution

[19] Mecke, *Zeit. f. Phys.* xxxvi. p. 375 (1926).

of the many problems raised which have so far been passed.

Sufficient has been said to show that the value of magnetic investigation extends far beyond the elucidation of atomic structure. Simple molecules only have been discussed here, but, as has been shown elsewhere [1], a study of the susceptibilities of complicated organic compounds may help to reveal the character of the electronic orbits constituting valency bonds. Further, the "anomalous" magnetic behaviour of many solids is closely connected with the rôle of the valence electrons when atoms combine into a crystalline aggregate.

As to two questions which are now of fundamental interest, all that may be said, in the present connexion, is that if the hypothesis of the spinning electron is necessary to account for atomic properties, and if a new formal type of mechanics is necessary to describe them simply and coherently, both will be equally necessary in considering molecular and crystal properties. Molecular theory may, however, have some reaction on atomic theory, for, from a model standpoint, molecular properties show that, in many cases, orbital planes of electrons do not invariably pass through a particular nucleus; suggesting that this may be true also, in view of the many analogies, for some of the electronic orbits in atoms.

Summary.

The magnetic properties of mononuclear and simple binuclear systems are discussed in relation to their spectroscopic and chemical properties.

For diamagnetic mononuclear systems (inert gas atoms, and ions of similar configuration) the magnetic susceptibilities are roughly of the same order as those to be anticipated from the ionization potential data. The helium model with $k=\frac{1}{2}$ for each electron orbit leads to a susceptibility six times smaller than that observed. The magnetic data suggest a model with two parallel approximately circular orbits.

The magnetic moments of the ions of the first transition series of elements (representative of mononuclear paramagnetic systems) are shown not to be in agreement, except in a few cases, with those appropriate to the ground terms predicted by the Hund treatment. The ions with a smaller number of electrons behave magnetically as though they were in S states.

The simpler binuclear diamagnetic systems behave analogously to ^1S atomic configurations. From a consideration of the numerical values of the susceptibilities it is shown that the Glaser anomaly is probably not to be attributed to a threefold increase in the molecular susceptibility at low pressures due to orientation. The significance of the high value of the susceptibility of H_2 is discussed.

The magnetic moments of the binuclear paramagnetic systems NO and O_2 suggest that these two molecules form a sequence with N_2, the three molecules behaving as atom-like configurations in ^1S, ^2S, and ^3S states. The magnetic and chemical properties may be closely correlated if it is assumed that ten "outer" electrons (as in N_2) are required to form an inert gas atom-like configuration. The electronic levels in the band spectra, on the other hand, suggest that eight are required; and the two views lead to divergent predictions as to the ground levels to be anticipated. The different lines of evidence, however, support the validity of the conception of the atom-like molecule, suggesting that in the simpler molecules the outer electrons distribute themselves about the binuclear centre in orbits in a similar way to the electrons in atoms.

Department of Physics,
University of Leeds,
August 1926.

Note added to proof (Dec. 1926).—Lehrer has recently confirmed his previous results for CO_2, and for argon also he finds proportionality between volume susceptibility and pressure between 60 and 720 mm. Hg (*Ann. der Phys.* lxxxi. p. 229, 1926); Hammar (Proc. Nat. Acad. Sci, xii. p. 594, Oct. 1926), using a method essentially similar to Glaser's, finds no evidence of a magnetic anomaly, but with imperfectly dried gases he obtains curves not unlike Glaser's. For a fuller account of the systematization of spectra see Sommerfeld's 'Three Lectures on Atomic Physics' (Methuen, 1926), and a paper by McLennan and McLay (Proc. Roy. Soc. cxii. p. 76, Aug. 1926).

XXXIV. *On Lines and Planes of Closest Fit.* *By* E. C. Rhodes, *M.Sc., Reader in Statistics, University of London* *.

THE problem of the determination of the best linear relationship between a number of variables, of which we have observations, has recently been considered by H. Glauert (Phil. Mag. vol. l. 1925), and was dealt with by K. Pearson in 1901 (Phil. Mag. 6th ser. vol. ii.). Pearson, starting out with the idea that at any rate a "plane" of *good* fit (even if not the *best* fit) would be obtained by making a minimum the sum of the squares of the "distances" of the observed "points" in n-dimensional space from this plane, obtained equations for determining the constants of the equation to the plane, and illustrated his work with many numerical examples. He was dealing with the case of many concurrent observations of any number of variables. Glauert considered a slightly different problem, the case where there are a number of variables determined by observation, and liable to error, in association with other variables, whose values are known accurately in each experiment. He outlines a proof that the "best-fitting" plane is that obtained by making the sum of the squares of the distances from the plane a minimum, and develops equations similar to those of Pearson in his paper. Both these writers assume that the precision of the errors involved in the measurements of the different variables is the same. It is of interest to consider the problem without this assumption, which would apply to only a very restricted field.

1. We will consider the case of any number of simultaneously varying quantities, where there is reason *à priori* to suppose that the quantities are connected by a linear relationship, or where we wish to write down an empirical linear equation connecting these quantities. We will suppose that the quantities are denoted by $X_1, X_2, \ldots X_m$, and that there are quantities $u_1, u_2, \ldots u_m$ measured in the same units as $X_1, X_2, \ldots X_m$ respectively and which we use to reduce the X's to a common base. Let us assume that the linear relationship between the X's is

$$l_1\frac{X_1}{u_1}+l_2\frac{X_2}{u_2}+\ldots+l_m\frac{X_m}{u_m}=p,$$

where $l_1^2+l_2^2+\ldots l_m^2=1$.

* Communicated by Sir J. J. Thomson, O.M., F.R.S.

Our problem is to find the l's and p from a number of observations of the X's.

Let us introduce $(m-1)$ variable quantities $t_1, t_2, \ldots t_{m-1}$ which will determine the X's by means of the equations below.

$$\begin{aligned}
\frac{X_1}{u_1} &= pl_1 + a_{11}t_1 + a_{12}t_2 + \ldots + a_{1\,m-1}t_{m-1},\\
\frac{X_2}{u_2} &= pl_2 + a_{21}t_1 + a_{22}t_2 + \ldots + a_{2\,m-1}t_{m-1},\\
&\cdots\cdots\cdots\cdots\\
\frac{X_m}{u_m} &= pl_m + a_{m1}t_1 + a_{m2}t_2 + \ldots + a_{m\,m-1}t_{m-1},
\end{aligned}$$

where the a's are unknown functions of the l's such that

$$\left.\begin{aligned}
l_1a_{11} + l_2a_{21} + \ldots + l_ma_{m1} &= 0,\\
l_1a_{12} + l_2a_{22} + \ldots + l_ma_{m2} &= 0,\\
\cdots\cdots\cdots\cdots\\
l_1a_{1\,m-1} + l_2a_{2\,m-1} + \ldots + l_ma_{m\,m-1} &= 0.
\end{aligned}\right\} \quad . \quad . \quad . \quad \text{(i.)}$$

We will suppose that the t's have assumed certain values which fix the $\left(\frac{X}{u}\right)$'s, which, being measured, involve errors which are independent with standard deviations $s_1, s_2, \ldots s_m$, and which are distributed according to the normal law. In this way, by introducing the t's, we can regard the X's as varying concurrently, none of them being regarded as prior to the others. The chance that the measurements made lie between the limits $x_1, x_1 + dx_1, \ldots x_m, x_m + dx_m$ is therefore

$$\frac{1}{(\sqrt{2\pi})^m s_1\, s_2 \ldots s_m} e^{-\frac{1}{2}E} \frac{dx_1}{u_1}\ \frac{dx_2}{u_2} \cdots \frac{dx_m}{u_m}, \quad . \quad \text{(ii.)}$$

where

$$E = \left(\frac{x_1}{u_1} - pl_1 - a_{11}t_1 - \ldots - a_{1\,m-1}t_{m-1}\right)^2 \Big/ s_1^2 + \ldots$$
$$+ \left(\frac{x_m}{u_m} - pl_m - a_{m1}t_1 - \ldots - a_{m\,m-1}t_{m-1}\right)^2 \Big/ s_m^2.$$

Now we come to consider the actual observations. We will suppose that we have one set of observations of these quantities, viz. $x_1, x_2, \ldots x_m$. What can we infer from these? We do not know the t's which determined the X's which were measured, but we can assume that the most likely t's are those which render the expression (ii.) a

maximum. This assumption will enable us to calculate the t's. We have, differentiating E with regard to $t_1, t_2, \ldots t_{m-1}$, in turn,

$$\left.\begin{aligned}
&\frac{Y_1}{{s_1}^2}a_{11} + \frac{Y_2}{{s_2}^2}a_{21} + \ldots + \frac{Y_m}{{s_m}^2}a_{m_1} = 0,\\
&\frac{Y_1}{{s_1}^2}a_{12} + \frac{Y_2}{{s_2}^2}a_{22} + \ldots + \frac{Y_m}{{s_m}^2}a_{m2} = 0,\\
&\quad\ldots\ldots\ldots\ldots\\
&\frac{Y_1}{{s_1}^2}a_{1\,m-1} + \frac{Y_2}{{s_2}^2}a_{2\,m-1} + \ldots + \frac{Y_m}{{s_m}^2}a_{m\,m-1} = 0,
\end{aligned}\right\}. \qquad \text{(iii.)}$$

$(m-1)$ equations from which we can determine the t's, where

$$Y_q = \frac{x_q}{u_q} - pl_q - a_{q1}t_1 - a_{q2}t_2 - \ldots - a_{q\,m-1}t_{m-1}. \quad (q=1, 2, \ldots m).$$

But we require the expression (ii.) when these t's, found from (iii.), are substituted; we do not require the t's themselves. If we call the co-factors of $a_1, a_2, \ldots a_m$ in the determinant Δ, $A_1, A_2, \ldots A_m$, where

$$\Delta = \begin{vmatrix} a_1 & a_2 & \ldots\ldots a_m, \\ a_{11} & a_{21} & \ldots\ldots a_{m1}, \\ \ldots & \ldots & \ldots \\ a_{1\,m-1} & a_{2\,m-1} & \ldots a_{m\,m-1} \end{vmatrix}$$

Then equations (i.) give

$$\frac{l_1}{A_1} = \frac{l_2}{A_2} = \ldots = \frac{l_m}{A_m},$$

and equations (iii.) give

$$\frac{Y_1/{s_1}^2}{A_1} = \frac{Y_2/{s_2}^2}{A_2} = \ldots = \frac{Y_m/{s_m}^2}{A_m}.$$

Therefore

$$\frac{Y_1/{s_1}^2}{l_1} = \frac{Y_2/{s_2}^2}{l_2} = \ldots = \frac{Y_m/{s_m}^2}{l_m},$$

and this system of equal ratios is equal to

$$\frac{E}{l_1Y_1 + l_2Y_2 + \ldots + l_mY_m},$$

since

$$E = {Y_1}^2/{s_1}^2 + {Y_2}^2/{s_2}^2 + \ldots + {Y_m}^2/{s_m}^2.$$

But

$$l_1Y_1 + l_2Y_2 + \ldots + l_mY_m = l_1\frac{x_1}{u_1} + l_2\frac{x_2}{u_2} + \ldots + l_m\frac{x_m}{u_m} - p = Z \text{ (say)},$$

using ${l_1}^2 + {l_2}^2 + \ldots + {l_m}^2 = 1$ and equations (i.).

Thus

$$\frac{Y_1/s_1^2}{l_1} = \frac{Y_2/s_2^2}{l_2} = \ldots = \frac{Y_m/s_m^2}{l_m} = \frac{E}{Z}.$$

From these we get

$$E = \frac{E^2}{Z^2}\{l_1^2 s_1^2 + l_2^2 s_2^2 + \ldots + l_m^2 s_m^2\};$$

i. e. $$E = Z^2/(l_1^2 s_1^2 + \ldots + l_m^2 s_m^2).$$

Thus we may say that the chance of measurements lying between x_1, $x_1 + dx_1$; $\ldots x_m$, $x_m + dx_m$ is

$$\frac{1}{(\sqrt{2\pi})^m s_1 s_2 \ldots s_m} \times e^{-\frac{1}{2}\left(l_1\frac{x_1}{u_1} + l_2\frac{x_2}{u_2} + \ldots + l_m\frac{x_m}{u_m} - p\right)^2 \Big/ (l_1^2 s_1^2 + \ldots + l_m^2 s_m^2)} \frac{dx_1}{u_1} \ldots \frac{dx_m}{u_m}$$

from (ii.). The part of this expression involving the l's and p is

$$e^{-\frac{1}{2}\left(l_1\frac{x_1}{u_1} + l_2\frac{x_2}{u_2} + \ldots + l_m\frac{x_m}{u_m} - p\right)^2 \Big/ L^2},$$

where $$L^2 = l_1^2 s_1^2 + \ldots + l_m^2 s_m^2.$$

2. If we consider now the combined chance of the result of n sets of measurements of the X's, the part which involves the unknowns is

$$e^{-\frac{1}{2}\Sigma\left(l_1\frac{x_1}{u_1} + l_2\frac{x_2}{u_2} + \ldots + l_m\frac{x_m}{u_m} - p\right)^2 \Big/ L^2}, \quad \ldots \quad \text{(iv.)}$$

where the Σ refers to all the n values of x_1, $x_2 \ldots$, x_m.

From this chance we can determine the best values to give to the l's and p, the criterion being that

$$\Sigma\left(l_1\frac{x_1}{u_1} + l_2\frac{x_2}{u_2} + \ldots - p\right)^2 \Big/ L^2 \quad \ldots \quad \text{(v.)}$$

should be a minimum, thus making the expression (iv.) a maximum.

Differentiation with regard to p gives immediately

$$\Sigma\left(l_1\frac{x_1}{u_1} + l_2\frac{x_2}{u_2} + \ldots - p\right) = 0,$$

i. e. $$l_1\overline{\frac{x_1}{u_1}} + l_2\overline{\frac{x_2}{u_2}} + \ldots = p.$$

Thus the best fitting "plane" goes through the "centroid" of the observations.

We can therefore consider

$$\Sigma\left(l_1\frac{x_1-\bar{x}_1}{u_1}+\ldots+l_m\frac{x_m-\bar{x}_m}{u_m}\right)^2\Big/\mathrm{L}^2$$

instead of (v.). This may be written

$$\frac{1}{\mathrm{L}^2}\left\{l_1{}^2\frac{\sigma_1{}^2}{u_1{}^2}+l_2{}^2\frac{\sigma_2{}^2}{u_2{}^2}+\ldots+2l_1l_2r_{12}\frac{\sigma_1\sigma_2}{u_1u_2}+\ldots\right\}=\mathrm{F}\text{ (say)},$$

where $\sigma_1, \sigma_2, \ldots$ are the standard deviations of the observed measurements and $r_{12}, \ldots$ are the coefficients of correlation between them.

The equations to determine the l's are given by

$$\frac{1}{l_1}\frac{d\mathrm{F}}{dl_1}=\frac{1}{l_2}\frac{d\mathrm{F}}{dl_2}=\ldots=\frac{1}{l_m}\frac{d\mathrm{F}}{dl_m}. \quad . \quad . \quad . \quad \text{(vi.)}$$

But

$$\frac{d\mathrm{F}}{dl_1}\mathrm{L}^2+2\mathrm{F}l_1s_1{}^2=2\frac{\sigma_1}{u_1}\left(l_1\frac{\sigma_1}{u_1}+l_2r_{12}\frac{\sigma_2}{u_2}+\ldots+l_mr_{1m}\frac{\sigma_m}{u_m}\right),$$

i. e.

$$\frac{d\mathrm{F}}{dl_1}=\frac{2}{\mathrm{L}^2}\left\{\frac{\sigma_1}{u_1}\left(l_1\frac{\sigma_1}{u_1}+l_2r_{12}\frac{\sigma_2}{u_2}+\ldots+l_mr_{1m}\frac{\sigma_m}{u_m}\right)-\mathrm{F}l_1s_1{}^2\right\}.$$

Similarly

$$\frac{d\mathrm{F}}{dl_2}=\frac{2}{\mathrm{L}^2}\left\{\frac{\sigma_2}{u_2}\left(l_1r_{12}\frac{\sigma_1}{u_1}+l_2\frac{\sigma_2}{u_2}+\ldots+l_mr_{2m}\frac{\sigma_m}{u_m}\right)-\mathrm{F}l_2s_2{}^2\right\}$$

and so on.

We see that

$$l_1\frac{d\mathrm{F}}{dl_1}+l_2\frac{d\mathrm{F}}{dl_2}+\ldots=0.$$

Therefore

$$\frac{d\mathrm{F}}{dl_1}=\frac{d\mathrm{F}}{dl_2}=\ldots=0$$

are the equations for the l's.
These give

$$\left.\begin{aligned}
l_1\left(\left(\frac{\sigma_1}{u_1}\right)^2-\mathrm{F}s_1{}^2\right)+l_2r_{12}\frac{\sigma_1\sigma_2}{u_1u_2}+\ldots+l_mr_{1m}\frac{\sigma_1\sigma_m}{u_1u_m}&=0,\\
l_1r_1\frac{\sigma_2\sigma_1}{u_2u_1}+l_2\left(\left(\frac{\sigma_2}{u_2}\right)^2-\mathrm{F}s_2{}^2\right)+\ldots+l_mr_{2m}\frac{\sigma_2\sigma_m}{u_2u_m}&=0,\\
\ldots\ldots\ldots\ldots\ldots\ldots&\\
l_1r_{1m}\frac{\sigma_m\sigma_1}{u_mu_1}+l_2r_{2m}\frac{\sigma_m\sigma_2}{u_mu_2}+\ldots+l_m\left(\left(\frac{\sigma_m}{u_m}\right)^2-\mathrm{F}s_m{}^2\right)&=0.
\end{aligned}\right\}$$

. . . (vii.).

The simplest way of finding the l's from these equations is to find F from the equation

$$\begin{vmatrix} \left(\frac{\sigma_1}{u_1}\right)^2 - \mathrm{F}s_1^2 & r_{12}\frac{\sigma_1\sigma_2}{u_1u_2} & \dots & r_{1m}\frac{\sigma_1\sigma_m}{u_1u_m} \\ r_{12}\frac{\sigma_2\sigma_1}{u_2u_1} & \left(\frac{\sigma_2}{u_2}\right)^2 - \mathrm{F}s_2^2 & \dots & r_{2m}\frac{\sigma_2\sigma_m}{u_2u_m} \\ \cdot\ \cdot\ \cdot\ \cdot\ \cdot, & \cdot\ \cdot\ \cdot\ \cdot\ \cdot\ \cdot & & \\ r_{1m}\frac{\sigma_m\sigma_1}{u_mu_1} & r_{2m}\frac{\sigma_m\sigma_2}{u_mu_2} & \dots & \left(\frac{\sigma_m}{u_m}\right)^2 - \mathrm{F}s_m^2 \end{vmatrix} = 0, \quad \text{(viii.)}$$

and substitute this value in (vii.) to obtain the l's. It must be remembered that the root of (viii.) to be chosen is the least; all the roots will be positive since F is positive.

3. It will be seen that the general solution of this problem involves two sets of entirely unknown quantities, viz. the u's and the s's. The u's are the standards of measurement involved in measuring the X's, which are not necessarily measured in the same units. The u's will involve the same units as the X's. Even if the X's are measured in the same units we may need the u's all different; for instance, X_1 may be measured with a metre rule and X_2 with a pair of fine calipers. It is essential to realize that any step forward we may take is only possible if some assumption is made as to these u's. The s's are the standard deviations of the errors involved in measuring the $\left(\frac{X}{u}\right)$'s, and we need to make some assumption as to these if we are to proceed further.

Let us assume that $s_1 = s_2 = \dots = s_m$, and that $u_1 = \sigma_1$, $u_2 = \sigma_2, \dots u_m = \sigma_m$. Then $\mathrm{F}s_1^2 = \mathrm{F}s_2^2 = \dots = \mathrm{F}s^2$ (say). L^2 is now equal to s^2 and

$$\mathrm{F}s^2 = 1 + 2l_1l_2r_{12} + 2l_1l_3r_{13} + \dots.$$

The equation (viii.) becomes

$$\begin{vmatrix} 1-\mathrm{F}s^2 & r_{12} & \dots & r_{1m} \\ r_{12} & 1-\mathrm{F}s^2 & \dots & r_{2m} \\ \cdot\ \cdot\ \cdot\ \cdot\ \cdot\ \cdot & & & \\ r_{1m} & r_{2m} & \dots & 1-\mathrm{F}s^2 \end{vmatrix} = 0,$$

and equations (vii.) become

$$\begin{aligned} l_1(1-\mathrm{F}s^2) + l_2r_{12} + \dots + l_mr_{1m} &= 0, \\ \cdot\ \cdot\ \cdot\ \cdot\ \cdot\ \cdot\ \cdot\ \cdot & \\ l_1r_{1m} + l_2r_{2m} + \dots + l_m(1-\mathrm{F}s^2) &= 0. \end{aligned}$$

4. We may re-write these equations when $m=2$, in this way $(1-\mathrm{F}s^2)^2=r^2$ (r is written instead of r_{12} in this case); and for l_1, l_2

$$l_1(1-\mathrm{F}s^2)+l_2r=0,$$

$$l_1r+l_2\,1-\mathrm{F}s^2)=0.$$

The values of F are $\frac{1\pm r}{s^2}$, the least being $\frac{1-r}{s^2}$ when r is positive, and $\frac{1+r}{s^2}$ when r is negative. Let us write $\frac{1-\rho}{s^2}$ where $\rho=|r|$.

Then

$$\left.\begin{aligned} l_1\rho+l_2r&=0\\ l_1r+l_2\rho&=0 \end{aligned}\right\}\text{are the equations for } l_1,\ l_2.$$

Thus $l_1=\pm l_2$ according as r is negative or positive, *i. e.* the best fitting straight line is

$$\frac{x_1-\bar{x}_1}{\sigma_1}\mp\frac{x_2-\bar{x}_2}{\sigma_2}=0$$

according as r is positive or negative.

(Note that this does not involve r.)

This result differs from Pearson's, owing to the introduction of the u's into the foregoing. Effectively Pearson has considered all the u's to be equal.

It is interesting to note in this special case that

$$\mathrm{F}s^2=1+2l_1l_2r,$$

which becomes unity when $r=0$.

This means that the position of the best-fitting line is indeterminate when $r=0$, *i. e.* if we have data giving measurements of two variable quantities, which data indicate that there is no correlation between the variables, we conclude that there is *no* best-fitting line, or *no* linear relationship between the variables.

We may further remark on the fact, above noted, that the best-fitting line in the case of two variables does not involve the correlation coefficient. This should not occasion surprise, if we remember that we are dealing with two variables which are assumed to be bound by a linear relationship, which we endeavour to find. Our variables are not assumed to be correlated. It happens to be convenient for us to use the notation of the calculus of correlation, and it may be that we find it convenient to show our data diagrammatically as a spot diagram, or in table form by means of a bi-variate

table. The errors introduced into the measurements mask the exact relationship between the variables, and suggest to us that our variables are correlated. The only function of the correlation coefficient in our connexion is to indicate, by means of its sign, whether x_1 on the average increases or decreases with x_2. The equation of the straight line is determined from the means and standard deviations of the variables.

XXXV. *The Flash Arc Spectrum of Sodium.* *By* F. H. Newman, *D.Sc., A.R.C.S., Professor of Physics, University College of the South-West of England, Exeter* *.

[Plate VIII.]

1. *Introduction.*

THE spark lines of sodium vapour are less easily excited than those of the heavier alkali metals. They lie in the ultra-violet region and are, as a rule, faint. Goldstein † and Nelthorpe ‡ experienced difficulty in exciting the "grund spectrum" of this element even when an intense electrical discharge was passed through the vapour. On the other hand, Foote, Meggers and Mohler § found that practically all of these enhanced lines were produced with impacting energy equivalent to 50 volts, the spark lines beginning to appear above 30 volts. These experimenters employed the electronic bombardment of sodium vapour at a low pressure. Their measurements of the wave-lengths of the spark lines extend down to λ 2318·0. Schillinger ‖ also investigated the spark spectrum of sodium, and most of the lines measured by him are among those listed by Foote, Meggers, and Mohler.

The valency electron is removed from the sodium atom when the latter is subjected to impacting energy equivalent to 5·1 volts, and an electron from the L orbit is ejected if the incident energy is equivalent to 35 volts ¶. The double ionization may be brought about, either by the removal of the valency electron followed by the ejection of one of the L electrons, or the latter may be removed first, followed by the removal of the valency electron. This second mode of

* Communicated by the Author.
† Astrophys. Journ. xxvii. p. 25 (1908).
‡ Astrophys. Journ. xli. p. 16 (1915).
§ Astrophys. Journ. lv. p. 145 (1922).
‖ *Akad. Wiss. Wien. Sitz.-Ber.* cxviii. 11 (*a*) (1909).
¶ See paper by Foote, Meggers, and Mohler, mentioned above.

double ionization should give the enhanced lines at 35 volts, but the first method requires higher energy, viz. 49 volts. The difference, 14 volts, is the requisite energy for exciting the spark lines if one of the L electrons has been displaced previously from its orbit by 35-volt energy. Now by three successive impacts resulting in (*a*) the removal of the valency electron, (*b*) a transition of an L electron to a new quantized orbit, (*c*) an ejection of this electron from its new orbit, the spark lines might appear at a lower voltage. Three successive impacts in this manner are not likely to occur, so that the spark lines will not be excited, in general, below 35 volts. These predictions have been verified by Foote, Meggers, and Mohler *, who used a discharge-tube in which the grid, a helical coil, was mounted extremely close to a tungsten hot wire cathode and was in metallic contact with a concentric hollow cylinder of relatively large diameter. Regulating the vapour pressure, they arranged that relatively few electron-atomic collisions occurred over the short path across which the accelerating field was applied, *i. e.* between the cathode and the grid. In this manner the majority of the electrons entered the force-free space between the grid and the plate with a velocity corresponding to the impressed field.

The sodium spark lines do not often appear in the sodium arc radiation, whereas in the potassium, rubidium, and cæsium arcs the enhanced lines are frequently present. Under ordinary conditions it is highly improbable that the accelerating voltage per mean free path of the impacting electron in the sodium arc will attain the value 30–40 volts which is required to excite the spark lines. In practice the potential difference across the entire arc, with the current passing, is not likely to exceed this voltage, but when the arc is first struck, *i. e.* at the instant of striking, the full applied potential difference must be operative across the electrodes, so that with low vapour pressure, conditions are favourable for an appreciable fraction of the electrons to attain the impacting energy necessary to excite the spark lines. Although no accurate measurements have been made on the thickness of the cathode fall region in arcs, theoretical considerations suggest that this space should be equal to the mean free path of the electrons from the cathode.

In previous work on the flash arc spectrum of potassium † it has been shown experimentally that the spark lines are intensified in this type of arc, and in the present investigations similar experiments on the flash arc spectrum of sodium have been made.

* *Loc. cit.*

† Phil. Mag. ii. p. 1042 (1926).

2. *Experiments.*

The discharge-tube used contained three electrodes. The two between which the arc was struck were encased in glass tubes and had metallic sodium packed round the ends of the iron, so that a sodium arc could be produced. A momentary electrical discharge from an induction-coil could be passed between the third electrode and one of the arc electrodes, and by means of a rotary commutator, the arc once struck could be rapidly quenched and started alternately. No difficulty was experienced in maintaining this flash arc provided that the time interval between make and break was short. In this way an intermittent arc, requiring no external heating, was produced. The discharge-tube was continuously exhausted to 10^{-3} mm. of mercury. One end of the tube was closed by means of a quartz window, and the spectrum was photographed with a quartz spectrograph, special rapid panchromatic plates being used. In the first investigations, with 200 volts across the arc terminals, the arc lines were present in the radiation, but when the light from the immediate neighbourhood of the cathode was focussed on the spectrograph, in addition to the arc lines, many of the more prominent spark lines appeared, although the latter did not approach the D lines in intensity. The difference between the ordinary and intermittent arc spectra is shown in Plate VIII. The lines appearing in the flash arc spectrum were measured, using an iron comparison, and their wave-lengths are given in Table I. There were no lines of wave-length shorter than λ 2493·8, this limit being explained by the comparative feebleness of the stimulation. The more intense of the lines correspond with the spark lines measured by Schillinger and by Foote, Meggers, and Mohler.

The configuration of the singly-ionized sodium atom resembles that of the normal neon atom, and the first spark spectrum of sodium should resemble the arc spectrum of neon. Hertz *, employing a special type of discharge-tube with an accelerating field 18·7–20·0 volts, has developed a group of red lines in the neon spectrum, and Déjardin † noted a second spark spectrum of this gas in the electrodeless discharge similar to the blue spectrum of argon, krypton, and xenon. This blue spectrum is excited when intense electrical stimulation is employed. It is to be expected therefore that the spark lines of sodium would fall into

* *Zeits. f. Phys.* xxii. 1–2. p. 18 (1924).
† *Comptes Rendus*, clxxxii. p. 452 (1926).

TABLE I.

The Flash Arc Spectrum of Sodium.

Wave-length.	Intensity.	Wave-length.	Intensity.
5228	0	3581	1
5183	0	3574	1
5087	0	3533	10
5045	0	3462·4	0
5007	0	3446·2	0
4928	0	3371·2	2
4713	0	3360·5	1
4705	0	3327·5	1
4679	0	3318·0	1
4573	2	3285·5	7
4539	1	3274·4	1
4451	1	3258·1	5
4443	1	3235·1	1
4418	0	3226·1	0
4336	5	3212·4	4
4305	1	3190·0	4
4274	2	3179·2	0
4233	0	3164·0	3
4207	0	3149·4	2
4183	1	3135·6	2
4174	1	3129·5	3
4132	0	3104·6	0
4120	0	3092·9	10
4098	1	3078·4	4
4085	0	3074·3	2
4066	0	3064·6	0
4064	0	3056·3	4
4059	0	3053·9	1
4045	2	3046·1	0
4042	4	3037·3	1
4024	0	3029·4	1
4004	0	3015·8	0
4001	0	3007·6	0
3988	0	2984·4	1
3967	0	2979·8	1
3953	0	2975·2	1
3943	0	2951·6	3
3909	5	2945·9	0
3883	1	2938·2	0
3869	1	2917·8	4
3859	1	2905·2	3
3816	1	2853·0	3
3800	0	2842·0	3
3795	0	2809·8	1
3752	0	2680·4	1
3711	5	2672·0	1
3682	0	2661·6	1
3672	0	2612·2	2
3664	0	2493·8	1
3631	7		

two divisions with a certain amount of overlapping. The first division, corresponding to the neon red spectrum, is excited with a low stimulus, and this is the spectrum produced in the present work. The spectral centre is approximately at $\lambda 3300$, a lower wave-length than the corresponding spectral centre of the potassium lines in the flash arc. This suggests that the group of lines given in Table I. form the first spark spectrum of sodium. Further work and measurements on the spark spectrum of this element seem desirable.

The author wishes to express his thanks to the Royal Society for a Government Grant which enabled this research to be carried out.

XXXVI. *On the Sparking Potentials of Glow Discharge Tubes.* *By* James Taylor, *M.Sc., Ph.D., A.Inst.P., Fellow of the International Education Board, and Earl Grey Memorial Fellow, The Physical Laboratory of the University, Utrecht* *.

Part I.

On Threshold Currents and the Sparking Potentials.

The Static Sparking Potential.

At the outset we shall define as "discharge-tube" any system of two electrodes placed in a gas and between which a spark or glow discharge may pass when conditions are suitable. Agents which can produce ionization of the gas between the electrodes, or electronic emission from the electrodes, are termed "ionizing factors," and the ionizing factors of a tube at any instant are the sum total of all such agents acting upon the tube at that moment.

There are numerous definitions of the so-called sparking potential, and it is not easy to select one free from inherent weaknesses. Nevertheless, if the term "sparking" is employed it is wisest to define the sparking potential with reference to the actual spark [or, for lower pressures, the glow discharge, as this takes the place of the spark when the pressure is sufficiently lowered], rather than with reference to the very small currents obtainable when the energy suppliable by the circuit is sufficiently limited.

* Communicated by Professor Ornstein.

Adopting this point of view it may be said that, under given conditions of pressure, temperature, and distance between the electrodes etc., a discharge-tube is characterized by a definite sparking potential if this is described in the following manner:—The discharge-tube is carefully protected from ionizing factors —that is to say they are reduced to a minimum—and a gradually increasing potential from a steady source is placed directly across the electrodes. The potential is raised very slowly—in the ideal case infinitely slowly—and at a definite value of this potential, $V=v_c$, a spark or glow discharge occurs. This value, v_c, is termed the normal static sparking potential or static upper critical voltage, using a more plastic nomenclature [1]. This is the least potential that will initiate a discharge when there is no initial ionization or electrons in the tube other than the occasional ion or electron produced in the gas or at the electrodes by small unavoidable ionizing factors such as radiations from radioactive substances, etc. The above definition is not entirely free from ambiguity, in that the residual ionizing factors are uncertain of character and intensity; it is more definite in nature, however, than one which excludes all mention of ionizing factors, for these latter, as will be seen in a later part, exert a considerable influence on the sparking potential of discharge-tubes which have layers of gas condensed on the electrodes.

It has been known for a very long time that there is usually a time-lag in the production of the discharge after the voltage across the electrodes has attained the value v_c. This time-lag is a subject of considerable controversy, some experimenters regarding it as of variable magnitude and others as of approximately constant value [2]. According to Züber (*loc. cit.*) the time-lag is determined by chance, and obeys a probability law. Zeleny [3], for the case of discharges from points, attributes the lags to surface layers of gas on the electrodes. Because of these lag effects and the practical methods usually adopted for the measurement of

[1] For these and many of the following considerations *cp.* Pedersen, *Ann. d. Phys.* lviii. p. 297 (1925); Züber, *ibid.* lxxvi. p. 231 (1925); Campbell, Phil. Mag. xxxviii. p. 214 (1919); Mauz & Seeliger, *Phys. Zeits.* xxvi. p. 47 (1925). For nomenclature of upper critical voltages etc., see Taylor & Sayce, Phil. Mag. l. p. 918 (1925).

[2] See ref. 1. Also Peak, 'Dielectric Phenomena,' New York, 1925; Hiller & Regener, *Zts. f. Phys.* xxiii. p. 129 (1924); Compton & Foulke, Gen. Elec. Rev. xxvi. p. 755 (1923); Zeleny, Phys. Rev. xvi. p. 102 (1920).

[3] Zeleny, Phys. Rev. xvi. p. 102 (1920).

the sparking potentials, the obtained values do not, as a rule, correspond exactly to the static value.

The following is a method of regarding the production of a spark or glow discharge [1]. At the static sparking potential v_c, there is a probability that a chance electron (or ion?) will build up a sufficiently strong current by ionization by collision to initiate a spark or glow discharge [4]. The condition whether a spark will or will not take place, will be determined by the nature and pressure of the gas, the form of the electrodes, and the actual place at which the electron is born [5]. Initially a "dark," very small current will flow owing to the presence of ionization due to the existing ionizing factors; this then builds up into a luminous discharge, which in the case of neon discharge-tubes [6] and argon-nitrogen tubes [7] increases in luminosity towards the anode, and is similar to the corona type of discharge [8]. In this diffuse type of luminous discharge the field appears to be distributed almost uniformly throughout the gas (with parallel electrodes), not concentrated at the cathode as in the ordinary type of glow discharge. A space charge is set up by the discharge and at a definite current density the normal glow discharge or spark discharge sets in (Seeliger and Schmekel, *loc. cit.*).

The phenomena of this discharge, which flows before the normal glow or spark discharge, are not, as a rule, visible [9] because they occur so near to the glow or spark. This is due to the fact that the external circuit is usually able to supply adequate quantities of energy to initiate the spark or glow extremely rapidly, and consequently the regime of the corona and Townsend types of current, associated as they are with very small energy transferences, is transitory and unstable. Nevertheless the regime, or one very closely akin to it, may be obtained by regulating the energy suppliable from the external circuit, by means of a high resistance

[4] Marx, *Hdb. der Radiologie*, i. p. 282, Leipzig, 1920; Townsend, 'Electricity in Gases.'

[5] Campbell, *loc. cit.*; Züber, *loc. cit.*

[6] Penning, *Phys. Zeits.* xxvii. p. 187 (1926); Seeliger & Schmekel, *Phys. Zeits.* xxvi. p. 471 (1925); *Cp.* Holst & Oosterhuis, Phil. Mag. xlvi. p. 1117 (1923).

[7] Work of W. Clarkson, not yet published. The present writer also obtains similar results with parallel plate electrode discharge tubes with air at pressures of less than about 1 mm. For higher pressures and point discharges see Zeleny, Phys. Rev. xxiv. p. 268 (1925).

[8] *Cp.* Peak, *loc. cit.*; Campbell, *loc. cit.*

[9] They may of course be studied stroboscopically, as Penning and Clarkson have done.

or thermionic-valve control [10]. In this way, by careful adjustment of the energy suppliable by the circuit, the "corona regime" becomes stable and may be studied [6]. Characteristics of this type have been studied by Seeliger and Schmekel, and Penning, for neon glow-lamps [6]. It is also the starting point for the Holst and Oosterhuis theory of sparking potentials [6].

It will be observed that, following an analogy of Seeliger and Schmekel, the word "corona" is employed here. The term is perhaps not very good, in so far as the corona which is obtained at higher pressures is of a rather different character. However, since in the following work it is employed throughout for the luminous discharges of small current density which precede the normal spark or glow discharge, or are obtained with high resistances in the tube circuit, there can be little ambiguity.

The writer has made some experiments upon this type of discharge in the case of several tubes filled with a mixture of neon-helium gas.

Description of the Discharge-Tubes.

No. (1) tube consisted of parallel rectangular electrodes of iron (18·5 by 18·5 mm.) and 3·5 mm. apart, filled with neon-helium mixture (about 78 per cent. neon, 22 helium), at a pressure of about 10 mm.

No. (2) tube comprised nickel electrodes 5 cm. in diameter and 15 mm. apart at the centres. These electrodes were slightly curved (10 cm. radius) so that the discharge took place between the central portions of the electrodes. The filling gas was neon-helium mixture at 7·8 mm. pressure.

No. (3) tube was identical in form with (2), but contained a side-tube and tungsten filament for the introduction of sodium by electrolysis [11]. The filling gas was neon-helium mixture at 6·2 mm. pressure.

Several other tubes of the same form containing air at different pressures were also used.

In the preparation of the tubes (with the exception of (1)) they were thoroughly cleaned and baked at about 300° C. at high vacuum for many hours. A discharge in neon-helium was run for some time with the electrodes red-hot. Neon-helium mixture was afterwards introduced at the required pressure and carefully purified by means of a quartz side-tube containing heated calcium [12]. The tubes were then sealed off.

[10] Penning, *loc. cit.*; Geffcken, *Phys. Zeits.* xxvi. p. 241 (1925).

[11] Burt, Phil. Mag. xlix. p. 1468 (1925); Taylor, Journ. Scient. Instrs. iii. Dec. 1926.

[12] Soddy, Proc. Roy. Soc. Lond. lxxviii. p. 429 (1902).

Polarization Effects.

Preliminary to the determination of the corona characteristics the sparking potentials of the tubes were investigated with great care under different conditions.

Now in the experimental determination of the sparking potentials the methods employed are not as a rule such as determine the static sparking potential. The conditions are usually of a dynamical or semi-dynamical nature, since the potential across the discharge-tube when the determination of the sparking potential is being made is raised slowly, but not extremely slowly. In these experiments the potential was usually raised to the sparking value in about 15 or 20 seconds. It was found that the passage of a discharge always produced a greater or less polarization at the electrodes—chiefly the cathode. This polarization effect will be considered in a later part, but it is necessary to mention a few facts here which are relevant to the study of the characteristics. These polarization effects are erratic and large in neon discharge-tubes containing traces of electronegative gases, but exist even in tubes where the most meticulous care has been taken to purify the gases and clean the electrodes. Even in the case of tube (3) with a fresh and pure sodium surface on the electrode, the polarization was observable although very small and of the order of 1 volt. Experiments indicated that the polarization effects were due to the charging up of gas layers on the electrodes, and largely to the positive charging up of a layer on the cathode. In this way double electrical layers were formed which persisted from times ranging from a few minutes to an hour or so, the intensity of the effect gradually diminishing with time of course[13]. The discussion of these effects is not included in our present purpose and they will be left to a later part; it is obvious, however, that the determination of the exact form of the characteristics is rendered somewhat difficult by the existence of these layers which alter the potential across the tube terminals from the value that would be adopted if the effect did not exist.

The method usually adopted to overcome the difficulty consisted in commencing the determination of the characteristics with the electrodes already polarized by having borne the corona current for some considerable time so that a condition of approximate equilibrium had been attained. The effect of this small polarization effect is shown in graph

[13] *Cp.* Zeleny, Phys. Rev. xix. p. 566 (1922); *ibid.* xvi. p. 102 (1920); *ibid.* xxiv. p. 255 (1925).

5 of fig. 4. As the corona current was increased the voltage across the tube actually increased for some time owing to the formation of an electrical double layer. On taking the results in the opposite direction, however, the change was not observed.

Determination of the Characteristics.

The details of measurement for such characteristics have been previously described[14]. The discharge-tube was connected to an adjustable source of potential through a high resistance of the order of several megohms (an adjustable carbon resistance was used) and the current was measured by means of a microammeter or mirror galvanometer. The potential across the tube was determined by means of a thermionic-valve electrostatic voltmeter[14]. It is not permissible to place a capacity such as an electrostatic voltmeter directly across the tube, for this alters the regime and may give rise to "flashing" or discontinuous discharges[15].

The general results with this type of tubes were very similar to those found by previous experimenters[6]. When the potential across the discharge-tube reached the static sparking potential v_c, a faint, diffuse glow became evident near the anode. This luminous discharge was easily observable for current densities of the order of 10^{-9} amp. cm^2.[16] The characteristic for tube (2) is shown in the graph of fig. 1. The current was increased by increase of the potential at the ends of the resistance, and it is seen that the potential across the tube remained almost of the value v_c until currents of about 5 microamperes were attained. During this increase of current the diffuse glow near the anode increased in brightness and began to extend. With further increase of the current the voltage across the tube began to fall slowly in value and the maximum of brightness of the discharge became of some 5 mm. or so in thickness and extended nearer towards the cathode. With further increase of the current the discharge developed a diffuse form, convex towards the cathode and very bright relative to

[14] Taylor & Sayce, Phil. Mag. *loc. cit.*, Journ. Scient. Instrs. ii. p. 9 (1925); see also Penning, *Phys. Zeits.* loc. cit.

[15] Taylor & Sayce, Phil. Mag. *loc. cit.*; also Penning, Seeliger, & Schmekel, *Phys. Zeits.* loc. cit.

[16] *Cp.* Holst & Oosterhuis, Phil. Mag. xlvi. p. 147 (1923). Zeleny (Phys. Rev. xxiv. p. 258, 1924), in experiments on the discharge from points in air (of the order of atmospheric pressure), obtained luminosity that could be seen by the eye for currents as low as $2\times$ 0 amp. (electrode a steel needle point (point negative)).

the rest of the glow. Further, when the point corresponding to A (fig. 1) is reached the potential across the tube falls abruptly in value and the form of the discharge alters discontinuously into a small crescent of negative glow upon the cathode, and concave away from the cathode (point B of fig. 1). The current density was then very much greater than in the previous type of discharge and approached very closely the normal type with normal cathode glow etc., and

Fig. 1.—Graphs for Tube (2).

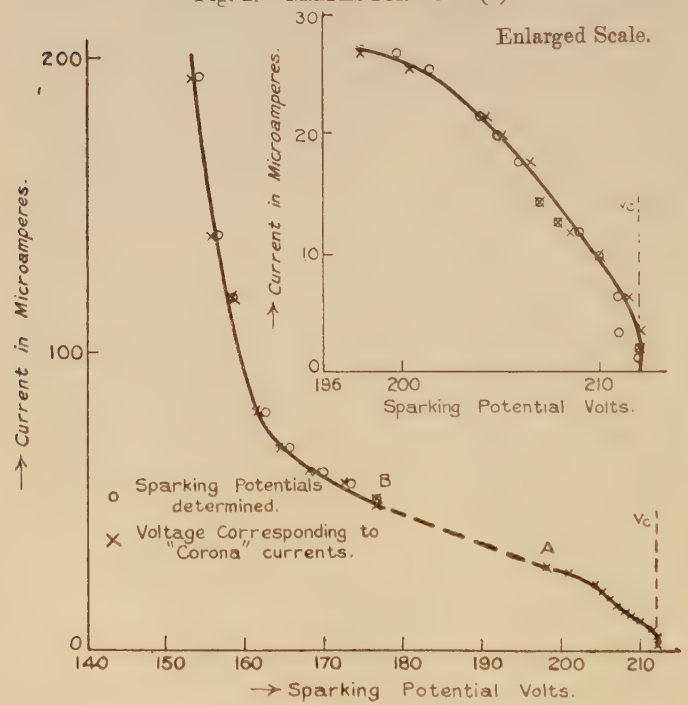

indeed the normal form is reached on further increasing the current, and the voltage across the tube falls to the "extinction" or lower critical voltage value [17]. The region A to B is characterized by intermittence of the discharge [6]. In the case of tube (2) a parallel capacity of about 0·002 microfarad gave a current which was intermittent with an audio-frequency. The intermittency which occurs without additional capacity in the circuit would appear to be due to the self-capacity of the discharge-tube system. This is

[17] See ref. 20.

usually greater than the capacity calculated from the tube dimensions and varies with the pressure of the filling-gas. At the higher pressures it was extremely difficult to obtain a non-intermittent corona type of discharge, and indeed when the filling-gas was air (with similar form of tubes) a steady corona was obtainable only at pressures less than about 1 mm.

A series of experiments were carried out with tube (1) to ascertain whether the potential at which these faint luminous discharges were produced was variable. It was found, however, that within the limits of experimental error the potential across the tube was always of the value of the static sparking potential (unless, of course, the electrodes were polarized), even for resistances as high as 121 megohms.

The graphs of fig. 4 show the form of the corona current function for small currents for tube (3). The graphs are almost straight lines, and in all cases the slope is very great.

The Threshold Current Hypothesis.

The Hypothesis of Threshold Currents appears to have been applied first to the problem of sparking potentials by Appleton, Emeléus, and Barnett[18], in the case of the Rutherford-Geiger α-particle counter. In the work of these experimenters the threshold current idea was merely a suggestion for explaining some of their results. The general nature of the volt-ampere characteristics for discharge-tubes of the type dealt with in this paper, when a voltage is connected directly (without resistance in the circuit) across the electrodes of the discharge-tube, are well known[19]. The diagram of fig. 2 illustrates the type of characteristic. At the sparking voltage v_c, discharge commences and a relatively large current traverses the tube. The current diminishes with decrease of the potential until, at a definite value v_b, the extinction or lower critical voltage[20], the discharge stops abruptly and the current falls to zero.

[18] Appleton, Emeléus, & Barnett, Proc. Phil. Soc. Camb. xxii. 3. p. 447 (1925).

[19] Pearson & Anson, Proc. Phys. Soc. Lond. xxxiv. p. 204 (1922); Shaxby & Evans, *ibid.* xxxvi. p. 4 (1924); Taylor & Clarkson, *ibid.* xxxvii. p. 3 (1925).

[20] This is merely descriptive. The lower critical voltage is itself subject to very considerable variations, but for the present purpose these do not concern us. For these variations see:—Penning, *Phys. Zeits.* loc. cit.; Taylor & Clarkson, Phil. Mag. xlix. p. 336 (1925); Taylor & Stephenson, *ibid.* xlix. p. 1081 (1925); Taylor & Sayce, *ibid.* l. p. 916 (1925).

We have seen, however, that there is another regime corresponding to the corona type of current, and that this regime precedes the normal discharge and corresponds to smaller currents. There is thus another part of the characteristic which falls below the normal one (see fig. 2). It was further seen (fig. 1) that as the current in the corona regime was increased the potential across the tube fell in value from v_c, the static sparking potential, down to the value v_b, the lower critical potential, and the characteristic was such that if at any point corresponding to a definite value V ($< v_c$) of the voltage across the tube electrodes, the

Fig. 2.

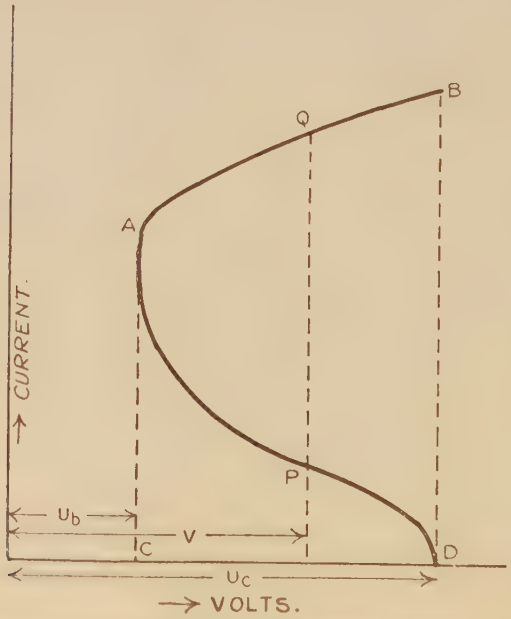

energy supplied by the circuit was increased, then the current through the tube would increase continuously. Considering fig. 2, ABDP represents the full characteristic [18], AB is the normal part (corresponding to no resistance in the circuit), and APD is the corona characteristic. The point P then corresponds to a voltage V across the discharge-tube electrodes, and a current i through it. If the energy suppliable from the circuit is increased whilst the voltage is maintained at the value V, then the current will increase continuously until the point Q on the normal characteristic

is reached. It is thus evident that V is the sparking potential corresponding to a current i through the tube, and i may be termed the threshold current for the potential V [18]. The minimum sparking potential is thus the extinction or lower critical voltage v_0, and the threshold current is then given by the ordinate of the point A, that is the "extinction current."

Experiments proved to be in agreement with the above considerations. The method was as follows (see fig. 3). A

Fig. 3.

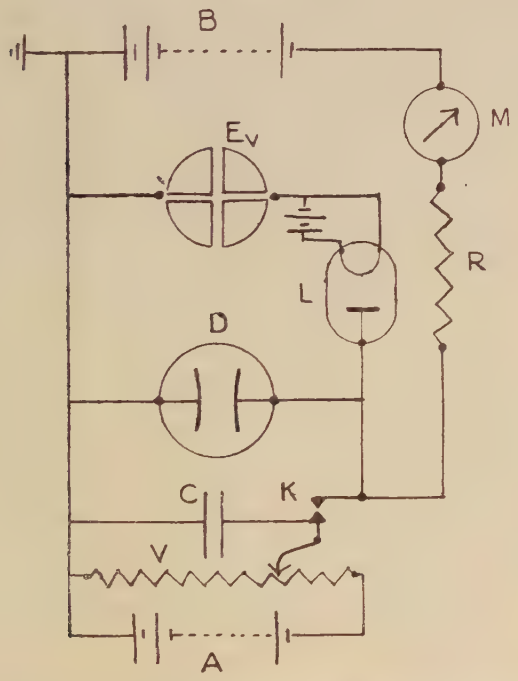

current of the required magnitude was maintained through the discharge-tube D by a battery of adjustable E.M.F., B, and a high resistance R (1·3 megohms for the results of fig. 1). The current was measured by means of a micro-ammeter M, and the voltage across the terminals was determined by the thermionic-valve voltmeter $E_V L$ (previously referred to). At a given instant a voltage V (from the low resistance potentiometer AV continuously charging the capacity C of 0·5 microfarad) from an independent source

was connected directly across the discharge-tube electrodes (in the same direction as the "corona voltage"), so as to ascertain whether a spark or flash would occur at this voltage. The voltage was adjusted and increased until, upon shutting the contact key K, a flash occurred. This measured voltage then corresponded to the sparking potential for the threshold current measured by the microammeter M.

The graphs of fig. 1 illustrate the results obtained for tube (2). It is seen that the sparking potential determined for the different threshold currents agreed almost exactly with the potential across the tube as given by the thermionic-valve voltmeter. Further, for this tube, as shown in the enlarged scale graph (in fig. 1), the value of the sparking potential for threshold currents up to 4 or 5 microamperes did not differ appreciably from the static sparking potential v_c. It is at once seen that with a type of characteristic such as this, which is almost tangential to the line $V = v_c$ (for small currents), the effect of radiating the cathode with light cannot alter the sparking potential—within the limits of measurement—from the value v_c, the static sparking value, for the currents involved due to the photoelectric effects on the cathode are very much less than 4 or 5 microamperes.

The form of the corona characteristic will, of course, depend upon the shape of the electrodes etc., and in the case of certain types of discharge-tube the ionization produced by α-rays and other ionizing factors may be of sufficient amount to produce a threshold current large enough to lower the value of the sparking potential. Consequently, if such a discharge-tube is adjusted critically, it may be utilized for the counting of α-particles and the measurement of ionizing factors [21]. Appleton, Emeléus, and Barnett appear to consider the above as the method of functioning of the Rutherford-Geiger α-particle counter. There is, however, another form of explanation of the action of this counter, based upon the idea of resistance layers on the point electrodes [22].

Experiments on Tubes with Sodium Electrodes.

It was thought that if cathodes of such metals as the alkalies, which liberate electrons by photoelectric actions with ease, were utilized, there would be a possibility that light radiations incident on the cathode might produce

[21] Rutherford & Geiger, Proc. Roy. Soc. A, lxxxi. p. 141 (1908); Appleton, Emeléus, & Barnett, *loc. cit.*; Baeyer & Kützner, *Zeits. f. Phys.* xxi. 1. p. 46 (1924); Zeleny, *loc. cit.*; Jönsson, *Zeits. f. Phys.* xxxvi. 6. p. 426 (1926) (contains many references to previous work).

[22] See Zeleny, *loc. cit.*, and works in ref. 21.

threshold currents of sufficient importance to lower the value of the sparking potential. The effect of such radiations would evidently depend upon the slope of the threshold characteristic (that is the corona characteristic) in the neighbourhood of $V = v_e$.

For these experiments the tube (3) was utilized. The sparking potentials, the polarization effects, and the form of the corona characteristics were carefully examined before and after the introduction of sodium into the tube. We shall denote the two electrodes by the letters A and B.

Initially, previous to the introduction of sodium, the static sparking potentials were about 213 volts with A as cathode, and 212·5 with B as cathode. The polarization effect (with

Fig. 4.—Graphs for Tube 3.

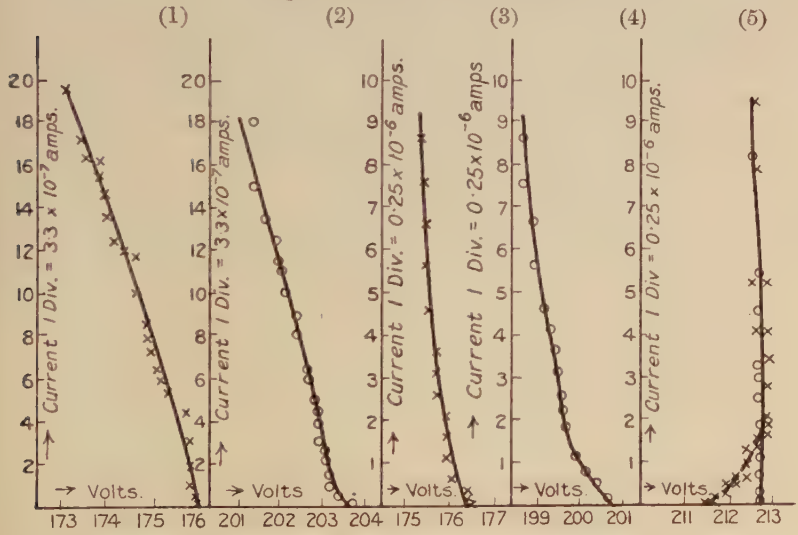

Graph (1). Electrode B cathode, sodium on electrode.
„ (2). „ A cathode, „ „ „
„ (3). Same as (1) taken on different day (larger scale).
„ (4). „ „ (2) „ „ „ „ „ „
„ (5). Electrode A cathode, before introduction of sodium.

a discharge from a capacity of 0·5 microfarad) gave values for the sparking potentials rising from 208 to 217 volts with A as cathode, and 208 to 218 with B as cathode. With much smaller currents, as in the corona, the polarization effect was not more than 2 or 3 volts. From the above results it is seen that the discharge-tube was symmetrical, and it was found that the values of the sparking potentials varied little, if at all, from day to day. The graph (5) of fig. 4 shows the form of the corona characteristic for small

currents. The (×) points were from readings obtained with an unpolarized tube and increasing current, and the (○) points were the readings obtained from decreasing currents. It is to be seen that even with the small quantity transferences of the corona currents, a polarization effect of almost 2 volts occurred. Allowing for the polarization effects it was determined that the corona current started at the static sparking potential value v_c, and increased upon increase of the current with a very steep slope : in fact, as is seen in the graphs, the characteristics are almost coincident with the line $V = v_c$.

After these results had been taken, sodium was introduced into the side-tube by electrolysis, in sufficient quantity to give a little of the vapour in the discharge-tube. The sparking potentials etc. were re-determined, but no alterations could be detected. Sodium was then introduced for several hours, and a strong electric field was put across the tube electrodes and the side-tube, to bring the heated sodium vapour over to the electrodes by the discharge. Owing to the form of the tube, the electrode B received more sodium upon it than the electrode A.

The constants for the tube were then immediately determined and the static sparking potentials were found to be 193·5 volts with A as cathode, and 173·5 with B as cathode. The polarization (with discharge from capacity of 0·5 microfarad) effect was found to be very small with B as cathode, the sparking potential rising by not more than 1 volt after "flashing" for a considerable time. With A as cathode, the polarization effect was greater—but less than before the introduction of the sodium,—the sparking potential rising from 193·5 to 198 volts after "flashing" for some time. The sparking potentials changed slightly from day to day, suggesting that the sodium was being absorbed into the electrodes.

The graphs (1) to (4) of fig. 4 show the corona characteristics for the tube (3) after the introduction of the sodium on to the electrodes. The graphs were not all taken at the same time, consequently the sparking potentials had changed slightly in between the results. Before taking the readings the corona current was allowed to flow for some time to reduce the effect of polarization on the form of the characteristics. It is seen that the actual form of the characteristic was very little altered by the presence of sodium on the electrodes, but the sparking potential was very considerably changed. On the whole, the slope of the characteristics are found to be less than in those where the sodium was absent, but the

change was not of such an order as to give any alteration in the value of the sparking potential when the cathode was illuminated by light. In graphs (2) and (4) a bending-up at the ends of the graphs near $V = v_c$ is to be seen (that is to say, there is an increase of the potential across the tube for small currents). This effect was found to be absent when the electrodes were unpolarized, and was, further, not observable when the electrode B was cathode (the polarization with this electrode was extremely small). Experiments appeared to point to the following explanation :—

There is a great tendency for the current through a discharge-tube to be intermittent for very low current densities if the cathode is subject to polarization effects. This tendency for intermittency of the discharge has been observed by several experimenters[23]. This intermittency is, in our view, brought about in the following manner. The polarized cathode acts as a leaky capacity. It has been shown that "flashes" (that is intermittency of a discharge-tube current) are obtainable by placing a discharge tube in series with a sufficiently high potential, and a capacity shunted by a high resistance[24]. This is actually the state of affairs in the polarized tube, though the energy and quantity transferences are further limited by the high resistance in the external circuit. When the E.M.F. in the circuit is greater than a certain value no intermittency is possible because the resistance of the polarization film is lower than the critical resistance for "flashing"[25]. If the current is reduced, however, by decrease of the E.M.F. in the circuit, at a definite value of this E.M.F. (corresponding to the smaller corona currents) the film resistance will be greater in value than the critical resistance for the circuit and intermittency is obtained. As soon as intermittency occurs the sparking potential, as measured by the thermionic-valve voltmeter, increases owing to the time-lag of the discharge behind the voltage across the tube electrodes (since the polarization gives a time-lag effect the voltage across the tube electrodes will attain a value greater than the normal sparking potential before discharge occurs). The increase

[23] Toepler, *Ann. d. Phys.* ii. p. 560 (1900) ; Zeleny, Phys. Rev. xxiv. pp. 257 & 259 (1924); i. 25. p. 310 (1907) ; xi. 3. p. 70 (1914).

[24] Taylor & Clarkson, Proc. Phys. Soc. Lond. xxxvii. 3. p. 134 (1925); Taylor, Clarkson, & Stephenson, Journ. Scient. Instrs. ii. 5. p. 154 (1925).

[25] Taylor & Clarkson, Proc. Phys. Soc. Lond. xxxvi. 4. p. 271 (1924) ; Phil. Mag. xlix. p. 339 (1925); Taylor & Sayce, Phil. Mag. l. p. 922 (1925).

in potential is observed as an increase in the voltage across the discharge-tube as is seen in graph (2) of fig. 4.

These experiments demonstrate the change of sparking potential with the nature of the cathode, for, apart from the introduction of sodium, the discharge-tube was identically the same throughout the whole work. Further, the change appears to be of a progressive nature depending upon the extent to which the cathode is covered, as is seen from the difference of the results with A and B as cathode. The nature of the cathode also appears to have a very considerable influence upon the polarization effects. These phenomena, however, will be considered in a later paper.

It is a pleasure to express my gratitude to the International Education Board for the Fellowship which enabled the above work to be undertaken, to Prof. Ornstein, under whose supervision the work was carried out, for all the valuable help and assistance given during the course of the experiments, and to the Staff of the University Physical Laboratory at Utrecht.

Summary.

A definition of the static sparking potential is given and the luminous discharges that flow through a discharge-tube prior to the actual spark or "flash" are discussed. The volt-ampere characteristics for small currents of the order of 10^{-6} and 10^{-7} amp. are discussed and some examples given for discharge-tubes consisting of circular parallel electrodes 15 mm. apart, and filled with neon-helium gas mixture. These characteristics are termed "corona" characteristics. The idea of threshold currents is described, and it is shown that corresponding to each current through the discharge-tube there is a definite sparking potential which diminishes as the current is increased. The threshold-current-sparking-potential function is shown to be the same as the "corona" characteristic.

Some electrical double layer effects on the electrode surfaces are described.

It is shown, by the introduction of sodium on to the electrodes by electrolysis through the glass of the discharge-tube, that the sparking potential values alter very considerably with the nature of the cathode.

XXXVII. *The Crystal Structure of Solid Oxygen.* By Prof. J. C. McLennan, *F.R.S.*, and J. O. Wilhelm, *M.A.**

[Plate IX.]

DURING the past two years we have been investigating by means of X-ray diffraction methods the crystal structure of gases solidified by the use of liquid air or of liquid hydrogen. The present paper deals with the work we have done and the results we have obtained for the crystal structure of solid oxygen at the temperature of liquid hydrogen, using a modification of the method we described in a paper on the crystal structure of solidified carbon dioxide.

The general cystallographic properties of solid oxygen were investigated by W. Wahl †, by examining thin layers (about 0·5 mm.) of the solidified gas under the polarization microscope. The thin sheets were obtained by freezing the gas between the flat sides of a specially prepared vessel of glass or quartz, which was cooled in a spray of liquid hydrogen. He found that solid oxygen existed in two modifications. The first one was found to be hexagonal, and to exist in this crystallographic form between the temperatures −230° and −219°. The second, which was the denser of the two, was formed at temperatures below −230°. Its crystal structure Wahl was unable to determine by the use of the optical method.

In a recent paper ‡ Keesom and de Smedt reported that they had been studying the crystal structure of solid oxygen and solid nitrogen, and that in their work they found the crystals of these two elements gave identical diffraction patterns. They reported further that they had been unable from the patterns to deduce a crystal structure for the two elements.

In our experiments we found that these two elements, when solidified, gave quite different diffraction patterns on being examined at the temperature of liquid hydrogen. The present paper gives an account of our work with oxygen.

* Communicated by the Authors.

† Wahl, Proc. Roy. Soc. Lond. A, lxxxviii. p. 61 (1913).

‡ Keesom & de Smedt, Comm. of Phys. Lab. of Univ. of Leyden, #178

Apparatus.

A modified Debye-Scherrer camera was used. The main body of the camera was similar to that described by us in our paper on the structure of carbon dioxide *. Figs. 1 and 2 show the horizontal and vertical sections of the camera. As glass was found to be unsatisfactory for the vacuum flask proper, one that we made up of German silver was used. The outer wall C of the vacuum flask was fitted into the ground opening K of the camera. The inner wall

Fig. 1.

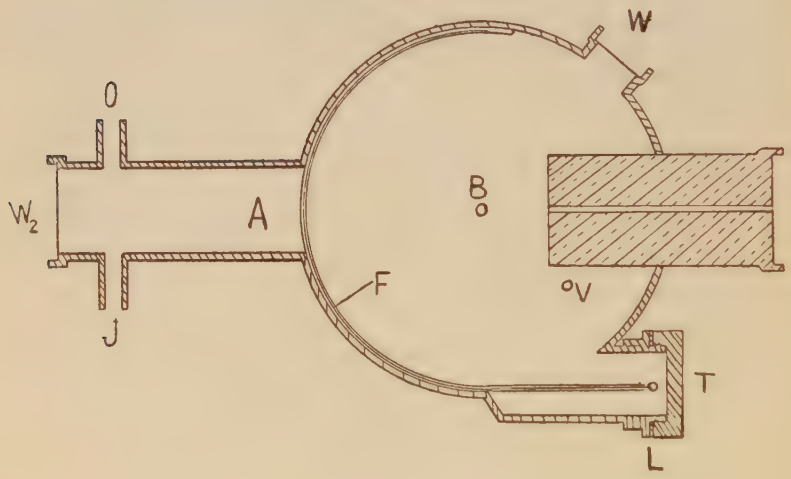

D terminated in a small tube B, which was made of copper and was 1·5 mm. in diameter.

To insure that the cooling liquid had a free flow through B this tube was continued and brought back into the chamber R to the opening H. It was possible and practicable to put a moderate pressure on the liquid in R to force it through B, but this was not found to be necessary. An iron tube of the same size as B was also tried in its place, but the gas would not condense on it as well as on the copper tube.

The tube B was centred as accurately as possible in the camera; but in reducing the observations, corrections were made by means of a graphical method that allowed for any

* McLennan & Wilhelm, Trans. Roy. Soc. Canada, xix. (1925).

eccentricity that might have arisen as a result of cooling strains set up in the flask when the liquid hydrogen was introduced. The camera and flask were evacuated by a mercury-diffusion pump backed by a Cenco air-pump.

Fig. 2.

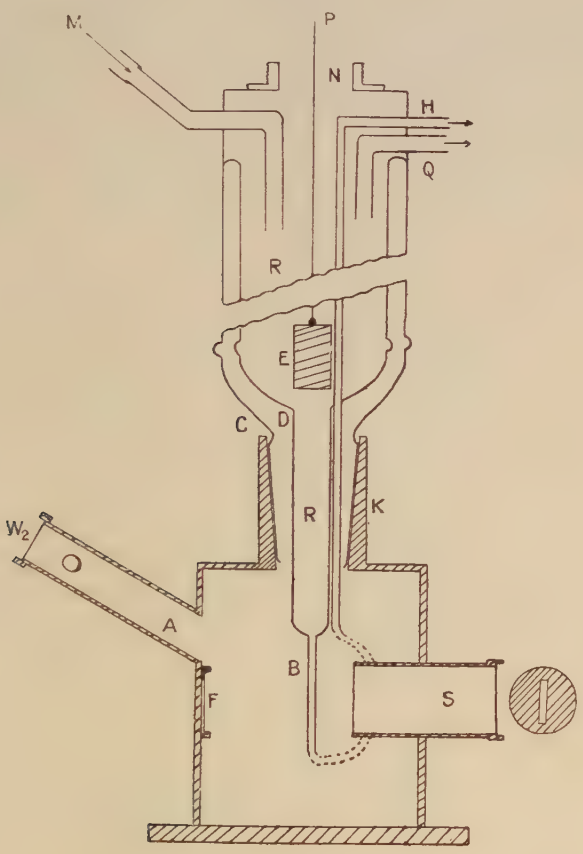

Liquid hydrogen was introduced into the chamber R through the opening M, and it was arranged that the evaporated hydrogen could escape through the opening H, or through Q to a gasometer. The level of the hydrogen in R was indicated by a float E that was attached to a

counterweight by means of the thread P. The float, counterweight, connecting-string, and pulley were enclosed in an inverted U-tube made of glass (fig. 3). One limb containing the counterweight was closed by a stop-cock, but the other was fitted with an annular end-piece made of brass by means of which a gas-tight joint could be made at N.

Fig. 3.

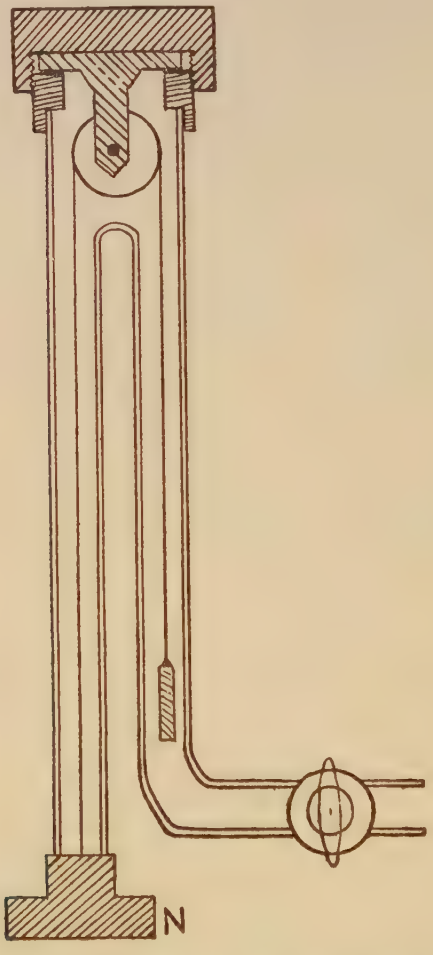

The X-rays entered through a 1-mm. × 10-mm. slit in a lead cylinder 40 mm. long, sealed into the wall of the camera. The slit was covered with aluminium foil ·003 mm. thick, which was sealed on with hard wax.

The photographic film was carried in a phosphor-bronze holder that slid into the camera through the opening T. The holder was held tightly to the wall of the camera by guideways attached to the wall. The opening in the front of the holder was such that an area 10 mm. × 100 mm. of the film could be irradiated. To prevent fogging, the film was covered with a thin sheet of black paper.

A Shearer tube with a removable target, generally of copper, was used to produce the X-rays. The tube was operated at 30–40 K.V. from an induction coil giving a maximum voltage of 50 K.V. The primary current used in the coil was about 7 amperes. It was drawn from the 220-volt D.C. main and was interrupted by a modified Wehnelt interrupter *. With secondary currents of about 5 M.A. the exposures were from 7 to 9 hours.

Experiment.

In carrying out an experiment on oxygen, the film was inserted in the camera and the latter was then kept exhausted for some time. The chamber R was afterwards filled with liquid hydrogen, and the gas to be condensed was slowly admitted through the opening O. The progress of the condensation on B could be observed through the glass window W_2 when a light was placed in front of the window W_1. A layer of solidified gas about ·5 mm. thick gave the best results.

The oxygen used was prepared by heating potassium permanganate. This gas was then passed through a liquid air-trap and through a set of drying tubes before it entered the camera. When oxygen prepared in this way was spectroscopically tested, no trace of any impurity was found to be detectable.

Diffraction Patterns.

Pl. I. shows the diffraction patterns obtained with oxygen when deposited on the copper tube B. The plate was taken without a filter in the X-ray beam, and on it the lines due to the copper K_α radiation and the copper K_β radiation occur. The latter were used as a check on the accuracy of the former. Other photographs were taken with a nickel filter placed in the X-ray beam, and on them K_β lines did not appear.

The data for oxygen are given in Table I., the columns of which are arranged as follows :—(1) number of the line ; (2) diffraction angle θ as measured from the film ; (3) sine

* F. H. Newman, Proc. Roy. Soc. Lond. A, xcix. p. 324 (1921).

of the angle θ; (4) indices of the planes giving rise to the lines; (5) H, where H equals $\left(\frac{h^2}{a^2}+\frac{k^2}{b^2}+\frac{l^2}{c^2}\right)$, a, b, and c being the axial ratios; (6) the square root of H; (7) the value of $\frac{\sin\theta}{\sqrt{\mathrm{H}}}=\frac{\lambda}{2b_0}$; (8) the value of the planar spacings as calculated on the basis of $b_0=3{\cdot}82$ Å; (9) the value of the planar spacings as given from the values of θ in column 2; (10) the estimated intensity of the lines.

TABLE I.

Data for Oxygen.

#.	θ.	$\sin\theta$.	hkl.	$\mathrm{H}=\frac{h^2}{a^2}+\frac{k^2}{b^2}+\frac{l^2}{c^2}$.	$\sqrt{\mathrm{H}}$.	$\frac{\sin\theta}{\sqrt{\mathrm{H}}}$.	d calculated.	d measured.	I.
1...	35°12	·5764	400	7·71	2·78	·2076	1·36	1·34	*m*
2...	32·01	·5302	202	6·87	2·62	·2023	1·46	1·45	*w*
3...	31·04	·5160	112	6·42	2·55	·2023	1·51	1·49	*w*
4...	28·48	·4818	121	5·71	2·39	·2015	1·60	1·60	*s*
5...	27·36	·4633	310	5·34	2·31	·2005	1·65	1·66	*w*
6...	26·36	·4478	002	4·94	2·22	·2016	1·72	1·72	*w*
7...	23·49	·4035	020	4·00	2·00	·2017	1·91	1·91	*m*
8...	17·22	·2985	011	2·23	1·494	·1998	2·56	2·58	*s*
9...	16·30	·2840	200	1·93	1·389	·2044	2·75	2·71	*s*
10...	15·27	·2664	101	1·71	1·307	·2038	2·92	2·89	*w*
11...	14·48	·2554	200	1·93	1·389		3·04	3·02	*m*
12...	14·12	·2453	110	1·48	1·216	·2017	3·14	3·14	*w*

$$\rho=\frac{64\times1{\cdot}649\times10^{-24}}{1{\cdot}44\times{\cdot}9\times(3{\cdot}82\times10^{-8})^3}=1{\cdot}46.$$

$a_0=5{\cdot}50$ Å, $b_0=3{\cdot}82$ Å, $c_0=3{\cdot}44$ Å.

The method of Hull and Davey * was used to find the structure from the values of the planar spacings. A match could not be found in the range of charts that had been prepared for the tetragonal and hexagonal systems, so additional charts were prepared for the orthorhombic system taking in the most likely values of the axial ratios.

* Hull & Davey, Phys. Rev. xvii. p. 549 (1921).

It was found from these new charts that at $-252°$ oxygen crystallized in the body-centred orthorhombic system with axial ratios $a:b:c=1{\cdot}44:1:0{\cdot}9$. The sides of the unit cell as calculated from the data of Table 1. are

$$a_0=5{\cdot}50\ \text{Å}, \quad b_0=3{\cdot}82\ \text{Å}, \quad c_0=3{\cdot}44\ \text{Å}.$$

The density of solid oxygen is then given by the relation

$$\frac{nM\times 1{\cdot}649\times 10^{-24}}{a\,c\,d^3}=1{\cdot}46,$$

if two molecules be supposed to be associated with each cell.

The density of solid oxygen as given in the International Critical Tables is 1·426. If we assume that this value is for the first modification, *i. e.* the one that is existent at the higher temperatures, we find, in the fact that our value is slightly higher than the value given in the Critical Tables, a satisfactory agreement with the observation of Wahl that the low temperature modification is the denser of the two forms for solid oxygen.

The existence of two modifications of oxygen is in agreement with the results that have been obtained for the other members of the same group of elements in the periodic table, for sulphur, selenium, and tellurium are well known as having several allotropic forms dependent on temperature and mode of preparation. Sulphur in its most stable form is orthorhombic *, while selenium and tellurium have been assigned to the rhombohedral division of the hexagonal system by mineralogical † and X-ray experiments ‡.

The writers wish to thank Dr. W. P. Davey and Dr. A. W. Hull for their assistance in the preparation and use of the new graphs. One of the writers, J. O. Wilhelm, is indebted to the Research Council of Canada for the grant of a Studentship which enabled him to take a part in the work.

* Bragg & Bragg, 'X-rays and Crystal Structure,' 4th edition.

† Dana, 'Text-book of Mineralogy.'

‡ Slattery, Phys. Rev. xxv. p. 333 (1925). Olshausen, *Zeit. für Kristallographie*, lxi. p. 463 (1925).

XXXVIII. *On the Fluorescence Spectra of the Sulphur Group.*

By Prof. J. C. McLennan, *F.R.S.*, I. Walerstein, *B.A.*, *and* H. Grayson Smith, *Ph.D.**

[Plates X. & XI.]

Introduction.

THE recent theoretical considerations of Lenz † and Kemble and Witmer ‡ on the origin of the fluorescence spectrum of iodine, which was studied experimentally by R. W. Wood § and McLennan ‖, have attracted fresh attention to a study of the fluorescence spectra of other gases and vapours. The band fluorescence spectrum of iodine, as studied by Wood, is distinguished by its very great complexity when excited by white light, by the fact that selected portions of the spectrum are excited by almost any monochromatic or line source of light, and by the variation of the spectrum with conditions of pressure and temperature. Band fluorescence spectra of this type will probably be excited by a suitable source of illumination in any vapours and gases having complicated molecules like that of iodine (I_6). Thus we should expect to observe a similar phenomenon for the elements of the sulphur and phosphorus groups, and perhaps for bromine and chlorine, when the conditions of pressure and temperature are suitable for the formation of large molecules. A simpler type of resonance spectrum should also be found for simple diatomic molecules.

The elements of the fifth and sixth columns of the periodic table have already been studied by Steubing ¶ (oxygen, sulphur, selenium, and tellurium), Diestelmeier ** (sulphur, selenium, and tellurium), Oldenberg †† (nitrogen) and others. Much work has also been done on other elements. Diestelmeier finds fluorescent spectra for these elements, however, only with unsaturated vapours at high temperatures, and ascribes the phenomenon to the diatomic form of the molecules. In the present paper spectra due to fluorescence of sulphur, selenium, and tellurium excited by the lines of the mercury arc in saturated vapours at lower temperatures

* Communicated by the Authors.

† Lenz, *Phys. Zeit.* xxi. p. 991 (1920).

‡ Kemble and Witmer, Phys. Rev. xxviii. p. 633, Oct. 1926.

§ R. W. Wood, Phil. Mag. Oct. 1912, p. 673, and other papers.

‖ J. C. McLennan, Proc. Roy. Soc. lxxxviii. p. 289 (1913).

¶ Steubing, *Phys. Zeit.* xiv. p. 887 (1913).

** Diestelmeier, *Zeit. f. wiss. Phot.* xv. p. 18 (1915).

†† Oldenberg, *Zeit. f. Phys.* xxxviii. p. 370 (1926).

are described. These spectra are apparently quite different from those described by Diestelmeier and Steubing, and in the case of selenium, two distinct spectra have been found by the authors at different temperatures. It is probable, therefore, that they are due to more complicated molecules which exist at the lower temperatures. A similar spectrum has also been found for bismuth vapour.

Apparatus.

The vapours were intensely illuminated by the light from a quartz mercury arc of the type shown in fig. 1 with a

Fig. 1.

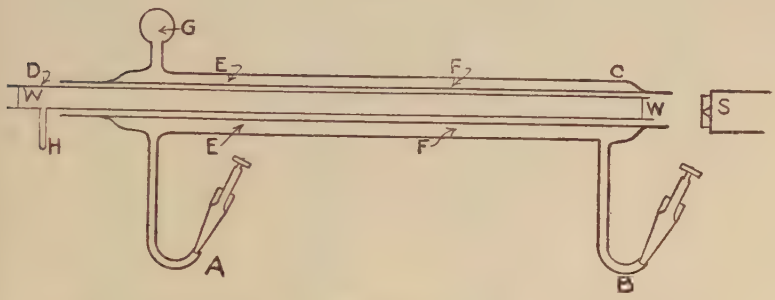

length of about 75 cm. The inner tube was open to the air and the arc was struck in the space between the two tubes. The vapour was contained in another quartz tube D which fitted loosely inside the lamp, and which was thus intensely illuminated from all sides. The fluorescence spectra were observed at the end of the inner tube. The mercury spectrum also appeared on the photographs due to diffusion from the walls of the inner tube. When necessary the inner tube was heated by means of a coil of nichrome wire wound around the tube to a higher temperature than that given by the mercury arc itself. The spectra were photographed by means of a large Hilger quartz spectrograph, covering the region from 2000 to 7000 Å. The exposures were from two to four hours, depending on the intensity of the fluorescent light.

Sulphur.

An extensive fluorescence spectrum was observed in sulphur vapour at the temperature of the inner tube of the mercury arc, without additional heating. A reproduction of this spectrum is shown in Plate X., and the wave-lengths

of the bands observed are listed in Table I. It consists of a large number of bands extending from $\lambda = 5670$ to 4050 Å.

TABLE I.—Sulphur.

Wave-length I.A.	Int.	Wave-number cm.$^{-1}$	Wave-length I.A.	Int.	Wave-number cm.$^{-1}$
5673·6	1d	17620·6	4622·9	2 d	21625·4
5653·8	1	17682·3	4593·7	3	21762·9
5609·6	2	17821·6	4590·3	3	21779·0
5584·6	2	17901·4	4579·9	3	21828·4
5548·9	3	18016·6	4571·4	3	21869·0
5482·9	1	18233·5	4562·9	3	21910·8
5424·2	1	18430·8	4551·9	1 d	21962·7
5400·4	1	18512·0	4545·0	5 d	21996·1
5359·5	2	18653·3	4540·1	3	22019·8
5315·6	2	18807·3	4536·4	2	22037·8
5300·1	3	18862·3	4531·2	1	22063·0
5265·2	3	18987·4	4529·6	5 d	22070·8
5246·1	3	19056·5	4527·3	2	22082·0
5213·3	2	19176·4	4518·9	1	22123·1
5202·7	2	19215·5	4509·9	1	22167·2
5146·4	5	19425·7	4496·8	3 d	22231·8
5137·4	5	19459·7	4475·9	1	22335·6
5124·4	1	19509·1	4468·8	1	22371·1
5104·6	2	19584·7	4462·8	3 d	22401·2
5087·1	2	19652·1	4454·1	1	22444·9
5059·0	2	19761·3	4450·4	2	22463·6
5042·7	2	19825·1	4446·6	3	22482·8
5025·8	1	19891·8	4439·2	4 d	22520·3
5011·8	1	19947·4	4435·9	2	22537·0
5001·6	1	19988·0	4432·5	2	22554·3
4993·9	1	20018·9	4420·2	3	22617·1
4990·5	5	20032·5	4415·6	2	22640·6
4982·0	5	20066·7	4404·7	3	22696·7
4980·1	5	20074·3	4334·1	1 d	23066·4
4965·3	1	20134·2	4327·4	2 d	23102·1
4937·4	1	20247·9	4323·6	2 d	23122·4
4891·3	1	20438·8	4319·5	4	23144·3
4880 9	1	20482·3	4317·3	5	23156·1
4867·1	1	20540 4	4314·2	3	23172·8
4858·3	1	20577·6	4312·5	3	23181·9
4850·9	1	20609·0	4285·8	1	23326·3
4843·2	5	20641·8	4279·6	1	23360·1
4835·8	4	20673·3	4217·5	1	23704·1
4832·8	5	20686·2	4206·6	2	23765·5
4816·7	1	20755·3	4204·3	2	23778·5
4805·9	1	20802·0	4201·4	2 d	23794·9
4794·6	1	20851·0	4197·2	2	23818·7
4740·6	1	21088·5	4174·6	1	23947·7
4724·3	1	21161·3	4169·9	1	23974·7
4710·8	1	21221·9	4163·4	1	24012·1
4704·3	5	21251·7	4098·4	1	24392·9
4698·4	2	21277·9	4092·8	1	24426·3
4694·7	2	21294·7	4088·0	1	24455·0
4685·0	2	21338·8	4082·3	1	24489·1
4682·0	2	21352·4	4065·6	1 d	24589·7
4675·0	5	21384·4	4063·5	1 d	24602·4
4757·9	5	21462·9	4056·7	1 d	24643·6

For the most part the bands are sharp, and those which have been marked "d" (diffuse) in the table are probably groups of unresolved bands. In spite of the apparent confusion of these bands certain sequences of approximately equally spaced bands can be seen on the reproduction. The plate also shows marked absorption of the diffused mercury spectrum in the region below $\lambda = 4050$ Å, indicating that this is probably the active region for the excitation of this spectrum.

Selenium.

The first fluorescence spectrum of selenium excited by the light of the mercury arc was observed when the tube containing the vapour was heated by an auxiliary coil to a temperature of about 325° C. The wave-lengths are listed in Table II. It extends over the greater part of the

TABLE II.—Selenium (325° C.).

Wave-length.	Int.	Wave-length.	Int.
5079	3 d	2882	1
4803	2 d	2874	1
4794	2 d	2838	1
4719	3 d	2835	2
4674	3 d	2825	2
4228	1	2811	1
4166	0	2782	2
4119	1	2773	1
4022	Faint	2766	1
3986		2761	0
3972	narrow	2679	1
3935		2665	4 d
3919	bands.	2663	0
3737	2	2629	3 d
3681	3 d	2616	3
3608	3 d	2610	1
3593	1	2583	1
3570	2	2580	1 d
3509	1	2524	1
3464	2 d	2516	1
3402	1	2477	1 d
3394	1	2445	1
3301	2 d	2414	1
3279	1	2402	1
3267	0	2394	3
3259	1 d	2395	1
3251	0	2334	Faint
3075	1	2330	broad
3067	4 d	2307	bands.
2993	1	2289	1 vd
2990	1	2281	2 vd
2939	2	2271	1 d
2926	1	2245	1 d
2899	2	2229	1 vd

spectrum which could be observed with the spectrograph used, namely from $\lambda = 5080$ to 2230 Å, and is probably analogous to the ultra-violet fluorescent spectrum observed by McLennan in the case of iodine. The greater number of the bands were broad, and could not be measured very accurately, and for this reason the wave-lengths have been given to the nearest Ångström unit only.

At temperatures slightly higher than 325° C. this spectrum disappeared, and at 430° C. a second spectrum consisting of nine faint broad bands appeared. The approximate wave-lengths of the centres of these bands are given in Table III. Neither of these spectra is the same as that observed by Diestelmeier with unsaturated vapour at temperatures above 450° C.

Table III.—Selenium (430° C.).

Wave-length.	Int.	Wave-length.	Int.
4178	0	4587	0
4242	0	4678	0
4311	0	4754	0
4443	0	4829	0
4515	0		

Tellurium.

A fairly intense fluorescence spectrum was excited by the mercury arc in tellurium vapour at 550° C. This is reproduced in Plate XI., and the wave-lengths are listed in Table IV. The spectrum consists of two groups of fairly

Table IV.—Tellurium.

Wave-length. I.A.	Int.	Wave-number. cm.$^{-1}$	Wave-length I.A.	Int.	Wave-number cm.$^{-1}$
6577·4	1	15199·4	5221·6	1 d	19145·9
6494·7	1 d	15392·9	5158·8	2 d	19379·0
6469·7	1	15452·4	5102·1	2	19594·3
6404·7	3 d	15609·2	5043·7	2	19821·2
6382·1	2	15664·5	4982·2	1	20065·9
6316·5	3 d	15827·2	4926·9	1	20291·1
6294·9	2	15881·5	4872·0	2	20519·7
6231·4	3 d	16043·3	4815·0	2	20762·6
6215·3	2	16084·9	4760·7	2	20999·5
6151·8	3 d	16250·9	4708·2	2	21233·6
6135·7	2	16293·6	4655·1	2	21475·8
6063·6	1	16487·3	4602·4	2	21721·7
5992·0	2	16684·3	4553·0	2	21957·4
5916·8	3	16896·4	4502·5	2	22203·7
5840·8	3	17116·2	4451·9	2	22456·0
5678·4	1 d	17605·7	4405·5	2	22692·5
5625·0	2	17772·9	4311·9	2	23185·1
5556·0	3	17993·6	4266·2	1	23433·5
5488·0	1	18216·5	4212·4	1	23732 8
5401·8	0	18507·2	4164·4	1	24006·3
5288 7	3 d	18903·0	4128·6	1	24214·5
5244·0	2 d	19064·1			

regularly-spaced bands, covering the region from $\lambda = 6580$ to 4130 Å. As in the cases of sulphur and selenium, this spectrum is quite different from that obtained by Diestelmeier at higher temperatures. However, it appears to be the same spectrum as that described by Rakowicz-Pogorzelska * for tellurium in a paper that has just reached us as we are writing up our results. A plate taken by us at a slightly higher temperature showed the same bands as those listed in the table, but in this case the group of bands of shorter wave-length was the more intense.

Bismuth.

A fluorescence spectrum was excited by the light from the mercury arc in saturated bismuth vapour at a temperature of about 500° C. The wave-lengths of the lines observed are given in Table V. 18 fairly sharp lines were observed in the region from 4890 to 4410 Å.

Table V.—Bismuth.

Wave-length I.A.	Int.	Wave-number cm.$^{-1}$	Wave-length I.A.	Int.	Wave-number cm.$^{-1}$
4890·0	2	20444·2	4635·1	1	21568·5
4872·1	1	20519·3	4620·6	1	21636·2
4823·9	1	20724·3	4602·0	1	21723·6
4799·2	2	20831·0	4574·8	1	21852·8
4773·3	2	20944·0	4554·5	1	21950·2
4752·0	2	21037·9	4536·5	2	22037·3
4731·2	2	21130·4	4511·5	1	22159·4
4683·8	1	21344·2	4473·6	2	22347·1
4663·2	2	21438·5	4416·8	2	22634·5

Summary.

New fluorescent spectra have been found in the vapours of sulphur, selenium, and tellurium, excited by intense illumination with the light from a quartz mercury arc. These are found with saturated vapours at comparatively low temperatures, and are apparently quite different from the fluorescence spectra found for these elements by Diestelmeier and others using superheated vapours. In the case of selenium two distinct spectra have been observed at different temperatures.

A fluorescence spectrum has also been found for bismuth vapour under similar conditions.

* Rakowicz-Pogorzelska, *Comptes Rendus de la Soc. Polonaise de Phys.* vii. p. 51 (1926).

XXXIX. *Studies on Precipitated Magnetite, with Particular Reference to Hysteresis.* *By* Dr. Lars A. Welo, *and* Dr. Oskar Baudisch, *The Rockefeller Institute for Medical Research* *.

[Plate XII.]

In the first part of this paper we shall describe three methods we have used in the preparation of magnetite which, in order to emphasize its mixed character as to the valence of the iron, may be written $FeO \cdot Fe_2O_3$. A brief summary will be given of their physical properties and their particularly interesting properties as chemical and biological catalysts. It will be seen that the three methods of preparation reduce, in principle, to two. In one method, due to Lefort †, precipitation takes place from a solution containing both ferrous and ferric ions and in just the proportion 1 : 2 necessary to form $FeO \cdot Fe_2O_3$, so that no oxidation is necessary during or after the precipitation. In the other two methods, which will be referred to as Haber's ‡ and B. & W.'s §, ferrous iron only is present in the solution from which the hydroxide is precipitated, so that it is necessary to oxidize two-thirds of the iron to the ferric form at the moment of precipitation or at some subsequent time. It will be shown that these two principal methods lead to magnetites which differ mainly as to the size of the average crystal. It is on that basis that we may explain their differences in catalytic activity and absorptive powers for water and oxygen.

In the latter part of the paper their magnetic properties are described with emphasis on the hysteresis. Finally, the decision is reached that, although the oxides differ as to hysteresis characteristics and crystal size, there is no direct relation between these two things. Differences in hysteresis disappear on annealing and are therefore referred to the phenomenon of magnetostriction. In the last section there is described a new method of preparing magnetite : the oxidation of ferrous hydroxide by nitric oxide.

* Communicated by the Authors.

† Lefort, *Compt. Rend. Acad.* xxxiv. p. 488 (1852); lxix. p. 179 (1869).

‡ Haber and Kaufmann, *Z. Elektrochem.* vii. p. 733 (1900-01).

§ Welo and Baudisch, J. Biol. Chem. lxv. p. 215 (1925).

The Preparation of Magnetite.

Lefort's.—281 grams of $Fe_2(SO_4)_3 + 10H_2O$ and 134 grams of $FeSO_4 + 7H_2O$ are separately dissolved in 750 c.c. and 500 c.c. of water, respectively. They are then mixed and poured into a boiling solution of NaOH containing 250 grams of the hydroxide in 3200 c.c. of water. The black mixture formed on the addition of the sulphates is boiled for an hour. The mixture is near-colloidal so that the precipitate does not settle readily. In washing we use the centrifuge. We alternately fill with water and centrifuge until the washings become neutral towards litmus paper. The precipitate is put away to dry, preferably in an evacuated desiccator. It is rather jelly-like and dries slowly and shrinks. When finally dry it breaks up into brittle cakes or lumps which are easily ground into a fine powder.

Haber's.—220 grams of a 20 per cent. solution of ammonia are added to 2200 c.c. of a 10 per cent. solution of crystalline ferrous sulphate and the mixture is brought to the boiling-point. While the mixture is boiling, 25·5 grams of KNO_3 dissolved in as little water as possible is poured in. Boiling is continued for 15 minutes. In contrast to Lefort's magnetite, this material settles rapidly and is easily decanted and washed without use of the centrifuge. We may mention that the decantation can be hurried by holding the containing vessel over a large electromagnet. This magnetite dries rapidly and does not shrink and cake on drying. In other words, the phenomenon of coagulation is not prominent in this method of preparing magnetite.

B. & W.'s.—This method involves the reaction first studied by Baudisch and Mayer *, in which KNO_3 is reduced by freshly-precipitated ferrous hydroxide in the presence of oxygen. Magnetite is formed as a by-product. 26 grams NaOH and 20 grams KNO_3 are dissolved in about 5 litres of water. To this solution is added 90 grams of $FeSO_4 + 7H_2O$ dissolved in 500 c.c. of water. The mixture is first greenish and finally becomes black. As in Haber's method, the precipitate settles rapidly and is easily washed and dried. It is not near-colloidal in its behaviour.

Their Physical, Chemical, and Biological Properties.

Table I. is a summary of the results we have obtained from a comparative study of these magnetites. The numbers in the table are average values. For a given sample the numbers

* Baudisch and Mayer, *Biochem. Z.* cvii. p. 1 (1920).

may depart much from the average. This is especially true as to the ferrous iron content. The theoretical value for ferrous iron, calculated as FeO, in $Fe_3O_4 = FeO \cdot Fe_2O_3$, is 31·03 per cent. In no sample was this attained. The chief precaution necessary seems to be to prevent oxidation during the washing and the drying. It has recently been shown * that, except for colour, the properties of precipitated magnetite are practically independent of the FeO content and that they are, in the main, the same after complete oxidation to Fe_2O_3 at a low temperature. We therefore took no special precaution to prevent over-oxidation other than to dry in an evacuated desiccator. It is to be noted that in Lefort's magnetite the FeO content is less than two-thirds that of Haber's and B. & W.'s. This was our first indication that the crystals in Lefort's are smaller and that they expose a relatively larger surface for oxidation and other actions of the nature of surface phenomena.

The permeabilities were measured by a method we have already described †. Although the maximum permeability of Lefort's magnetite is higher, Haber's and B. & W.'s are really more ferromagnetic because their permeabilities vary differently with the magnetizing field. As we shall show in another section of this paper, the saturation value of the magnetization in Haber's magnetite is of the order twice that of Lefort's. The most striking feature of Table I. when it is considered from the magnetic standpoint is the fact that in Lefort's magnetite the permeability maximum appears at a magnetizing field of 50 to 85 gausses, whereas in Haber's and B. & W.'s it appears at 250 to 300 gausses. It was this observation which led to our detailed study of the hysteresis.

The three magnetites give identical X-ray diffraction patterns as shown in Pl. XII. We have made no direct comparison with the pattern given by natural magnetite.

* Welo and Baudisch, Phil. Mag. l. p. 399 (1925). Sosman and Posnjak, J. Wash. Acad. Sci. xv. p. 329 (1925).

Footnote.—In our paper, two equations contain typographical errors. The last equation but one on p. 402 should read:

$$d_0 = C[(A_e - A_0)H + A_0 \mu H]$$

and the first equation on p. 403 should read:

$$\mu = \frac{A_e}{A_0} R - \frac{A_e - A_0}{A_0}.$$

† Welo and Baudisch, Phil. Mag. l. p. 399 (1925).

TABLE I.

	Magnetite.		
	Lefort's.	Haber's.	B. & W.'s.
Ferrous Iron, per cent. FeO	16·9	26·9	26·7
Impurities, per cent. (mainly occluded sulphates).	0·7	0·1	2·0
Maximum Magnetic Permeability (for packing density of 1·32 $\frac{gr.}{(cm.)^3}$)	3·4	2·8	2·6
Maximum Permeability at Magnetizing Field of ——	50–85	250–300	300
Crystal Unit	Cubic.	Cubic.	Cubic.
Character of Diffraction Lines.....	Diffuse.	Sharp.	Sharp.
Absorption of Water, per cent. ...	2·0	2·1	1·9
Absorption of Oxygen, average initial rate, $\frac{cm.^3}{gr.\ hr.}$.	0·0044	0·0019	—
Blood Test. Oxidation of benzidine hydrochloride by H_2O_2 in presence of——	Good.	Fair.	—
Oxidation of Guajac Resin by H_2O_2 in presence of——	Strong.	Strong.	—
Growth of Bact. lepisepticum in broth and in presence of——	Good.	Fair.	—

But an indirect comparison is possible. We* have shown that ferromagnetic ferric oxide made by oxidizing precipitated magnetite gives the same pattern as the magnetite with which we started. Sosman and Posnjak† have made a direct comparison of ferromagnetic ferric oxide made by oxidation of precipitated magnetite with natural magnetite, and found practically complete identity of pattern except for the line nearest the centre. This line from natural magnetite seemed to be more intense and indicated a greater spacing of these particular diffracting planes by about 2·5 per cent. However, they remarked that "the films are rather weak

* *Loc. cit.*
† *Loc. cit.*

with much scattering (the technique has since been improved) and it cannot be asserted that this one difference is real." In this paper we are not primarily concerned with this question, but rather with a comparison between magnetites prepared in different ways. The patterns are identical, but we note a difference in the character of the lines. Lefort's magnetite gives broad diffuse lines, while the lines given by Haber's and B. & W.'s are relatively sharp. By the Debye-Scherrer relation *

$$B = 2\sqrt{\frac{\log_e 2}{\pi}}\,\frac{\lambda}{D}\cdot\frac{1}{\cos\frac{\theta}{2}} + b$$

connecting line half widths, B, with crystal edges, D, this means that Lefort's magnetite is composed of smaller crystals than the others. This fact has already been assumed in order to account for the smaller FeO content in Lefort's magnetite. It accounts completely for the relative behaviour of the magnetites as absorbers of water and oxygen and for their action as catalysts and biocatalysts as recorded in the last five rows of Table I. The small crystals expose relatively large areas for these actions which take place mainly on the surfaces of the crystals. The crystal size should not be confused with the particle size. The particles of magnetite are porous and are aggregates of a large number of sub-microscopic crystals.

Four of the five absorptive and catalytic actions recorded in Table I. have been described elsewhere † and those interested in them should consult that paper. The Guajac resin test as applied to these magnetites has not yet been published as it is only recently that we have used it. Guajac resin is dissolved in either alcohol or chloroform. A brilliant blue oxidation product appears if blood or finely-powdered magnetite is added with hydrogen peroxide to the resin solution. Hydrogen peroxide alone does not give this blue colour. This test for catalysis is more sensitive than any of the others we have used. In fact, it is so sensitive that, as far as our purely qualitative tests go, Haber's gives just as strong a test as Lefort's magnetite and it does not serve as a means of differentiating between the two.

It is seen that the differences between Lefort's magnetite and the others may be referred, ultimately, to the difference

* Bragg, W. H. and Bragg, W. L., 'X-rays and Crystal Structure,' 4th edition, 1924, p. 133.

† Welo and Baudisch, J. Biol. Chem. lxv. p. 215 (1925).

in size of the average crystal. A difference in crystal size is just what we might expect from a consideration of the precipitation law of von Weimarn. In making Lefort's magnetite we precipitated with a hydroxide from a mixture of $FeSO_4$ and $Fe_2(SO_4)_3$. When making Haber's and B. & W.'s we precipitated from $FeSO_4$ alone. The two cases may be represented by :—

1.

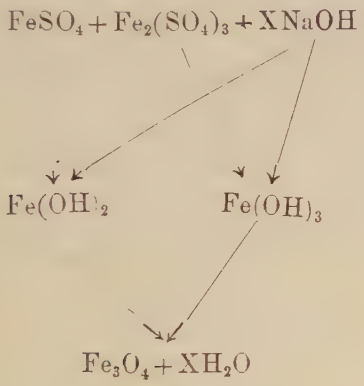

2.

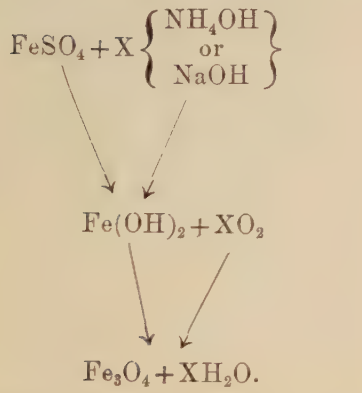

The precipitation law in its simplest form is *

$$\delta = \frac{N_p}{S_p}\eta,$$

where δ is the dispersion coefficient, η the viscosity of the solution and the ratio $\frac{N_p}{S_p}$ is the degree of supersaturation of

* Washburn, 'Principles of Physical Chemistry,' 2nd edition, 1921, p. 433.

the solution. When we are working at approximately the same concentrations, as we did while preparing the three magnetites, the controlling factor, as regards the degree of dispersion, is the solubility, S_p, of the precipitate. $Fe(OH)_3$ is less soluble than $Fe(OH)_2$. When $Fe(OH)_3$ is present, as it is when using Lefort's method, the ratio $\frac{N_p}{S_p}$ and hence δ becomes large. In Lefort's magnetite, δ is in fact so large that the precipitate behaves much like a colloid. It is difficult to dry and in doing so shrinks, cracks, and forms lumps.

The Permeabilities.

The curves showing the permeabilities as functions of the magnetizing fields are very interesting in that the magnetites

Fig. 1.

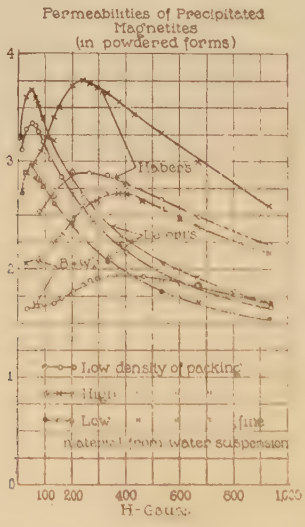

are sharply differentiated as to the position of the permeability maximum. They are shown in fig. 1. The oxides of Lefort and Haber used here were prepared in the usual way. If prepared in the way we have described, B. & W.'s magnetite gives the same kind of permeability curve as Haber's. However, if we vary the method of preparing B. & W.'s magnetite the permeability maximum can be pushed out to a magnetizing field of 380 to 400 gausses as shown in the figure. B. & W.'s magnetite is ordinarily made by pouring

$FeSO_4$ into a *cold* solution of NaOH and KNO_3. The sample studied for the data of fig. 1 was made by pouring $FeSO_4$ into a *boiling* solution of KNO_3 and 20 per cent. excess of NaOH and boiling the mixture for two hours. We had observed that preparation in a hot alkaline solution had this effect, and the sample used for the study recorded in fig. 1 was purposely made in that way in order to provide, as we shall see in a later section, an extreme case of high hysteresis.

The density of packing in the measuring tube was varied as widely as possible in order to make sure that the position of the permeability maximum is not dependent on the density and on the air gaps. The low density represents the packing obtained by jarring the tube containing the magnetite until no shortening took place in the column. The high density was obtained by alternate addition of a small quantity and tamping with a rod. With each addition and tamping the column was lengthened by about 2 mm. A test was made to see if the position of the permeability maximum depends on the grain or particle size. Lefort's magnetite was used and the separation was made in a water suspension. The fine material which remained suspended in water after the coarser material had settled for 3 minutes represents about one-fifth of the total material. In fig. 1 it is seen that, within the limits of the densities attained and of the range of particle size used, the position of the permeability maximum is independent of these two factors.

The densities of packing pertaining to the results shown in fig. 1 are given in Table II.

TABLE II.

	Density of packing, $\frac{gr.}{cm.^3}$.		
	Lefort's.	Haber's.	B. & W.'s.
Low density	1·35	1·42	1·076
High density	1·45	1·84	1·68
Low density, fine material from water suspension.	1·13	—	—

Table II. brings out another difference between Lefort's magnetite and the others. The particles in Lefort's magnetite feel hard and brittle and will pack nearly as well by

mere jarring as by packing. The difference in density between the jarred and the tamped packing density is $\frac{1{\cdot}45-1{\cdot}35}{1{\cdot}40} = 7{\cdot}1$ per cent. Haber's and B. & W.'s magnetites, on the other hand, are fluffy and feel soft and smooth, almost like graphite. The density differences obtained by the two packing methods were, respectively, 25 and 44 per cent.

The Hysteresis.

It has been seen that the magnetites differ as to the position of the permeability maximum. This indicates that

Fig. 2.

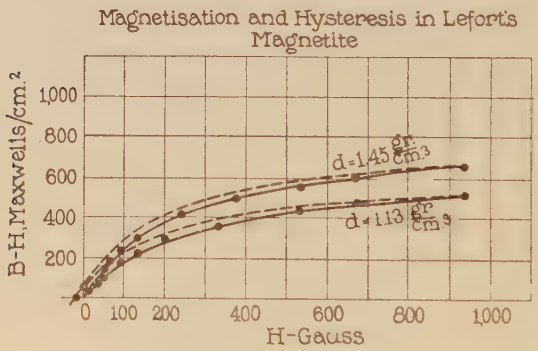

Fig. 3.

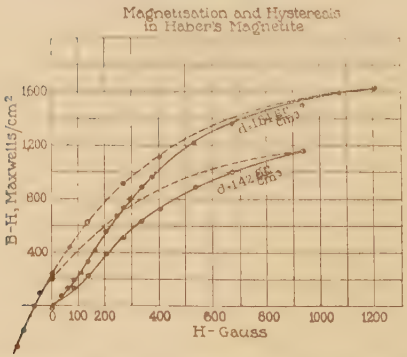

they differ markedly as to hysteresis and this property was therefore studied. The one-point method of Ewing * was used. The results appear in figs. 2, 3, and 4, which also

* Starling, 'Electricity and Magnetism,' 4th edition, 1924, p. 275.

give the magnetization curves obtained from the data used to draw the permeability curves of fig. 1. The whole first quarter of the hysteresis loop was obtained only for Haber's magnetite. With Lefort's and B. & W.'s magnetites the only points determined were those on the B-H axis and those near the axis of H. These are sufficient to determine the two principal quantities, the remanence and the coercivity.

Fig. 4.

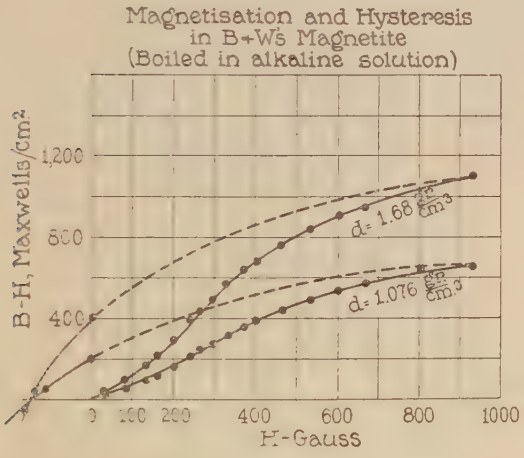

The remaining part of the first quarter of the hysteresis loops for Lefort's and B. & W.'s magnetites was merely sketched in. The areas within the whole hysteresis loops may be considered to be nearly proportional to the areas between the magnetization curve and the first quarter of the loop. These areas were measured with a planimeter. The approximate relative areas for Lefort's, Haber's, and B. & W.'s magnetites were found to be, respectively, as 1, 5, and 7.

Fig. 5 is a large-scale drawing intended to show more clearly the remanences and the coercivities of the three magnetites. All of our measurements are included for the various densities of packing and for various values of the magnetizing field. It is clear that the remanences and the coercivities divide themselves into three groups according to the magnetite used. For Lefort's, Haber's, and B. & W.'s magnetites the average remanences are, respectively, 8, 18, and 34 per cent. The corresponding average values of the coercivities are 14, 67, and 149 gausses.

Fig. 5.

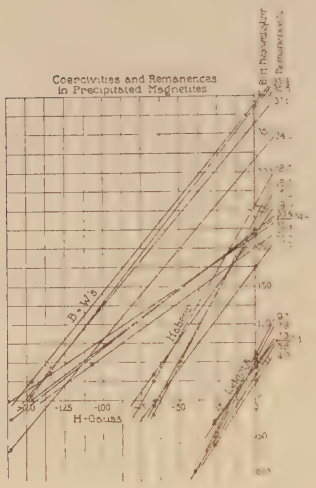

Does Hysteresis depend on Crystal Size?

The idea that the hysteresis loss in ferromagnetic materials depends on the size of the crystal has been advanced by several investigators. The evidence has been contradictory. Yensen * and Gerlach † agree that the hysteresis loss diminishes with increase of crystal size. Edwards ‡ concludes from his experiments with nickel that the relation is the opposite. v. Auwers § finds no relation. Our results with magnetite appeared to have a bearing on this question and seem, on their face, to support the conclusion of Edwards that the hysteresis loss increases with increased crystal size. They were discussed with Dr. L. W. McKeehan, who suggested that the results may have been influenced by magnetostrictive effects brought about by irregularities in the lattices, with consequent internal strains. It is particularly in Lefort's magnetite that these irregularities and strains may appear. The material is precipitated out with great velocity so that the ions do not have time to adjust themselves into the positions required in a perfect lattice. We should keep in mind still another source of strain in Lefort's magnetite. As has been mentioned, Lefort's magnetite is precipitated as a jelly-like substance which shrinks and cracks on drying. The fact that strains develop on

* Yensen, J. Amer. Inst. Elect. Eng. xliii. p. 558 (1924).
† Gerlach, *Phys. Zeit.* xxvi. p. 914 (1925).
‡ Edwards, Phys. Rev. xxvii. p. 252 (1926).
§ v. Auwers, *Phys. Zeit.* xxvi. p. 699 (1925).

drying is obvious. It is doubtful, however, if the strains introduced in this way are large enough appreciably to affect the magnetic properties.

Dr. McKeehan suggested that we should anneal the magnetites and then make observations on the hysteresis. His suggestion was carried out. Magnetite in powdered form must be annealed in a vacuum in order to prevent oxidation. Annealing at 700° C. produced no change. After annealing at 1000° C. the two magnetites tried, Lefort's and Haber's,

Fig. 6.

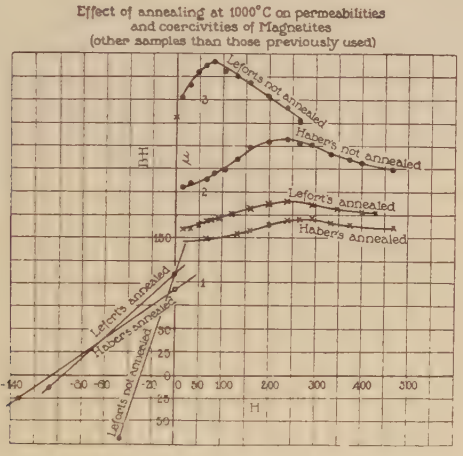

became nearly alike as to the position of the permeability maximum and as to the value of the coercive force. The results appear in fig. 6 *. It seems that Haber's magnetite

* Experiments other than those recorded in fig. 6 deserve mention. Lefort's magnetite which had been used to obtain the data of figs. 1 and 2 was partly reduced to FeO with hydrogen at about 600° C. On exposure to air the cold substance oxidized spontaneously and became hot enough to glow. The temperature of glow was evidently above the annealing temperature. The magnetite had given a permeability maximum at 50 gausses and a coercive force of 14. After partial reduction and spontaneous oxidation the permeability maximum appeared at 260 gausses and the coercive force had become 102 gausses; both in very close agreement with the value for annealed magnetite as shown in fig. 6.

Lefort's and B. & W.'s magnetites were completely reduced to iron with hydrogen at 1000° C. The reduced irons were compared as to coercivity. The respective values found were 20 and 19 gausses. The large differences in coercivity shown by these two magnetites do not appear on reduction to iron. If coercivity were dependent on crystal size one would expect such differences to persist, since both sets of crystals should grow at the same rate during like conditions and like times of reduction. At least, it is highly improbable that the final average size is the same.

is fairly free from strain previous to annealing since the permeability maximum was shifted relatively little. The large effects of annealing appear in Lefort's magnetite. The permeability maximum is shifted from 80 to 250 gausses and the coercive force is changed from about 30 gausses to 95.

We must not ignore the possibility that the crystals in both magnetites grew during the annealing process and that they have here happened to grow to the same average size. The water absorption affords a ready test. It is a measure of the total crystal surface, and is therefore an inverse measure of the average crystal's dimensions. After annealing, Lefort's still absorbs 9·6 per cent. while Haber's absorbs only 2 per cent. As we have found the water absorption to be a reliable inverse index of the crystal size, we are satisfied in our own minds that the average crystals in the two magnetites are not of like size after annealing *. We are not pursuing the matter further. It does not seem worth while to do so as long as no theoretical basis exists for the belief that hysteresis is a function of crystal size.

One question suggested by fig. 6 is still unsettled. Why do not the permeability maxima and the coercivities approach the extreme values found in B. & W.'s magnetite? There are two possibilities. Either the magnetites were not thoroughly annealed or else B. & W.'s magnetite is under strain which is, on the whole, of opposite sign. The first possibility is more probable. The question does not seem to be important enough to merit further investigation.

Another fact brought out in fig. 6 is easily explained. It is noted that both magnetites show much lower permeabilities after they have been annealed. Both magnetites contain Fe_2O_3 in excess of the theoretical amount represented by the formula $FeO \cdot Fe_2O_3$. This excess portion of Fe_2O_3 becomes paramagnetic on heating to 550° C., or more, and serves only to dilute the ferromagnetic part.

* We have tried to test this point by taking X-ray diffraction patterns after annealing. Both Lefort's and Haber's magnetites gave sharp lines indicating that the crystals in Lefort's magnetite had grown beyond the range of size in which line character is a practicable index of crystal size.

The presence of irregularities and strains in Lefort's magnetite, as brought out by the change in hysteresis on annealing, casts some doubt on the value of the diffuseness of the diffraction lines as proof that the crystals in Lefort's magnetite were small before annealing. We do not know how much of the diffuseness is due to irregular lattice planes. The other evidence, however, retains its full validity. A small average crystal is to be expected from the precipitation laws, and it is the most natural way to account for the high water absorption and good catalytic action of Lefort's as compared with the other magnetites.

The Permeability Maximum Shift on Oxidation to Fe_2O_3.

In our paper on "The Two Stage Transformation of Magnetite into Hematite"* we showed that a small shift in the permeability maximum took place when magnetite was oxidized to Fe_2O_3 at a temperature of 300° C. In that particular sample of Lefort's magnetite the shift was from 85 gausses to 65 gausses. We remarked in that paper that no reason was known for this. We have since observed a similar but larger shift in Haber's magnetite. The permeability maximum moved from 250 gausses to 195, a total shift of 55 gausses. This shift in the permeability maximum means, in the light of our later results, that there was in both cases a decrease in the hysteresis. We may infer that there was an increase in the internal strains. We explained the oxidation of magnetite to form Fe_2O_3 without a change in structure by considering that there is room for additional oxygen in the lattice of magnetite. But we found the available room to be rather small. We had to be content with the result that, in magnetite, the radii of some of the iron atoms are reduced to 1·145 Å. The smallest radius which has been observed in iron and in its simple compounds is, as near as we know, about 1·25 Å. In our calculations we assumed the radius of oxygen to be fixed at 0·65 Å. It is evident that if oxygen really enters into combination with magnetite to form Fe_2O_3, it fits in very tightly and the whole structure is seriously strained. It is not strained beyond the point of stability, however, for it is not until oxidized magnetite is heated to 550° C., or more, that it becomes unstable and changes to the usual hematite structure.

Oxidation of Ferrous Hydroxide to Magnetite with Nitric Oxide.

In this, the concluding section of our paper, it appears to be appropriate to record the fact that ferrous hydroxide can be oxidized with nitric oxide, NO, and that the final product is also a magnetite. The method we employed is essentially the same as B. & W.'s described in the first section of this paper. The presence or absence of KNO_3 seems to be immaterial. The solutions were boiled to drive off dissolved oxygen, and the precipitation took place in an oxygen-free hydrogen atmosphere in an apparatus we have designed for

* *Loc. cit.*

working under oxygen-free conditions *. After precipitation, NO gas was bubbled through the mixture. The precipitate, which was white at first, turned green and finally became black. The washed and dried precipitate is magnetite. Its diffraction pattern is shown in Pl. XII. Its magnetic and other physical properties are those of Haber's and B. & W.'s magnetites. The resemblance to these magnetites rather than to Lefort's was to be expected since ferrous hydroxide alone was precipitated and a part of it subsequently oxidized. In this case the oxygen was obtained by reduction of NO. The free nitrogen passed off as a gas.

March 27, 1926.

Notes added on reading Proof:—

(1) Gerlach has recently also come to the conclusion that it is not the size of the crystal but rather its quality which controls the hysteresis loss in ferromagnetic materials. He says: "Nicht die Grösze der Kristallite (oder ihre Zahl pro Volumeneinheit) ist in erster Linie für die Magnetischen Eigenschaften maszgebend, sondern die Güte ihrer Ausbildung." *Zeit. f. Phys.* xxxix. p. 327 (1926).

(2) It has been suggested by those who have read our paper in the manuscript that the results may have been influenced by small amounts of impurities. They had in mind particularly the presence of KNO_3 when preparing Haber's and B. & W.'s magnetites, whereas this salt is not used when preparing Lefort's magnetite. We have prepared magnetite by precipitating ferrous hydroxide alone and oxidizing part of it by bubbling with oxygen. No KNO_3 was used. The product corresponded to Haber's and B. & W.'s magnetites in every way. The permeability maximum appeared at from 250 to 300 gausses, and the remanence and the coercivity were, in general, the same as in Haber's and B. & W.'s. It is, therefore, not the presence of potassium ions or nitrates which give to Haber's and B. & W.'s magnetites the large hysteresis losses as compared with Lefort's magnetite.

* Baudisch and Welo, J. Biol. Chem. lxiv. p. 757 (1925).

XL. *Determination of the Lattice Spacing and of the Rhombohedral Angle of Magnesium Carbonate from a Microcrystalline Powder.*

By J. Brentano, *D.Sc., Lecturer in Physics, Manchester University, and* W. E. Dawson, *B.Sc., Research Student, Manchester University* *.

Summary.

A determination of the lattice constants of magnesium carbonate is undertaken with the purpose of securing a more exact measurement of the rhombohedral angle and of the spacing of the member of the calcite series of carbonates farthest away from calcite. The determination is carried out with a microcrystalline powder using an X-ray method previously described by one of the writers. The result is discussed in connexion with recent theoretical calculations of the lattice constants of the isomorphous series of carbonates of calcite type.

EXACT determinations of the lattice constants of crystals have assumed a particular interest in connexion with work referring the physical properties of crystals to their lattices.

Professors W. L. Bragg and S. Chapman † and S. Chapman, J. Topping, and J. Morrall ‡ have calculated the rhombohedral angles of the members of the isomorphous series of carbonates forming the calcite group. While the crystallographic data belonging to calcite are well known §, information concerning the carbonates of the lighter elements is less abundant, owing to imperfect growth of their crystals. For this reason a determination has been undertaken by X-ray methods of the lattice constants of magnesium carbonate, which in order of molecular volume stands farthest from calcite in the series. The X-ray determination has the advantage over

* Communicated by Prof. W. L. Bragg, F.R.S.

† W. L. Bragg and S. Chapman, Proc. R. Soc. vol. cvi. p. 369 (1924).

‡ S. Chapman, J. Topping, and J. Morrall, Proc. R. Soc. A, vol. cxi. p. 25 (1926).

§ A verification of the rhombohedral angle for calcite has recently been made by H. N. Beets, Phys. Rev. vol. xxv. p. 621 (1925), by observing the reflexions from lattice planes parallel to the cleavage faces of a large crystal.

the goniometric measurement of giving more direct information of the lattice constants, unaffected by any deviation of the cleavage faces of the crystal and of being applicable to very imperfect crystals when a powder method is used.

X-ray determinations confirming the structure of magnesium carbonate have been made respectively by W. L. Bragg using the ionization spectrometer with a single crystal * and by R. C. Wyckoff† using the Laue method, whilst a determination of the edge a of the elementary cleavage rhomb and also of the molecular volume has been made by Levi and Ferrari with a crystal powder using the Debye method ‡. The rhombohedral angle α was not, however, determined in these experiments, and the value $\alpha = 103° 21'$, commonly given, originates from a goniometric determination by Schröder §.

The determination of the rhombohedral angle from experimental data can be based on the relation

$$d_{hkl} = \frac{a\sqrt{1+2\cos^3\alpha-3\cos^2\alpha}}{\sqrt{(h^2+k^2+l^2)\sin^2\alpha+2(hk+kl+hl)(\cos^2\alpha-\cos\alpha)}},$$

holding good for a trigonal system of axes, where d_{hkl} is the spacing of the planes with the indices hkl.

By measuring the values of two different spacings of d_{hnl}, a and α can be calculated.

The difficulty in calculating α lies in the fact that for values not far from 90° a small change in α has little effect on the relative values of any two spacings d_{hkl}. It proved best therefore to effect the determination of α by utilizing a greater number of spacings. Special precautions had further to be taken to ensure their exact measurement. Some details of the method may therefore be discussed.

The crystals were examined in the form of a powder with the arrangement described by one of us ‖, in which a thin plane layer of powder moving at varying speed is used in conjunction with a rotating slit.

The magnesite examined was of fine microcrystalline structure (magnesite compatta del Senese) and was kindly given to us by Prof. Levi, who had found it to be practically free from impurities.

* W. L. Bragg, Proc. R. Soc. vol. lxxxix. p. 468 (1914).

† R. C. Wyckoff, Am. Journ. Science, vol. l. p. 317 (1920).

‡ G. R. Levi and A. Ferrari, *Rend. Lincei,* vol. xxxiii. ser. 5. p. 516 (1924).

§ Schröder, *Pogg. Ann.* (4) vol. xvi. p. 226 (1859).

‖ J. Brentano, Proc. Phys. Soc. London, vol. xxxvii. p. 184 (1925).

Copper K_α radiation was used, the β and γ components having been greatly reduced by passage through a Nickel filter. Owing to the small absorption of X-rays in magnesium carbonate, the layer of crystal powder had to be made 0·2 mm. thick with a consequent broadening of the lines. In order that this broadening should not be detrimental to the determination of their position, powder of nickel oxide in the ratio of two parts by weight of nickel oxide was added to every five of magnesium carbonate. The intensity distribution over the nickel oxide lines was then much the same as that over those of magnesium carbonate, and the positions of the latter were determined in terms of those of the first. The procedure consisted in calculating the glancing angles of the nickel oxide reflexions and plotting them against the corresponding distances measured on the photographic film; the angles of the different magnesium carbonate reflexions can so be found from their positions on the film by a graphical method. By interposing in this manner the lines due to the nickel oxide reflexions, not only can the effect of the width of the lines arising from the thickness of the layer be counteracted, but also errors due to any divergence of the photographic film from the correct position with respect to the setting of the powder layer and to its axis of rotation can be eliminated.

For such comparative measurements the indirect way of using nickel oxide is preferable to adding sodium chloride, owing to its greater reflecting power per unit volume, and for this purpose a determination of the lattice constant of nickel oxide in terms of rock-salt had been previously made by one of us* giving $d_{100}=4{\cdot}172\pm0{\cdot}005$ Å. A more exact determination recently made in a similar way, gave $d_{100}=4{\cdot}1705$, which agrees with the former value within the margin of error claimed. This latter value was used in calculating the glancing angles of the nickel oxide reflexions and so also in determining those of magnesium carbonate. The table gives in the first column the $\log\sin\theta$ of the glancing angles θ found in this way for the magnesium carbonate reflexions, which were used in the calculation of the lattice constants. These reflexions were the best for accurate measurement, the lines being neither broadened by over exposure nor too faint.

For determining the rhombohedral angle α the relation

$$\sin\theta=\frac{\lambda}{2a\sin\alpha\sin\epsilon}\sqrt{(h^2+k^2+l^2)-2(hk+kl+hl)\cos\epsilon}$$

was employed, where hkl are the indices corresponding to

* J. Brentano, *loc. cit.*

any particular reflexion and ϵ is the angle between the adjacent faces of the rhomb, connected with the rhombohedral angle α by

$$\cos\epsilon = \frac{\cos\alpha - \cos^2\alpha}{\sin^2\alpha}.$$

For $\alpha = 103^\circ\ 21'$ is found $\epsilon = 107^\circ\ 29'$ and so a diagram was prepared, in which for different indices the quantity L_{hkl},

$$L_{hkl} = \log[(h^2+k^2+l^2) - 2(hk+kl+hl)\cos\epsilon],$$

was plotted against ϵ for values between $106^\circ\ 31'$ and $108^\circ\ 30'$ for all eligible indices. The curves corresponding to any given indices were sensibly straight lines over this interval and were drawn as such. Fig. 1 is a reproduction on a reduced scale of the central part of this graph, which was originally drawn on a scale in which 10 cm. represented a change of 1° in ϵ. The L values are drawn as abscissæ, the distance between two arrows corresponding to a change of the logarithm by 0·1, and the angle ϵ is taken as ordinate.

By plotting the values of $2\log\sin\theta$ of the magnesite reflexions on the same scale along the straight edge of a strip of paper and applying this to the graph, the position was found in which each line on the strip most nearly coincided with a curve of the graph, following the procedure introduced by Hull. The best fit gave $\epsilon = 107^\circ\ 26'$. For this setting the actual readings for the values of the L curves associated with the magnesium carbonate reflexions are given in the second column of the table. Expressing the distances between the lines on the strip and the curves on the graph in terms of the glancing angles θ the greatest discrepancy is $\Delta\theta = 1{\cdot}5'$, which falls within the limit of the possible error in determining the positions of the lines on the photograph. The indices of the magnesium carbonate lines are given in the last column of the table. In some cases the curves on the diagram were so close that two indices fit equally well.

From the value $\epsilon = 107^\circ\ 26'$ the rhombohedral angle α is calculated to be $103^\circ\ 19'$, which confirms the value found goniometrically by Schröder. By means of the graph it was possible to utilize the whole group of magnesium carbonate lines on which exact measurements had been made, to derive a value for d_{100} and in this way was found $d_{100} = 5{\cdot}477 \pm 0{\cdot}005$Å.

Comparing the results of our experiment with the result of the theoretical calculation, we see that W. L. Bragg and

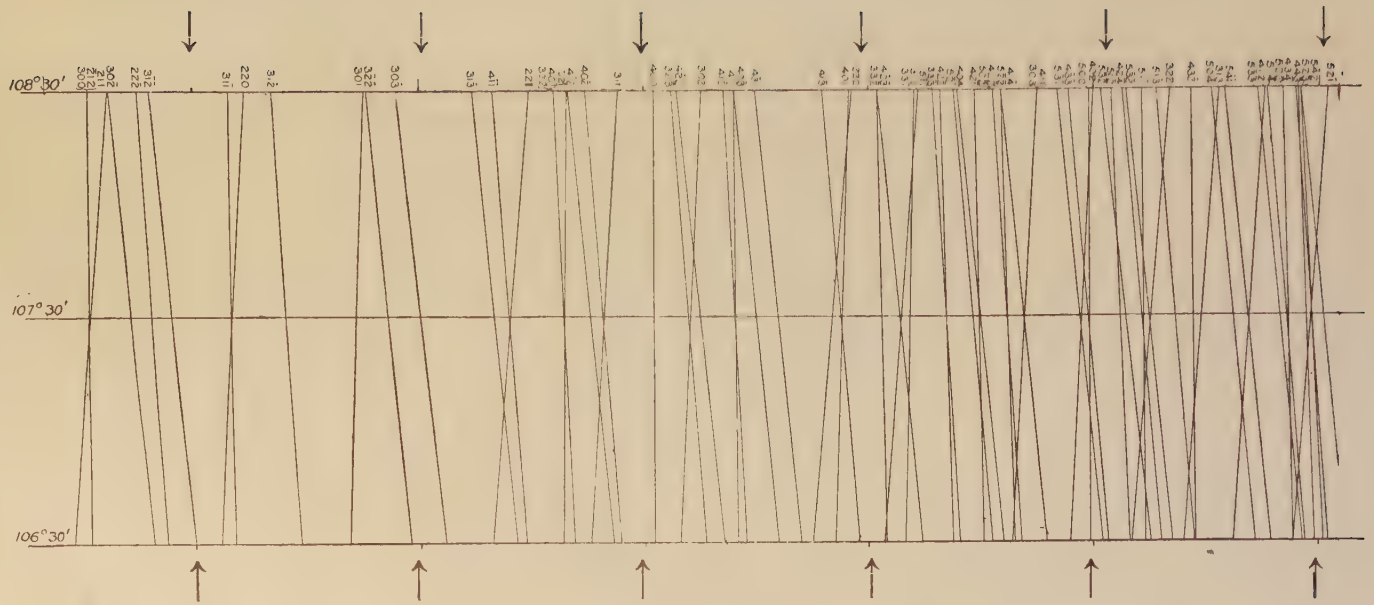

Fig. 1.

Table.

Log sin θ.	$\frac{L}{2}$.	Indices.
9·6378	9·6380	$22\bar{2}$
9·7140	9·7142	$31\bar{3}$
9·7383	9·7383	$40\bar{2}$
9·7492	9·7493	400
9·7600	9·7601	$4\bar{2}\bar{2}$
9·7889	9·7887	222
9·8147	9·8146	$42\bar{2}$ $33\bar{3}$
9·8535	9·8533	$51\bar{2}$
9·8583	9·8582	$42\bar{4}$ $51\bar{1}$

S. Chapman arrive at values for the rhombohedral angles which follow closely the changes of those angles observed through the series of the carbonates, but the numerical values of which are about four degrees greater than the values obtained from measurement. This result is obtained assuming a fixed value 1·25 Å for the distance b between the oxygen and carbon atoms in the CO_3 group and assuming "contact" between the atoms with respect to repulsive forces, the condition of minimum potential energy of the electrostatic fields being responsible for the position of equilibrium. It is shown in addition, that a close numerical agreement can be obtained, when a smaller value for b is assumed, which however is not in accord with the result of X-ray intensity measurements for calcite. In the paper by S. Chapman, J. Topping, and J. Morrall a polarized O ion is considered, for which evidence is given. In this way a smaller effective value for the parameter b can be introduced without affecting the value responsible for X-ray intensities. The values of the rhombohedral angles so calculated, assuming the parameter $b = 0{\cdot}92$ Å, are 102° 4′ for calcite and 103° 28′ for magnesium carbonate, while the experimental values are 101° 55′ and 103° 19′ respectively, referring for magnesium carbonate to the present determination. The rhombohedral angle of magnesium carbonate was calculated by Chapman, Topping, and Morrall assuming the distance between adjacent Mg atoms to be 4·61 Å. From the present experimental determination this distance is found to be 4·627 Å and using this value in the calculation the theory gives the rhombohedral angle 103° 24′. The difference between the calculated and the experimental values of the rhombohedral angles becomes thus

9′ for calcite and 5′ for magnesium carbonate; the calculated value being in each case greater. If we are allowed to confine ourselves to these two carbonates and to assume that the more irregular discrepancies of the other members of the series could be attributed to the uncertainty of the experimental values,—in the first place probably in determining the density and the lattice spacings—a small reduction in the size of the CO_3 group could bring perfect agreement between the theoretical and the experimental result within the margin of error of observation. We may consider this as confirming the hypothesis made in the theoretical calculation of Bragg and Chapman, that the effective dimensions of the CO_3 group remain unchanged through the whole series of the carbonates. In bringing the experimental finding in this relation to the theoretical result, we must not overlook that the theory in arriving at numerical results involves a number of definite assumptions and the possible departure from one of them has to be considered. For instance, it is assumed that for all ions including the polarized O ion, the centre of the attractive forces coincides with the centre of the repulsive forces; it is shown by Chapman, Topping, and Morrall that the effect of a relative displacement is small, still it may not be permissible to neglect these possible effects, when drawing close numerical relations.

From the value for the spacing $d_{100}=5{\cdot}477$ Å and from the rhombohedral angle the edge of the elementary cleavage rhomb is calculated from the relation

$$a=\frac{d_{100}}{\sin\alpha\sin\epsilon}$$

to be $a=5{\cdot}899$ Å, and its volume from the relation $v=a^3\sin^2\alpha\sin\epsilon$ to be $v=1{\cdot}854\pm0{\cdot}015\,.\,10^{-22}$ cm.^{3} Now this volume includes four molecules of magnesium carbonate, and with the molecular weight equal to 84·325 and the mass of the H atom equal $1{\cdot}662\,.\,10^{-24}$ the density results $\rho=3{\cdot}000$ g./cm.^{3}.

The accepted values obtained for magnesite from direct density measurements range from 3·0 to 3·1 g./cm.^{3}; the higher value directly observed may be partly due to impurities of greater density. The present value for magnesium carbonate is also lower than the value 3·08 found by Levi and Ferrari from X-ray measurements, corresponding to the lower value found by them for the spacing d_{100}, viz. 5·420 Å, as compared with our value of 5·477 Å.

In the course of our experiments we have had the opportunity of taking exposures with another variety of magnesite, Giobertite found in Casellette (Piemont), which shows a coarse structure. The glancing angles stood in good agreement with those determined with the magnesite from the Senese. We were unable, however, to confirm an observation made by Levi and Ferrari, that the lines obtained from the latter variety were broader, thus indicating an extremely fine microcrystalline structure *.

In conclusion we wish to thank Prof. W. L. Bragg, F.R.S., for facilities placed at our disposal during the course of this investigation. We are also obliged to Prof. Levi for the specimens of magnesite.

XLI. *The Bending of Columns of varying Cross-section.* By J. A. Wilcken, *B.Sc., Ph.D., Lecturer in Electrical Engineering at Armstrong College, Newcastle-upon-Tyne* †.

In connexion with the mechanical design of Transmission lines, the question arises as to the stability of the supporting structures, such as wooden or concrete masts and steel-frame towers. It is obvious that the assumption of a purely transverse load, due to the horizontal pull of the conductors, is inadequate, and a closer investigation of the problem involves the consideration of the structure as a column, and requires, therefore, an extension of the classical theory to deal with the universally adopted type of a column of non-uniform cross-section. Such columns are also widely used in architecture, mainly for artistic reasons, and it is of interest to note that some of the most important problems of this class are amenable to rigorous analysis, under the assumptions customary in structural engineering.

The question of the symmetrically tapering strut, now prominent in connexion with aeroplane design, has received

* In a discussion Prof. Levi suggested that the effect observed might be due to the comparatively great penetration of Cu K radiation in magnesium carbonate, so that by using a rod of powder as he did, the lines could be more or less broadened according to the experimental conditions. It also seems possible that one of the varieties is more likely than the other to break up into minute fragments during the process of grinding and that we did not perhaps push this process so far as to produce this effect, which has to be avoided when fine lines are desired.

† Communicated by the Author.

much attention in recent years*, mainly with a view to establishing the correct shape of a strut of uniform stress, but the conditions obtaining, and the methods employed, differ essentially from those of our problem.

The present investigation follows the lines of Euler's theory, leaving out of consideration the numerous empirical formulæ that have been suggested as alternatives; and the results are obtained by exact integration of the relevant differential equations, and may therefore be expected to possess the same range of application, as defined by

(1) the deflexions being small enough to admit of the approximate expression $\frac{d^2y}{dx^2}$ for the curvature, as in the ordinary theory of bending;

(2) the shortening due to bending and compression being negligible.

To approach the general problem, we consider first the simple case of a purely axial load; the extension to eccentric and oblique loading, applicable to masts and supporting towers, will be given in a subsequent publication.

Axial Load.

(A)—*A column simply supported at both ends.* The equation of bending moment is written in the usual notation,

$$\mathrm{EI}\frac{d^2y}{dx^2}+\mathrm{P}y=0, \quad . \quad . \quad . \quad . \quad . \quad (1)$$

E being the modulus, I the moment of inertia of the cross-section at x from one end, y the deflexion, and P the load; the solution being subject to the conditions

$$y_{/0}=y_{/l}=0 \quad . \quad . \quad . \quad . \quad . \quad . \quad . \quad (2)$$

The equation (1) is of the type

$$\frac{d^2y}{dx^2}+n^2y=0, \quad . \quad . \quad . \quad . \quad . \quad . \quad (3)$$

where n^2 is a (real) function of x, and the integral to this equation can be obtained in finite form in two cases, namely, when

$$\text{(i.)}\ n^2=(\alpha+\beta x)^{-4}, \quad \text{or} \quad \text{(ii.)}\ n^2=(\alpha+\beta x)^{-2}.$$

* Wallace, 'Engineering,' xciv. p. 831 (1912). Morley, *ibid.* xcvii. p. 567 (1914). Bairstow and Stedman, *ibid.* xcviii. p. 403 (1914). For a more complete bibliography the reader is referred to modern text-books, *e.g.*, Case, 'Strength of Materials,' Arnold. Salmon, 'Columns,' Oxford, U.P. And, for the older literature, Todhunter and Pearson, 'History of the Theory of Elasticity,' Camb., U.P.

These two forms cover, in our problem, in the first instance the cases of a solid square or circular cross-section, for which the moment of inertia is proportional to the fourth power of the linear measure, with either (i.) a linear or (ii.) a parabolic variation of the radius or side, corresponding to a "straight tapering" or "bulging" solid column, respectively.

Denoting by S the area, and by k the radius of gyration of the cross-section, and writing $I = Sk^2$, it is seen that the relations (i.) and (ii.) refer also to the usual type of braced lattice-work column, in which the cross-section of the main members is constant and their distance varies, in the manner that (ii.) represents a linear variation of k, and (i.) corresponds to a concave outline of the column. It is thus seen that, by a suitable choice of constants, the most important types of structures are included.

The solutions to the equation (1) have been given elsewhere *, together with a brief discussion, of which a summary is here added.

(i.) $P/EI = (\alpha+\beta x)^{-4}$. The solution may be written

$$y = C(\alpha+\beta x)\sin(\chi-\chi_0), \quad . \quad . \quad . \quad . \quad (4)$$

where

$$\left.\begin{aligned} \chi &= (\alpha\beta+\beta^2 x)^{-1} \\ \chi_0 &= (\alpha\beta)^{-1} \end{aligned}\right\}, \quad . \quad . \quad . \quad . \quad . \quad (5)$$

thus satisfying the condition $y/^0 = 0$. The second condition, $y/^l = 0$, requires

$$l/\alpha(\alpha+\beta l) = n\pi,$$

n being any integer, and leads, after substituting

$$\left.\begin{aligned} \alpha &= (EI_0/P)^{1/4} \\ \alpha+\beta l &= (EI_1/P)^{1/4} \end{aligned}\right\}. \quad . \quad . \quad . \quad . \quad . \quad (6)$$

to the value for "the crippling load" in the Eulerian sense.

$$P_1 = \pi^2 E \sqrt{I_0 I_1}/l^2, \quad . \quad . \quad . \quad . \quad . \quad (7)$$

where I_0 and I_1 are the moments of inertia at the ends.

We thus have that the crippling load of a column of type (i.) depends on the geometric mean of the extreme moments of inertia.

(ii.) $P/EI = (\alpha+\beta x)^{-2}$. The equation (1) integrates into

$$y = C(\alpha+\beta x)^{1/2}\sin(\chi-\chi_0), \quad . \quad . \quad . \quad . \quad (8)$$

* Proc. Durham Phil. Soc. vii. 3, p. 125.

where

$$\left.\begin{aligned} \chi &= \mu \log (\alpha+\beta x), \\ \chi_0 &= \mu \log \alpha, \\ \mu &= \sqrt{\beta^{-2}-1/4}, \end{aligned}\right\} \quad . \quad . \quad . \quad . \quad . \quad . \quad (9)$$

supposing μ real, or $\beta^2<4$. The condition $y/^l=0$ leads to

$$\mu \log (1+\beta l/\alpha)=n\pi,$$

and thus gives, for the crippling load,

$$P_1=(E/l^2)(\sqrt{I_1}-\sqrt{I_0})^2\{(\pi/\log \sqrt{I_1/I_0})^2+1/4\}. \quad (10)$$

We proceed to discuss the above results more in detail, considering first the type (i.). Defining by

$$\rho_1=(I_1/I_0)^{1/4}=1+\beta l/\alpha, \quad . \quad . \quad . \quad . \quad (11)$$

what may be termed the taper-ratio, we write

$$P_1=\rho_1^2\pi^2 E I_0/l^2, \quad . \quad . \quad . \quad . \quad . \quad (12)$$

showing that the strength of a tapering column, for the loading and supports as specified, is ρ_1^2 times the strength of a uniform column on the same base.

The volume of a solid straight tapering column bears to that of a uniform column, on the same base, the ratio $(1+\rho_1+\rho_1^2)/3$, and the volume of a tapering column bears to that of an equally strong uniform column the ratio $(1+\rho_1+\rho_1^2)/3\rho_1$; the tapering solid column, when simply supported, is therefore not economical.

Introducing the notation, of which frequent use will be made,

$$l/\alpha(\alpha+\beta l)=\lambda, \quad . \quad . \quad . \quad . \quad . \quad . \quad . \quad . \quad (13)$$

$$\begin{aligned} (\alpha\beta)^{-1}-(\alpha\beta+\beta^2 x)^{-1} &= x/\alpha(\alpha+\beta x), \\ &= (\lambda\rho_1 x/l)/\{1-(1-\rho_1)x/l\}, \quad (14) \end{aligned}$$

the deflexion may be written, for the crippling load $\lambda=\pi$,

$$y=C\{1-(1-\rho_1)x/l\} \sin [(\pi\rho_1 x/l)/\{1-(1-\rho_1)x/l\}], \quad . \quad . \quad . \quad . \quad . \quad . \quad (15)$$

and the point of maximum deflexion determined in the usual way by differentiation, which leads to an equation of the form

$$u \cot u=(1-\rho_1)x/l, \quad . \quad . \quad . \quad . \quad . \quad (16)$$

where u stands for the argument of the sine function in (15).

The function $u \cot u$, which occurs frequently in connexion with this work, is tabulated and represented graphically in the Appendix *.

* The function $(\tan x)/x$ is found in Jahnke u. Emde, *Funktionen-Tafeln,* but for a range insufficient for our purpose.

The solution to the equation (16) can then be found graphically as follows.

Plot $(\pi\rho_1 x/l)/\{1-(1-\rho_1)x/l\}$ for any given value of ρ_1, as abscissæ, choosing some probable values of x/l; plot corresponding values of $(1-\rho_1)x/l$ as ordinates, and by means of the tables plot to the same vertical scale the corresponding values of $u\cot u$; the intersection with the function $(1-\rho_1)x/l$ determines the solution.

As an example is shown the determination of the point of maximum deflexion for a taper-ratio 0·5, plotting the points corresponding to $x/l=0{\cdot}5$, 0·6, 0·7.

The point is at $x/l=0{\cdot}6$.

Fig. 1.

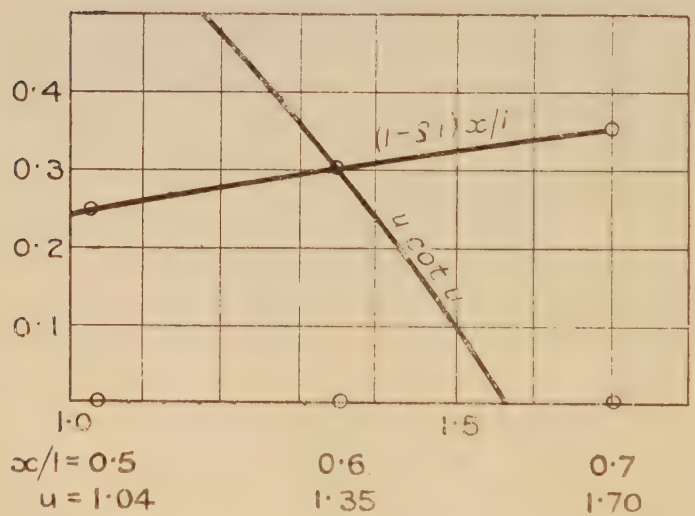

(ii.) When $P/EI=(\alpha+\beta x)^{-2}$ it is more convenient to define the taper-ratio by

$$\rho_2=(I_1/I_0)^{1/2}=1+\beta l/\alpha, \quad . \quad . \quad . \quad . \quad (17)$$

and in this notation the crippling load is written

$$P_1=(1-\rho_2)^2\{(1/\log\rho_2)^2+1/4\pi^2\}(\pi^2 EI_0/l^2). \quad . \quad (18)$$

As above, the classical formula appears as a special case, for $\rho=1$.

When $\beta^2\geq 4$, μ is imaginary; the solution to the fundamental equation involves real exponentials or hyperbolic functions, and the boundary conditions are not satisfied for

any finite value of the integration constants. The physical interpretation is, obviously, that the column cannot be maintained in a bent position by the corresponding load. Since, however, the condition for real μ, or $\beta^2<4$, is equivalent to

$$(EI_0/Pl^2)(1-\rho_2)^2<4,$$

or, with an obvious notation,

$$P>P_0=(1-\rho_2)^2EI_0/4l^2, \quad . \quad . \quad . \quad . \quad (19)$$

and therefore provides a limit for P less than that determined by (18), the case is mainly of theoretical interest. It is worth noting that, for $\rho_2=1$, P_0 vanishes, and for very small values of ρ_2—of the order 10^{-6}—P_0 approaches P_1.

For the limiting value $\beta^2=4$, the equation integrates into

$$y=(\alpha+\beta x)^{1/2}\{A\log(\alpha+\beta x)+B\}. \quad . \quad . \quad (20)$$

Comparing the volume of a solid column of this type to that of a uniform column on the same base, a simple integration gives the volume-ratio $(1+\rho_2)/2$. Defining the strength-ratio from (18) by

$$\sigma_2=(1-\rho_2)^2\{(1/\log\rho_2)^2+1/4\pi^2\},$$

we find that the volume of a solid column of type (ii.) bears to that of an equally strong uniform column the ratio $(1+\rho_2)/2\sqrt{\sigma_2}$.

Adopting the notation

$$\lambda=\mu\log\rho_2, \quad . \quad . \quad . \quad . \quad . \quad . \quad (21)$$

the deflexion at any point may be written, similarly to above,

$$y=C\{1-(1-\rho_2)x/l\}^{\frac{1}{2}}\sin[\lambda\log\{1-(1-\rho_2)x/l\}/\log\rho_2], \quad . \quad . \quad . \quad . \quad . \quad (22)$$

and the point of maximum deflexion is determined by

$$\cot[\lambda\log\{1-(1-\rho_2)x/l\}/\log\rho_2]=-(1/2\pi)\log\rho_2. \quad (23)$$

(B)—*A column built in at one end and free at the other end.* The equation to the bending-moment is now

$$EI\frac{d^2y}{dx^2}+P(y-h)=0, \quad . \quad . \quad . \quad . \quad . \quad (24)$$

with the boundary conditions

$$y/^0=\frac{dy}{dx}\Big|^0=0, \quad y/^l=h. \quad . \quad . \quad . \quad . \quad (25)$$

The taper-ratios are taken less than unity throughout.

Fig. 2.

(i.) $P/EI=(\alpha+\beta x)^{-4}$. The solution may be written in the form

$$y=h+(\alpha+\beta x)\{A\cos\chi+B\sin\chi\}, \quad . \quad . \quad . \quad (26)$$

and the conditions (25) are equivalent to

$$A\cos\chi_0+B\sin\chi_0+h/\alpha=0, \quad . \quad . \quad . \quad (27)$$

$$A\Big(\beta\cos\chi_0-\alpha\sin\chi_0\cdot\frac{d\chi}{dx}\Big|^0\Big)+B\Big(\beta\sin\chi_0+\alpha\cos\chi_0\cdot\frac{d\chi}{dx}\Big|^0\Big)$$

$$=0,$$

or, since

$$\frac{d\chi}{dx}\Big|^0=-\alpha^{-2},$$

$$A(\beta\cos\chi_0+\frac{1}{\alpha}\sin\chi_0)+B(\beta\sin\chi_0-\frac{1}{\alpha}\cos\chi_0)=0, \quad . \quad (28)$$

and

$$A\cos\chi_1+B\sin\chi_1=0. \quad . \quad . \quad . \quad . \quad (29)$$

The consistency of these equations requires the vanishing of the determinant

$$\begin{vmatrix} \cos\chi_0 & \sin\chi_0 & h/\alpha \\ \cos\chi_1 & \sin\chi_1 & 0 \\ \beta\cos\chi_0+\frac{1}{\alpha}\sin\chi_0 & \beta\sin\chi_0-\frac{1}{\alpha}\cos\chi_0 & 0 \end{vmatrix}$$

or, after reduction,

$$\beta\sin(\chi_0-\chi_1)-\frac{1}{\alpha}\cos(\chi_0-\chi_1)=0.$$

In our previous notation, by (13) and (14), this becomes

$$\lambda\cot\lambda=-(1-\rho_1)/\rho_1 \quad . \quad . \quad . \quad . \quad (30)$$

and, by means of the tables in the Appendix, the solution is easily found for any given taper-ratio. As an example,

the values of λ corresponding to $\rho_1=0{\cdot}1,\ 0{\cdot}2\ \ldots\ 0{\cdot}9$ are given below, together with the corresponding ratios $\eta=\lambda/(\pi/2)$.

$\rho_1=$	0·1	0·2	0·3	0·4	0·5	0·6	0·7	0·8	0·9	1·0
$(1-\rho_1)/\rho_1=$	9·000	4·000	2·333	1·500	1·000	0·667	0·429	0·250	0·111	0·000
$\lambda=$	2·84	2·57	2·35	2·18	2·03	1·91	1·80	1·71	1·63	1·57
$\eta=$	1·80	1·63	1·50	1·38	1·30	1·21	1·15	1·09	1·04	1·00

We may thus write the crippling load

$$P_1=\eta^2\pi^2E\sqrt{I_1I_0}/4l^2, \quad . \quad . \quad . \quad . \quad . \quad (31)$$
$$=\eta^2\rho_1{}^2\pi^2EI_0/4l^2,$$

and the classical formula is obtained from this, taking $\eta=\rho_1=1$.

To determine the deflexion and the bending moments, the integration constants are found from the equations (27) and (29). Thus

$$B=-A\cot\chi_1$$

and, substituting,

$$A=(h/\alpha)\sin\chi_1\operatorname{cosec}\lambda,$$

whence

$$B=-(h/\alpha)\cos\chi_1\operatorname{cosec}\lambda,$$

and so,

$$y=h+(\alpha+\beta x)\ (h/\alpha)\operatorname{cosec}\lambda\sin(\chi_1-\chi).$$

Substituting here

$$\chi_1-\chi=(x-l)/(\alpha+\beta x)\ (\alpha+\beta l),$$
$$=-\lambda(1-x/l)/\{1-(1-\rho_1)x/l\},$$

we have,

$$y=h\left[1-\ 1-(1-\rho_1)x/l\}\operatorname{cosec}\lambda\sin\left\{\lambda\cdot\frac{1-x/l}{1-(1-\rho_1)x/l}\right\}\right]$$
$$. \quad . \quad . \quad . \quad . \quad (32)$$

and thus the bending-moment becomes,

$$-Ph\{1-(1-\rho_1)x/l\}\operatorname{cosec}\lambda\sin\left\{\lambda\cdot\frac{1-x/l}{1-(1-\rho_1)x/l}\right\}.$$

The maximum bending-moment occurs at $x/l=0$.

(ii.) Passing now to the bulging column, $P/EI=(\alpha+\beta x)^{-2}$, the solution may be written

$$y=h+(\alpha+\beta x)^{1/2}\{A\cos\chi+B\sin\chi\}, \quad . \quad . \quad (33)$$

where

$$\chi=\mu\log(\alpha+\beta x), \quad . \quad . \quad . \quad . \quad . \quad (34)$$

in case μ is real. The boundary conditions require the vanishing of the determinant

$$\begin{vmatrix} \cos\chi_0 & \sin\chi_0 & h/\sqrt{\alpha} \\ \cos\chi_1 & \sin\chi_1 & 0 \\ \cos\chi_0 - 2\mu\sin\chi_0 & \sin\chi_0 + 2\mu\cos\chi_0 & 0 \end{vmatrix}$$

or, the equivalent,

$$\sin(\chi_0-\chi_1) + 2\mu\cos(\chi_0-\chi_1) = 0.$$

Substituting

$$\chi_0-\chi_1 = -\mu\log\rho_2,$$

the condition may be written

$$(\mu\log\rho_2)\cot(\mu\log\rho_2) = \tfrac{1}{2}\log\rho_2, \quad . \quad . \quad . \quad (35)$$

an equation of the type referred to above, which for any given taper-ratio is easily solved by means of our tables of $u\cot u$— as an example, values of $\lambda = -\mu\log\rho_2$ are given below for $\rho_2 = 0{\cdot}1,\ 0{\cdot}2 \ldots 0{\cdot}9$, together with $\eta = \lambda/(\pi\ 2)$:—

$\rho_2 =$	0·1	0·2	0·3	0·4	0·5	0·6	0·7	0·8	0·9	1·0
$-\frac{1}{2}\log\rho_2 =$	1·151	0·805	0·602	0·458	0·347	0·255	0·178	0·112	0·053	0·000
$\lambda =$	2·08	1·96	1·88	1·82	1·76	1·72	1·68	1·64	1·60	1·57
$\eta =$	1·32	1·25	1·20	1·15	1·12	1·09	1·07	1·04	1·02	1·00

We then get, for the crippling load,

$$P_1 = (1-\rho_2)^2\{(\eta/\log\rho_2)^2 + 1/\pi^2\}(\pi^2 EI_0/4l^2). \quad . \quad (36)$$

Making $\eta = \rho_2 = 1$, the classical formula is obtained.

To determine the deflexion, we have, from the boundary conditions,

$$A = (h/\sqrt{\alpha})\sin\chi_1\operatorname{cosec}\lambda,$$

$$B = -(h/\sqrt{\alpha})\cos\chi_1\operatorname{cosec}\lambda,$$

and so, substituting in (33),

$$y = h + (h/\sqrt{\alpha})(\alpha+\beta x)^{1/2}\operatorname{cosec}\lambda\sin(\chi_1-\chi),$$

or, in the usual notation,

$$y = h\Big[1 - \{1-(1-\rho_2)x/l\}^{1/2}\operatorname{cosec}\lambda\sin$$

$$\Big\{(\lambda/\log\rho_2)\log\frac{\rho_2}{1-(1-\rho_2)x/l}\Big\}\Big]. \quad . \quad (37)$$

The bending-moment at any point is given by

$$-Ph\{1-(1-\rho_2)x/l\}^{1/2}\operatorname{cosec}\lambda\sin\left\{(\lambda/\log\rho_2)\log\frac{\rho_2}{1-(1-\rho_2)x/l}\right\}.$$

The maximum occurs, as before, at the foot, $x/l=0$.

The case $\beta^2>4$ requires special consideration, since it is now apparently possible to satisfy the boundary conditions, also when hyperbolic functions are involved.

Writing

$$\nu=\sqrt{1/4-\beta^{-2}},$$

we may take the solution in the form

$$y=h+(\alpha+\beta x)^{1/2}\{A\cosh\chi'+B\sinh\chi'\}, \quad . \quad (38)$$

$$\chi'=\nu\log(\alpha+\beta x).$$

Similarly to above, the boundary conditions lead to

$$(\nu\log\rho_2)\coth(\nu\log\rho_2)=\tfrac{1}{2}\log\rho_2. \quad . \quad . \quad (39)$$

Since, however, $\log\rho_2$ is essentially negative, and the function $u\coth u$ is always positive, it is not possible, in our case, to satisfy the conditions when $\beta^2>4$. The case $\beta^2=4$ leads also to results of no practical interest in this problem.

Comparing the strength of tapering columns with that of uniform columns on an equal base, when the columns are built in at one end and axially loaded, it is seen from (31) and (36) that a column of type (i.) is $\eta^2\rho_1^2$ as strong, and of type (ii.) $(1-\rho_2)^2\{(\eta/\log\rho_2)^2+1/\pi^2\}$ as strong as a uniform column. The volume ratios are, of course, the same as given above.

Comparing the volumes of equally strong columns of the type specified, we observe that a uniform column of the same strength as a column of type (i.) must have a moment of inertia equal to $\eta^2\rho_1^2 I_0$, and therefore a volume proportional to $\eta\rho_1\sqrt{I_0}$, whereas the volume of the tapering column is proportional to $\tfrac{1}{3}(1+\rho_1+\rho_1^2)\sqrt{I_0}$—the volume-ratio is thus $(1+\rho_1+\rho_1^2)/3\eta\rho_1$.

For a solid column of type (ii.) the volume is proportional to $\tfrac{1}{2}(1+\rho_2)\sqrt{I_0}$, and an equally strong uniform column would have a moment of inertia equal to $(1-\rho_2)^2\{\eta/\log\rho_2)+1/\pi^2\}I_0$, and this volume-ratio thus becomes

$$(1+\rho_2)/\{2(1-\rho_2)\sqrt{(\eta/\log\rho_2)^2+1/\pi^2}\}.$$

The values of these volume-ratios are tabulated below for values of $\rho = 0{\cdot}1, 0{\cdot}2 \ldots 0{\cdot}9$:—

$\rho =$	0·1	0·2	0·3	0·4	0·5	0·6	0·7	0·8	0·9
vol.-ratio (i.)	2·050	1·249	1·042	0·940	0·894	0·890	0·907	0·928	0·962
vol.-ratio (ii.)	0·933	0·897	0·890	0·898	0·913	0·922	0·944	0·958	0·975

It appears from these values that the most economical taper-ratios are

for a solid column of type (i.) ..... 0·6,

for a solid column of type (ii.) ..... 0·3,

the economy in material being, in both cases, about 11 per cent. as compared with a uniform column.

The column of type (ii.) is always more economical than a uniform column, but the type (i.) is only so for taper-ratios greater than 0·35.

Appendix.

Fig. 3.—The function $u \cot u$, from $u = 0$ to $u = 2{\cdot}00$.

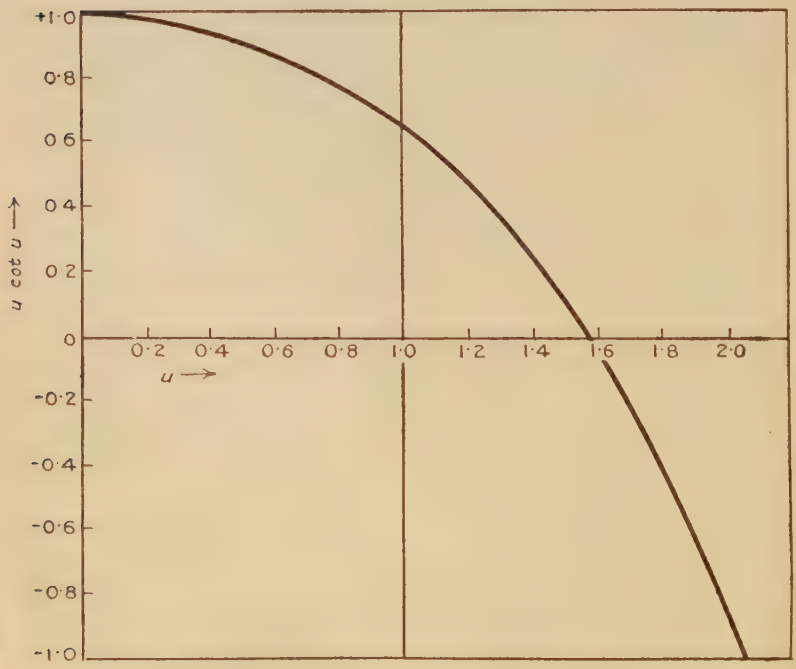

Table of $u \cot u$ for $u=0$ to $u=3{\cdot}00$.

u	$u \cot u$	u	$u \cot u$	u	$u \cot u$
0·00	1·000	1·00	0·642	2·00	−0·903
0·05	0·999	1·05	0·602	2·05	−1·068
0·10	0·997	1·10	0·560	2·10	−1·229
0·15	0·992	1·15	0·515	2·15	−1·405
0·20	0·987	1·20	0·467	2·20	−1·602
0·25	0·979	1·25	0·415	2·25	−1·814
0·30	0·970	1·30	0·361	2·30	−2·061
0·35	0·957	1·35	0·303	2·35	−2·321
0·40	0·946	1·40	0·242	2·40	−2·619
0·45	0·932	1·45	0·186	2·45	−2·96
0·50	0·915	1·50	0·106	2·50	−3·36
0·55	0·897	1·55	0·032	2·55	−3·80
0·60	0·877	1·60	−0·047	2·60	−4·32
0·65	0·855	1·65	−0·136	2·65	−4·96
0·70	0·831	1·70	−0·225	2·70	−5·71
0·75	0·805	1·75	−0·322	2·75	−6·66
0·80	0·777	1·80	−0·421	2·80	−7·85
0·85	0·747	1·85	−0·531	2·85	−9·50
0·90	0·714	1·90	−0·649	2·90	−11·75
0·95	0·679	1·95	−0·767	2·95	−15·20

XLII. *A Note on Certain Experiments on the Supposed Variation of the Coefficient of Viscosity with the Rate of Shear.* *By* J. W. Lewis, *M.Sc., Lecturer in Physics, Artillery College, Woolwich* *.

THE variation of the coefficient of viscosity with the rate of shear has been referred to by several writers, and there is some doubt as to whether or when it exists. While it has been shown that there is no variation in the case of water or glycerine over a considerable range in the rate of shear, it has been claimed that in the case of oil a variation does take place, the viscosity decreasing with the rate of shear. K. Molin † arrived at the conclusion that the viscosity of a very viscous liquid such as treacle is dependent on the rate of shear, and his conclusion has been quoted by W. N. Bond ‡. The object of this note is to point out that Molin's conclusion is based on an erroneous interpretation of his experimental results.

Molin measured the viscosity of treacle in the viscometer

* Communicated by Prof. E. N. da C. Andrade, D.Sc., Ph.D.

† K. Molin, Proc. Camb. Phil. Soc. vol. xx. pt. 1, p. 23 (1920).

‡ W. N. Bond, Proc. Phys. Soc. vol. xxxiii. p. 225 (1921).

designed by G. F. C. Searle* for use with very viscous liquids, The liquid is contained in the space between two coaxial cylinders, the outer one of which is fixed and the inner one rotated by a couple applied by the weight of two equal masses, M, which are supported by a pair of threads attached to a drum on the inner cylinder. When the couple set up by the viscous forces in the liquid balances the applied couple, the inner cylinder rotates with a constant angular velocity. Then, assuming the viscosity is independent of the rate of shear, it can be shown that

$$\eta = C \cdot \frac{MT}{l+k},$$

where C is the apparatus constant, l the length of the inner cylinder, and k the length that must be added to l to correct for the viscous forces acting on the bottom of the inner cylinder. The experiment consists in measuring T the period of revolution. Even for a given value of T, the rate of shear varies throughout the liquid, and by altering the couple a considerable variation can be obtained. In Molin's experiments the maximum variation in the rate of shear at the wall of the outer cylinder was from 0·066 to 2·00 radians per sec.

Molin made six series of observations of the value of T for six values of l varying from 10·0 to 2·15 cm. Now, if the viscosity is independent of the rate of shear, the equation shows that as M is varied, the product MT should be constant for each value of l. Molin plotted MT against M for each value of l. These curves are reproduced in fig. 1. Instead of a series of straight lines parallel to the M axis, each curve has a hyperbolic appearance; the value MT tends towards infinity for small values of M. Molin explained the nature of these curves by assuming that for small rates of shear the viscosity increased, and deduced the relation

$$\eta_{19\cdot8} = 274\cdot7 + 79\cdot44e^{-5\cdot694\Omega}$$

between η the viscosity and Ω the angular velocity of the inner cylinder, *i.e.*, as Ω increases, the viscosity tends to the value 274·7 c.g.s.

All the abnormal portions of the curve obtained by plotting MT against M can be explained by the existence of a small pivot friction. Using Molin's values, I have plotted M against 1/T. For each value of l, a straight line is obtained which, as shown in fig. 2, cuts the M axis on the

* G. F. C. Searle, Proc. Camb. Phil. Soc. vol. xvi. p. 600 (1912).

positive side and indicates that $(M-m)T$ is a constant for all values of M. m is the load used in overcoming pivot friction and differs slightly for the different values of l, but

Fig. 1.

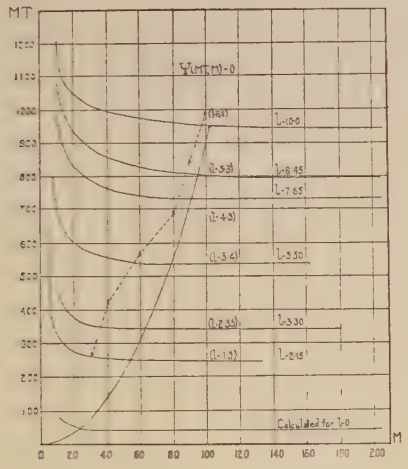

Fig. 2.

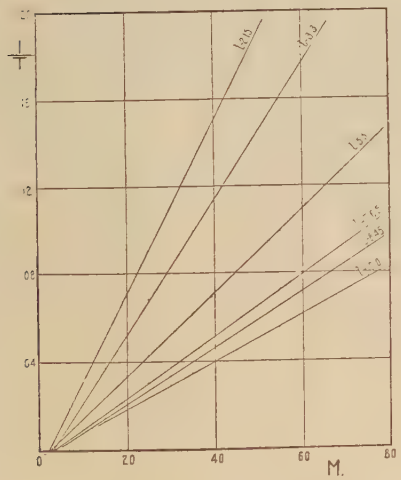

is between 2 and 3 grams. This is a large percentage of M and readily accounts for the hyperbolic nature of the curves in fig. 1, in which it has not been allowed for. Using the data given by Molin, it is found that for each value of l

the product MT continually decreases, but that there is no systematic variation in $(M-m)T$ where m is the pivot friction obtained from the curves in fig. 2 pertaining to the selected value of l.

Molin did not entirely overlook the possibility of pivot friction, for he states: "Before the liquid was put into the apparatus I adjusted the pivots so that the rotation due to the weights of the two empty pans (5 gm. each) was so rapid that I was hardly able to measure, for instance, 3T by a stop watch." The fact that the rotation is very rapid when M is 5 gm. does not preclude a pivot friction of 2–3 gm. I find that to overcome the pivot friction of a similar apparatus* it is necessary to add a mass of 0·75 gm. to each scale pan, making a total of 5·75 gm.; then, on adding a further 3 gm., 3T is certainly difficult to measure. Furthermore, the value of the pivot friction obtained in this way is no measure of its value when the viscometer contains a liquid, since the friction is reduced by the buoyancy effect of the liquid. When pivot friction is taken into account, as indicated above, the mean value of $(M-m)T$ plotted against the corresponding value of l represents a straight line from which k can be found, and hence η evaluated. The mean value obtained from Molin's data is 280·4 c.g.s.

Contrary to Molin's own conclusion, the conclusion now drawn from the experimental data is that the viscosity of the liquid tested, namely treacle, is independent of the rate of shear over the range used. It should be noted, however, that G. F. Davidson †, in experiments on the flow of liquids through an orifice, makes measurements of the viscosity of oil at different rates of shear and finds a decrease with the rate of shear. On the other hand, this result for treacle is in accord with experimental evidence for other liquids. Using the capillary tube method, Bond ‡ found no variation in the case of glycerine at 0° C. ($\eta=46$) between rates of shear at the walls of 4·1 and 0·6 radians per sec., nor at 14° C. ($\eta=14·8$) between rates of shear of 15·7 and 0·6 radians per sec. Also, it is well known from the experiments of A. and C. H. Griffiths § that the viscosity of water at the extremely low rates of shear of from 0·0017 to 0·0233 radians per sec. is not different from its values at normal rates (5000 to 1000 radians per sec.).

* This apparatus is made by Messrs. W. G. Pye & Co., Cambridge, and illustrated in their catalogue of Scientific Apparatus, p. 43 (1926).

† G. F. Davidson, Proc. Roy. Soc. A, vol. lxxxix. p. 91 (1913).

‡ W. N. Bond, Proc. Roy. Soc. vol. xxxiv. p. 139 (1922).

§ A. Griffiths and C. H. Griffiths, Proc. Phys. Soc. vol. xxxiii. p. 242 (1921).

XLIII. *The Refractivity of some Anisotropic Molecules.*

By Prof. T. H. Havelock, *F.R.S.**

Introduction.

1. THE type of molecular model discussed in this paper is the simple model of the ordinary electromagnetic theory of dispersion. The atoms or ions in each molecule are assumed to be isotropic polarizable units in fixed relative positions within the molecule; taking into account the mutual electrostatic action between these units according to the structure of the molecule, we can obtain the dispersion formula for a gas composed of such molecules. In addition we can calculate the depolarization ratio for light scattered by the gas. In a recent paper † I examined from this point of view some simple di- and tri-atomic gases, and in particular the series HCl, HBr, H_2O, H_2S and their relation to the corresponding inert gases. The following calculations for molecules with four and five atoms were made primarily to extend this series to such cases as NH_3 and CH_4 and to examine some structures which have been proposed recently for these molecules.

There are several cases of tetrahedral or pyramidal structures of atoms or ions of this kind; and as explicit refraction or dispersion formulæ do not seem to have been given previously, they are worked out in some detail in the following sections. The particular cases are: (i.) three equal atoms at the corners of an equilateral triangle with a fourth atom equidistant from them but not in the same plane, (ii.) the same with the four atoms in one plane, (iii.) four equal atoms at the corners of a regular tetrahedron with a fifth atom at the centroid, (iv.) four equal atoms at the corners of a square with a fifth atom equidistant from them but not in the same plane. Numerical calculations are then made for some molecular models for NH_3 and CH_4 which have been suggested chiefly with reference to the infra-red spectra. Here they are examined with respect to refractivity and scattering; but as the experimental data for the optical effects are not very concordant, one is unable to arrive at a definite conclusion meantime. Reference is also made to other similar molecules, such as CCl_4.

2. The general method for obtaining the dispersion formula may be summarized briefly. We consider a gas composed

* Communicated by the Author.

† Phil. Mag. iii. p. 158 (Jan. 1927).

of N molecules per unit volume. Choose axes $O(x, y, z)$ fixed in a molecule, and let $(X, Y, Z)\, e^{ipt}$ be the electric force in the incident radiation. If (u_r, v_r, w_r) is the induced electric moment of any assigned atom in the molecule, we have three equations of the form

$$a_r(p_r^2 - p^2)u_r = E_x, \quad . \quad . \quad . \quad . \quad . \quad (1)$$

where E_x includes, in addition to X, the components of force at this point due to all the other polarized atoms in the molecule. Writing down the equations for each atom, we have to solve for the total induced moment (U, V, W) of the molecule. From symmetry in the cases we shall consider, it is easy to choose principal axes such that U, V, W are proportional to X, Y, Z respectively. Averaging for all possible orientations of the molecular axes in space, and summing for all the molecules, we obtain the dispersion formula for the gas :

$$n^2 - 1 = \frac{4\pi N}{3}\left(\frac{U}{X} + \frac{V}{Y} + \frac{W}{Z}\right). \quad . \quad . \quad . \quad (2)$$

We shall use the notation

$$R = n^2 - 1 ; \quad P_r = a_r(p_r^2 - p^2) = 4\pi N/R_r. \quad . \quad (3)$$

The molecular refractivity, for gases under standard conditions, is taken as 7470 R.

Molecules with Four Atoms.

3. Let the structure consist of three equal isotropic units, of

Fig. 1.

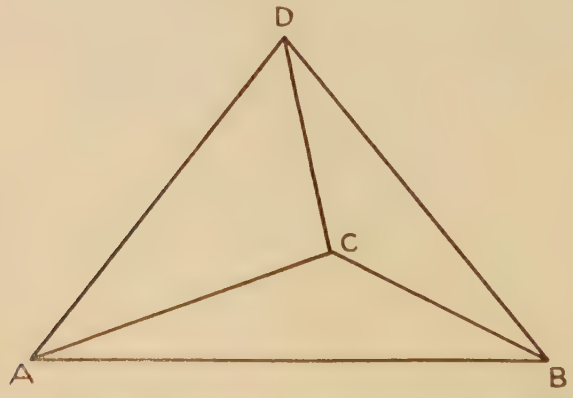

parameter P_1, at the corners of an equilateral triangle ABC, with a fourth unit (P_2) equidistant from these. The molecule is optically symmetrical round the perpendicular from

D on to the plane ABC, as can be verified by direct calculation. Take the origin O at the middle of AB, with Ox along OB and Oy along OC and Oz perpendicular to the plane ABC; these will be principal axes for the molecule.

First take the field to be Z parallel to Oz. Then from the symmetry of the molecule we can take the induced moments in the atoms to be the following:

$(\frac{1}{2}u\sqrt{3}, -\frac{1}{2}u, w)$ at the point $(\frac{1}{2}d, 0, 0)$,

$(-\frac{1}{2}u\sqrt{3}, -\frac{1}{2}u, w)$ at $(-\frac{1}{2}d, 0, 0)$,

$(0, u, w)$ at $(0, \frac{1}{2}d\sqrt{3}, 0)$,

$(0, 0, w')$ at $(0, \frac{1}{6}d\sqrt{3}, q)$,

where $AB=BC=CA=d$; $DA=DB=DC=r$;

$$q^2=r^2-\tfrac{1}{3}d^2.$$

We get sufficient equations by resolving at B parallel to Ox and Oz, and at D parallel to Oz; working out the components due to the constituent doublets, these equations reduce respectively to

$$\frac{\sqrt{3}}{2}\left(P_1+\frac{7}{2d^3}\right)u+\frac{3}{2}\frac{dq}{r^5}w'=0,$$

$$\left(P_1+\frac{2}{d^3}\right)w+\frac{1}{r^3}\left(1-\frac{3q^2}{r^2}\right)w'=Z,$$

$$P_2w'+3\sqrt{3}\frac{dq}{r^5}u+\frac{3}{r^3}\left(1-3\frac{q^2}{r^2}\right)w=Z. \quad . \quad . \quad (4)$$

The total moment W is $3w+w'$, and the solution of these equations gives

$$W/d^3Z=[(P_1+\tfrac{7}{2})\{3P_2+P_1+2-6\alpha^3(1-3\beta^2)\}-27\alpha^8\beta^2]$$
$$\div[(P_1+\tfrac{7}{2})\{P_2(P_1+2)-3\alpha^6(1-3\beta^2)^2\}-9\alpha^8\beta^2(P_1+2)], \quad . \quad . \quad . \quad (5)$$

where for convenience we have written P for d^3P, and have put

$$\alpha=d/r, \quad \beta=q/r.$$

Next take the field to be Y parallel to Oy, and we have the system of moments

(u_1, v_1, w_1) at $(\frac{1}{2}d, 0, 0)$,

$(-u_1, v_1, w_1)$ at $(-\frac{1}{2}d, 0, 0)$,

$(0, v_2, w_2)$ at $(0, \frac{1}{2}d\sqrt{3}, 0)$,

$\{0, v_3, -(2w_1+w_2)\}$ at $(0, \frac{1}{6}d\sqrt{3}, q)$.

We calculate the components of force at B parallel to Ox, Oy, and Oz, at C parallel to Oy and Oz, and at D parallel to Oy; using the same notation the corresponding equations reduce to

$$(\mathrm{P}_1+2)u_1+\frac{3}{4}\sqrt{3}v_2+\frac{\sqrt{3}}{4}\alpha^5 v_3-\frac{3}{2}\alpha^4\beta(2w_1+w_2)=0,$$

$$(\mathrm{P}_1+1)v_1-\frac{5}{4}v_2+\alpha^3\left(1-\frac{1}{4}\alpha^2\right)v_3+\frac{\sqrt{3}}{2}\alpha^4\beta(2w_1+w_2)=d^3\mathrm{Y},$$

$$(\mathrm{P}_1+1)w_1+w_2-\frac{\sqrt{3}}{2}\alpha^4\beta v_3-\alpha^3(1-3\beta^2)(2w_1+w_2)=0,$$

$$\mathrm{P}_1v_2+\frac{3}{2}\sqrt{3}u_1-\frac{5}{2}v_1+\alpha^3(1-\alpha^2)v_3-\sqrt{3}\alpha^4\beta(2w_1+w_2)=d^3\mathrm{Y},$$

$$\mathrm{P}_1w_2+2w_1+\sqrt{3}\alpha^4\beta v_3-\alpha^3(1-3\beta^2)(2w_1+w_2)=0,$$

$$\mathrm{P}_2v_3+\frac{\sqrt{3}}{2}\alpha^4\beta u_1+2\alpha^3\left(1-\frac{1}{4}\alpha^2\right)v_1+\alpha^3(1-\alpha^2)v_2-\sqrt{3}\alpha^4\beta(w_1-w_2)=d^2\mathrm{Y}. \quad . \quad . \quad . \quad (6)$$

Solving for the total moment $\mathrm{V}(=2v_1+v_2+v_3)$, we obtain eventually

$$\begin{aligned}\mathrm{V}/2d^3\mathrm{Y}=&\\ &[(\mathrm{P}_1-1)\{6(2\mathrm{P}_1+1)\mathrm{P}_3+4\mathrm{P}_1{}^2-2(12\alpha^3-6\alpha^5+1)\mathrm{P}_1\\ &-12\alpha^3+24\alpha^5-9\alpha^{10}-11\}-27\alpha^8\beta^2(2\mathrm{P}_1+1)]\\ &\div[(\mathrm{P}_1-1)\{2(4\mathrm{P}_1{}^2-2\mathrm{P}_1-11)\mathrm{P}_2-12\alpha^6(2-2\alpha^2+\alpha^4)\mathrm{P}_1\\ &-3\alpha^6(4-16\alpha^2+5\alpha^4)\}-9\alpha^8\beta^2(4\mathrm{P}_1{}^2-2\mathrm{P}_1-11)]. \quad . \quad (7)\end{aligned}$$

It may be verified, by taking the electric force parallel to Ox, that we get the same value for the corresponding ratio U/X.

For the index of refraction of the gas, we have the expression (2). Returning to the original notation, substituting for P in terms of partial refractivity according to (3), and also putting

$$k=1/2\pi\mathrm{N}d^3, \quad . \quad . \quad . \quad . \quad . \quad . \quad . \quad (8)$$

we obtain the refractivity of the gas in the form

$$\mathrm{R}=n^2-1=\tfrac{1}{3}(2\mathrm{A}+\mathrm{C}), \quad . \quad . \quad . \quad . \quad (9)$$

where

$$\begin{aligned}
A = 4[&12(2-kR_1)(4+kR_1)R_1\\
&+R_2\{(2-kR_1)[16-4(1+12\alpha^3-6\alpha^5)kR_1\\
&-(11+12\alpha^3-24\alpha^5+9\alpha^{10})k^2R_1^2]-27\alpha^8\beta^2k^2R_1^2(4+kR_1)\}]\\
&\div[4(2-kR_1)(16-4kR_1-11k^2R_1^2)\\
&-kR_2\{kR_1(2-kR_1)[24\alpha^6(2-2\alpha^2+\alpha^4)\\
&+3\alpha^6(4-16\alpha^2+5\alpha^4)kR_1]\\
&+9\alpha^8\beta^2kR_1(16-4kR_1-11k^2R_1^2)\}],\\
C = 2[&6(4+7kR_1)R_1\\
&+R_2\{(4+7kR_1)[2+\{2-6\alpha^3(1-3\beta^2)kR_1\}]\\
&-54\alpha^8\beta^2k^2R_1^2\}]\div[4(4+7kR_1)(1+kR_1)\\
&-kR_2\{3\alpha^6(1-3\beta^2)^2(4+7kR_1)kR_1+36\alpha^8\beta^2kR_1(1+kR_1)\}].
\end{aligned}$$

. . . (10)

4. We may deduce the particular case of a plane structure, the three similar atoms being at the corners of an equilateral triangle and the fourth atom at the centroid. In (10) we put

$$\alpha = \sqrt{3}\,; \quad \beta = 0, \quad . \quad . \quad . \quad . \quad . \quad (11)$$

and we obtain

$$\begin{aligned}
A = 4[&12(4+kR_1)R_1+R_2\{16-4kR_1-2198k^2R_1^2\\
&+36\sqrt{3}kR_1(2+5kR_1)\}]\div[4(16-4kR_1-11k^2R_1^2)\\
&-81k^2R_1R_2(40+kR_1)],\\
C = 4[&3R_1+R_2\{1-(9\sqrt{3}-1)kR_1\}]\\
&\div[4(1+kR_1)-81k^2R_1R_2].
\end{aligned}$$

. . . . . (12)

Molecules with Five Atoms.

5. We make similar calculations for structures with five atoms, of which four are alike. In the first place, let the four similar atoms be at the corners of a regular tetrahedron ABCD and the fifth at the centroid E. It appears that this arrangement is optically isotropic. We shall take the same axes as in § 3, with Oz perpendicular to the plane ABC. Assuming the electric force to be parallel to Oz, and taking account of the symmetry of the structure we have the

following system of doublets :

$$(\tfrac{1}{2}u\sqrt{3}, -\tfrac{1}{2}u, w) \text{ at } (\tfrac{1}{2}d, 0, 0),$$
$$(-\tfrac{1}{2}u\sqrt{3}, -\tfrac{1}{2}u, w) \text{ at } (-\tfrac{1}{2}d, 0, 0),$$
$$(0, u, w) \text{ at } (0, \tfrac{1}{2}d\sqrt{3}, 0),$$
$$(0, 0, w') \text{ at } (0, \tfrac{1}{6}d\sqrt{3}, \tfrac{1}{3}d\sqrt{6}),$$
$$(0, 0, w'') \text{ at } (0, \tfrac{1}{6}d\sqrt{3}, \tfrac{1}{12}d\sqrt{6}),$$

where d is the edge of the tetrahedron, and the distance of the central atom from each of the corner atoms is $\frac{1}{4}d\sqrt{6}$.

We require four equations and we obtain them by resolving at B parallel to Ox and Oz, and at D and E parallel to Oz. Writing temporarily P for Pd^3, these equations reduce to

$$\frac{\sqrt{3}}{4}(2P_1+7)u + \frac{\sqrt{6}}{2}w' + \frac{32}{9}w'' = 0,$$

$$(P_1+2)w - w' + \frac{32\sqrt{6}}{27}w'' = d^3Z,$$

$$3\sqrt{2}u - 3w + P_1w' - \frac{32\sqrt{6}}{9}w'' = d^3Z,$$

$$\frac{64\sqrt{3}}{9}u + \frac{32\sqrt{6}}{9}w - \frac{32\sqrt{6}}{9}w' + P_2w'' = d^3Z. \quad (13)$$

Solving for the total moment $W(=3w+w'+w'')$, we find

$$W/d^3Z =$$
$$[108(2P_1+1)P_2 + 27(2P_1^2+P_1-9) - 32768 + 2304\sqrt{6}]$$
$$\div[27(2P_1^2+P_1-9)P_2 - 8192P_1]. \quad . \quad . \quad . \quad . \quad . \quad (14)$$

It can be verified directly by taking the force parallel to Ox and Oy, that we get the same value for the ratios U/X and V/Y.

Hence, with the same notation as in (8), we find the refractivity of the medium to be given by

$$R = n^2 - 1 =$$
$$[216(4+kR_1)R_1 + R_2\{216 + 54kR_1$$
$$- (33011 - 2304\sqrt{6})k^2R_1^2\}]$$
$$\div[27(8+2kR_1 - 9k^2R_1^2) - 8192k^2R_1R_2]. \quad . \quad . \quad (15)$$

6. We consider now a pyramid with a square base. The

similar atoms are at the corners of the square (of side d), and the fifth is at the vertex of the pyramid at equal distances (r) from the other atoms. Take the origin at a corner of the

Fig. 2.

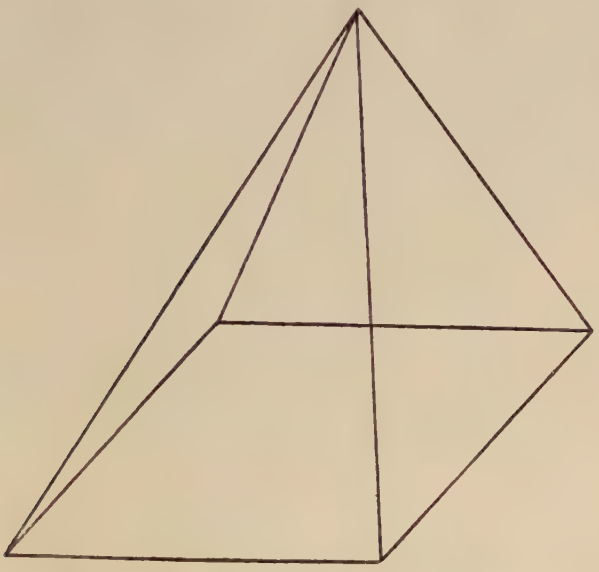

square, with Ox and Oy along the adjacent sides; and write q for the height of the pyramid. With the electric force parallel to Oz, we have the system of doublets :

$$(-u, -u, w) \text{ at } (0, 0, 0),$$
$$(u, -u, w) \text{ at } (d, 0, 0),$$
$$(u, u, w) \text{ at } (d, d, 0),$$
$$(-u, u, w) \text{ at } (0, d, 0),$$
$$(0, 0, w') \text{ at } (\tfrac{1}{2}d, \tfrac{1}{2}d, q).$$

We write down the x- and z- components of force at the origin, and the z-component at the vertex of the pyramid, and so obtain the necessary equations. With the same notation as in § 3, these are

$$(\mathrm{P}_1+3+\tfrac{1}{2}\sqrt{2})u+\tfrac{3}{2}\alpha^4\beta w' = 0,$$
$$(\mathrm{P}_1+2+\tfrac{1}{4}\sqrt{2})w+\alpha^3(1-3\beta^2)w' = d^3\mathrm{Z},$$
$$12\alpha^4\beta u+4\alpha^3(1-3\beta^2)w+\mathrm{P}_2 w' = d^3\mathrm{Z}. \quad . \quad . \quad (16)$$

With $W = 4w + w'$, these give the result

$$W/d^3Z =$$
$$[(P_1+3+\tfrac{1}{2}\sqrt{2})\{4P_2+P_1+2+\tfrac{1}{4}\sqrt{2} - 8\alpha^3(1-3\beta^2)\} - 72\alpha^8\beta^2]$$
$$\div[(P_1+3+\tfrac{1}{2}\sqrt{2})\{(P_1+2+\tfrac{1}{4}\sqrt{2})P_2 - 4\alpha^6(1-3\beta^2)^2\} - 18\alpha^8\beta^2(P_1+2+\tfrac{1}{4}\sqrt{2})]. \quad (17)$$

Next take the electric force parallel to Ox, and we have the doublet system

$(u_2, -v_2, w_2)$ at $(0, 0, 0)$,
$(u_1, -v_1, w_1)$ at $(d, 0, 0)$,
(u_1, v_1, w_1) at $(d, d, 0)$,
(u_2, v_2, w_2) at $(0, d, 0)$,
$(u_3, 0, -2w_1-2w_2)$ at $(\frac{1}{2}d, \frac{1}{2}d, q)$.

Here we require seven equations, and we get them by resolving parallel to the three axes at $(0, 0, 0)$ and at $(d, 0, 0)$ and resolving parallel to Ox at $(\frac{1}{2}d, \frac{1}{2}d, q)$. After some reduction these give respectively the equations

$$(P_1+1)u_2 - \left(2+\frac{\sqrt{2}}{8}\right)u_1 - \frac{3\sqrt{2}}{8}v_1 + \alpha^3(1-\tfrac{3}{4}\alpha^2)u_3 + 3\alpha^4\beta(w_1+w_2) = d^3X,$$
$$(P_1+2)v_2 + \frac{3\sqrt{2}}{8}u_1 + \left(1+\frac{\sqrt{2}}{8}\right)v_1 + \tfrac{3}{4}\alpha^5 u_3 - 3\alpha^4\beta(w_1+w_2) = 0,$$
$$(P_1+1)w_2 + \left(1+\frac{\sqrt{2}}{4}\right)w_1 - 3\alpha^4\beta u_3 - 2\alpha^3(1-3\beta^2)(w_1+w_2) = 0,$$
$$(P_1+1)u_1 - \left(2+\frac{\sqrt{2}}{8}\right)u_2 + \frac{3\sqrt{2}}{8} + \alpha^3(1-\tfrac{3}{4}\alpha^2)u_3 - 3\alpha^4\beta(w_1+w_2) = d^3X,$$
$$(P_1+2)v_1 - \frac{3\sqrt{2}}{8}u_2 + \left(1+\frac{\sqrt{2}}{8}\right)v_2 - \tfrac{3}{4}\alpha^5 v_3 - 3\alpha^4\beta(w_1+w_2) = 0,$$
$$(P_1+1)w_1 + \left(1+\frac{\sqrt{2}}{4}\right)w_2 + \tfrac{3}{2}\alpha^4\beta u_3 - 2\alpha^3(1-3\beta^2)(w_1+w_2) = 0,$$
$$P_2u_3 + 2\alpha^3(1-\tfrac{3}{4}\alpha^2)(u_1+u_2) - \tfrac{3}{2}\alpha^5(v_1-v_2) + 3\alpha^4\beta(w_1-w_2) = d^3X.$$
$$\ldots \quad (18)$$

With $U=2u_1+2u_2+u_3$, the solution of these equations leads to

$$U/Xd^5X=$$
$$\left[\left(P_1-\frac{\sqrt{2}}{4}\right)\left\{16P_2\left(P_1+1-\frac{\sqrt{2}}{8}\right)+4P_1^2\right.\right.$$
$$-(\sqrt{2}+32\alpha^3-24\alpha^5)P_1-5+(4\sqrt{2}-32)\alpha^3$$
$$\left.+(6\sqrt{2}+24)\alpha^5-36\alpha^{10}\right\}-144\alpha^8\beta^2\left(P_1+1-\frac{\sqrt{2}}{8}\right)\Bigg]$$
$$\div\left[\left(P_1-\frac{\sqrt{2}}{4}\right)\left\{2P_2\left(2P_1^2-\frac{\sqrt{2}}{2}P_1-\frac{5}{2}\right)\right.\right.$$
$$-\alpha^6(16-24\alpha^2+18\alpha^4)P_1+(2\sqrt{2}-16)\alpha^6+(6\sqrt{2}+24)\alpha^8$$
$$\left.\left.-\frac{9\sqrt{2}}{2}\alpha^{10}\right\}-18\alpha^8\beta^2\left(2P_1^2-\frac{\sqrt{2}}{2}P_1-\frac{5}{2}\right)\right]. \quad . \quad (19)$$

Obviously we should get the same ratio for V/Y if we took the electric force parallel to Oy. Thus we obtain finally, in the same notation as before,

$$R=n^2-1=\tfrac{1}{3}(2A+C),$$
$$\tfrac{1}{2}A=\left[\left(2-\frac{\sqrt{2}}{4}kR_1\right)\left\{32\left[2+\left(1-\frac{\sqrt{2}}{8}\right)kR_1\right]R_1\right.\right.$$
$$+R_2[16-2(\sqrt{2}+32\alpha^3-24\alpha^5)kR_1$$
$$\left.-\{5-(4\sqrt{2}-32)\alpha^3-(6\sqrt{2}+24)\alpha^5+36\alpha^{10}\}k^2R_1^2]\right\}$$
$$\left.-144\alpha^8\beta^2k^2R_1^2R_2\left\{2+\left(1-\frac{\sqrt{2}}{8}\right)kR_1\right\}\right]$$
$$\div\left(2-\frac{\sqrt{2}}{4}kR_1\right)\left[4(8-\sqrt{2}kR_1-\tfrac{5}{2}kR_1^2)\right.$$
$$-k^2R_1R_2\{2\alpha^6(16-24\alpha^2+18\alpha^4)$$
$$\left.-\alpha^6(2\sqrt{2}-16+6\sqrt{2}\alpha^2+24\alpha^2-\tfrac{9}{2}\sqrt{2}\alpha^4)kR_1\}\right]$$
$$-18\alpha^8\beta^2k^2R_1R_2(8-\sqrt{2}kR_1-\tfrac{5}{2}k^2R_1^2),$$
$$\tfrac{1}{2}C=\left\{2+\left(3+\frac{\sqrt{2}}{2}\right)kR_1\right\}\left[8R_1+2R_2\right.$$
$$\left.+kR_1R_2\left\{2+\frac{\sqrt{2}}{4}-8\alpha^3(1-3\beta^2)\right\}\right]-72\alpha^8\beta^2k^2R_1^2R_2$$
$$\div\left\{2+\left(3+\frac{\sqrt{2}}{2}\right)kR_1\right\}\left[2\left\{2+\left(2+\frac{\sqrt{2}}{4}\right)kR_1\right\}\right.$$
$$\left.-4\alpha^6(1-3\beta^2)^2k^2R_1R_2\right]$$
$$-18\alpha^8\beta^2k^2R_1R_2\left\{2+\left(2+\frac{\sqrt{2}}{4}\right)kR_1\right\}. \quad . \quad . \quad . \quad (20)$$

Numerical Applications.

7. NH_3.—As a first example we consider ammonia. Taking Cuthbertson's measurements and adopting 5461 Å. as our standard wave-length as in the previous paper, we have

$$R = n^2 - 1 = 7{\cdot}5738 \times 10^{-4}. \quad . \quad . \quad . \quad (21)$$

The polarization of light scattered at right angles has been examined recently by Ramanathan and Srinavasan, who give for the ratio of the weak to the strong component the value

$$\rho = 0{\cdot}008. \quad . \quad . \quad . \quad . \quad . \quad . \quad (22)$$

For axial symmetry, in the notation used in the previous sections, we have

$$\rho = 2(A-C)^2/(9A^2+4C^2+2AC). \quad . \quad . \quad (23)$$

A pyramidal structure, derived from consideration of equilibrium of the nuclei, has been proposed for this molecule by F. Hund *. It is of the form which we have examined in § 3, the distance between the hydrogen nuclei being 1·4 Å. and the distance of each from the nitrogen nucleus 1·35 Å.

Assuming as an approximation that these may be taken as the distances between the polar elements of the theory, we have in the notation of § 3

$$\alpha = 1{\cdot}037\,; \quad \beta = 0{\cdot}801\,; \quad k = 0{\cdot}2126 \times 10^4. \quad . \quad (24)$$

Putting these values in (10) we obtain A and C as functions of R_1 and R_2. In our previous study of the gases HCl, HBr, H_2O, H_2S we found it possible to take throughout the same value for the refractivity of the hydrogen in these compounds, namely $0{\cdot}175 \times 10^{-4}$, which was derived initially from the refractivity and scattering of HCl.

We shall use this value now for R_1, and then determine R_2 from the equation

$$2A + C = 22{\cdot}72 \times 10^{-4}. \quad . \quad . \quad . \quad . \quad (25)$$

We find that this gives $R_2 = 6{\cdot}5 \times 10^{-4}$ for the refractivity of the nitrogen, or a molecular refractivity for N^{---} of 4·86. However, with these values we have

$$A = 7{\cdot}16 \times 10^{-4} \quad \text{and} \quad C = 8{\cdot}39 \times 10^{-4}\,;$$

putting these in (23) we obtain the value 0·0035 for the scattering ratio ρ instead of the experimental value 0·008.

* F. Hund, *Zeit. für Phys.* xxxi. p. 81 (1925).

Another way of treating this model is not to assume the hydrogen refractivity, but to determine both R_1 and R_2 directly so that the two optical conditions are satisfied. With $\rho=0{\cdot}008$, we have, from (23), $A=0{\cdot}79\,C$; hence from (25)

$$10^4 A = 6{\cdot}957\,; \quad 10^4 C = 8{\cdot}806.$$

Writing x for kR_1 and substituting the known quantities in the expressions (10) for A and C, we obtain after some reduction the two equations

$$10^4 R_2 = \frac{(4+7x)(35{\cdot}22-91{\cdot}67x)}{16+64{\cdot}63x+214x^2}$$

$$= \frac{4(2-x)(111{\cdot}3-254x+133x^2)}{128-22{\cdot}47x-504x^2-139x^3} \quad . \quad . \quad (26)$$

These give $x=0{\cdot}08$, or finally

$$10^4 R_1 = 0{\cdot}376\,; \quad 10^4 R_2 = 5{\cdot}64. \quad . \quad . \quad (27)$$

The criticisms to be made on this solution are that the hydrogen value seems too large and the nitrogen too small compared with the rest of this series; it may be noted that the value of R_2 means a molecular refractivity of 4·2 for N^{---}, which is probably too small in relation to the values for Neon and O^{--}.

It is of interest to consider a plane structure for the Ammonia molecule, such as we worked out in § 4. With the two optical data, we have two equations for the three quantities k, R_1, and R_2. We shall choose again to take $R_1=0{\cdot}175\times10^{-4}$, and so determine R_2 and the size of the structure.

With the given value of ρ, we have, since the structure is of the oblate type,

$$A = 1{\cdot}3\,C.$$

This, combined with (25) and the value of R_1, enables us to obtain from (12) two equations for k and R_2; omitting the numerical reductions here, the solution is

$$10^{-4}k = 0{\cdot}0474\,; \quad 10^4 R_2 = 6{\cdot}3. \quad . \quad . \quad (28)$$

This gives a molecular refractivity of 4·7 for N^{---}; and the value of k gives $d=2{\cdot}315$ Å., using the standard value for N the number of molecules per unit volume. The distance from the nitrogen nucleus, which is $\frac{1}{3}d\sqrt{3}$, works out as 1·34 Å. It is interesting that this is practically the same as Hund's value for the pyramidal model.

8. CH_4.—Several investigations have been made into the molecular structure of methane. A natural assumption, from a chemical point of view, is to suppose the hydrogen atoms to be at the corners of a regular tetrahedron with the carbon at the centroid; this model has been examined by various writers, for example by Dennison *, in relation to the band spectrum. The most recent study of the structure is that of Guillemin †, using the methods applied by Hund to the series of so-called pseudo-atoms HF, H_2O, NH_3. Guillemin considers first the regular tetrahedron and gives the distance of each hydrogen nucleus from the carbon as 1·14 Å.; he also works out a symmetrical pyramidal structure, the hydrogen nuclei being at the corners of a square of side 1·05 Å. and the carbon at the vertex at a distance 1·15 Å. from each hydrogen nucleus.

For the optical properties under consideration here, we have Cuthbertson's ‡ determinations of refractive index, which give at 5461 A.

$$n^2-1 = 8{\cdot}832\times10^{-4}. \quad . \quad . \quad . \quad . \quad (29)$$

An interesting point arises in regard to the dispersion of methane. It was pointed out in the previous paper that if we consider the constants of a simple dispersion formula

$$n^2-1 = C/(p_0^2-p^2), \quad . \quad . \quad . \quad . \quad (30)$$

the hydrides can be arranged in groups headed by the corresponding inert gas; for instance, we have the group

Gas.	$C\times10^{-27}$.	$p_0^2\times10^{-27}$.
Neon	5·1865	38916
HF	—	—
H_2O	5·2540	10697
NH_3	5·9316	8135

The value of C is of the same order in any one group, and the effective natural frequency p_0 decreases with increasing effective radius of the negative ion; we may picture the negative ion in this group as being neon-like with increasing radius and with increasing disturbance due to the hydrogen

* D. M. Dennison, Astrophys. Journ. lxii. p. 84 (1925); also Phil. Mag. i. p. 195 (1926).

† V. Guillemin, *Ann. der Phys.* lxxxi. p. 173 (1926).

‡ C. & M. Cuthbertson, Proc. Roy. Soc. A, xcvii. p. 152 (1920).

nuclei. We should expect CH_4 to take its place in this sequence, but Cuthbertson gives the values

$$10^{-27}C = 10{\cdot}05536\,; \quad 10^{-27}p_0^2 = 11689{\cdot}3. \quad . \quad (31)$$

If this is really the case, it would seem to indicate a difference of constitution of the atoms or ions in CH_4 compared with the other members of the group. Earlier experimental work on methane, used by various writers on refractivity, is that of St. Loria *, who expressed the dispersion in a formula of different type from (20) ; it is, however, easy to bring his results under the same form with sufficient accuracy for comparison with those of Cuthbertson. It is found that St. Loria's results, in the form (20), give approximately

$$10^{-27}C = 6{\cdot}314\,; \quad 10^{-27}p_0^2 = 7373{\cdot}8. \quad . \quad . \quad (32)$$

These values agree better with the sequence given in the Table for the Neon group. The matter is, however, one for experiment to decide.

The depolarization ratio for scattered light for methane vapour is given by Cabannes and Gauzit † as

$$\rho = 0{\cdot}015. \quad . \quad . \quad . \quad . \quad . \quad . \quad (33)$$

It should be mentioned that experimental values of this ratio are not always as concordant as could be desired. Generally speaking, the values found by Cabannes seem to be smaller than those obtained by Rayleigh, or by Raman and his coworkers. This may be illustrated by the series of values of ρ for carbon tetrachloride, CCl_4, which are 0·032 (Rayleigh), 0·03 (Raman and Rao), 0·019 (Ganesan), and 0·0082 (Cabannes). However, we shall not attempt to discuss disputed points of experimental technique ; reference may be made in this connexion to a recent paper by Cabannes ‡. The only measurement for CH_4 appears to be that quoted in (33). Cabannes states that the value is certainly greater than for CCl_4 ; further, as he considers the molecule to be a symmetrical structure, he concludes that it is the carbon atom itself which is anisotropic. That may well be the case ; but here we are simply working out the consequences of anisotropy due to an arrangement of isotropic units.

As we have seen in § 5, the symmetrical centred-tetrahedron is isotropic and the expression (15) shows the effect of the interaction of the units upon the refractivity of the gas.

* St. Loria, *Ann. der Phys.* xxix. p. 605 (1909).
† Cabannes and Gauzit, *Journ. de Phys.* vi. p. 182 (1925).
‡ Cabannes, *Journ. de Phys.* vii. No. 11 (1926).

Let us ignore, for the moment, the anisotropy of methane as shown by the depolarization ratio, and see what value can be deduced for the refractivity of the carbon ion. If we take Guillemin's value of 1·14 Å. for the distance from the carbon to a hydrogen, then the edge of the tetrahedron is 1·86 Å. and the value of k in (15) is $0{\cdot}0914 \times 10^4$. Taking the same value as before for the hydrogen, namely $10^4 R_1 = 0{\cdot}175$, and using (29), we obtain on solving (15)

$$R_2 = 5{\cdot}58 \times 10^{-4},$$

or a molecular refractivity of 4·2 for the carbon. Consider now the square pyramidal model of Guillemin. In the notation of § 6, we have

$$d = 1{\cdot}05 \text{ Å.}; \quad k = 0{\cdot}5081 \times 10^4; \quad \alpha = 0{\cdot}912; \quad \beta = 0{\cdot}77.$$

Using the same value for R_1, the expressions (20) reduce to

$$A = \frac{65{\cdot}71 + 53{\cdot}69\, R_2}{61{\cdot}86 - 2{\cdot}67\, R_2},$$

$$C = \frac{6{\cdot}52 + 11{\cdot}92\, R_2}{10{\cdot}29 - 0{\cdot}54\, R_2}, \qquad \ldots \quad (34)$$

omitting some factors of 10^{-4}. From

$$2A + C = 26{\cdot}496,$$

we obtain $R_2 = 5{\cdot}74 \times 10^{-4}$, or a molecular refractivity of 4·3. Further, the value of A/C is 0·77, and from (23) the corresponding value of ρ works out as 0·01.

We may remark in the first place that the value of ρ is smaller than the experimental value. In the second place, a molecular refractivity of 4·3 for the carbon is too small if we suppose it to be a C^{4-} ion. The molecular refractivity of Neon is 1·0; and, from H_2O and NH_3, we have calculated O^{--} and N^{---} to be 2·58 and 4·7 respectively. If CH_4 is the fifth member of this sequence, we should expect the value for C^{4-} to be greater than for N^{---}. The reason for it coming out less is the relatively small distance of the hydrogen nuclei from the carbon, according to the calculations of Dennison and Guillemin to which we have referred; this distance is given as about 1·14 Å. The corresponding distances for H_2O and NH_3 are 1·02 Å. and 1·34 Å. approximately. Doubtless the presence of the hydrogen nuclei contracts the effective radius of the negative ion considerably compared with what it would be in a hypothetical free condition, but one would not expect it to be actually less in CH_4

than in NH_3. The distance 1·14 Å. for CH_4 involves, among other considerations, the calculation of moments of inertia from the band spectrum. It may of course prove to be a correct deduction, but if so it indicates that CH_4 is different in some respect from the earlier members of the group; the discussion may be left meantime by referring again to Cuthbertson's values of the constants in the dispersion formula, which also seem to lead to the same conclusion.

9. *CCl_4.*—Consider briefly the molecule of carbon tetrachloride. The refractivity, at the D line, is given as

$$n^2-1 = 35{\cdot}39\times10^{-4}. \quad . \quad . \quad . \quad . \quad (35)$$

We have seen in the previous section that there is a considerable range of experimental values of the depolarization ratio ρ, the largest being 0·032 given by Lord Rayleigh.

In this case there are no available calculations of the structure to examine. Let us assume a square pyramidal structure, like the model we examined for CH_4; and let us suppose that in this case the carbon is in the form C^{4+}. The refractivity of carbon in this form is very small, and as a first approximation we shall neglect it. We are left with four Cl^- ions at the corners of a square. It follows from (35) that the refractivity of each Cl^- in this combination cannot in any case exceed $8{\cdot}85\times10^{-4}$; let us take the value we found in the previous paper from HCl, namely

$$R_1 = 8{\cdot}22\times10^{-4}. \quad . \quad . \quad . \quad . \quad . \quad (36)$$

With $R_2=0$, the expressions (20) reduce to

$$A = 16\left\{2+\left(1-\frac{\sqrt{2}}{8}kR_1\right)R_1\right\}\Big/(8-\sqrt{2}kR_1-\tfrac{3}{2}k^2R_1^2),$$

$$C = 4R_1\Big/\left\{1+\left(1+\frac{\sqrt{2}}{8}\right)kR_1\right\}. \quad . \quad . \quad . \quad . \quad . \quad . \quad (37)$$

From (35), (36), and (37) we solve for k and obtain the value $0{\cdot}0406\times10^4$. From (8), using the standard value of N, this gives for the side of the square

$$d = 2{\cdot}44\text{ Å}.$$

In addition, from the values of A and C, we obtain the depolarization ratio

$$\rho = 0{\cdot}032. \quad . \quad . \quad . \quad . \quad . \quad . \quad (38)$$

It is easy to see that if a larger value is taken for R_1, d will be increased and the value of ρ diminished.

Summary.

10. The molecule is treated as a structure of isotropic polarizable constituents in fixed relative positions. Expressions are obtained, in terms of the constants of the constituents and of the structure, for the refractivity and depolarization ratio of a gas whose molecules are of the following types: (i.) three equal atoms at the corners of an equilateral triangle, with a fourth atom equidistant from them but not necessarily in the same plane, (ii.) four equal atoms at the corners of a regular tetrahedron with a fifth atom at the centroid, (iii.) four equal atoms at the corners of a square, with a fifth atom equidistant from them but not necessarily in the same plane. Numerical applications are made to some molecular models which have been proposed for NH_3 and CH_4, and the results are discussed in relation to other members of the series of compounds of the form XH_n.

XLIV. *The Relativity Law of Refraction. An illustration of the transition from one observer's space to the fourfold and from the fourfold to another observer's space.* By D. B. Mair *.

The Classical Law.

1. ON the classical view of the refraction of light at a plane surface we have two media separated by a plane interface, an incident ray arriving in the first medium at the interface with a speed proper to that medium, and departing as the refracted ray in the second medium with a speed proper to it. We call the proper speed in the arrival medium $\tanh\alpha$, and the proper speed in the departure medium $\tanh\beta$, the speed of light in a vacuum being unity.

2. We take vector $\mathbf{a}_2$ normal to the interface and heading into the departure medium, $\mathbf{h}$ along the incident ray, $\mathbf{x}$ along the refracted ray, $\mathbf{p}$ perpendicular to the plane of incidence, and $\mathbf{q}$ along the line of intersection of the interface and the plane of incidence. $\mathbf{q}$ is to head in the same sense as the projection of the incident ray upon it.

3. The capital letters H X (fig. 1) mark the heads of vectors $\mathbf{h}$ $\mathbf{x}$, and so for all vectors at the origin. Let the projections of H X on $\mathbf{q}$ $\mathbf{a}_2$ be K L and U V. Let θ be the angle of incidence. The classical law of refraction is

$$\mathrm{OU}/\mathrm{OX}\tanh\beta = \sin\theta/\tanh\alpha.$$

* Communicated by the Author.

To distinguish between OX as a vector and as a scalar length we denote the vector by $\mathbf{x}$ or $\overrightarrow{OX}$ and the size or length or magnitude by σ_{OX} or $\sigma_{\mathbf{x}}$. We then write the law

$$\sigma_{\mathbf{u}}/\sigma_{\mathbf{x}} \tanh\beta = \sin\theta/\tanh\alpha. \quad . \quad . \quad . \quad . \quad (1)$$

Fig. 1.

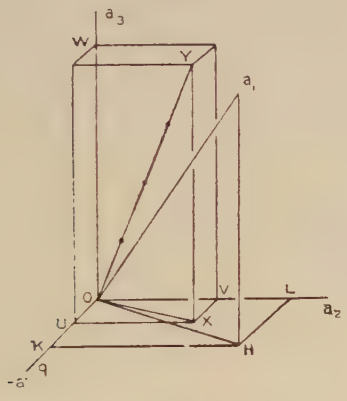

Stationary observer's reference system in the Fourfold.

4. The classical law is the law as determined by a stationary observer S, an observer at rest relative to the apparatus. To obtain the figure in the fourfold we draw the world lines of S and of the incident and refracted rays, and lay the vectors $\mathbf{a}_3$ $\mathbf{a}_1$ $\mathbf{y}$ along them. The world line for S is perpendicular to S's space. The speed of the incident ray being $\tanh\alpha$, its world line makes with $\mathbf{a}_3$ the hyperbolic angle α; $\mathbf{a}_1$ is taken of such size that $\mathbf{h}$ is its projection. The world line $\mathbf{y}$ of the refracted ray makes the angle β with $\mathbf{a}_3$, and is taken of such size that its projection is $\mathbf{x}$.

5. For S the interface is a biplane, that is to say a two-dimensional plane. Every point of it has a world line parallel to $\mathbf{a}_3$ and the totality of these world lines form a triplane which we will call the triplane interface. The triplane interface contains the vectors $\mathbf{a}_3$ $\mathbf{p}$ $\mathbf{q}$ and may be considered to be determined by them. The vector $\mathbf{a}_2$ is perpendicular to the vectors $\mathbf{a}_3$ $\mathbf{p}$ $\mathbf{q}$ and is thus the normal to the triplane interface.

6. S is concerned with only three dimensions of the fourfold, namely, with the triplane that is determined by $\mathbf{a}_2$ $\mathbf{a}_3$ $\mathbf{q}$ or by $\mathbf{a}_2$ $\mathbf{a}_3$ $\mathbf{a}_1$. Let S measure the phenomenon by means of a reference lattice of which $\mathbf{a}_1$ $\mathbf{a}_2$ $\mathbf{a}_3$ are the prime

vectors ; and let $b_{\rho\sigma}$ be the lattice constants, that is to say let

$$b_{\rho\sigma}=\mathbf{a}_\rho\,.\,\mathbf{a}_\sigma \qquad \rho\ \sigma=1\ 2\ 3. \quad . \quad . \quad . \quad . \quad (2)$$

With this reference lattice we associate another whose prime vectors $\mathbf{a}^1$ $\mathbf{a}^2$ $\mathbf{a}^3$ carry upper affixes and are defined by

$$\mathbf{a}^\rho\,.\,\mathbf{a}_\sigma=\delta_\sigma{}^\rho. \quad . \quad . \quad . \quad . \quad . \quad . \quad (3)$$

Let this lattice have constants $b^{\rho\sigma}$, so that

$$b^{\rho\sigma}=\mathbf{a}^\rho\,.\,\mathbf{a}^\sigma. \quad . \quad . \quad . \quad . \quad . \quad . \quad (4)$$

Then $b^{\rho\sigma}$ $b_{\rho\sigma}$ are connected by the relations

$$b^{\rho\sigma}b_{\rho\tau}=\delta_\tau{}^\sigma. \quad . \quad . \quad . \quad . \quad . \quad . \quad (5)$$

7. We take the fundamental quadratic expression $b_{\rho\sigma}x^\rho x^\sigma$ to be positive when the vector $\mathbf{x}\equiv x^1a_1+x^2a_2+x^3a_3$ is time-like and negative when it is spacelike. The vector $\mathbf{a}^1$ is by definition perpendicular to $\mathbf{a}_2$ $\mathbf{a}_3$ and therefore lies along q. Since $\mathbf{a}^1\,.\,\mathbf{a}_1$ is unity and $\mathbf{a}^1$ is spacelike, $\mathbf{a}^1$ and the projection of $\mathbf{a}_1$ upon it have opposite senses ; that is to say, q has the same sense as $-\mathbf{a}^1$.

8. Let $\mathbf{w}\equiv\overrightarrow{\mathrm{OW}}$ be the projection of y on $\mathbf{a}_3$. Then

$$\begin{aligned}\mathbf{y}&=\mathbf{u}+\mathbf{v}+\mathbf{w}\\&=\sigma_{\mathrm{u}}\left(\frac{-\mathbf{a}^1}{\sigma_{\mathbf{a}^1}}\right)+\sigma_{\mathrm{v}}\frac{\mathbf{a}_2}{\sigma_{\mathbf{a}_2}}+\sigma_{\mathrm{w}}\frac{\mathbf{a}_3}{\sigma_{\mathbf{a}_3}}.\end{aligned}$$

We use the expression for $\mathbf{a}^1$ in terms of the lower-affix lattice, namely

$$\mathbf{a}^1=b^{11}\mathbf{a}_1+b^{12}\mathbf{a}_2+b^{13}\mathbf{a}_3$$

and have

$$\begin{aligned}\mathbf{y}&=\mathbf{a}_1\left(-\frac{b^{11}\sigma_{\mathrm{u}}}{\sigma_{\mathbf{a}^1}}\right)+\mathbf{a}_2\left(\frac{\sigma_{\mathrm{v}}}{\sigma_{\mathbf{a}_2}}-\frac{b^{12}\sigma_{\mathrm{u}}}{\sigma_{\mathbf{a}^1}}\right)+\mathbf{a}_3\left(\frac{\sigma_{\mathrm{w}}}{\sigma_{\mathbf{a}_3}}-\frac{b^{13}\sigma_{\mathrm{u}}}{\sigma_{\mathbf{a}^1}}\right)\\&=\sigma_{\mathrm{u}}\sigma_{\mathbf{a}^1}\sigma_{\mathbf{a}_1}\left[\frac{\mathbf{a}_1}{\sigma_{\mathbf{a}_1}}+\frac{\mathbf{a}_2}{\sigma_{\mathbf{a}_2}}\left(\frac{\sigma_{\mathrm{v}}}{\sigma_{\mathrm{u}}\sigma_{\mathbf{a}_1}\sigma_{\mathbf{a}^1}}+\frac{b^{12}\sigma_{\mathbf{a}_2}}{b^{11}\sigma_{\mathbf{a}_1}}\right)\right.\\&\qquad\left.+\frac{\mathbf{a}_3}{\sigma_{\mathbf{a}_3}}\left(\frac{\sigma_{\mathrm{w}}}{\sigma_{\mathrm{u}}\sigma_{\mathbf{a}_1}\sigma_{\mathbf{a}^1}}+\frac{b^{13}\sigma_{\mathbf{a}_3}}{b^{11}\sigma_{\mathbf{a}_1}}\right)\right]. \quad . \quad . \quad . \quad (6)\end{aligned}$$

9. Since $\mathbf{y}$ makes the angle β with $\mathbf{a}_3$

$$\sigma_{\mathrm{w}}=\sigma_{\mathrm{y}}\cosh\beta. \quad . \quad . \quad . \quad . \quad . \quad . \quad (7)$$

From the law of refraction, equation (1), we have

$$\sigma_u=\sigma_y\sinh\beta\tanh\beta\sin\theta/\tanh\alpha. \quad . \quad . \quad . \quad (8)$$

The relation $\sigma_y^2=\sigma_w^2-\sigma_u^2-\sigma_v^2$ gives from these

$$\sigma_v=\sigma_y\frac{\sinh\beta\tanh\beta}{\tanh\alpha}\sqrt{\cos^2\theta+\kappa}, \quad . \quad . \quad . \quad (9)$$

where κ denotes $\dfrac{\tanh^2\alpha-\tanh^2\beta}{\tanh^2\beta}$.

10. Since $\sigma_h=\sigma_{a_1}\sinh\alpha$ and $b_{12}=\mathbf{a}_1\,.\,\mathbf{a}_2=1\,.\,\mathbf{a}_2=-\sigma_1\sigma_{a_2}$ we have

$$\cos\theta=\sigma_1/\sigma_h=-b_{12}/\sigma_{a_1}\sigma_{a_2}\sinh\alpha. \quad . \quad . \quad (10)$$

We use $b_{\kappa\lambda\mu\nu}$ to mean the determinant $\begin{vmatrix} b_{\kappa\mu} & b_{\kappa\nu} \\ b_{\lambda\mu} & b_{\lambda\nu} \end{vmatrix}$ and b to mean the determinant of the lattice constants, and remembering that $b_{23}=\mathbf{a}_2\,.\,\mathbf{a}_3=0$, we have

$$\frac{b^{12}\sigma_{a_2}}{b^{11}\sigma_{a_1}}=\frac{bb^{12}\sigma_{a_2}}{bb^{11}\sigma_{a_1}}=\frac{b_{2331}\sigma_{a_2}}{b_{2323}\sigma_{a_1}}=-\frac{b_{12}b_{33}\sigma_{a_2}}{b_{22}b_{33}\sigma_{a_1}}$$

$$=\frac{b_{12}}{\sigma_{a_1}\sigma_{a_2}}=-\sinh\alpha\cos\theta. \quad . \quad . \quad . \quad . \quad (11)$$

and

$$\frac{b^{13}\sigma_{a_3}}{b^{11}\sigma_{a_1}}=\frac{b_{2312}\sigma_{a_3}}{b_{2323}\sigma_{a_1}}=-\frac{b_{13}\sigma_{a_3}}{b_{33}\sigma_{a_1}}=-\frac{b_{13}}{\sigma_{a_1}\sigma_{a_3}}=-\cosh\alpha. \quad (12)$$

Since $\sigma_k=\sigma_h\sin\theta=\sigma_{a_1}\sinh\alpha\sin\theta$

and $\sigma_{a^1}\sigma_k=\mathbf{a}^1\,.\,\mathbf{k}=\mathbf{a}^1\,.\,\mathbf{a}_1=1,$

we have $\sigma_{a^1}\sigma_{a_1}=1/\sinh\alpha\sin\theta. \quad . \quad . \quad . \quad . \quad . \quad (13)$

11. We use the equations 7–13 in equation (6) and thus find

$$\mathbf{y}=\sigma_y\frac{\sinh\beta\tanh\beta}{\sinh\alpha\tanh\alpha}\left[\frac{\mathbf{a}_1}{\sigma_{a_1}}+\frac{\mathbf{a}_2}{\sigma_{a_2}}\left(\sqrt{\cos^2\theta+\kappa}-\cos\theta\right)\sinh\alpha\right.$$

$$\left.+\frac{\mathbf{a}_3}{\sigma_{a_3}}\kappa\cosh\alpha\right]. \quad . \quad . \quad . \quad . \quad (14)$$

Let $y^1\ y^2\ y^3$ be the components of $\mathbf{y}$ in the $\mathbf{a}_p$ lattice, that is to say let

$$\mathbf{y}=y^1\mathbf{a}_1+y^2\mathbf{a}_2+y^3\mathbf{a}_3$$

and we have from equation (14), for the law of the refracted ray,

$$y^1\sigma_{a_1}=\frac{y^2\sigma_{a_2}}{\left(\sqrt{\cos^2\theta+\kappa}-\cos\theta\right)\sinh\alpha}=\frac{y^3\sigma_{a_3}}{\kappa\cosh\alpha}, \quad (15)$$

in which $\kappa=(\tanh^2\alpha-\tanh^2\beta)/\tanh^2\beta$

and $\cos\theta=-b_{12}/\sigma_{a_1}\sigma_{a_2}\sinh\alpha.$

Moving observer's reference system in the Fourfold.

12. We consider now an observer M who is in motion with a constant velocity relative to the apparatus, and take vector $\mathbf{c}_4$ lying along his world line. Let him use as prime vectors for a reference lattice $\mathbf{c}_1$ $\mathbf{c}_2$ $\mathbf{c}_3$ $\mathbf{c}_4$ of which $\mathbf{c}_1$ $\mathbf{c}_2$ $\mathbf{c}_3$ are identical with $\mathbf{a}_1$ $\mathbf{a}_2$ $\mathbf{a}_3$, and let the lattice constants be

$$d_{\rho\sigma}=\mathbf{c}_\rho . \mathbf{c}_\sigma \qquad \rho\ \sigma=1\ 2\ 3\ 4.$$

13. We use $\mathbf{z}\equiv z^\rho \mathbf{c}_\rho$ to denote in the c-system the vector $\mathbf{y}\equiv y^\rho \mathbf{a}_\rho$ of the a-system. Since the vector lies in $\mathbf{c}_{123}$ z^4 is zero; and since $\mathbf{c}_1$ $\mathbf{c}_2$ $\mathbf{c}_3$ are identical with $\mathbf{a}_1$ $\mathbf{a}_2$ $\mathbf{a}_3$ we have

$$z^1=y^2 \qquad z^2=y^2 \qquad z^3=y^3.$$

Also $b_{12}=\mathbf{a}_1 . \mathbf{a}_2=\mathbf{c}_1 . \mathbf{c}_2=d_{12}$ so that in the c-system the law is

$$\frac{z^1\sigma_{c_1}}{1}=\frac{z^2\sigma_{c_2}}{(\sqrt{\cos^2\theta+\kappa}-\cos\theta)\sinh\alpha}=\frac{z^3\sigma_{c_3}}{\kappa\cosh\alpha}=\frac{z^4\sigma_{c_4}}{0}, \quad (16)$$

in which $\kappa=(\tanh^2\alpha-\tanh^2\beta)/\tanh^2\beta$

$$\cos\theta=-d_{12}/\sigma_{c_1}\sigma_{c_2}\sinh\alpha.$$

Reference system for the moving observer's space.

14. From the law expressed in the fourfold in terms of the c-lattice we wish to pass to the law expressed in terms of M's space. As prime vectors of the reference lattice in M's space we take $\mathbf{e}_1$ $\mathbf{e}_2$ $\mathbf{e}_3$ the projections of $\mathbf{c}_1$ $\mathbf{c}_2$ $\mathbf{c}_3$ on M's space. Let the lattice constants in M's space be $g_{\rho\sigma}$ so that $g_{\rho\sigma}=e_\rho . e_\sigma$.

15. Let the vector $\mathbf{z}\equiv z^1\mathbf{c}_1+z^2\mathbf{c}_2+z^3\mathbf{c}_3$ which is the world line of the refracted ray project in M's space into the vector $\mathbf{u}\equiv u^1\mathbf{e}_1+u^2\mathbf{e}_2+u^3\mathbf{e}_3$ which lies along the path of the refracted ray in M's space. u is thus the sum of the projections of $z^1\mathbf{c}_1$ $z^2\mathbf{c}_2$ $z^3\mathbf{c}_3$. Projection shortens parallel lines in the same ratio, so that while $\mathbf{c}_1$ projects to $\mathbf{e}_1$, $z^1\mathbf{c}_1$ projects to $z^1\mathbf{e}_1$; and so for the other two components. That is to say,

$$u^1=z^1 \qquad u^2=z^2 \qquad u^3=z^3. \quad . \quad . \quad . \quad (17)$$

16. Since $\mathbf{c}_1$ is the world line of the incident ray, $\mathbf{e}_1$ is for M in the customary terminology the path of the incident ray. In the same way the apparatus is, for M, travelling along the vector $\mathbf{e}_3$.

For M the interface between the two media is the biplane in which M's space cuts the triplane interface. As $\mathbf{c}_2$ is

perpendicular to the triplane interface it is also perpendicular to M's biplane interface ; and as E_2C_2 is perpendicular to every line in M's space, it is perpendicular to the biplane interface. Hence e_2, which is the vector sum of c_2 and $\overrightarrow{C_2E_2}$, is perpendicular to the biplane interface ; that is to say, in M's space e_2 is the normal to the interface between the two media.

17. We wish to have the refraction problem stated and solved in terms of the data of M's space. These data are :—An arrival medium in which the proper speed of light is $\tanh\alpha$, a departure medium of proper speed $\tanh\beta$, the vector e_2 normal to the interface between the media and heading into the departure medium, the vector e_3 along which the apparatus is travelling relative to M with a speed which we will call $\tanh\gamma$, and the vector e_1 which is the path of the incident ray relative to M.

We have to express the quantities of equation (16) in terms of these data.

18. Let k be the projection of c_1 on the biplane c_4e_2, and let l m r be the projections of k on e_2 c_4 c_2. Thus r is also the projection of c_1 on e_2, and when r has the same sense as c_2

$$d_{12}=c_1\,.\,c_2=r\,.\,c_2=-\sigma_r\sigma_{c_2}. \quad . \quad . \quad . \quad (18)$$

19. Let the hyperbolic angle between c_4 and c_1 be ψ, that between c_2 and e_2 ω, let those made by k with c_4 c_1 RK be ξ η ζ respectively. Then

$$\tanh\xi=\frac{\sigma_l}{\sigma_m}=\frac{\sigma_{e_1}(-g_{12}/\sigma_{e_1}\sigma_{e_2})}{\sigma_{c_1}\cosh\psi}=-\frac{g_{12}}{\sigma_{c_1}\sigma_{e_2}}\tanh\psi \quad (19)$$

$$\cosh\eta=\frac{\sigma_k}{\sigma_{c_1}}=\frac{\sigma_k}{\sigma_m}\frac{\sigma_m}{\sigma_{c_1}}=\frac{\cosh\psi}{\cosh\xi} \quad . \quad . \quad . \quad . \quad . \quad . \quad (20)$$

$$\zeta=\xi-\omega. \quad . \quad . \quad . \quad . \quad . \quad . \quad . \quad . \quad . \quad . \quad . \quad . \quad (21)$$

20. Hence we have

$$\sigma_r=\sigma_k\sinh\zeta,$$

$$\sigma_k=\sigma_{c_1}\cosh\eta=\sigma_{c_1}\cosh\psi/\cosh\xi.$$

$$\begin{aligned} d_{12}/\sigma_{c_1}\sigma_{c_2} &= -\sinh(\xi-\omega)\cosh\psi/\cosh\xi \\ &= -(\tanh\xi\cosh\omega-\sinh\omega)\cosh\psi \\ &= (\cosh\omega\tanh\psi\, g_{12}/\sigma_{e_1}\sigma_{e_2}+\sinh\omega)\cosh\psi \\ &= \frac{g_{12}\sinh\psi\cosh\omega+\sigma_{e_1}\sigma_{e_2}\cosh\psi\sinh\omega}{\sigma_{e_1}\sigma_{e_2}}. \end{aligned} \quad (22)$$

21. Equation (22) along with

$$\sigma_{c_1}=\sigma_{e_1}/\sinh\psi \quad \sigma_{c_2}=\sigma_{e_2}/\cosh\omega \quad \sigma_{c_3}=\sigma_{e_3}/\sinh\gamma \quad (23)$$

and equation (17) give the quantities of equation (16) in terms of ψ ω and the data of M's space. We have still to determine ψ ω in terms of M's data.

22. The preceding discussion applies to the first of the figures (fig. 2) in which ω ξ ζ are taken to be positive. Any of ω ξ ζ may become negative, as the other four figures show. The result in equation (22) is true for all the cases.

In these figures lines lying in the biplane c_4 e_2 are drawn as full lines. Of the lines lying out of this biplane those in triplane c_4 e_2 e_1 are shown by dashes, and those in triplane c_4 e_2 e_3 by dots.

Calculation of ω and ψ.

23. Let $\mathbf{p}$ be the projection of $\mathbf{c}_3$ on biplane $\mathbf{c}_4\mathbf{e}_2$, and let $\mathbf{q}$ $\mathbf{t}$ be the projections of $\mathbf{p}$ on $\mathbf{e}_2$ $\mathbf{c}_4$. The vectors $\mathbf{c}_2$ $\mathbf{c}_3$ were originally chosen at right angles, and $\mathbf{C}_3\mathbf{P}$ is perpendicular to $\mathbf{c}_2$ because it was drawn perpendicular to the biplane $\mathbf{c}_1\mathbf{c}_2$; therefore $\mathbf{p}$ which is the sum of $\mathbf{c}_3$ and $\mathbf{C}_3\mathbf{P}$ is perpendicular to $\mathbf{c}_2$, and $\mathbf{p}$ makes with $\mathbf{c}_4$ the same angle ω that $\mathbf{c}_2$ makes with $\mathbf{e}_3$.

24. Hence

$$\tanh\omega=\frac{\sigma_q}{\sigma_t}=\frac{\sigma_{e_3}(-g_{23}/\sigma_{e_2}\sigma_{e_3})}{\sigma_t},$$

or since $\tanh\gamma=\sigma_{e_3}/\sigma_t$

$$\tanh\omega=-g_{23}\tanh\gamma/\sigma_{e_2}\sigma_{e_3}, \quad . \quad . \quad . \quad . \quad (24)$$

whence also

$$\sinh\omega=\frac{-g_{23}\sinh\gamma}{\sqrt{G_{2233}}}. \quad . \quad . \quad . \quad . \quad . \quad . \quad . \quad (25)$$

$$\cosh\omega=\frac{\sigma_{e_2}\sigma_{e_3}\cosh\gamma}{\sqrt{G_{2233}}}, \quad . \quad . \quad . \quad . \quad . \quad . \quad . \quad (26)$$

in which $G_{2233}=g_{22}g_{33}+g_{2323}\sinh^2\gamma$.

The expression for $\sinh\omega$ has a minus sign because ω is positive when $\mathbf{e}_2$ $\mathbf{e}_3$ meet at an acute angle, that is when g_{23} is negative.

25. Let $\mathbf{t}$ be the projection of $\mathbf{c}_3$ on the biplane $\mathbf{c}_4\mathbf{e}_1$ (fig. 3), and let $\mathbf{u}$ $\mathbf{v}$ $\mathbf{w}$ be the projections of $\mathbf{t}$ on the vectors $\mathbf{e}_1$ $\mathbf{c}_4$ $\mathbf{c}_1$. Let the hyperbolic angles made by $\mathbf{t}$ with $\mathbf{c}_4$ $\mathbf{c}_1$ $\mathbf{c}_3$ be λ μ ϕ. Then

$$\tanh\lambda=\frac{\sigma_u}{\sigma_v}=\frac{\sigma_u}{\sigma_{e_3}}\frac{\sigma_{e_3}}{\sigma_v}=\frac{-g_{13}}{\sigma_{e_1}\sigma_{e_3}}\tanh\gamma, \quad . \quad . \quad (27)$$

Fig. 2.

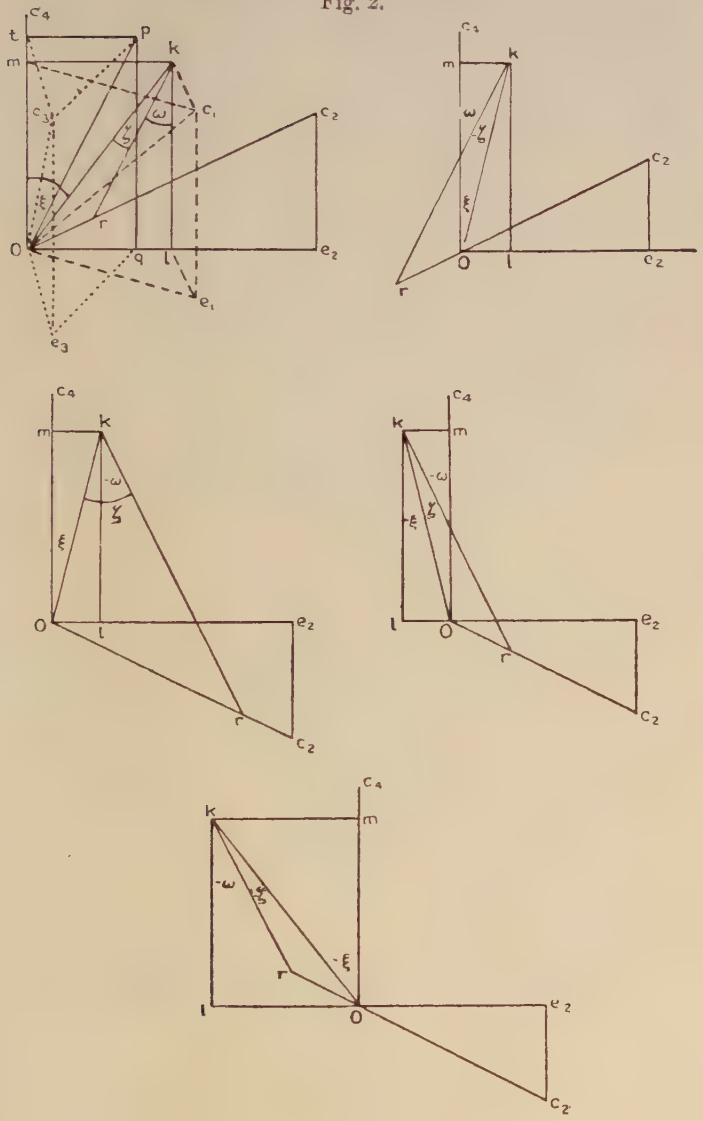

whence also

$$\sinh\lambda = \frac{-g_{13}\sinh\gamma}{\sqrt{G_{1133}}}. \quad . \quad . \quad . \quad . \quad . \quad . \quad . \quad (28)$$

$$\cosh\lambda = \frac{\sigma_{e_1}\sigma_{e_3}\cosh\gamma}{\sqrt{G_{1133}}}, \quad . \quad . \quad . \quad . \quad . \quad . \quad . \quad (29)$$

in which $G_{1133} = g_{11}g_{33} + g_{1313}\sinh^2\gamma$.

The expression for $\sinh\lambda$ has a minus sign because λ is positive when e_1 e_3 make an acute angle, that is when g_{13} is negative.

Fig. 3.

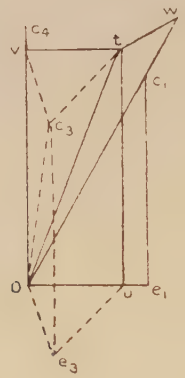

26. For ϕ we have

$$\cosh\phi = \frac{\sigma_t}{\sigma_{c_3}} = \frac{\sigma_t}{\sigma_v}\frac{\sigma_v}{\sigma_{c_3}} = \frac{\cosh\gamma}{\cosh\lambda} = \frac{\sqrt{G_{1133}}}{\sigma_{e_1}\sigma_{e_3}}, \quad . \quad (30)$$

whence

$$\sinh\phi = \frac{\sqrt{g_{1313}}\sinh\gamma}{\sigma_{e_1}\sigma_{e_3}} \quad . \quad . \quad . \quad . \quad . \quad (31)$$

$$\tanh\phi = \frac{\sqrt{g_{1313}}\sinh\gamma}{\sqrt{G_{1133}}}. \quad . \quad . \quad . \quad . \quad . \quad (32)$$

27. For μ we have

$$\cosh\mu = \frac{\sigma_w}{\sigma_t} = \frac{\sigma_w}{\sigma_{c_3}}\frac{\sigma_{c_3}}{\sigma_t} = \frac{\cosh\alpha}{\cosh\phi} = \frac{\sigma_{e_1}\sigma_{e_3}\cosh\alpha}{\sqrt{G_{1133}}}. \quad (33)$$

$$\sinh\mu = \frac{R}{\sqrt{G_{1133}}} \quad . \quad . \quad . \quad . \quad . \quad . \quad . \quad . \quad (34)$$

$$\tanh\mu = \frac{R}{\sigma_{e_1}\sigma_{e_1}\cosh\alpha}, \quad . \quad . \quad . \quad . \quad . \quad . \quad (35)$$

in which $$R = \sqrt{g_{11}g_{33}\sinh^2\alpha - g_{1313}\sinh^2\gamma}.$$

28. Since $\psi = \lambda + \mu$, we have by means of the values

found for λ μ

$$\sinh\psi = \sinh\lambda\cosh\mu + \cosh\lambda\sinh\mu$$

$$= \frac{\sigma_{e_1}\sigma_{e_3}}{G_{1133}}(R\cosh\gamma - g_{13}\cosh\alpha\sinh\gamma) \quad . \quad . \quad (36)$$

$$\cosh\psi = \cosh\lambda\cosh\mu + \sinh\lambda\sinh\mu$$

$$= \frac{1}{G_{1133}}(g_{11}g_{33}\cosh\alpha\cosh\gamma - Rg_{13}\sinh\gamma). \quad (37)$$

The law in the moving observer's space.

29. Using the values found for ω ψ we have

$$\frac{d_{12}}{\sigma_{c_1}\sigma_{c_2}} = \frac{1}{\sigma_{e_1}\sigma_{e_2}}(g_{12}\sinh\psi\cosh\omega + \sigma_{e_1}\sigma_{e_2}\cosh\psi\sinh\omega)$$

$$= \frac{1}{\sigma_{e_1}\sigma_{e_2}G_{1133}\sqrt{G_{2233}}}[g_{12}\sigma_{e_1}\sigma_{e_3}(R\cosh\gamma - g_{13}\cosh\alpha\sinh\gamma)\sigma_{e_2}\sigma_{e_3}\cosh\gamma + \sigma_{e_1}\sigma_{e_2}(g_{11}g_{33}\cosh\alpha\cosh\gamma - Rg_{13}\sinh\gamma)(-g_{23}\sinh\gamma)]$$

$$= \frac{1}{G_{1133}\sqrt{G_{2233}}}[-RG_{3312} - g_{33}g_{1213}\cosh\alpha\sinh\gamma\cosh\gamma] \quad . \quad . \quad . \quad . \quad (38)$$

in which $G_{3312} = g_{33}g_{12} + g_{3132}\sinh^2\gamma$.

30. For the quantities σ_{c_p} we have

$$\sigma_{c_1} = \sigma_{e_1}/\sinh\psi = \frac{G_{1133}}{\sigma_{e_3}(R\cosh\gamma - g_{13}\cosh\alpha\sinh\gamma)} \quad (39)$$

$$\sigma_{c_2} = \sigma_{e_2}/\cosh\omega = \frac{\sqrt{G_{2233}}}{\sigma_{e_3}\cosh\gamma} \quad . \quad . \quad . \quad . \quad . \quad . \quad . \quad (40)$$

$$\sigma_{c_3} = \sigma_{e_3}/\sinh\gamma. \quad . \quad . \quad . \quad . \quad . \quad . \quad . \quad . \quad . \quad . \quad . \quad (41)$$

31. We know that, if $\mathfrak{u} \equiv u^1e_1 + u^2e_2 + u^3e_3$ is the path in M's space of the refracted ray whose world line is

$$z \equiv z^1c_1 + z^2c_2 + z^3c_3,$$

then u^1 u^2 u^3 are equal to z^1 z^2 z^3. Consequently equation (16) now takes the form

$$\frac{u^1G_{1133}}{R\cosh\gamma - g_{13}\cosh\alpha\sinh\gamma} = \frac{u^2\sqrt{G_{2233}}}{\sinh\alpha\cosh\gamma(\sqrt{\cos^2\theta + \kappa} - \cos\theta)}$$

$$= \frac{-u^3g_{33}}{\kappa\cosh\alpha\sinh\gamma}, \quad . \quad . \quad . \quad . \quad (42)$$

in which

$$\cos\theta = \frac{RG_{3312} + g_{33}g_{1213}\cosh\alpha\sinh\gamma\cosh\gamma}{G_{1133}\sqrt{G_{2233}}\sinh\alpha},$$

$$\kappa = \frac{\tanh^2\alpha - \tanh^2\beta}{\tanh^2\beta},$$

$$G_{\lambda\rho\mu\sigma} = g_{\lambda\rho}g_{\mu\sigma} + g_{\lambda\mu\rho\sigma}\sinh^2\gamma,$$

$$g_{\lambda\mu\rho\sigma} = \begin{vmatrix} g_{\lambda\rho} & g_{\lambda\sigma} \\ g_{\mu\rho} & g_{\mu\sigma} \end{vmatrix}$$

$$R = \sqrt{g_{11}g_{33}\sinh^2\alpha - g_{1313}\sinh^2\gamma}.$$

32. The vector $\mathbf{c}_1$, the world line of the incident ray, is one of the intersections between the biplane $\mathbf{c}_4\mathbf{e}_1$ and a tricone which has axis $\mathbf{c}_3$ and semi-vertical angle α. The condition for the reality of intersections between these loci is that R should be real, that is to say that

$$\sinh\alpha > \frac{\sqrt{g_{1313}}}{\sigma_{e_1}\sigma_{e_3}}\sinh\gamma. \quad . \quad . \quad . \quad . \quad (43)$$

33. In addition to being real $\mathbf{c}_1$ must head towards the future. First let us suppose that λ is positive and numerically greater than μ. This means that $\mathbf{u}$ in fig. 3 has the same sense as $\mathbf{e}_1$, and that there are two possible positions for $\mathbf{c}_1$. For one position μ is positive, $\mathbf{c}_1$ lies between $\mathbf{t}$ and $\mathbf{e}_1$, and ψ is greater than λ; for the other μ is negative, $\mathbf{c}_1$ lies between $\mathbf{t}$ and $\mathbf{c}_4$, and ψ is less than λ.

$\tanh\lambda$, which is equal to $-g_{13}\tanh\gamma/\sigma_{e_1}\sigma_{e_3}$, is the velocity that the apparatus has in the direction of the incident ray. There are two possible speeds relative to M with which a ray of light may travel along $\mathbf{e}_1$, and in order that our problem may be definite, the data must for this case include a statement whether the speed of the ray is greater or less than the speed of the apparatus in this direction.

Expressed in terms of M's data this case occurs when γ is greater than α and the angle between $\mathbf{e}_1$ $\mathbf{e}_3$ is acute.

34. Next let us suppose that λ is negative and numerically greater than μ. In this case the intersection of the two loci give vectors heading into past time, there is no position for $\mathbf{c}_1$, and the data are not possible data for a refraction problem.

35. Finally let λ be either positive or negative and numerically less than μ. Then the positive value of μ always gives a position for $\mathbf{c}_1$ and the negative value does not. In this case the problem is definite without any

information as to the speed of the incident ray relative to M, this speed being calculable from the other data.

36. We have seen in which cases the data are consistent with the existence of a real incident ray. With a real incident ray there is always a real refracted ray if α is greater than β. When the arrival medium is denser than the departure medium, that is to say when α is less than β, the condition for a real refracted ray is that

$$\kappa + \cos^2\theta > 0,$$

or

$$\frac{RG_{3312} + g_{33}g_{1213}\cosh\alpha\sinh\gamma\cosh\gamma}{G_{1133}\sqrt{G_{2233}}\sinh\alpha} > \sqrt{1 - \frac{\tanh^2\alpha}{\tanh^2\beta}}. \quad (44)$$

XLV. *The Existence of Silver Hydroxide in the Solid State.* *By* H. L. Riley, *B.Sc., D.I.C., A.R.C.S., Beit Scientific Research Fellow, Demonstrator in Chemistry at the Imperial College of Science and Technology* *.

DURING the course of an investigation of the properties of silver oxide Carey Lea (Amer. J. Sci. (3) xliii. p. 249, 1892) noticed that all the water cannot be removed from the precipitated silver oxide by prolonged desiccation. Even after drying for 20 hours at 100° C. the oxide still retains 0·5 per cent. water. E. H. Madsen (*Zeit. anorg. Chem.* lxxix. p. 200, 1913) states that it is impossible to remove all the water from silver oxide without the latter undergoing slight decomposition.

It was necessary whilst carrying out some investigations on the atomic weight of silver (Riley and Baker, J. C. S. cxxviii. p. 2510, 1926) to analyse a large number of samples of silver oxide. The results of these analyses lent striking confirmation to the above observation of Carey Lea. The following are the percentages of water present in the various samples of silver oxide analysed :—

0·324	0·315	0·342	0·301
0·349	0·469	0·277	0·367
0·460	0·332	0·306	0·281
0·371	0·271	0·322	0·231
0·379	0·305	0·283	0·306
0·451	0·339	0·287	

That the remarkable constancy of the amount of water present in the various samples is not accidental is shown by the following. The time of desiccation over phosphorus

* Communicated by Prof. H. B. Baker, C.B.E., F.R.S.

pentoxide varied from two to eight months. In one experiment a sample of forty grams of oxide had been dried over phosphorus pentoxide for three months. Twenty grams of it were analysed and found to contain 0·377 per cent. H_2O. The remaining 20 gms. were well mixed and exposed to fresh pentoxide for another month. On analysis it was found to contain 0·451 per cent. H_2O. Another sample of oxide was analysed before it had had time to dry to the full extent. It contained 4·891 per cent. H_2O. Another portion of the same sample after only another week's drying contained only 0·315 per cent. H_2O. Caustic potash, when used as the drying agent, proved just as efficient as the pentoxide, the limit of desiccation being reached when the oxide still contained approximately 0·3 per cent. of water.

In view of the above results one is forced to the conclusion that this last 0·3 per cent. H_2O is not accidentally occluded in the silver oxide but held there by chemical forces. The following is an attempt to explain the exact nature of this small amount of water which is retained by the silver oxide.

If it is assumed that the water is present as OH groups in silver hydroxide and that the substance analysed was a "double salt," silver oxide-hydroxide, then it must be assigned a formula $n\mathrm{Ag_2O}\,.\,\mathrm{AgOH}$, where n is in the neighbourhood of 20. At first sight this is an improbable type of compound, but subsequent considerations indicate that this is the correct mode of formulation.

Silver oxide is decidedly amorphous and shows no tendency to crystallize. It is, therefore, highly probable that the individual particles approximate to colloids with regard to size. It is known that colloidal particles of radius greater than 10^{-6} cm. coagulate after a short time, so it may safely be assumed that the radius of each individual particle of silver oxide is slightly greater than that of an unstable colloid, *i. e.* between 10^{-6} and 10^{-5} cm. Suppose that on each individual particle there is an adsorbed unimolecular film of water. It will then be possible to calculate approximately the percentage of water one would expect in a sample of oxide so constituted. The volume of a single water molecule is 18/N, where N = Avogadro's Number $= 6 \times 10^{23}$ c.c.

The diameter of the water molecule, calculated from this value of the volume, $= 3{\cdot}9 \times 10^{-8}$ cm.

Assuming the radius of the individual particle of silver oxide to be 10^{-5} cm., then

$$\text{Volume of particle} = 4/3\pi \times 10^{-15} \text{ c.c.},$$

$$\text{Weight of particle} = 4/3\pi \times 10^{-15} \times 7{\cdot}1 \text{ gms.},$$

where 7·1 = the density of the silver oxide.

The weight of water on one individual particle will be to a first approximation

$$4/3\pi R^2 \times D \times M,$$

where R = radius of silver oxide particle, D the diameter of the water molecule, and M the density of water.

The percentage of water present in a sample of silver oxide so constituted will therefore be

$$\frac{4/3\pi 10^{-10} \times 3{\cdot}9 \times 10^{-8} \times 100}{4/3\pi 10^{-15} \times 7{\cdot}1}$$

$$= \underline{0{\cdot}06 \text{ per cent.}}$$

Assuming the radius of the silver oxide particle to be 10^{-6} cm. then, repeating the above, amount of water present

$$= \underline{0{\cdot}6 \text{ per cent.}}$$

The actual experimental value was about 0·3 per cent. A sample of silver oxide which is constituted of particles of radius somewhere between 10^{-5} and 10^{-6} cm., each being surrounded by a unimolecular film of water, will therefore have a composition the same as the samples of oxide investigated.

If one considers the mechanism of the precipitation of substances which have no tendency to crystallize, then it becomes apparent that it is highly probable that such compounds will be precipitated in particles, the size of which is just greater than the size of particles which form stable colloidal solutions.

But how are these water molecules attached to the silver oxide? Do they exist actually as water molecules attached to the oxide by some stray chemical forces, or is it not conceivable that each particle of oxide is surrounded by a film of hydroxide? The amounts of water present in the two cases would be very nearly the same. It is well known that the forces at the surface of a solid are different from those in the interior, so it is quite possible that silver hydroxide might exist and be quite stable at the surface of a silver oxide lattice.

In view of the above considerations it was decided to carry out an experiment which, it was hoped, would indicate to some extent which of these two explanations is correct.

Suppose some thoroughly desiccated silver oxide, containing the usual 0·3 per cent. H_2O, be treated with carbon dioxide and then subjected to further desiccation. If the water were present as a film of hydroxide, then one would expect that this treatment would result in the liberation of

the water and further desiccation would lead to the complete dehydration of the sample. If the water were mechanically occluded or adsorbed on the surface of the silver oxide particles in the form of water molecules, then it is doubtful if carbonating and further desiccation would lead to complete dehydration; for it is quite conceivable that similar stray chemical forces or mechanical occlusion may lead to a retention of the water in silver carbonate.

In order to determine the result of carbonating silver oxide, a sample of about 20 gms. was prepared and dried over potash for two months. It was then placed in a desiccator over phosphorus pentoxide. Dry carbon dioxide was passed into the desiccator each day for a week, a large excess being used. The oxide was then allowed to remain in the desiccator for a further period of eighteen days and then analysed. The following unexpected results were obtained :—

Weight of carbonated oxide used	18·4396 gms.
Weight of water	0·0321 „
Weight of carbon dioxide	0·1777 „
Weight of residual silver	16·9714 „

showing that the desiccated silver oxide had only become carbonated to the extent of one-twentieth although it had been treated with a large excess of carbon dioxide over a period of one week. The only satisfactory explanation of the above experiment, in view of the work of H. B. Baker, is that desiccated silver oxide contains no free water, and that 0·3 per cent. H_2O shown on analysis must be present in the combined form, *i. e.* as silver hydroxide.

That silver hydroxide may exist on the surface of silver oxide particles is made highly probable if the structure of the silver oxide lattice is considered. By analogy with cuprous oxide, silver oxide belongs to the cubic octahedral system, a unit lattice cube of which is shown in fig. 1.

The black circles represent oxygen atoms and the white ones silver atoms. In the centre of the crystal each of the oxygen atoms at the corners of the unit cube is associated with eight cubes. Therefore, the number of oxygen atoms directly associated with four silver atoms in the centre of the unit cube will be, the oxygen atom in the centre plus 8/8, *i. e.* 2. This gives the correct stoichiometric ratio of silver to oxygen in silver oxide, viz. 4Ag : 2 O. Now in a unit cube at the surface of the lattice a different state of affairs exists, for each of the oxygen atoms at the surface corners of the unit cube is only associated with four, instead

of eight, unit cubes. The ratio of silver to oxygen in such an arrangement would be $4Ag : (1+4/8+4/4)O = 4Ag : 2\frac{1}{2}O$, showing an excess of oxygen over the correct ratio.

Fig. 1.

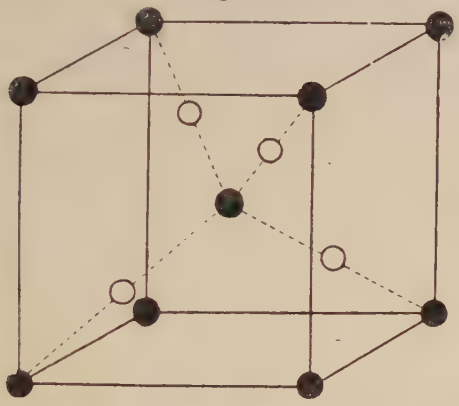

In order that the valency forces may be satisfied at the surface of a crystal the lattice must either lose symmetry at the surface or some adsorption effect must take place. In crystals with a radius greater than 10^{-4} cm. any adsorption effect would not be detected by ordinary chemical analysis, but in amorphous bodies, where the individual crystals are very small, this surface effect will cause a pronounced alteration in the composition of the substance.

Fig. 2.

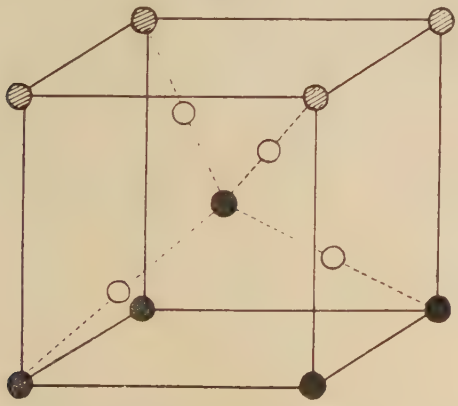

In the case of silver oxide, if instead of putting oxygen atoms, we put hydroxyl groups (see fig. 2: the shaded

circles represent hydroxyl groups), it will be seen that the valencies of both silver and oxygen are satisfied. The four silver atoms in the unit cube are associated with

$$O + 4/8\,O + 4/4\,OH,$$

which gives the stoichiometric relationship

$$4Ag\,.\,1\tfrac{1}{2}\,O\,.\,OH = 3Ag_2O\,.\,2AgOH,$$

which satisfies the valencies of both silver and oxygen.

Summary.

The above considerations indicate that the water present in precipitated silver oxide after prolonged desiccation is probably there in the form of a surface film of silver hydroxide. This view is in conformity with the size of the individual particles of silver oxide and with the chemical inactivity of the substance when treated with carbon dioxide. This view can be correlated quite simply with theories of crystal structure.

Further experiments are in progress in which it is hoped to correlate adsorption phenomena with the size and structure of the precipitated particle.

XLVI. *Magnetic Anisotropy of Cubic Crystals.* *By* J. Forrest, *M.A., D.Sc., Carnegie Teaching Fellow, Dundee University College of St. Andrews* *.

THIS paper is a continuation of a more general one just published in the Trans. of the Roy. Soc. of Edin. (1926, No. xiv.), a *résumé* of which appeared in the Philosophical Magazine (November 1925).

Prof. P. Weiss was the first to point out, by his experimental researches on crystals of magnetite, the exact nature of the magnetic anisotropy of that cubic crystal. He showed that only to a first order was the crystal magnetically isotropic, and that its variations from magnetic uniformity are represented in general by a quartic central surface, approximating in form to a cube with rounded corners, bevelled edges, and depressions in the centres of the faces. While this surface gives magnetic isotropy in octahedral planes, the work of Quittner (*Ann. d. Physik*, xxx. 1909) indicates hexagonal variation therein. For varying orientation of a magnetizing field in a cube face plane of magnetite, the variation of the component of magnetization parallel to the external field is represented by a central

* Communicated by the Author.

almost circular oval, with minima along the quaternary axes and maxima along the binary axes. A similar and extensive research on large crystals of iron has been carried out by K. Beck (1918), but I have not been able to obtain the published account of his work. Weiss, in some of his papers in the *Journal de Physique* and elsewhere ('Le Magnétisme,' par P. Weiss et G. Foëx, p. 128), remarks that Beck's results for iron are similar to those found for magnetite; but apparently this is true only in a limited sense, as recent work of W. L. Webster on iron crystals (Proc. Roy. Soc. A, cvii. 1925) indicates that while the general nature of the curves for the two substances is the same in cube-face planes of iron, maxima occur along the quaternary axes and minima along the binary axes.

The experimental work of the writer on other cubic crystals (Trans. Roy. Soc. Edin. xiv. 1926), such as the cubic alums, iron pyrites, sodium chloride, fluorspar, copper, &c., indicates that the general structure found for magnetite and iron is common to all cubic crystals. In effect, with reference to magnetic quality in cube-face planes, cubic crystals may be classified into two classes :—(A) those with maxima along the binary axes and minima along the quaternary axes—examples : magnetite and the alums ; (B) those with maxima along the quaternary axes and minima along the binary axes—examples : iron, iron pyrites, fluorspar, sodium chloride, copper.

On the theoretical side, the above experimental results have led to analysis designed to predict this quality by estimation of the variation of the internal force within regular arrangements of magnetic doublets. The first work of this nature is that of Prof. W. Peddie, who in three papers communicated to the Royal Society of Edinburgh (1905, 1908, 1912) deals in this way with a Face-centred Cube arrangement of doublets, a Simple Cube arrangement, and finally gives a general discussion applicable to any regular array of doublets. In particular, with reference to the subject of this paper, he has found that a Face-centred arrangement of magnetic doublets has the same variation of magnetic quality as was found by Weiss in magnetite, and that a Simple Cube system has exactly the opposite variation of quality. The quartic form of the magnetization surface is also deduced and the hexagonal variation in octahedral planes is shown to be represented by a surface of higher order.

The writer (Trans. Roy. Soc. Edin. xiv. 1926) has applied the above theory in detail to a series of crystals, much less strongly magnetic than magnetite and iron, chosen from

all the crystal systems. Curves showing the variation of magnetization in principal planes of these are found for varying orientation of a magnetic field therein, and compared with theoretically deduced modes of variation of internal force in regular arrangements of doublets. This leads to discrimination of the equivalent Magnetic Lattice of the crystal—*i. e.*, the singly homogeneous arrangement of magnetic doublets identical with the crystal in its departure from magnetic isotropy.

The present discussion is limited to crystals belonging to the cubic system, and is intended to indicate that the doublet conception is sufficient to explain the known facts, and to show that there are other possibilities in the theory than discrimination of the magnetic lattice. The theoretical basis of the argument is essentially that laid down in the papers above referred to. Two fundamental assumptions are made : (1) the law of force between magnetic poles induced in a crystal is that of the inverse square ; (2) the ratio $\frac{a}{\rho}$ is small, where a is the semi-length of a doublet and ρ is the distance apart of nearest neighbours in the array of doublets.

As relevant to the structures to be investigated, the force at a pole of either of two parallel dissimilar magnetic doublets is required.

Consider two parallel magnetic doublets, similarly co-directed, of semi-lengths a_1 and a_2, pole-strengths m_1 and m_2, the distance apart of the centres being r, and the inclination of the pair to r being θ, where θ is measured from the south to north direction of an axis. Then, in general, the components of force at the pole of strength $+m_1$, these components being taken parallel and transverse to the pair, are respectively L and T, where

$$\mathrm{L} = m_2(a_1-a_2-r.\cos\theta).\left[(a_1-a_2)^2-2(a_1-a_2)r.\cos\theta+r^2\right]^{-3/2}$$
$$-m_2(a_1+a_2-r\cos\theta).\left[a_1+a_2)^2-2(a_1+a_2)r.\cos\theta+r^2\right]^{-3/2}$$

and

$$\mathrm{T} = m_2.r.\sin\theta.\left[(a_1-a_2)^2-2(a_1-a_2)r.\cos\theta+r^2\right]^{-3/2}$$
$$-m_2.r\sin\theta.\left[(a_1+a_2)^2-2(a_1+a_2).r.\cos\theta+r^2\right]^{-3/2}.$$

These expanded in terms of Zonal Harmonics in $\cos\theta$ become

$$\mathrm{L} = \frac{2\mathrm{M}_2}{r^3}.\left[\mathrm{P}_2+\frac{3a_1}{r}.\mathrm{P}_3+\frac{2}{r_2}.(3a_1^2+a_2^2).\mathrm{P}_4+\ldots.\right]. \quad (1)$$

and

$$\mathrm{T} = \frac{\mathrm{M}_2\sin\theta}{r^3}.\left[\mathrm{P}_2'+\frac{2a_1}{r}.\mathrm{P}_3'+\frac{1}{r^2}.(3a_1^2+a_2^2).\mathrm{P}_4'+\ldots\right], \quad (2)$$

where P_n is Zonal Harmonic in $\cos\theta$ of order n, and $\frac{a_1}{r}, \frac{a_2}{r}$ each less than 1 ; M_1 and M_2 are the magnetic moments of the doublets.

Similarly, for the components of force at $-m_1$ due to the second doublet there result

$$L' = \frac{2M_2}{r^3} \cdot \left[P_2 - \frac{3a_1}{r} \cdot P_3 + \frac{2}{r^2} \cdot (3a_1^2 + a_2^2) \cdot P_4 - \ldots \right] \quad . \quad (3)$$

and

$$T' = \frac{M_2 \sin\theta}{r^3} \cdot \left[P_2' - \frac{2a_1}{r} \cdot P_3' + \frac{1}{r^2} \cdot (3a_1^2 + a_2^2) \cdot P_1 - \ldots \right] . \quad (4)$$

Now (3) and (3) differ from (1) and (2) only in the signs of the odd Zonal Harmonics. For singly homogeneous cubic arrangements, the first two terms on summation to include the force at $\pm m_1$ due to a surrounding system of doublets like the second member of the above pair vanish either identically or on the whole (Proc. Roy. Soc. Edin. 1912, vol. xxxii. no. 17) ; and hence for such arrangements (1), (2) and (3), (4) give the same force.

Hence for such arrays

$$L = L' = 4M_2 \cdot (3a_1^2 + a_2^2) \cdot \Sigma \frac{P^4}{r^5} \cdot \quad . \quad . \quad . \quad . \quad (5)$$

and

$$T = T' = M_2 \cdot (3a_1^2 + a_2^2) \cdot \Sigma \frac{\sin\theta}{r^5} \cdot P_4', \quad . \quad . \quad (6)$$

where the summation includes a surrounding cubic array of doublets each of magnetic moment M_2.

Thus up to this order the force at each pole of the doublet of magnetic moment M_1 due to a surrounding cubically-arranged set, each of which has magnetic moment M_2, has the same value, and its components are given effectively by (5) and (6).

By putting $a_2 = a_1$ we obtain the force when all members are alike, viz. :

$$L = 16M_1a_1^2 \cdot \Sigma \frac{P_4}{r^5} \quad \text{and} \quad T = 4M_1a_1^2 \cdot \Sigma \frac{\sin\theta}{r^5} P_4'.$$

When the force lies in a face plane of a cubic array these become

$$L_1 = -\frac{M_1a_1^2}{2\rho_1^5} \cdot (G_1 - D_1)(\cos 4\theta + \tfrac{3}{5})$$

and

$$T_1 = \frac{M_1a_1^2}{2\rho_1^5} \cdot (G_1 - D_1) \cdot \sin 4\theta \quad . \quad . \quad . \quad . \quad . \quad (I.)$$

(see Proc. Roy. Soc. Edin. xxxii. 1917), where

$$(G - D) = \tfrac{35}{2} \cdot [\Sigma f^{-5/2} - \Sigma\lambda^4 \cdot f^{-9/2}] \text{ with } f = (\lambda^2 + \mu^2 + \nu^2);$$

(λ, μ, ν) are integers chosen so as to include all members in the system, the effect of which, at the pole of the first doublet, is being found ; ρ is the distance apart of nearest neighbours ; and θ is the angle between the force and a cube edge.

Correspondingly, in a face plane of a cubic array, (5) and (6) become

$$L_2 = -\frac{M_2}{8\rho_2^5}.(3a_1^2+a_2^2).(G_2-D_2).(\cos 4\theta+\tfrac{3}{5})$$

and

$$T_2 = \frac{M_2}{8\rho_2^5}.(3a_1^2+a_2^2)(G_2-D_2).\sin+\theta, \quad . \quad . \quad (II.)$$

which give the variational components of force at a pole of a member of a first set due to all members of a second set ; *i. e.* (G_2-D_2) has to be effected for all centres of the second set referred to a member of the first set.

It is necessary now to connect (L, T) with the actual components of magnetization as found by experiment, parallel and transverse to the externally applied field.

Consider a plane of the crystal in which the applied field H is inclined at α to some direction of stability OX, and let the magnetization be inclined at θ to OX. Thus at saturation all the doublets are directed at an angle θ with OX. The cubic arrangements to be dealt with are of such high symmetry that this common co-direction will hold in the case of the two sets of doublets involved. Theory as above gives L and T in terms of constants and θ, where L and T are the components of force, parallel and perpendicular to the magnetization, on a doublet at the origin, due to the members within the directional sphere of influence, beyond which the other members have no appreciable effect on the summation coefficients in L and T, *i. e.* in the cubic system, on (G—D). For the members beyond this limit we may substitute a uniform distribution which will be magnetized in the direction of H. Hence, so far as the effect on the origin magnet is concerned, we may put $H_1 = H + \frac{4}{3}\pi I$ in place of H, where I is the mean intensity of magnetization throughout the substance.

Remembering now that (L, T) is the same at each pole of any member of one set, we may identify (L, T) with the induction. Then parallel to the applied field the induction relation " $B=(H+4\pi I)$ " becomes

$$L.\cos\phi + T.\sin\phi = H_1 + 4\pi.I_p,$$

where $\phi=(\theta-\alpha)$ and I_p is the directional component of magnetization parallel to H. But also $T=H_1.\sin\phi$. To

simplify the analysis, let ϕ be small and so T small compared with H_1, and the induction relation parallel to the applied field becomes $L = H_1 + 4\pi . I_p$. Hence the total component of magnetization parallel to H is $I_P = I_p + I = \frac{L - H_1}{4\pi} + I$, giving $4\pi I_p = (L + \frac{8}{3}\pi I)$; and thus the parallel magnetization curves are given by the addition of a constant magnetization to L.

Perpendicular to the external field the induction relation becomes $L . \sin\phi - T . \cos\phi = 4\pi . I_N$, where I_N is in this case the total component of magnetization perpendicular to H. With the same limitation as above this gives

$$\frac{T}{H}(L - H_1) = 4\pi . I_N.$$

To a first order this becomes $4\pi I_N = -T$, since L and T contain the same power of $\frac{a}{\rho}$ as a factor. Hence zero values of I_N and T occur simultaneously, as is always found in the experimental curves of the transverse component of magnetization. T is always proportional to $\sin 2\theta$, $\sin 4\theta$, &c. (see Roy. Soc. Edin. papers above referred to); and so the variation of T with θ is represented by a curve of symmetrical loops. The curve showing the variation of I_N will be composed of the same number of loops, but these will not be symmetrical. From the above expression for I_N, since $(H_1 - L)$ is positive at saturation, the loops representing I will be flatter on approach to the directions of minimum L than at approach to the directions of maximum L. The smaller $\frac{L}{H_1}$ is, *i.e.* at high fields, the greater will be this effect. This is found in all the transverse magnetization curves.

For investigation of maxima and minima of induction for any cubic arrangement, simple or compound, we need only deal with the expressions for L and T as given by equations (I.) and (II.) for a cube-face plane.

It is now possible to investigate the magnetic structure of several well-known cubic crystals, identifying the magnetic doublet with the atom.

Iron.—For a Body-centred Cubic system of similar doublets, $(G_1 - D_1) = \frac{35}{2} . (+1{\cdot}0990)$ with $2\rho_1 =$ the edge of the elementary body-centred cube (Trans. Roy. Soc. Edin. xiv. 1926). This value substituted in (I.) gives maxima along the

binary axes and minima along the quaternary axes. This is the opposite of the experimental results, and hence the equivalent Magnetic Lattice cannot be a Body-centred Cube one.

However, the Body-centred array given by X-rays can be regarded in two other ways. We may regard it as two interpenetrating Simple Cube arrangements, which do not act independently, but in which corresponding doublets act in pairs. The structure then becomes a Simple Cube one with members composed of similar compound pairs. For such an array $(G_1-D_1)=\frac{35}{2}.(-3{\cdot}8461)$ (Roy. Soc. Edin. papers), and so gives in a face plane the experimental variation of quality.

There is still another possibility, as the two sets may be dissimilar and also act independently, in which case

$$L=L_1+L_2.\,(G_1-D_1)=\frac{35}{2}.(-3{\cdot}8461)$$

for a Simple Cube set with ρ_1 = the edge of the elementary Simple Cube, and

$$(G_2-D_2)=\frac{35}{2}.(2{\cdot}314)\quad\text{with}\quad\rho_2=\tfrac{1}{2}\rho_1.$$

These give in a cube-face plane

$$L=\frac{35}{4}\cdot\frac{3{\cdot}846}{\rho_1^{\,5}}\cdot[M_1a_1^{\,2}-0{\cdot}481M_2(3a_1^{\,2}+a_2^{\,2})]\,.\,(\cos 4\theta+\tfrac{3}{5}).$$

Hence, if $M_1.a_1^{\,2}$ is greater than $\cdot481M_2(3a_1^{\,2}+a_2^{\,2})$, maxima lie along $\theta=0$, *i. e.* cube edges, and minima along $\theta=\frac{\pi}{4}$, *i. e.* face diagonals, as is required by the experimental results. The above condition means in effect that $M_1a_1^{\,2}$ must be greater than $1{\cdot}44M_2a_1^{\,2}$ or M_1 greater than $1{\cdot}44M_2$ with M_1 and M_2 both positive. Hence for the magnetic quality to be satisfied by such a structure, the doublet in one set must have at least about one and a half times the magnetic moment of a member of the other set.

Sodium Chloride.—The structure of crystals of this class, as given by X-rays, consists of two interpenetrating Face-centred cubically-arranged systems, the members of one set being at the mid-points of the face-centred cube edges of the other set. Hence a member of either set is similarly surrounded by those of its own set and those of the other set. Again, in view of the high cubic symmetry of the

arrangement, the two sets of doublets will assume a common co-direction at saturation under an applied field.

For a simple Face-centred system, $(G_1-D_1)=\frac{35}{2}.(\cdot226)$, which, substituted in L, gives in a face-plane diamagnetic minima in the direction of the quaternary axes, and maxima in the direction of the binary axes. The substance has diamagnetic quality, and the above variation is the opposite of the experimental results (Trans. Roy. Soc. Edin. xiv. 1926). Hence a face-centred arrangement of diamagnetic doublets will not suit as the Magnetic Lattice. However, since for a Simple Cube system $(G-D)=(-3\cdot8461)$, it results that a Simple Cube array of diamagnetic doublets can be chosen as the Magnetic Lattice.

The more general possibility is again to regard the two sets as independent, in which case $(G_2-D_2)=\frac{35}{2}.(-4\cdot112)$ with $\rho_2=\rho_1=$ the elementary face-centred cube edge; and then the total variational force at a pole of the first set is given by

$$L'=-\frac{35}{4\rho_1{}^5}.[\cdot266M_1a_1{}^2-1\cdot028M_2(3a_1{}^2-a_2{}^2)].(\cos 4\theta+\tfrac{3}{5})$$

and

$$T'=\frac{35}{4\rho_1{}^5}.[\cdot266M_1a_1{}^2-1\cdot028M_2(3a_1{}^2+a_2{}^2)].\sin 4\theta.$$

Similarly, the components at a pole of the second set are, in face planes,

$$L''=-\frac{35}{4\rho_1{}^5}.[\cdot266M_2a_2{}^2-1\cdot028M_1(3a_2{}^2+a_1{}^2)].(\cos 4\theta+\tfrac{3}{5})$$

and

$$T''=\frac{35}{4\rho_1{}^5}.[\cdot266M_2a_2{}^2-1\cdot028M_1(3a_2{}^2+a_1{}^2)].\sin 4\theta.$$

But common co-direction of the two sets gives (*a*) $T'=T''$ if M_1 and M_2 are of the same sign, and (*b*) $T'=-T''$ if M_1 and M_2 are of opposite signs.

(*a*) With M_1 and M_2 of the same sign, we have two paramagnetic sets or two diamagnetic sets, for which $T'=T''$ gives

$$\cdot266M_1a_1{}^2-1\cdot028M_2(3a_1{}^2+a_2{}^2)=\cdot266M_2a_2{}^2-1\cdot028M_1(3a_2{}^2+a_1{}^2).$$

This means that $L'=L''$ and $\frac{a_1{}^2}{a_2{}^2}=\frac{M_2-2\cdot38M_1}{M_1-2\cdot38M_2}$, which

must thus be positive. In the Sodium Chloride series of crystals, examples of this type are $\overset{+}{Ca}\overset{+}{O}$, $\overset{+}{Mg}\overset{+}{O}$, $\overset{+}{Ba}\overset{+}{O}$, $\overset{+}{Sr}\overset{+}{O}$, $\overset{-}{Ag}\overset{-}{Cl}$, $\overset{-}{Ag}\overset{-}{Br}$, all of which have the same structure as that above. It is notable that all of the series are diamagnetic. If we identify M_1 and M_2 with the atomic magnetic moment of the corresponding element, and put $M_1=\chi . Aw$, where χ is the Specific Susceptibility of the element of atomic weight A, and w is the mass of a hydrogen atom, the susceptibilities of gas elements being taken at low temperatures, then it is found that $\frac{M_2-2{\cdot}38M_1}{M_1-2{\cdot}38M_2}$ is positive for all of the above series.

Members of this class have not yet been investigated experimentally in respect of positions of maxima and minima; but as indicating the possibility of prediction, take $\overset{+}{Ca}\overset{+}{O}$ as an example, for which

$$M_1=1{\cdot}8\times10^{-6}\times40\times w,\quad M_2=1{\cdot}8\times10^{-6}\times16\times w.$$

This gives $\frac{a_1^2}{a_2^2}={\cdot}93$, whence, using the above values of M_1 and M_2, the force becomes

$$L=\frac{35a_1^2}{4\rho_1^5}.[113{\cdot}2\times10^{-6}\times w].(\cos4\theta+\tfrac{3}{5}),$$

which has absolute maxima, *i. e.* diamagnetic minima in the direction of the quaternary axes ($\theta=0$) and diamagnetic maxima along the binary axes $\left(\theta=\frac{\pi}{4}\right)$. This has still to be verified experimentally.

(*b*) M_1 and M_2 are of opposite sign in cases where one set of members is paramagnetic and the other set diamagnetic. Here $T/=-T''$ gives

$$\cdot266M_1a_1^2-1{\cdot}028(3a_1^2+a_2^2)M_2 = 1{\cdot}028M_1(3a_2^2-a_1^2)-\cdot266M_2a_2^2,$$

whence $-\frac{a_1^2}{a_2^2}=\frac{M_2+4{\cdot}05M_1}{M_1+4{\cdot}05M_2}$, which must be negative.

Examples of this class are $\overset{+}{Na}\overset{-}{Cl}$, $\overset{+}{K}\overset{-}{Cl}$, $\overset{+}{K}\overset{-}{Br}$, $\overset{+}{K}\overset{-}{I}$, $\overset{+}{Cd}\overset{-}{O}$, $\overset{+}{Na}\overset{-}{I}$, for which substitution of $M=\chi . A . w$ as before gives in each case $\frac{M_2+4{\cdot}05M_1}{M_1+4{\cdot}05M_2}$ a negative value. Again, each of the series is diamagnetic.

Taking the case of $\overset{+}{\text{Na}}\overset{-}{\text{Cl}}$, from which the whole class takes its name,

$$M_1 = \cdot 5 \times 10^{-6} \times 23w \text{ and } M_2 = -\cdot 2 \times 10^{-6} \times 35\cdot 5w,$$

which gives $\frac{a_1^2}{a_2^2} = 42$, which values lead to

$$L = -\frac{35}{4} \cdot \frac{a_1^2}{\rho_1^5} \cdot (42\cdot 77 \times 10^{-6} w) \cdot (\cos 4\theta + \tfrac{3}{5}),$$

and this has diamagnetic maxima along the cube edges, and minima along the cube-face diagonals. The writer has shown that this is the actual magnetic structure (Trans. Roy. Soc. Edin. xiv. 1926). Alternatively the Magnetic Lattice may be a Simple Cube one, composed of compound doublets of diamagnetic quality.

Zinc Blende.—X-ray analysis indicates that ZnS consists of two interpenetrating Face-centred Cubic Lattices. One set of points lie at the body-centres of alternate small cubes in the Face-centred cubic lattice on which the other set lies, and so one set can be made to coincide with the other by motion of either set along a body diagonal a distance equal to half the body-diagonal of an octant cube. This means that an $\bar{\text{S}}$ atom is surrounded by both sets exactly as a $\bar{\text{Zn}}$ atom is surrounded. Taking a Zn doublet at the origin, the force due to the rest of the Zn set depends on

$$(G_1 - D_1) = \frac{35}{2} \cdot (\cdot 266)$$

for a face-centred system; for the force on the same Zn member due to the S system calculation gives

$$(G_2 - D_2) = \frac{35}{2} (\cdot 046),$$

with $\rho_2 = \frac{1}{2}\rho_1$ and $2\rho_1 =$ the edge of the elementary face-centred cube. This gives

$$L' = -\frac{35}{4\rho_1^5} \cdot [\cdot 266 M_1 a_1^2 + \cdot 368 M_2 (3a_1^2 + a_2^2)] \cdot (\cos 4\theta + \tfrac{3}{5}).$$

With $T' = T''$ we obtain $\frac{a_2^2}{a_1^2} = \frac{M_1 - 10\cdot 82 M_2}{M_2 - 10\cdot 82 M_1}$,

which with

$$M_1 = -\cdot 15 \times 10^{-6} \times 65w \text{ and } M_2 = -\cdot 5 \times 10^{-6} \times 32w$$

gives $\frac{a_2^2}{a_1^2} = 2\cdot 31$, and so $L =$ (a positive quantity) $\times (\cos 4\theta + \frac{3}{5})$.

This gives diamagnetic minima in the directions of the quaternary axes, and maxima along the binary axes. The crystals of this substance generally contain iron, and it is very difficult to obtain a pure specimen exhibiting diamagnetism, and more difficult accordingly to verify this result.

A Face-centred system of compound doublets—such we may regard the above structure to be—would of course interchange maxima and minima in the above result.

Calcium Fluoride.—For this diamagnetic cubic crystal, X-ray analysis indicates that the $\overset{+}{\mathrm{Ca}}$ atoms are arranged on a Face-centred Cubic lattice, and the $\overset{-}{\mathrm{F}}$ atoms occupy the centres of all the octant cubes in that Face-centred system; *i. e.*, the latter by themselves form a Simple Cubic array. Hence, for the force at a pole of a Ca doublet,

$$(\mathrm{G}_1-\mathrm{D}_1)=\frac{35}{2}.(\cdot 266),$$

with $2\rho_1$ = the edge of the face-centred cube, and

$$(\mathrm{G}_2-\mathrm{D}_2)=\frac{35}{2}.(\cdot 092) \quad \text{with} \quad 2\rho_2=\rho_1.$$

This gives as the variable part of the force at a pole of a Ca atom

$$\mathrm{L}'=-\frac{35}{4\rho_1{}^5}.[\cdot 266\mathrm{M}_1a_1{}^2+\cdot 736\mathrm{M}_2(3a_1{}^2+a_2{}^2)].(\cos 4\theta+\tfrac{3}{5})$$

for the magnetization lying in a cube-face plane.

In this case, however, there is not the same correspondence between the two systems, as an F member is not surrounded by both sets as a Ca member is. Taking the origin now at an F doublet $(\mathrm{G}_1'-\mathrm{D}_1')=\frac{35}{2}.(-3\cdot 85)$ for a Simple Cubic array, and, as the Ca doublets occupy alternate octants in that Simple Cubic structure, calculation gives

$$(\mathrm{G}_2'-\mathrm{D}_2')=\frac{35}{2}.(\cdot 046) \quad \text{with} \quad 2\rho_2'=\rho_1'=\rho_1.$$

Hence at a pole of an F member there results

$$\mathrm{L}''=-\frac{35}{4\rho_1{}^5}.[-3\cdot 85\mathrm{M}_2a_2{}^2+\cdot 368\mathrm{M}_1(3a_2{}^2+a_1{}^2)].(\cos 4\theta+\tfrac{3}{5}).$$

But $T' = -TT''$ gives

$$\cdot 266 M_1 a_1^2 + \cdot 736 M_2 (3a_1^2 + a_2^2) = 3\cdot 85 M_2 a_2^2 - \cdot 386 M_1 (3a_2^2 + a_1^2),$$

from which with

$$M_1 = \cdot 7 \times 10^{-6} \times 40w \text{ and } M_2 = -\cdot 4 \times 10^{-6} \times 19w$$

we obtain $\frac{a_1^2}{a_2^2} = 30$. These values when substituted in L'' give diamagnetic maxima in the direction of the cubic axes, and minima along the binary axes, as is required by the experimental results as found by the writer (Trans. Roy. Soc. Edin. xiv. 1926). Some difficulty has been experienced in obtaining reliable values for the susceptibilities of Ca and F, and in view of the conditions that of F is probably greater than the value taken ; but a greater value renders the signs more uncertain.

The structure may also be regarded as composed of an array of compound diamagnetic doublets in Simple Cube arrangement ; and from that point of view the Magnetic Lattice can be a Simple Cube one.

Copper.—This diamagnetic cubic crystal has been shown by the writer to have in cube faces diamagnetic maxima in the directions of the cube edges, and minima along the binary axes (Trans. Roy. Soc. Edin. xiv. 1926), and X-ray analysis has indicated that the atoms are arranged on a Face-centred cubic lattice.

As already indicated here and elsewhere (Roy. Soc. Edin. papers quoted above), $(G_1 - D_1)$ is positive for a Face-centred cubic array of doublets and for a Body-centred one, but negative for a Simple Cube one. Hence, since

$$L_1 = -\frac{M_1 a_1^2}{\rho_1^5} (G_1 - D_1)(\cos 4\theta + \tfrac{3}{5})$$

for a cube-face plane, it follows that the only possible Magnetic Lattice is the Simple Cube system for which we must assume a compound diamagnetic doublet.

We may regard the Face-centred Lattice as composed of two sets of members, one set arranged in a Simple Cube System, and the other at the centres of the cube faces of the former set. A member of the first set is not surrounded by both sets as a member of the second set is. Examination of the two systems indicates that for the common co-direction

lying in a cube-face plane,

$$L' = -\frac{35}{4\rho_1^5}\cdot[-3{\cdot}85M_1a_1^2 + 3{\cdot}095M_2(3a_1^2 + a_2^2)]\,.\,(\cos 4\theta + \tfrac{3}{5})$$

and

$$L = -\frac{35}{4\rho_1^5}\cdot[-3{\cdot}192M_2a_2^2 + 1{\cdot}574M_1(3a_2^2 + a_1^2)]\,.\,(\cos 4\theta + \tfrac{3}{5}).$$

Hence with both M_1 and M_2 diamagnetic but different in values, it is possible for the Face-centred structure when regarded as two systems to give the experimental result quoted above. The same is also true with one of the atomic magnetic moments diamagnetic and the other paramagnetic, or with both equally diamagnetic but a_1 and a_2 unequal.

Conclusion.

The foregoing analysis identifies the magnetic element with the atom, and the agreement of the theoretical results with those of actual experiment, where such are available, appears to support the assumption. It is not desired meantime to push the arithmetical results too far, as these are dependent on the values assumed for M_1 and M_2, for which are substituted the average values of the atomic element mass susceptibilities. However, these are always such as to render at least the final signs in L quite certain, and the latter alone are vital to the present argument. The summations have been calculated to six figures, and the values of (G − D) used are probably correct at least to the second decimal place.

This correspondence between theory and experiment gives further support to the assumption of the inverse square law between magnetic poles in a crystal, and also indicates the relative smallness of a compared with ρ. No attempt is made here to calculate the value of the constant part of the induction, which is dependent on the value of I, the mean magnetic moment throughout the substance.

In conclusion, I wish to thank Prof. Peddie for helpful discussion on several of the points dealt with above.

XLVII. *The Derivation of Energy from Action.* By P. Du Val, *B.Sc.**

THE world to which the following discussion refers is that described by Eddington in 'The Mathematical Theory of Relativity,' Ch. VII. Part II. References such as (100) or (61·3) are to the sections and formulæ of that work.

If $\mathfrak{K}$ be any invariant-density, which is a function of the ${}^*G_{\mu\nu}$ and their derivatives to any order, its variation for an arbitrary variation of ${}^*G_{\mu\nu}$ can be expressed in the form

$$\delta\mathfrak{K} = \text{a divergence} + \mathfrak{S}^{\mu\nu}\delta\,{}^*G_{\mu\nu}.$$

This defines the Hamiltonian derivative :

$$\mathfrak{S}^{\mu\nu} = \frac{\mathfrak{n}\mathfrak{K}}{\mathfrak{n}\,{}^*G_{\mu\nu}}.$$

If the variation $\delta\,{}^*G_{\mu\nu}$ be solely due to a change of coordinates, $\int\mathfrak{K}\,d\tau$ over any region whose boundary is unaffected by a change of coordinates is invariant, so that $\delta\mathfrak{K}$ must in this case reduce to a divergence.

If the coordinates x^μ be changed to $x^\mu+\delta x^\mu$, then exactly as in (63·1),

$$-\delta\,{}^*G_{\mu\nu} = {}^*G_{\mu\beta}\frac{\partial(\delta x^\beta)}{\partial x^\nu} + {}^*G_{\alpha\nu}\frac{\partial(\delta x^\alpha)}{\partial x^\mu} + \frac{\partial\,{}^*G_{\mu\nu}}{\partial x}\delta x^\alpha,$$

so that

$\delta\mathfrak{K}$ = a divergence

$$-\mathfrak{S}^{\mu\nu}\left({}^*G_{\mu\beta}\frac{\partial(\delta x^\beta)}{\partial x^\nu} + {}^*G_{\alpha\nu}\frac{\partial(\delta x^\alpha)}{\partial x^\mu} + \frac{\partial\,{}^*G_{\mu\nu}}{\partial x^\alpha}\delta x^\alpha\right)$$

= a divergence

$$-(\mathfrak{S}^{\rho\nu}\,{}^*G_{\rho\mu} + \mathfrak{S}^{\nu\rho}\,{}^*G_{\mu\rho})\frac{\partial(\delta x^\mu)}{\partial x^\nu} - \mathfrak{S}^{\alpha\beta}\frac{\partial\,{}^*G_{\alpha\beta}}{\partial x^\mu}\delta x^\mu$$

= a divergence

$$+\left[\frac{\partial}{\partial x^\nu}(\mathfrak{S}^{\rho\nu}\,{}^*G_{\rho\mu} + \mathfrak{S}^{\nu\rho}\,{}^*G_{\mu\rho}) - \mathfrak{S}^{\alpha\beta}\frac{\partial\,{}^*G_{\alpha\beta}}{\partial x^\mu}\right]\delta x^\mu,$$

and since the quantities δx^μ are entirely arbitrary (so long as they are small, and vanish at the boundary of the region)

* Communicated by the Author.

we must have

$$\frac{\partial}{\partial x^\nu}(\mathfrak{S}^{\rho\nu}\,{}^*G_{\rho\mu}+\mathfrak{S}^{\nu\rho}\,{}^*G_{\mu\rho})-\mathfrak{S}^{\alpha\beta}\frac{\partial\,{}^*G_{\alpha\beta}}{\partial x^\mu}=0, \quad . \quad \text{(i.)}$$

which, if the symmetric and antisymmetric parts of $\mathfrak{S}^{\mu\nu}$ are $\mathfrak{P}^{\mu\nu}$ and $\mathfrak{H}^{\mu\nu}$ respectively, reduces to

$$\frac{\partial}{\partial x^\nu}(R_{\mu\rho}\mathfrak{P}^{\rho\nu}-F_{\mu\rho}\mathfrak{H}^{\rho\nu})-\tfrac{1}{2}\mathfrak{P}^{\alpha\beta}\frac{\partial R_{\alpha\beta}}{\partial x^\mu}-\tfrac{1}{2}\mathfrak{H}^{\alpha\beta}\frac{\partial F_{\alpha\beta}}{\partial x^\mu}=0, \quad \text{(ii.)}$$

i. e.

$$\begin{aligned}\frac{\partial}{\partial x^\nu}(R_{\mu\rho}\mathfrak{P}^{\rho\nu})-\tfrac{1}{2}\mathfrak{P}^{\alpha\beta}\frac{\partial R_{\alpha\beta}}{\partial x^\mu}&=\frac{\partial}{\partial x^\nu}(F_{\mu\rho}\mathfrak{H}^{\rho\nu})+\tfrac{1}{2}\mathfrak{H}^{\alpha\beta}\frac{\partial F_{\alpha\beta}}{\partial x^\mu}\\&=F_{\mu\rho}\frac{\partial\mathfrak{H}^{\rho\nu}}{\partial x^\nu}+\mathfrak{H}^{\rho\nu}\frac{\partial F_{\mu\rho}}{\partial x^\nu}+\tfrac{1}{2}\mathfrak{H}^{\rho\nu}\frac{\partial F_{\rho\nu}}{\partial x^\mu}\\&=F_{\mu\rho}\frac{\partial\mathfrak{H}^{\rho\nu}}{\partial x^\nu}+\tfrac{1}{2}\mathfrak{H}^{\rho\nu}\left(\frac{\partial F_{\mu\rho}}{\partial x^\nu}+\frac{\partial F_{\nu\mu}}{\partial x^\rho}+\frac{\partial F_{\rho\nu}}{\partial x^\mu}\right)\end{aligned}$$

by the antisymmetry of $F_{\mu\nu}$ and $\mathfrak{H}^{\mu\nu}$

$$=F_{\mu\rho}\frac{\partial\mathfrak{H}^{\rho\nu}}{\partial x^\nu}, \quad . \quad . \quad . \quad . \quad . \quad . \quad . \quad . \quad . \quad \text{(iii.)}$$

since $F_{\mu\nu}$ is a curl.

If $\mathfrak{K}$ involves the ${}^*G_{\mu\nu}$ only, and not their derivatives (for instance, if $\mathfrak{K}=\sqrt{-|{}^*G_{\mu\nu}|}$), the last term of (i.) becomes

$$\frac{\partial\mathfrak{K}}{\partial x^\mu}=\frac{\partial}{\partial x^\nu}(\mathrm{I}_\mu\mathfrak{K})$$

(I write I_μ^ν instead of g_μ^ν for the idemfactor, simply because we have yet no metric-tensor). Hence (i.) becomes

$$\frac{\partial}{\partial x^\nu}(\mathfrak{S}^{\rho\nu}\,{}^*G_{\rho\mu}+\mathfrak{S}^{\nu\rho}\,{}^*G_{\mu\rho}-\mathrm{I}_\mu^\nu\mathfrak{K})=0,$$

and (ii.) accordingly

$$\frac{\partial}{\partial x^\nu}(R_{\mu\rho}\mathfrak{P}^{\rho\nu}-F_{\mu\rho}\mathfrak{H}^{\rho\nu}-\tfrac{1}{2}\mathrm{I}_\mu^\nu\mathfrak{K})=0. \quad . \quad . \quad \text{(iv.)}$$

Representing the quantity in brackets by $\mathfrak{A}_\mu^\nu$, it is fairly clear that if $\dfrac{\partial\mathfrak{A}_\mu^\nu}{\partial x^\nu}$ is to vanish in all coordinate systems,

$\mathfrak{A}^\nu_\mu$ itself must vanish identically. For if we choose any arbitrary tensor $g_{\mu\nu}$ for a metric, and form the Christoffel 3-index symbols from it in the ordinary way, we know that

$$\frac{\partial \mathfrak{A}^\nu_\mu}{\partial x^\nu} - \{\mu\alpha, \beta\}\, \mathfrak{A}^\alpha_\beta = (\mathfrak{A}^\nu_\mu)_\nu$$

is a tensor. Now by a suitable choice of coordinates any or all of the 3-index symbols may be made to vanish, so that for some coordinates

$$\mathfrak{A}^\nu_{\mu\nu} = \frac{\partial \mathfrak{A}^\nu_\mu}{\partial x^\nu};$$

hence for all coordinates

$$\mathfrak{A}^\nu_{\mu\nu} = 0.$$

Hence also for all coordinates

$$\{\mu\alpha, \beta\}\, \mathfrak{A}^\alpha_\beta = 0.$$

Thus, as the 3-index symbols may be given any value we please, by choosing coordinates such that all but one of them vanish, we can destroy each component in turn of $\mathfrak{A}^\nu_\mu$. (iv.) now reduces to

$$R_{\mu\rho}\mathfrak{P}^{\rho\nu} = F_{\mu\rho}\mathfrak{H}^{\rho\nu} + \tfrac{1}{2}\mathrm{I}^\nu_\mu \mathfrak{K}. \quad . \quad . \quad . \quad . \quad \text{(v.)}$$

The meaning of our formulæ seems now clear. If $\mathfrak{H}^{\mu\nu}$ be taken as the electromagnetic induction, so that

$$\mathfrak{C}^\mu = \frac{\partial \mathfrak{H}^{\mu\nu}}{\partial x^\nu}$$

is the charge and current, then $F_{\mu\rho}\mathfrak{C}^\rho$ is the ponderomotive force, and $\mathfrak{E}^\nu_\mu$ = each member of (v.) is the ordinary electromagnetic energy, momentum, and stress. Moreover, whether or not the equation

$$\delta \mathfrak{K} = \mathfrak{S}^{\nu\mu}\delta^* G_{\mu\nu}$$

holds, enabling us to replace (ii.) by (v.), (iii.) shows us a tensor-density whose divergence, in Eddington's "natural gauge," is equal to the ponderomotive force, namely, if

$$\mathfrak{E}^\nu_\mu = R_{\mu\rho}\mathfrak{P}^{\rho\nu}, \quad \lambda g_{\mu\nu} = R_{\mu\nu},$$

$$(\mathfrak{E}^\nu_\mu)_\nu = \frac{\partial \mathfrak{E}^\nu_\mu}{\partial x^\nu} - \tfrac{1}{2}\mathfrak{E}^{\alpha\beta}\frac{\partial g_{\alpha\beta}}{\partial x^\mu} = F_{\mu\rho}\mathfrak{C}^\rho \quad . \quad . \quad \text{(vi.)}$$

(since $\mathfrak{E}^{\mu\nu} = \lambda\, \mathfrak{P}^{\mu\nu}$ is symmetrical, and since in the second term the factor λ cancels between the $g_{\alpha\beta}$ and the $g^{\alpha\gamma}$

which raises the suffix of $\mathfrak{E}^{\beta}_{\gamma}$). Since, in the special case of

$$\delta\mathfrak{K} = \mathfrak{S}^{\mu\nu}\delta^{*}G_{\mu\nu},$$

$\mathfrak{E}^{\nu}_{\mu}$ is the electromagnetic, not the material, energy, I should think we must use it in this sense generally. The only case in which we could regard $\mathfrak{E}^{\mu\nu}$ (or $\mathfrak{P}^{\mu\nu}=\lambda\mathfrak{E}^{\mu\nu}$) as the material mass, momentum, and stress, is that in which $\mathfrak{K}=\mathfrak{K}_{\mathrm{E}}-\mathfrak{K}_{\mathrm{T}}$, where $\mathfrak{K}_{\mathrm{E}}$ involves $F_{\mu\nu}$ (and allowably $R_{\mu\nu}$) but not their derivatives, and $\mathfrak{K}_{\mathrm{T}}$ involves $R_{\mu\nu}$ (and allowably its derivatives) but not $F_{\mu\nu}$. We make the corresponding division of $\mathfrak{P}^{\mu\nu}$ into

$$\mathfrak{P}^{\mu\nu}_{\mathrm{E}} = \frac{n\mathfrak{K}_{\mathrm{E}}}{nR_{\mu\nu}} \quad \text{and} \quad -\mathfrak{P}^{\mu}_{\mathrm{T}} = -\frac{n\mathfrak{K}_{\mathrm{T}}}{n\mathfrak{K}_{\mu\nu}};$$

of course

$$\mathfrak{H}^{\mu\nu} = \frac{n\mathfrak{K}_{\mathrm{E}}}{nF_{\mu\nu}}, \qquad \frac{n\mathfrak{K}_{\mathrm{T}}}{nF_{\mu\nu}} = 0.$$

Thus we have

$$\left.\begin{gathered}\mathfrak{E}^{\nu}_{\mu\mathrm{T}} = \mathfrak{E}^{\nu}_{\mu\mathrm{E}} - \mathfrak{E}^{\nu}_{\mu} = \mathfrak{E}^{\nu}_{\mu\mathrm{E}} + \mathfrak{E}^{\nu}_{\mu\mathrm{M}}, \\ (\mathfrak{E}^{\nu}_{\mu\mathrm{T}})_{\nu} = 0, \quad (\mathfrak{E}^{\nu}_{\mu\mathrm{E}})_{\nu} = \mathrm{F}_{\mu\rho}\mathfrak{C}^{\rho}, \quad (\mathfrak{E}^{\nu}_{\mu\mathrm{M}}) = -F^{\nu}_{\mu\rho}\mathfrak{C}^{\rho},\end{gathered}\right\} \quad \text{(vii.)}$$

so that we may, if we like, call $\mathfrak{E}^{\nu}_{\mu\mathrm{T}}$ the total energy, $\mathfrak{E}_{\mu\mathrm{E}}$ the electromagnetic energy, and $\mathfrak{E}^{\nu}_{\mu\mathrm{M}} = -\mathfrak{E}^{\nu}_{\mu}$ the material energy. This division must seem a little artificial, and one may perhaps guess that in a more advanced stage of the theory the total energy will become of secondary importance, or disappear altogether, since already the quantity which spontaneously appears is that whose divergence is the ponderomotive force, not that whose divergence vanishes.

In particular it may be remarked that the "generalized volume" $\int\sqrt{-|{}^{*}G_{\mu\nu}|}\,d\mathrm{T}$ cannot profitably be taken as action function if we insist on a material and an electromagnetic energy with equal and opposite divergences, as in (vii.). This objection does not hold if we are ready to admit that the criterion for the presence of matter is not the existence of an energy distinct from $\mathfrak{E}^{\nu}_{\mu\mathrm{E}}$, but rather (as in Mie's theory) the departure of $\mathfrak{H}^{\mu\nu}$ from the form $\sqrt{-g}\,g^{\mu\alpha}g^{\nu\beta}F_{\alpha\beta}$.

Presumably, however, what we really want is an action function which will enable us to identify empty space, *i. e.* regions in which $\mathfrak{E}^{\nu}_{\mu}=0$ (or, if we retain both kinds of energy in which $\mathfrak{E}^{\nu}_{\mu\mathrm{M}}=\mathfrak{E}^{\nu}_{\mu\mathrm{E}}=0$), with those in which ${}^{*}G_{\mu\nu}=G_{\mu\nu}$ (*cf.* (94·61), (95·3)) in natural metric. This condition

again, being reduced to the vanishing of some function of

$$2K_{\mu\nu,\rho} = \frac{\partial g_{\mu\nu}}{\partial x^\rho} - \Gamma^{\alpha}_{\mu\rho} g_{\alpha\nu} F - \Gamma^{\beta}_{\nu\rho} g_{\mu\beta} \quad (93{\cdot}3)$$

$$= {}^*\nabla_\rho g_{\mu\nu},$$

or $$2\lambda K_{\mu\nu,\rho} = {}^*\nabla_\rho R_{\mu\nu},$$

where ${}^*\nabla_\rho$ indicates the affine or in-covariant derivative (Note 13), suggests that ${}^*\nabla_\rho {}^*R_{\mu\nu}$ or ${}^*\nabla_\rho {}^*G_{\mu\nu}$ should appear in the action. We are also inclined to demand that where $\mathfrak{E}^\mu = 0$, $\mathfrak{E}^\nu_{\mu M}$ (if there is such a function) should also $= 0$, and that in these regions also $\mathfrak{H}^{\mu\nu}$ should reduce to the form $\sqrt{-g}\, g^{\mu\alpha} g^{\nu\beta} F_{\alpha\beta}$, so that

$$\mathfrak{K} \text{ (or } \mathfrak{K}_E) = \tfrac{1}{2}\sqrt{-g}\, g^{\mu\rho} g^{\nu\sigma} F_{\mu\nu} F_{\rho\sigma},$$

still of course in natural metric.

Perhaps the only thing of real importance in this investigation

> (" Which, now that I review it, needs must seem
> Unduly dwelt on, prolixly set forth,")

is the illustration it gives of the way in which the world may be "self-gauging," as Eddington supposes (95). His natural metric here presents itself automatically, both as gravitational potential, whose gradient, multiplied by "mass," gives "force," and as lowering a suffix to convert "mass" to "energy." This is the physical statement; and it implies also, with the condition ${}^*\nabla_\rho R_{\mu\nu} = 0$, that the natural metric is the one which defines the geodesics which form the world-lines of particles in empty space. The geometrical interpretation of (iii.) is of course that a vector occurs in it which in natural gauge would be the covariant divergence of $\mathfrak{E}^\nu_\mu$, and that this disposes us to adopt the natural gauge for simplification.

[It may finally be noted that, if natural gauge be assumed at the outset, instead of at the end, of the analysis, the investigation is equivalent to that of (100). My $\mathfrak{E}^{\mu\nu}$ is Eddington's $\mathfrak{P}^{\mu\nu}$, my $\mathfrak{H}^{\mu\nu}$ is his $-\mathfrak{H}^{\mu\nu}$ (this change of sign is compensated by the identification $\mathfrak{E}^\nu_{\mu M} = -(\mathfrak{E}^\nu_\mu)$, and (iii.), or (vi.), on dividing by $\sqrt{-g}$, is (100·43). It was largely to show the independence of (100) of the natural gauge, and yet its powerful suggestion of it, that the present investigation was first undertaken.]

XLVIII. *The Photo-electric Activity of the Silver Halides and Silver Sulphide.* *By* F. C. Toy, *D.Sc.*, *F.Inst.P.*, H. A. Edgerton, *B.Sc.*, *and* J. O. C. Vick, *B.Sc.*, *D.I.C.**

[Communication No. 58 from the British Photographic Research Association Laboratories.]

THE work to be described in this paper was undertaken to ascertain if any parallelism could be traced between the photo-electric and photographic properties of the silver halides. A study of silver sulphide has also been included in this investigation in view of the recent work of S. E. Sheppard (Phot. J. lxv. pp. 380–387, 1925) indicating that the high sensitivity of modern photographic emulsions is largely due to the presence of traces of silver sulphide in the silver halide crystals.

Few previous investigations have been found in the literature in which the photo-electric activity of the silver halides has been measured in sufficient detail to enable a definite conclusion to be drawn as to its relation to photographic sensitivity, in particular no account can be traced of a study of the effect of different methods of preparation of the silver halides on their photo-electric properties; so far as it goes, however, previous work indicates that no parallelism exists. For example the work of Dima (*Compt. Rend.* clvi. p. 1366, clvii. p. 590, 1913) on silver iodide, bromide, and chloride, and that of W. Wilson (*Ann. d. Physik*, xxiii. pp. 107–130, 1907) on silver iodide, show that the photo-electric effect from these salts is not produced by violet light and that the critical frequency is in the ultra-violet and not less than about λ 1800. According to Dima the relative activities of the silver halide are as follows:—

chloride : bromide : iodide : : 1 : 2·15 : 3·75,

though Allen (Photo-Electricity, p. 246, 1925) states that the order is bromide > chloride > iodide. G. C. Schmidt (*Wied. Ann. d. Physik*, lxiv. p. 708, 1898), on the other hand, states that the silver halides all give about the same effect. Beyond these somewhat contradictory statements, there seems to be no very definite information, and from the photographic point of view it is of great interest to determine whether *any* method of preparation of these silver salts can be found which will give an extension of their photo-electrical sensitivity into the visible region, far enough to cover completely the photographic range, which, in the case of silver bromide, extends to about λ 5000.

* Communicated by T. Slater Price, O.B.E., D.Sc., F.R.S.

Experimental.

A valve method of measuring the photo-electric current was used because it has the advantage of being very simple and utilizes to a large extent apparatus present in any laboratory. In general, against these advantages may be placed the facts that such arrangements are not extremely accurate and are sensitive to outside disturbances. The latter disadvantage was easily overcome by suitable shielding, and the accuracy was more than sufficient for the work in hand.

The arrangement adopted is shown diagrammatically in fig. 1, and since it is, in principle, now well known as a

Fig. 1.

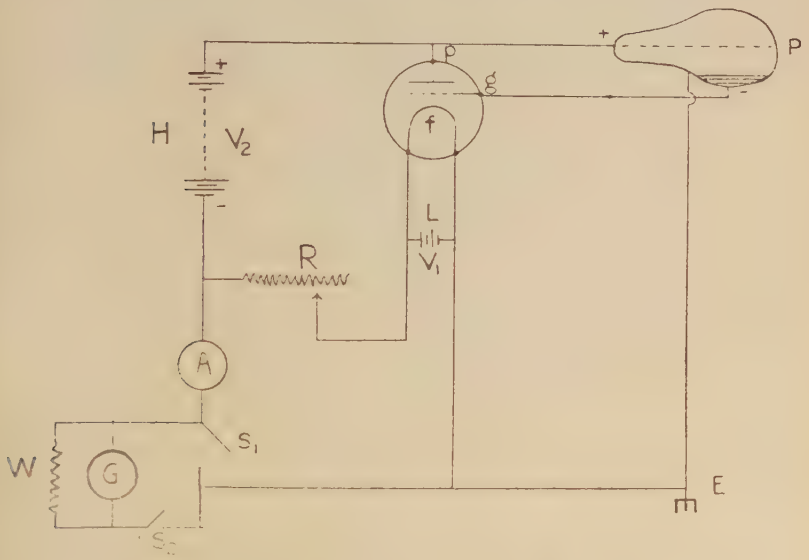

method of amplifying small currents, only brief reference need be made.

The essential principle is that the photo-electric cell is arranged between the grid and plate in a valve circuit (any of the usual types of receiving valves will do admirably). When the cell is in the dark there is a certain current through the plate circuit, depending on the filament voltage and that of the high-tension battery. This current, which we may call the dark current, flows through a moving coil galvanometer which is not specially sensitive (*e. g.* 1 mm. scale deflexion at 1 metre for 10^{-8} amp.).

Such an instrument can be used quite well in technical laboratories without the necessity of taking extreme precautions. The dark current through the galvanometer is compensated by an opposing e.m.f., so that the galvanometer reads zero. The deflexion produced on illumination of the cell is due, therefore, to the *change* in plate current. By this means the photo-electric current can easily be magnified one or two hundred thousand times. The plate, grid, and filament of the valve are represented at p, g, and f respectively. P is the photo-electric cell, H the high-tension battery having a voltage V_2. L is the filament battery, voltage V_1. A is a milliammeter and G the galvanometer, so arranged that by means of switches S_1 and S_2 the galvanometer need not be inserted in the circuit until approximate compensation of the plate dark current is obtained. This prevents the galvanometer being damaged, and is a very important precaution in work of this kind. In the arrangement used,

Fig. 2.

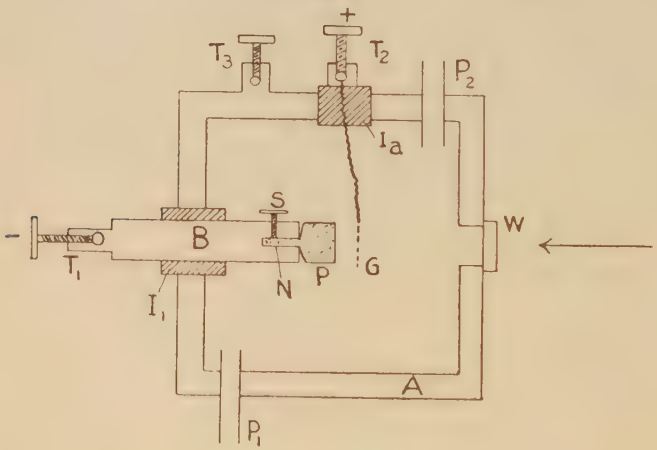

compensation was obtained from the battery L, which feeds the filament, and is connected across the galvanometer through the variable resistance R. A shunt was placed across the galvanometer, which whilst rendering the instrument dead-beat did not appreciably affect its sensitivity.

The photo-electric currents were measured in a cell built up by Kays Instrument Co., and shown in fig. 2.

This represents a section through the centre of the cell, which consists of a rectangular copper box, provided with a quartz window W, in the centre of one side. Through the

opposite side runs a thick cylindrical copper rod B, at the outer end of which is a terminal T_1, the whole being insulated from the case by the ebonite sheath I_1. The other end of B is drilled so as to take the nickel stem N of a pure silver disk P. This can be clamped firmly to B by means of the screw S. In front of P is arranged a fine nickel grid G, which is connected to the terminal T_2, itself insulated from the case by I_2. The grid may be moved (by an arrangement not shown) in a direction perpendicular to the surface of the plate P, and can be set at a known distance from P, with an approximate accuracy of 1/20 mm. T_3 is an earthing terminal connected direct to the case. P_1 and P_2 are inlet and outlet tubes. When using air in the cell, as in the following experiments, P_2 is closed and P_1 connected to the apparatus for producing a vacuum. This consists of a mercury vapour pump, backed by an ordinary water pump. The high and low vacuum sides are "short-circuited" by means of a piece of rubber tubing and clip, the adjustment of the latter giving the desired pressure.

One side of the cell is open and provided with a flange round the edges. This is ground flat so as to take a thick flat plate glass cover. The latter is held in position by Sira wax. With this arrangement the cell can be opened or closed very easily and the vacuum quickly obtained. When the cover is off, the silver disk P can be removed by unscrewing S, and pushing the grid to one side; the surface of the silver can then be treated in any desired way, and replaced in the cell.

Throughout the experiments, a quartz mercury vapour lamp was used as the source of illumination.

Since only comparative photo-electric measurements were desired, there was no need to work in a very high vacuum, and the presence of a small amount of gas had distinct advantages. One was the magnification of the true photo-electric current, produced by ionization by collision, and another, that as the apparatus had continually to be opened it was simpler and quicker to work at a comparatively high pressure. Since it is known that in general the magnification produced depends enormously on the pressure it was necessary to ensure either (1) that the pressure could be measured extremely accurately, or (2) that the conditions were such that relatively large variations in the pressure did not affect the number of electrons collected by the positive grid. The latter course was adopted.

From the theory of ionization of gases by collision we may write with sufficient accuracy, neglecting ionization

due to positive ions,

$$n = n_0 \epsilon^{lpN\epsilon - \frac{NV}{X}p}, \quad . \quad . \quad . \quad . \quad . \quad (1)$$

where

n_0 = number of electrons emitted from sensitive surface,
n = number of electrons reaching positive grid,
l = distance between electrodes in cms.,
p = pressure of the gas in mms.,
N = number of collisions made by an ion passing through 1 cm. of the gas at 1 mm. pressure,
V = ionizing potential,
X = the electric force per cm.

In order that in different experiments any variation in n should not be due to a change in p it was necessary to work at such a pressure that the variation of n with p is a minimum, *i. e.* at the maximum of the (n, p) curve. The pressure (p_m) at which n is a maximum is given by

$$p_m = X/NV. \quad . \quad . \quad . \quad . \quad . \quad . \quad (2)$$

In the experiments it was found convenient to use air as the gas and to work at a pressure of not less than 1 mm., as this can be read approximately on the usual U type of vacuum gauge. For air, NV may be taken as equal to 365 volts. The value of X was 590 volts, corresponding to 59 volts with the electrodes 1 mm. apart. This value of X had to be chosen with reference to the particular type of valve employed. The value of P_m is, under these conditions, $590/365 = 1{\cdot}6$ mm., which means that considerable variations in pressure will produce the least change in n, when the average pressure is 1·6 mm. That in this region it was only necessary to measure its actual value very roughly is shown by Table I., where galvanometer deflexions are given for different values of the pressure, using a surface of silver sulphide as the source of electron emission. (This was selected because it was found to be constant over a long period.)

Table I.

Pressure. mm.	Galvanometer deflexions, cm.
1	19
1·4	20
2·0	19
3·0	19
5·0	16
7·5	13
11·0	12

Since all the experiments to be described were carried out at pressures between 1·8 and 2·3 mm., large differences in the effects observed were due to true differences in the photo-electric activity of the substances examined and not to variation in pressure.

The photo-electric effects have been measured for three different methods of preparation of the silver halides, as follows :—

(1) By the action of the vapour on silver metal.
(2) By fusion of the salt prepared as in (1).
(3) By precipitation from aqueous solution.

The materials used in the preparation of the halides were the purest obtainable. The alkali halides used were the pure samples prepared by Clark in his work on electrometric titrations (J. C. S. 1925, pp. 749–755). The bromine and the iodine were the purest obtainable commercially, and the chlorine was prepared from pure recrystallized potassium permanganate and hydrochloric acid. The precipitated halides were allowed to settle slowly on to the silver disks, after the method used by Weiss (Brit. J. Phot. liv. p. 960, 1907). The layers so obtained were washed in distilled water and dried. In the later experiments the precipitate was forced on to the disks by centrifuging. All experiments were carried out in dull red light.

In this method of procedure there exists the difficulty that as soon as the substance is illuminated it commences to decompose, so that care must be taken to ensure that the photo-electric effect of the original salt is being measured. The rate of decomposition of the silver halides, if prepared by methods (1) or (2) above, is, however, slow compared with the time taken to observe the first deflexion of the galvanometer, and quite good end-points were obtained. In the case of the precipitated halides, this rapid decomposition of the salt under the influence of light was much more serious.

It was found that the photo-electric activity of the salts which had been fused and allowed to crystallize depends greatly on the conditions of cooling, as in shown in Table II. by experiments on the silver bromide.

TABLE II.

Method of Cooling.	Deflexion, cm.
(1) Slowing cooling in presence of bromine vapour...	4·4
(2) Slow cooling in air	6·3
(3) Rapid cooling in air	10·0

In order therefore to get some kind of comparison, the fused salts were in every case allowed to solidify and cool very slowly in contact with their respective vapours.

The results obtained by the first two methods of preparation are given in Table III. For comparative purposes the deflexion produced by a freshly scraped pure silver surface under the same conditions is given. This value could be repeated to within an accuracy of 3 per cent.

TABLE III.

The relative photo-electric activities of the silver halides. Measured in air at 2 mm. pressure.

Deflexion for freshly scraped silver surface = 178 cm.

Number.	Substance.	Technique.	First deflexion in cm.
1.....	Silver iodide.	Silver disk warmed and cooled slowly in halogen vapour.	60
2.....	Silver bromide.		5
3.....	Silver chloride.		0·2 approx.
4.....	Silver iodide.	Silver disk heated and salt fused and allowed to cool slowly in halogen vapour.	26
5.....	Silver bromide.		4 to 5
6.....	Silver bromide.		1 to 2

In view of the recent publications of S. E. Sheppard (*loc. cit.*) dealing with the formation of silver sulphide in the surface layers of the silver bromide crystals, it was of interest to see what would be the effect photo-electrically of forming traces of silver sulphide in a silver bromide surface. In order to do this it was first necessary to know the activity of pure silver sulphide, that of silver bromide already having been measured. Silver sulphide surfaces were prepared in two ways, by treating a silver surface with (*a*) sulphuretted hydrogen, and (*b*) dilute sodium sulphide solution, followed by washing with distilled water and drying. The results were of the same order, the gas treated surface being about 30 per cent. higher. The results given below in Table IV. are for method (*a*) only, since the conditions there corresponded most nearly to those under which the silver bromide was prepared. To obtain traces of

silver sulphide in a silver bromide surface, the latter was prepared as already described (Table III. (2)), and then fumed for a certain time with sulphuretted hydrogen.

TABLE IV.

Surface.	Photo-electric activity. Galvanometer deflexion in cm.
1. Silver bromide only	5
2. Silver bromide fumed for 0·5 sec. with H_2S gas, largely diluted with air	25
3. As in (2), but fumed for 2 secs. in almost pure H_2S	50
4. Silver sulphide	125

These results are not of special interest, in so far as they show a perfectly normal increase of effect with increasing amounts of sulphide. It is, however, possible that in these experiments the silver sulphide did not enter into the crystal lattice in the same way as when present in actual emulsion crystals.

The main point to notice is that silver sulphide is enormously more active photo-electrically than silver bromide, and about twice as active as silver iodide.

In the case of the precipitation of the halides from aqueous solutions much more difficulty was experienced in the repetition of results. This was thought to be due to one or more of the following causes :—

(1) Variation in the intensity of the lamp.

(2) Variation in the silver halide.

(3) Variation in thickness of layer and effect of metallic surface of disk.

(4) Variation in drying.

(1) To overcome this, a thermopile was arranged so that the energy of the green and yellow lines of the mercury lamp could be determined immediately before and after a photo-electric measurement was made; in this way any inconsistency in the intensity of the lamp could be detected. It was easily shown that this was not the cause of variable results.

(2) Careful precautions were taken to avoid any possible differences in the characteristics of the silver halide. In the original method the silver disk—on to which the

precipitate was centrifuged—was placed as shown in fig. 3 at the bottom of the glass tube. A certain quantity of ammonium bromide was run in, and then the required quantity of silver nitrate, *without stirring*. Although the mixture was shaken up immediately after the silver nitrate was added, it is quite possible that owing to local concentrations on the addition of the silver nitrate, some silver body (*i. e.* silver halide with adsorbed silver ions) might have been formed, even though there was always an excess of total halide, the amount of the silver body varying from

Fig. 3.

one tube to another. To overcome this difficulty the apparatus shown in fig. 4 was devised. The glass vessel A was fitted with a rubber bung B in which were 4 holes numbered 1, 2, 3, and 4 (only 1 and 2 are shown in the figure). Across the open top of the vessel A was placed a wooden cover C. Through holes in C passed four glass rods, G_1–G_4 (which had been drawn out at their lower ends to fit in the corresponding holes), a stirrer S, and an inlet tube T. The whole of this apparatus was fixed vertically, and four tubes of the type shown in fig. 3, and each containing a disk, were placed below the holes 1, 2, 3, and 4. With the rods fitted in the holes, ammonium bromide (or other halide) was run into the apparatus, and then with the stirrer rotating rapidly the desired quantity of silver nitrate was run in very slowly.

When thoroughly mixed and with the stirrer still working, the rods were loosened so that small quantities of precipitate could be run into the disk tubes below *. Since only approximately the same quantity of silver halide was wanted in each tube no exact measurements were made, but what this apparatus did ensure was, that the halide in all the

Fig. 4.

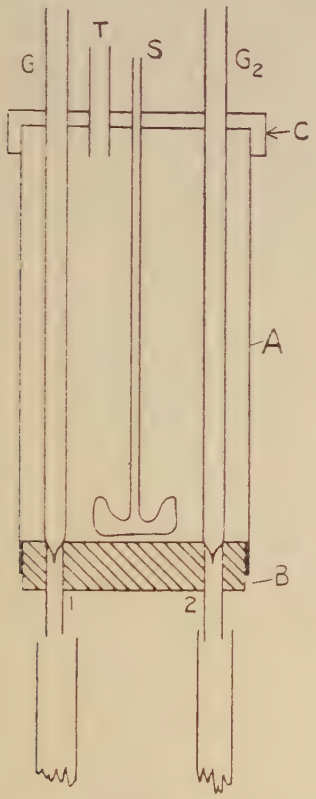

tubes had been formed under the same conditions. The precipitate was centrifuged down on to the disks as before. Even with these precautions, however, widely differing values were obtained.

(3) In order to investigate possible error due to photo-electric effect from the metallic surface of the disk itself, experiments were tried with both nickel and silver disks over

* Experiments with the precipitate before and after thorough washing showed no difference in the photo-electric effect obtained.

a wide range of thickness of halide layer. The results obtained indicated that there was no appreciable error due to this cause.

In these experiments no special precautions as to drying had so far been taken, the disks being allowed to dry in warm air in a small oven. It seemed therefore, that differences in drying were the cause of the irregular results.

(4) A long series of experiments, which need not be described in detail here, was undertaken to test this point. A special drying-cupboard was constructed and arranged so that the disk could be dried in a small space at the centre of the cupboard, where it was thought inequalities in drying would be inappreciable. Still, however, great differences were found. As an example, there are given below the values of the galvanometer deflexion in cms., obtained for seven different silver disks coated with silver bromide :—

39·4, 37·4, 30·3, 34·3, 32·9, 46·1, 35·9.

This was one of the best sets obtained. It was shown that these differences were still due to slight variations in drying owing to the small differences in the positions occupied by the disks in the cupboard.

Experiments were then carried out to test the effect of drying in a desiccator, over calcium chloride, but even then results could not be accurately repeated.

In view of all these difficulties, it was decided that the only way was to compare sets of disks, coated with different halides and dried together at the same time. By taking the *average* for each set, some comparison might be possible.

When these experiments were carried out, for the pure precipitated bromide and iodide, it was noticed that there was a great difference in the kind of deflexion observed. In the case of the iodide, the final deflexion was obtained fairly rapidly (about 15 secs.), the end-point being quite definite. But in the case of the bromide, the rise of deflexion was fairly slow and no marked end-point was reached. This was obviously due to the decomposition of the silver bromide by the light, with the resulting photo-electric emission from metallic silver. The kind of result obtained is shown in fig. 5, and it will be seen that it is quite impossible to specify for the silver bromide what is the value of the deflexion due to photo-electric emission from the unchanged halide. (This difficulty was also found later with Bromide + 10 per cent. Iodide precipitates.) With the iodide, however, the decomposition is relatively so slow that the definite deflexion obtained may be taken as due to the unchanged halide.

Since the direct decomposition of the silver halides is brought about by light of much longer wave-lengths than that active photo-electrically, the obvious procedure was to cut out all the radiations except those active photo-electrically—thus greatly diminishing the rate of decomposition, without appreciably lowering the photo-electric current. With the mercury lamp, the very strong lines at

Fig. 5.

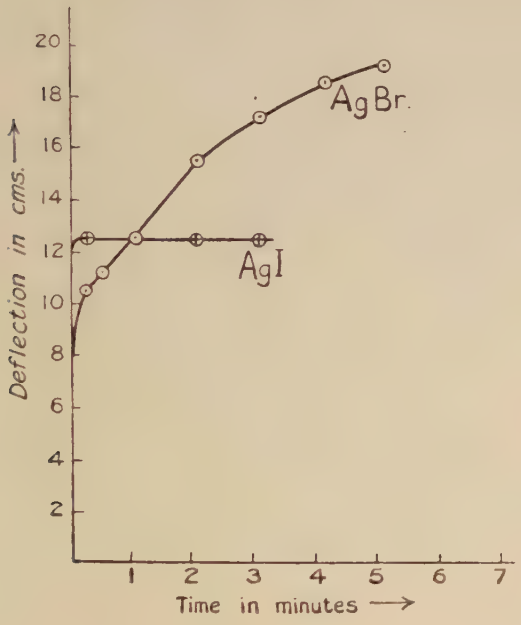

4358, 4060, 3650 Å. contribute nothing to the photo-electric effect but can all bring about the decomposition of silver bromide. By suitable chosen filters of chlorine and bromine vapours these can be practically cut out and the ultra-violet light of wave-length less than 3100 Å. transmitted. Preliminary experiments along these lines were actually undertaken, but in view of the fact that in the experiments to be described below all the evidence pointed very definitely to there being no connexion between photo-electric and photographic properties, it was considered inadvisable to continue these experiments.

The conclusion reached as the result of numerous experiments was that the order of photo-electric activity of the pure halides was very probably the same as for the previous methods of preparation.

These results confirm those of Dima (*loc. cit.*), in that the chloride shows the least effect, and the iodide the greatest, though the actual relative values are different.

In view of the well-known fact that traces of silver iodide in a silver bromide emulsion usually give chromatic sensitization, *i. e.* extend the spectral sensitivity into the longer wave-length region, experiments were also tried with silver bromide +5 per cent. and +10 per cent. silver iodide to try and detect any similar characteristics in the case of the photo-electric effect.

No noticeable increase in photo-electric effect relative to that of the pure bromide could be discovered for the iodobromide, although the latter appeared to show greatly increased sensitivity to direct print out effect.

In the experiments carried out to ascertain if any chromatic sensitization of the photo-electric effect could be obtained, a vita glass filter, which cut out all lines below about wave-length 2804, was placed between the light source and the cell. As with this filter no photo-electric effect could be obtained for pure silver (critical wave-length 3250) which without a filter gave a photo-electric effect equivalent to 350 mm. deflexion, it will be seen that most of the energy effective photo-electrically on pure silver lies below λ 2800—probably a large portion of it in the λ 2537 line. A similar experiment was tried with pure silver iodide and pure silver bromide, with a like result, as was to be expected, nor could any deflexion be obtained using the vita glass filter with iodobromide coated disks, so that no chromatic sensitization of the photo-electric effect to longer wave-lengths could be observed within the accuracy obtainable with the apparatus used.

In the photographic case, however, the chromatic sensitization is of the order of 500 Å., and it is probable that a shift of this order in the photo-electric effect could have been detected if present.

In all the cases investigated the photo-electric effect was due to light of wave-length less than 2800 Å., and greater than 1800 Å., at which points the absorption of vita glass and quartz begin. Photographically, on the other hand, a silver bromide emulsion is sensitive up to about λ 5000 and an iodobromide emulsion up to about λ 5500.

These results show that there is no parallelism between

the photo-electric properties of the pure silver halides and the photographic properties of silver halide emulsions.

In conclusion the authors wish to express their thanks to Dr. T. Slater Price, Director of Research of the British Photographic Research Association, for his interest and advice.

Summary.

1. If the silver halides are prepared by fuming metallic silver or by subsequent fusing, the order of photo-electric activity is

   Iodide > Bromide > Chloride.

   The order is very probably the same when the salts are precipitated from aqueous solutions.
2. Silver sulphide, prepared by fuming metallic silver with sulphuretted hydrogen, is from 2 to 3 times as active photo-electrically as silver iodide prepared in a similar way, and about 25 times more active than silver bromide.
3. Traces of silver sulphide in silver bromide have no abormal sensitizing effect photo-electrically, for the method of preparation used.
4. A trace of silver iodide in silver bromide causes no abnormal increase of photo-electric sensitivity.
5. It is improbable that the presence of small percentages of iodide in bromide results in any appreciable shift of the critical photo-electric wave-length towards the visible spectrum, comparable with the chromatic sensitization observed photographically.
6. All the effects observed were due to light of wave-length less than λ 2800.

The results show that there is no parallelism between the true photo-electric properties (*i. e.* complete ejection of electrons) and the photographic properties of the silver halides.

Physics Department,
British Photographic Research Association,
October 1926.

XLIX. *Dimensional Analysis.*

RECENTLY some papers on dimensional analysis and similar problems have been published in this magazine. The authors of most of these articles arrive at the conclusion that dimensional analysis on the basis of the old Fourier concept of dimensions is no longer possible in our days, and that this type of theory must be replaced by another, which may be designated "Theory of Similitudes." Opinions differ, however, as to the reliability of this theory. Mrs. Ehrenfest-Afanassjewa * regards the results as dependable, whereas Dr. N. Campbell † is of the opinion that the method can only be used successfully if one applies the utmost care in examining the physical peculiarities of the individual case.

In this way the theory of dimensions would be eliminated without being replaced by an equivalent one. That is unacceptable for all those who, from their own experience, have learned to appreciate the conception of dimensions. I should like to direct their attention to a method which establishes dimensional analysis in such a way that the objections raised to it fall to the ground. It has been worked out in two papers of mine issued in 1922 ‡. I demonstrate therein how, by utilizing the conceptions of the "Grössengleichungen" and the "Einheitengleichungen," we may give the whole doctrine of dimensions, units, and systems of units a reliable basis which will hold good for any theoretical and practical question in particular. All our fundamental conceptions involve, of course, conventions ; yet it may be evidenced that, departing from certain general principles, we arrive at *quite definite* dimensions of all quantities, and that, correspondingly, dimensional analysis, if carried out correctly, leads to as dependable results as any other kind of analysis.

Siemensstadt, Aug. 7, 1926. J. WALLOT.

* T. Ehrenfest-Afanassjewa, Phil. Mag. (7) i. p. 257 (1926).

† N. Campbell, Phil. Mag. (7) i. p. 1145 (1926).

‡ J. Wallot, *Zeitschrift für Physik*, x. p. 329 (1922) ; *Elektrotechnische Zeitschrift*, xliii. pp. 1329, 1381 (1922). A detailed treatise of the subject in question will shortly be published in *Handbuch der Physik*, edited by Geiger and Scheel, vol. ii.

L. *The Effect of the Presence of an "Indifferent" Gas on the Concentration and Activity of a Vapour in Equilibrium with a Condensed Phase or System of Condensed Phases.* (Part II.) *By* Ivan Roy McHaffie, 1851 *Exhibition Senior Student* *.

THE effect of the presence of air on the concentration and activity of water vapour in equilibrium with the solid phases $Na_2SO_4 10H_2O - Na_2SO_4$, at 25° C., has been described in a previous paper (Phil. Mag. 1926 (7), i. pp. 561–583). The results described were of such an anomalous nature that further investigation seemed desirable; furthermore, the activity coefficient as a function of pressure of air differed markedly from that calculated from the results of Pollitzer and Strebel (*Zeitschr. physik. Chemie,* cx. p. 768, 1924), who measured the concentration of water vapour in equilibrium with liquid water and in the presence of air up to a pressure of 200 kg. per cm.^{2} at temperatures of 50° and 70° C. The present paper describes the results obtained by the author using water at 25° C. as the condensed phase with pressures of air from 1 to 100 atmospheres.

The thermodynamic aspect of the problem has been discussed in the previous paper for vapour in equilibrium with a condensed liquid phase, and for a system of two solid condensed phases. As the present investigation is concerned with the concentration of water vapour in equilibrium with liquid water that which follows need only be considered in its relation to such a system. The relative activity of the vapour has been defined, and denoting this by a_p, it has been shown that,

$$\log a_p = \frac{PV_s}{RT}, \quad . \quad . \quad . \quad . \quad . \quad . \quad (1)$$

where P is the partial pressure of the indifferent gas, V_s is the molar volume of liquid water, in the condensed phase, and R and T have their usual significance. As an approximation a_p may be put equal to $\frac{c_p}{c_0}$; whence

$$\log \frac{c_p}{c_0} = \frac{PV_s}{RT}, \quad . \quad . \quad . \quad . \quad . \quad . \quad (2)$$

and if c_0 (the concentration of water vapour when the system is in a standard state) be known, c_p (the concentration of water vapour in equilibrium with the liquid phase when

* Communicated by Prof. F. G. Donnan, F.R.S.

the partial pressure of the indifferent gas is P) may be calculated with the validity involved in the assumption that $a_p = \frac{c_p}{c_0}$. The *relative activity coefficient*, f_p has also been defined, and is given by the equation

$$\log f_p = \frac{PV_s}{RT} + \log c_0 - \log c_p, \quad . \quad . \quad . \quad . \quad (3)$$

where c_0 is the concentration of water vapour in a standard state, and c_p is the concentration experimentally determined at the partial pressure P of the indifferent gas, and at the temperature T. The indifferent gas used was air freed from carbon dioxide. The lowering of the vapour pressure of water due to the increased solubility of air in water with increasing pressure has been calculated, and the decrease was found to be less than the experimental error of the apparatus, so this effect may be neglected. The standard state has been defined as that of pure water vapour in equilibrium with liquid water at 25° C. Hence, if from the experimental data c_p as a function of P is known, f_p as a function of P can be calculated.

The Method.

The air was maintained in contact with the water at constant pressure and temperature, until equilibrium was established between the partial pressure of the water vapour it contained and the vapour pressure of the water. The amount of water vapour contained in a small amount of this air was determined after releasing to atmospheric pressure. The pressure of the air was accurately determined from a hydrogen filled Cailletet tube, mounted in a suitable mercury-filled steel block.

The method employed for determining the amount of water vapour present in the air has been described elsewhere (J. Amer. Chem. Soc. xlviii. p. 1143, 1926), and is briefly as follows:—The water vapour from a known volume of air is frozen out, by means of liquid air, in a condensation tube of known volume to which a mercury manometer is attached. The air is then removed from the condensation tube, still maintained at the temperature of liquid air, by mercury diffusion pumps. The temperature of the condensation tube is then raised until all the water frozen out has been converted into vapour. The pressure of this vapour, at known volume, is then read off. Hence it is possible to calculate the mass of water present.

The Apparatus.

The apparatus has been described, and need not be given in detail here. Certain modifications were necessary in order that a condensed liquid phase might be used. These modifications are shown in fig. 1, in which D is a steel cylinder containing the vessel in which the water was placed. This vessel was made from a brass tube of suitable

Fig. 1.

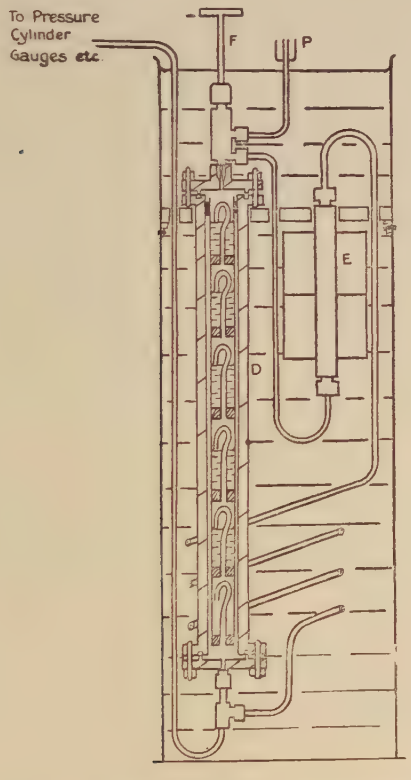

dimensions, and was divided into six compartments by brass plugs soldered into the tube. The free passage of air was provided for by copper tubes, shaped as shown in the diagram, soldered into the centre of each of the plugs. The water was placed in the five upper chambers, the surface of the water in each chamber being just below the openings in the connecting tubes. The lower chamber served as a trap to retain any water that might be forced back when the

pressure was released. The upper end of the brass tube fitted tightly into D so that the air passed through the saturator and not around it. All parts of this vessel which were in contact with liquid water, *i. e.* the portions inside, were tinned. E is an electromagnetic circulator (Trans. Faraday Soc. No. 63, xxii. 1926) which continuously circulated the air in an upwards direction through the saturators. A small electric heater was placed around the stem of the release valve F, and the temperature of the protruding portion of the valve maintained a few degrees above that of the thermostat. Thus any possible chance of condensation occurring at the release valve was prevented. Connexion was made to the glass portion of the apparatus by means of a mercury seal in the steel cup P. The oil thermostat, shown in the diagram, and the circulator E were maintained in continuous operation. The variation in temperature was not more than 0·05° C. over a period of several days. The experimental technique is similar to that previously employed, and need not be described here.

The arrangement of the water container was such that, with a very slow rate of circulation of air, there should be no water contained in the air as a very fine mist or spray. The results obtained, however, varied in a very peculiar manner, and when plotted against pressure gave a whole series of maxima and minima. The increase in the concentration of water vapour varied from a few per cent. at the minima to 100 per cent. at the maxima from 1·5 to 75 atmospheres, and from 75 to 100 atmospheres the variation was from 50 per cent. at the minima to 700 per cent. at the maxima. There was also a certain reproducibility among the results. The maxima and minima were found to occur at the same pressure of air for different series of measurements, although identical values were sometimes, but not always, obtained at any one pressure. These results being highly improbable the whole of the apparatus was thoroughly tested. The analysis of the air for water vapour was carried out by means of weighed phosphorus pentoxide tubes; at the same time the air was carefully tested for carbon dioxide, and was finally passed through sulphuric acid of known strength. The two latter analyses gave negative results, but the concentration of water vapour determined by this method still gave the peculiar variations referred to. The method of measuring very small amounts of water vapour by means of the condensation tube was then tested by measuring the vapour pressure of water over sulphuric acid-water mixtures of known strength. (The

results of these measurements will be published in a separate paper.) It was found that the method was reliable when the partial pressure of water vapour present was as low as 0·08 mm. of mercury. This value is much below the concentration required in any of the analyses of the present research. A filter was then inserted in the top end of the cylinder D so that the air, after passing through the saturators, must pass through the filter before being released through F. Filters composed of cotton-wool, asbestos-wool, and fine copper turnings were used. The results in each case were in good agreement, but still showed the same anomalies as the sodium-sulphate system. The air used in these experiments had been compressed in the laboratory, and it was thought that these peculiar anomalies might be due to something present in the air which had not been removed by the purifying system. In order to test this, cylinders of compressed air were obtained from another source. Two cylinders approximately two and one-half feet in length with an inch and a quarter hole, were placed in the pressure portion of the apparatus between the balancer cylinder and the thermostat. The first of these was filled with caustic soda (solid), the second was filled with glass, asbestos, and cotton-wool in three separate layers. The air was therefore efficiently "filtered" before entering the saturators, but the results obtained were in good agreement with those using air compressed in the laboratory.

The Results.

The readings obtained for the various experiments and for the different filters are given in Table I.; the results found when using compressed air from a different source are given at the end of the table. P is the pressure of air in atmospheres; T_a the temperature of the aspirator; V the number of c.c. of air passed through the condensation tube; B.p. the barometric pressure; (PV) the product of pressure and volume calculated from the data of Amagat (*Ann. de Chim. et Physique*, xix. p. 375, 1880), the value of this product for 1 c.c. of air at a pressure of 1 atmosphere and a temperature of 25° C. being taken as unity; T_u is the temperature of the condensation tube at which the pressures p, due to water vapour, were read. The concentrations of water vapour expressed in millimoles of water per litre are calculated from the data of Table I. by the expression

$$\frac{1000.273.1000}{298{\cdot}22410} \cdot \frac{AT_aP_p}{VB(PV)T_u},$$

where A is the volume of the condensation tube and B is

TABLE I.

With cotton-wool filter.

P.	T_a.	V c.c.	B.p. at	° C.	(PV).	T_w.	p.
5·0	21·0	89	756·0	20	0·9987	38·0	19·89
5·3	20·1	89	763·9	20	·9987	38·5	19·36
9·2	20·8	165	758·1	20	·9972	37·5	19·08
10·9	21·2	145	761·3	20	·9962	34·0	14·00
11·1	20·5	145	763·2	19	·9962	32·4	13·75
15·8	21·2	218	757·7	20	·9941	36·8	16·40
16·3	18·6	214	760·0	18	·9939	32·6	15·10
16·7	22·0	220	753·0	21	·9937	36·4	15·39
17·5	21·9	268	754·9	21	·9936	40·5	19·52
17·6	20·1	318	764·8	19	·9936	39·0	23·62
17·9	20·0	318	767·4	18	·9933	38·7	22·40
18·0	19·6	318	768·0	18	·9933	39·3	22·75
18·4	20·0	319	768·1	18	·9932	37·9	21·65
18·6	19·9	318	768·3	18	·9931	38·0	21·43
19·1	20·2	318	762·8	19	·9928	38·1	20·54
19·4	18·0	267	760·0	18	·9926	35·3	16·95
19·4	21·6	319	764·4	21	·9926	38·6	20·90
20·1	21·0	319	765·2	21	·9924	38·9	20·10
20·4	18·0	266	757·1	17	·9924	35·2	15·94
21·3	17·8	267	757·0	17	·9920	34·3	14·95
22·4	21·7	318	765·8	21	·9916	36·0	17·22
22·5	17·9	318	752·1	17	·9916	34·6	16·29
23·8	20·2	398	760·7	19	·9908	37·1	19·92
24·1	20.0	420	761·9	19	·9908	39·0	21·35
24·7	21·2	421	766·6	21	·9908	38·6	20·71
26·1	17·3	521	751·7	17	·9900	36·6	21·02
26·2	19·2	420	762·5	18	·9900	39·0	18·89
27·3	22·1	421	763·6	21	·9893	37·0	17·51
28·2	19·6	421	757·7	18	·9886	37·8	16·88
28·3	19·1	418	757·2	18	·9886	36·0	16·91
28·7	22·5	420	763·8	21	·9885	34·8	16·00
30·0	19·7	521	753·0	18	·9882	36·0	19·07
31·5	23·0	523	761·8	21	·9878	36·0	17·62
32·6	22·3	523	762·6	22	·9874	36·7	16·70
32·9	17·8	522	747·5	17	·9873	32·5	15·40
33·6	22·2	574	764·3	21	·9871	37·0	17·81
34·2	22·0	623	764·9	21	·9867	39·1	19·02
34·7	21·7	624	765·0	19	·9866	36·6	18·72
38·5	19·7	625	757·8	19	·9855	37·0	16·17
39·8	20·0	625	762·0	19	·9850	38·5	16·63
40·4	17·5	521	747·5	17	·9848	32·1	12·92
45·1	17·8	625	749·4	18	·9836	33·0	13·91
50·2	17·5	625	749·1	17	·9826	30·4	12·83
50·3	20·1	827	762·0	19	·9826	34·0	17·01
51·1	21·3	727	755·3	20	·9825	36·0	15·52
55·3	18·3	625	748·2	18	·9816	29·2	11·70
58·3	18·0	829	748·7	17	·9811	34·5	15·21
58·5	19·7	827	763·2	19	·9811	31·6	15·25
59·6	18·9	624	752·5	18	·9811	28·0	11·72
60·0	18·0	523	755·2	18	·9811	27·7	9·68
61·4	19·2	823	764·2	18	·9811	34·7	14·76
65·0	18·9	823	764·2	18	·9811	37·2	14·45
68·7	19·2	930	759·2	18	·9810	36·3	15·92
70·3	18·6	1032	757·1	18	·9810	36·8	17·34
71·8	19·0	1029	771·2	19	·9810	38·3	17·34
76·5	21·0	1032	764·8	20	·9808	36·6	16·30
78·4	18·2	1032	754·7	18	·9807	34·1	16·12
79·4	19·0	1032	768·7	18	·9806	35·4	16·07

TABLE I.

With cotton-wool filter (*con.*).

P.	T_a.	V c.c.	B.p. at ° C.		(PV).	T_u.	p.
80·6	18·7	1031	769·1	19	0·9806	34·2	16·02
81·5	20·2	1032	766·1	20	·9806	37·0	15·86
83·8	20·2	1032	766·8	20	·9806	37·5	14·91
83·8	18·9	1032	768·8	18	·9806	35·6	15·25
84·2	20·0	1032	767·5	20	·9806	35·3	15·18
84·3	18·3	1032	768·8	18	·9806	35·6	15·53
86·9	18·9	1032	755·7	18	·9806	32·2	14·96
87·8	20 0	1033	765·3	19	·9806	34·8	14·52
88·0	19·0	1033	764·1	18	·9806	36·5	14·65
88·4	19·2	1032	766·0	19	·9806	35·5	14·88
88·6	18·8	1026	763·9	18	·9806	36·9	15·02
91·9	19·8	1032	767·0	19	·9809	34·0	13·95
92·5	19·6	1032	762·4	19	·9809	37·2	13·97
92·6	19·2	1032	767·6	19	·9809	34·3	14·13
97·3	19·7	1033	770·1	19	·9816	33·5	13·47
98·5	19·3	1032	771·2	19	·9818	33·0	14·68
			With asbestos-wool filter.				
4·9	17·3	72	756·2	16	·9987	34·0	15·54
12·1	17·1	152	754·7	16	·9955	31·8	13·77
15·8	16·7	206	757·6	16	·9941	31·5	15·09
17·9	16·8	234	752·9	15	·9933	35·0	16·14
18·6	16·2	264	754·4	15	·9931	35·5	17·44
19·6	18·0	260	745·0	17	·9926	37·0	17·20
20·2	17·8	264	743·3	17	·9924	35·2	16·28
21·1	18·1	314	754·5	17	·9922	37·0	18·20
25·5	17·9	368	756·3	17	·9904	36·0	17·25
30·0	18·2	523	759·8	17	·9882	37·5	19·37
30·6	17·8	521	762·6	17	·9881	37·1	18·77
30·7	17·4	521	764·7	16	·9880	37·0	18·77
36·1	17·9	617	769·8	16	·9864	34·8	17·31
52·5	17·8	825	771·5	16	·9822	35·0	16·90
72·1	15·2	1034	764·5	15	·9810	36·4	17·70
88·6	16·7	1032	756·1	15	·9806	33·2	15·03
92·5	17·0	1032	757·3	16	·9809	33·0	14·85
96·6	17·7	1034	754·9	17	·9815	34·0	14·48
98·5	17·5	1032	754·5	16	·9818	33·0	14·54
			With copper-wool filter.				
9·9	16·0	151	751·4	17	·9964	36·0	16·30
19·9	16·2	257	749·6	17	·9925	34·2	15·79
28·3	15·8	420	749·2	16	·9886	35·0	16·89
31·3	16·1	523	750·3	17	·9879	35·0	18·24
32·2	15·5	523	752·9	16	·9876	34·6	17·48
40·7	16·5	624	762·3	18	·9847	33·0	15·48
64·0	16·1	930	764·4	16	·9811	34·5	16·69
86·0	16·0	1034	769·7	17	·9806	36·1	15·20
92·5	14·8	1031	771·4	16	·9809	31·8	14·29
			With compressed air from another source and the copper-wool filter.				
18·7	18·4	267	739·1	18	·9931	35·0	17·05
30·6	17·8	472	742·5	18	·9881	35·0	16·42
37·6	18·1	624	732·5	19	·9857	34·8	16·05
100·0	18·7	1036	752·2	16	·9820	31·0	12·85

TABLE II.

P.	Millimoles of H_2O per litre. Found.	Calculated.	log *f*.
	Cotton-wool filter.		
5·0	1·393	1·282	−0·0356
5·3	1·417		− ·0429
9·2	1·328	1·287	− ·0137
10·9	1·327		− ·0128
11·1	1·326		− ·0122
15·8	1·496	1·293	− ·0632
16·3	1·445		− ·0479
16·7	1·488		− ·0607
17·5	1·598		− ·0913
17·6	1·610		− ·0944
17 9	1·550		− ·0778
18·0	1·574		− ·0846
18·4	1·536		− ·0740
18·6	1·540		− ·0750
19·1	1·530		− ·0721
19·4	1·530		− ·0721
19·4	1·581		− ·0862
20·1	1·568	1·297	− ·0824
20·4	1·526		− ·0703
21·3	1·493		− ·0607
22·4	1·521		− ·0682
22·5	1·451		− ·0478
23·8	1·489		− ·0587
24·1	1·518		− ·0670
24·7	1·508	1·302	− ·0637
26·1	1·313		− ·0043
26·2	1·454		− ·0475
27·3	1·431		− ·0402
28·2	1·415		− ·0349
28·3	1·438		− ·0419
28·7	1·392		− ·0278
30·0	1·392	1·307	− ·0274
31·5	1·353		− ·0143
32·6	1·319		− ·0030
32·9	1·244	1·310	+ ·0226
33·6	1·315		− ·0015
34·2	1·307		+ ·0016
34·7	1·315	1·312	− ·0005
38·5	1·257		+ ·0197
39·8	1·322		− ·0018
40·4	1·259	1·317	+ ·0199
45·1	1·286	1·322	+ ·0120
50·2	1·330	1·327	− ·0014
50·3	1·314		+ ·0041
51·1	1·395		− ·0225
55·3	1·350	1·331	− ·0064
58·3	1·370		− ·0112
58 5	1·375		− ·0130
59·6	1·456		− ·0375
60·0	1·442	1·336	− ·0332
61·4	1·387		− ·0160
65·0	1·425	1·341	− ·0263
68·7	1·483		− ·0427
70·3	1·488	1·346	− ·0435
71·8	1·492		− ·0442
76·5	1·526	1·353	− ·0523
78·4	1·552		− ·0592
79·4	1·538		− ·0549

TABLE II.

Cotton-wool filter (*con.*).

P.	Millimoles of H_2O per litre. Found.	Calculated.	log *f*.
80·6	1·567	1·357	−0·0627
81·5	1·568		− ·0626
83·8	1·529		− ·0509
83·8	1·545		− ·0555
84·2	1·558	1·360	− ·0590
84·3	1·577		− ·0642
86·9	1·618		− ·0743
87·8	1·560		− ·0583
88·0	1·563	1·364	− ·0592
88·4	1·599		− ·0689
88·6	1·626		− ·0747
91·9	1·569		− ·0594
92·5	1·573	1·368	− ·0605
92·6	1·593		− ·0658
97·3	1·597		− ·0657
98·5	1·759	1·374	− ·1071
	Asbestos-wool filter.		
4·9	1·311	1·283	− ·0094
12·1	1·369	1·290	− ·0257
15·8	1·450	1·293	− ·0496
17·9	1·540		− ·0750
18·6	1·527		− ·0713
19·6	1·636		− ·1008
20·2	1·583	1·297	− ·0865
21·1	1·524		− ·0696
25·5	1·492	1·303	− ·0591
30·0	1·379	1·307	− ·0231
30·6	1·362		− ·0177
30·7	1·360		− ·0170
36·1	1·251	1·316	+ ·0208
52·5	1·330	1·329	− ·0005
72·1	1·516	1·348	− ·0512
88·6	1·633	1·364	− ·0780
92·5	1·684	1·368	− ·0903
96·6	1·717	1·372	− ·0974
98·5	1·761	1·374	− ·1076
	Copper-wool filter.		
9·9	1·322	1·288	− ·0116
19·9	1·534	1·297	− ·0729
28·3	1·427	1·306	− ·0387
31·3	1·370	1·309	− ·0201
32·2	1·345		− ·0118
40·7	1·262	1·317	+ ·0188
64·0	1·424	1·340	− ·0273
86·0	1·551	1·362	− ·0565
92·5	1·578	1·368	− ·0619
	With compressed air from another source and the copper-wool filter.		
18·7	1·531	1·296	− ·0722
30·6	1·362	1·308	− ·0176
37·6	1·252	1·314	+ ·0211
100·0	1·606	1·376	− ·0671

the barometric pressure corrected to that of mercury at 0° C. and for the vapour pressure of water at the temperature of the aspirator T_a. The temperatures in the expression are in degrees absolute. These values are given in the second column in Table II. The values in the third column are calculated from equation (2). The last column gives the values of $\log f_p$ calculated from equation (3).

Fig. 2 shows the curve obtained by plotting the concentrations measured against pressure. The value of the concentration of water in the gas phase when the pressure on the system is that defined by the standard state is given

Fig. 2.

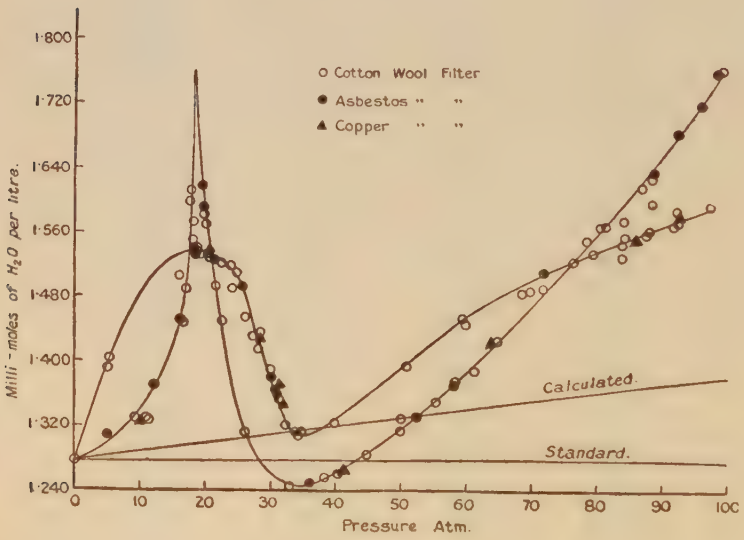

by the horizontal line marked "standard." The calculated values are also given. The results for the filters used are indicated in the figure. As with the sodium sulphate system investigated, two distinct curves have been obtained. The exact conditions which give rise to the change in equilibrium from one value to another at any one pressure have not been determined, but one may say that, with a freshly-inserted cotton-wool filter, the values along the lower portions of the curves will be obtained from 10 to 77 atmospheres both with increasing and decreasing pressure; from 77 to 100 atmospheres, with increasing pressure, the values along the upper portion of the curves will be obtained; but by

increasing the rate of circulation of air for as short a period as 2 hours before making a second determination, the lower value in this pressure region will be obtained; if the rate of circulation be again slowed down, and a determination of the concentration made after 20 hours, the value found will be intermediate between these two values—even 40 hours at constant pressure and temperature and with a very slow rate of circulation was not sufficient to allow the higher equilibrium to be reached. At 5 atmospheres the concentration measured fell on the upper curve, but from 10 to 17 atmospheres the values of the concentration found were those along the lower curve. After the filter had been in use for some time, the values of the concentration found were those on the upper portions of the curves from 17 to 77 atmospheres, but no change was noted from 5 to 17 atmospheres, nor from 77 to 100 atmospheres. In the narrow region between 17 and 21 atmospheres, values were now obtained along the sides of the high and very sharp maximum; but it was not found possible to trace this portion of the curve to the same degree as was possible with the sodium-sulphate system. Two separate cotton-wool filters were used, and they both behaved in a similar manner. Altering the rate of circulation at any pressure up to 77 atmospheres had no effect whatever on the values of the concentration found. The asbestos-wool filter had a slightly different effect from the cotton-wool filter. The values on the lower portions of the curves were obtained from 5 to 17 atmospheres; then at 18 atmospheres the value of the concentration was that on the lower maximum at this pressure, and at 19·6 and 20 atmospheres the values found were on the high and sharp maximum. From 21 to 34 atmospheres the values found were on the upper curve, and from 34 to 77 atmospheres the values were along the lower curve, and were on the upper curve again from 77 to 100 atmospheres. No change in the value of the concentration could be found by altering the rate of circulation at any pressure. The copper-wool filter gave the same results as the asbestos-wool filter, with the exception that in the neighbourhood of 18 atmospheres no values were found on the high and sharp maximum, and from 77 to 100 atmospheres the values fell along the lower curve. Changes in the rate of circulation had again no effect on the values of the concentration found. The comparison of these curves with those obtained for the sodium-sulphate system is of interest. The curve, which may be designated as that with the lower maximum at 18 atmospheres, corresponds in shape and in the pressures at which the maximum

and minimum occur to the similar curve for the sodium-sulphate system. The other curve, while of the same general shape as that for sodium sulphate, differs considerably in that the maximum and minimum occur at lower pressures. The respective ratios of the pressures at which these occur for water and for sodium sulphate is almost the inverse of the ratio of the concentrations of water vapour in equilibrium with the systems at their standard states. With water it has been found possible to trace this curve from 5 to 100 atmospheres, and the point of intersection with the other curve at 77 atmospheres corresponds to that of the sodium-sulphate system at 77·6 atmospheres. This fact would indicate that the discontinuity in the results for sodium sulphate is not due to any change occurring in the solid phases.

It is evident that the filters used have exerted some effect on the concentration of the water in the gas phase. The concentrations were much lower than when filters were not used. The peculiarities observed when filters were not employed cannot be readily explained. It cannot be definitely stated that they were due to a fine mist produced in the saturators, due to the circulation of air, since the same variations were noted whether the circulator was or was not in operation. It has also been suggested that they might be due to dust particles, having an adsorbed film of water molecules on their surface, which were carried by the air through the release valve giving rise to too high values; but copper-wool is not generally considered as being capable of removing dust particles from a gas, and yet when a copper-wool filter was used these peculiar variations disappeared. These considerations, together with the fact that there was a certain reproducibility in the variations, would indicate that they may be due to a metastable state of supersaturation of water in air, brought about by the effect of pressure on the condensed phase. If such were the case it can readily be seen why these variations were not observed in the sodium-sulphate system, as a supersaturated condition of water vapour would be impossible in the presence of anhydrous sodium sulphate. The effect of the filters could then be explained by the large amount of surface exposed supplying a sufficient number of points on which condensation could occur, giving rise to a stable equilibrium. This does not, however, explain the possibility of two apparently equilibrium values at any one pressure which has been experimentally observed in the case of sodium sulphate and of water. Any explanation of this phenomenon must be postponed until

further data are available concerning the effect of indifferent gas-pressure on heterogeneous equilibria.

The values of log f_p as a function of P are shown in fig. 3. The values calculated from the data of Pollitzer and Strebel (*loc. cit.*) are also indicated. It may be pointed out that their experimental error was several times greater than that calculated for the apparatus used in the present research, which was not greater than 0·2 per cent. With the exception

Fig. 3.

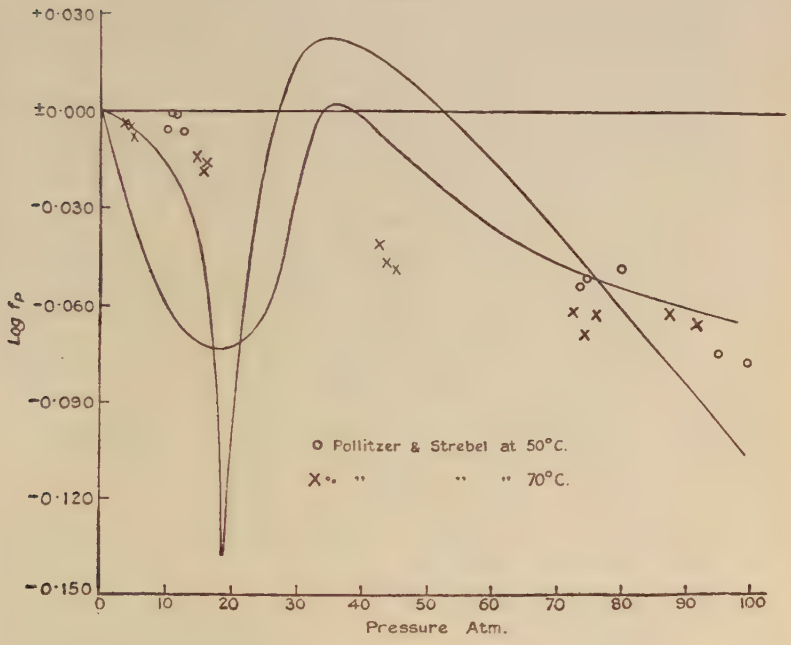

of the values for a temperature of 70° C. and a pressure of 45 atmospheres, there is a fairly good agreement between the values of log f_p calculated. It is also of interest that at 50° C. they do not give any values of the concentration of water vapour measured in the pressure range from 13 to 73 atmospheres ; and it is in this region that the most marked anomalies have been observed in the present research.

In conclusion, the author wishes to express his thanks to His Majesty's Royal Commissioners for the Exhibition of 1851 for a Senior Studentship during the carrying out

of this research; to the Royal Society for a grant to aid in the purchase of apparatus; and to Prof. F. G. Donnan, C.B.E., F.R.S., at whose suggestion the investigation was undertaken, for his interest and instructive advice during the progress of the research.

Summary.

1. The concentration of water in the gas-phase, in equilibrium with liquid water and in the presence of air up to a pressure of 100 atmospheres, has been measured.

2. The presence of filters in the high-pressure portion of the apparatus has been found to exert a marked influence on the values of the concentration determined.

3. The probable influence of such filters on the concentration of water in the gas-phase has been discussed.

4. The results for water have been compared with those obtained for the sodium-sulphate system.

5. The activity coefficient for water vapour in equilibrium with liquid water and in the presence of air has been calculated, and has been shown to be in good agreement with that calculated from the results of Pollitzer and Strebel.

The Sir William Ramsay Laboratories of
Physical and Inorganic Chemistry,
University College, London.

LI. *Notices respecting New Books.*

An Introduction to Surface Chemistry. By E. K. Rideal. (Cambridge University Press. 18*s.* net.)

THE importance of the subjects treated in this work, which really constitutes the first connected English account of them, is well brought out by Professor Donnan in a foreword to the book. While the work of Willard Gibbs, van der Waals and others has given an effective account of the thermodynamical and more general statistical phenomena relating to surfaces of separation, the "more intimate" study, on a molecular basis, of the structure and the kinetics of such surfaces has only advanced rapidly in very recent years, and the author is one of the chief pioneers in one of the successful modes of attack. Remarkable phenomena involving molecular orientations have been found to occur in such cases, and a full account appears in its due sequence in the course of the book.

The fundamental theme may not unreasonably be stated to be colloid chemistry, and in view of the growing importance of

the study of colloids, both to the pure chemist and on account of the increasing applications to industry, a treatise on the subject, such as the work now before us, is most valuable at the present moment.

The first chapter is concerned with the surface tension of liquids, and the second with the same property of solutions. Thermodynamical modes of argument are somewhat hard to find, in view of the author's expressed wish to present the subject from other aspects than those at one time considered sufficient. He goes on to discuss the surface films of insoluble materials, and subsequently the various types of interface, such as liquid-liquid, gas-solid, liquid-solid, and the differences of potential which can be found there. This is one of the most interesting parts of the work.

Colloid chemistry proper appears mainly in the two remaining chapters, of which the first deals generally with conditions of stability valid for various types of suspension or emulsion.

The form of the work reflects the usual great credit on the Cambridge University Press.

The Kinetics of Chemical Change in Gaseous Systems. By C. N. Hinshelwood. (Oxford: Clarendon Press. 12*s.* 6*d.* net.)

This work supplies a very definite need in the literature of physical chemistry, and more particularly in that section which is concerned with the mechanism of reactions. This is, at present, a rapidly expanding subject of a type only recently understood in general terms at all. The author is in the forefront of those who are at present investigating the phenomena in a strictly quantitative way.

The aim in this work is to give a connected account of such phenomena of chemical change as can be interpreted in the light of kinetic theory,—necessarily these are confined to gaseous systems, and hence the restriction of the scope of the book. The author explicitly points out, in his preface, that he has tried not to suggest any illusory simplicity in the subject, for its coordination is in fact only now beginning in a tentative manner.

The work is founded on lectures given in Oxford, where the school of physical chemists engaged on these problems is very strong and progressive, and the work can be regarded as quite authoritative. The various types of chemical reactions, uni-, bi-, and termolecular, are fully discussed, with a special chapter on the energy of activation. A long chapter deals with the general kinetics of heterogeneous reactions, and subsequently the nature of the activation in such cases is taken up.

The book is pleasant to read, and misprints seem few. It is a valuable addition to the series of scientific works from the Clarendon Press, and should prove indispensable to most teachers of physical chemistry.

LII. *Intelligence and Miscellaneous Articles.*

Absorption and selective dispersion of the hydrogen Balmer lines.

To the Editors of the Philosophical Magazine.

Gentlemen,—

MAY I make some remarks concerning the very interesting paper of Prof. R. W. Wood in the October issue of your Magazine on "The Self-Reversal of the Red Hydrogen Line"? In the experiments described, Prof. Wood did not note absorption of the H_α-line when sending the light of a discharge tube A through another tube B. The tubes were excited independently by two transformers. From my experiments with luminous hydrogen I believe the reason for Prof. Wood's negative result may be that the two discharge tubes A and B were not exactly in phase and the current density was not strong enough.

As a matter of fact, Dr. Agathe Carst and I have obtained strong selective dispersion at the H_α- and the H_β-line using a long tube of atomic hydrogen prepared by the known method of Wood and excited by strong continuous current of more than 100 m.a. per sq. cm. * Under these conditions the hydrogen is therefore doubtless in the absorbing state.

With neon and helium it is much easier to get absorption (Meissner, Dorgelo, and McCurdy) on account of the metastable atomic states in these gases, which according to experiments of J. Franck and others last a relatively long time and therefore accumulate. So Dr. H. Kopfermann and I were able to get also selective dispersion at many lines of neon and helium at very much lower currents than in hydrogen †, and it follows from the arrangement of the series-lines of hydrogen that in this case we probably do not meet with such long-lasting metastable atoms as in neon or helium.

Yours faithfully,
Dr. R. Ladenburg,
Prof. of Physics.

Berlin—Dahlem, Kaiser Wilhelm-Institut für physikalische Chemie und Elektrochemie. 11 December, 1926.

* See *Sitzungsber. d. Pr. Akad. d. Wiss.* 1926, S. 255, and *Die Naturwissensch.* xiv. p. 1208 (1926).

† *L. c.*, and *Phys. Zeitschr.* xxvi. p. 688 (1925); see also W. H. McCurdy and A. Bramley, Phys. Rev. xxvii. p. 314 (1926).

[*The Editors do not hold themselves responsible for the views expressed by their correspondents.*]

Flash Arc Spectrum of Sodium.

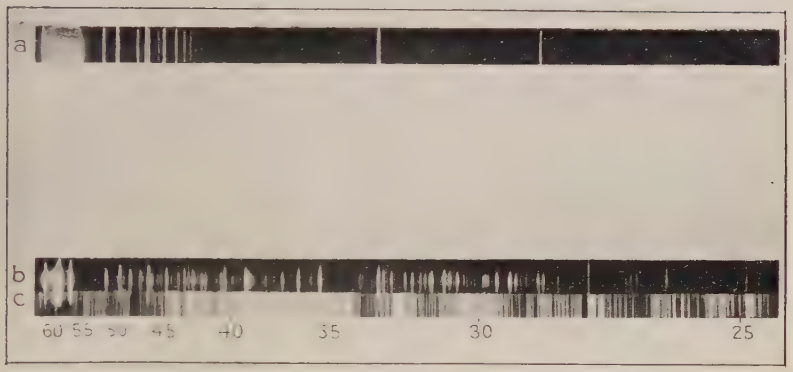

a. Sodium Arc Spectrum.

b. Sodium Flash Arc Spectrum.

c. Iron Comparison Spectrum.

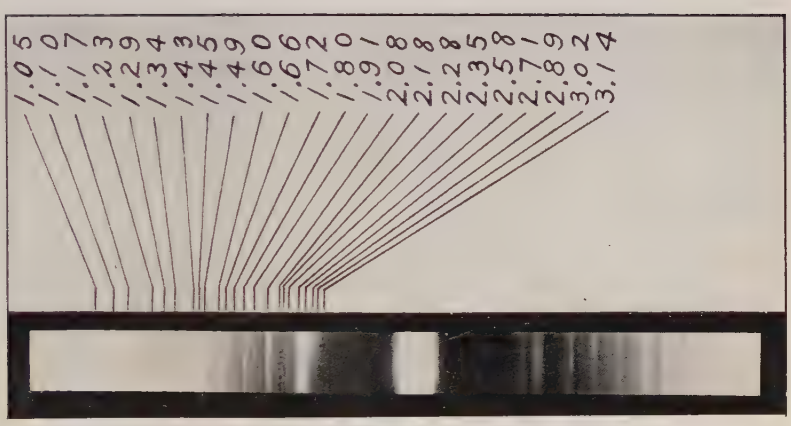
1.05
1.07
1.23
1.29
1.34
1.43
1.45
1.49
1.60
1.66
1.72
1.80
1.91
2.08
2.18
2.28
2.35
2.58
2.71
2.89
3.02
3.14

OXYGEN.

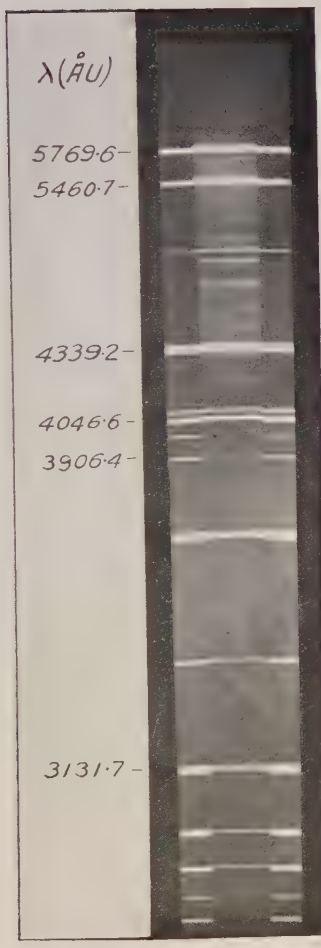

Fluorescence Spectrum of Sulphur.

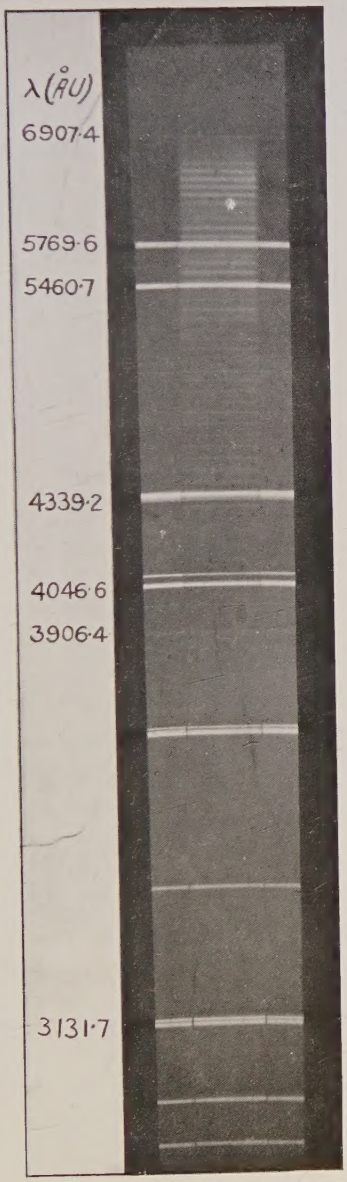

Fluorescence Spectrum of Tellurium.

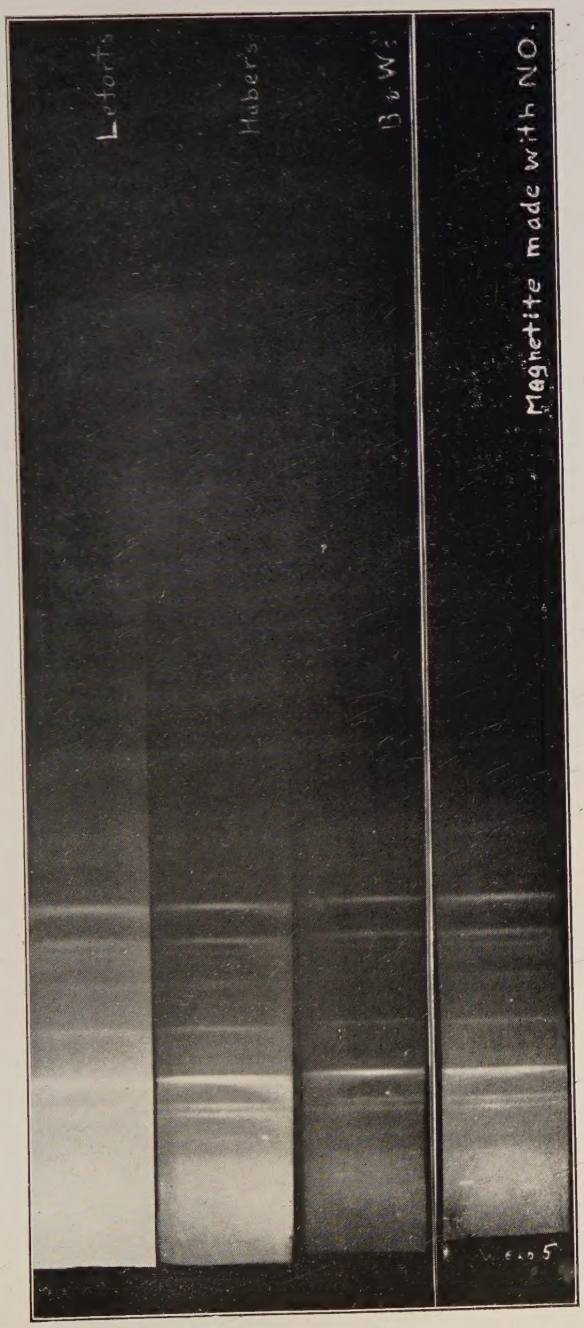
Lefort
Hubers
B & W
Magnetite made with NO.